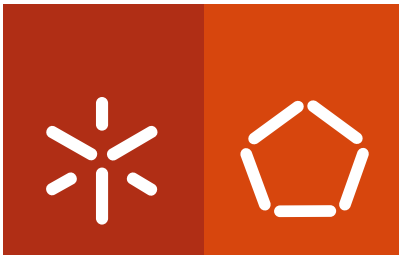


**Universidade do Minho**  
Escola de Engenharia

Elisabete Ramos Fernandes

**Development of a Phage-based Biosensor  
to Detect *Salmonella* in Food Stuff**

Fevereiro de 2013



**Universidade do Minho**  
Escola de Engenharia

Elisabete Ramos Fernandes

**Development of a Phage-based Biosensor  
to Detect *Salmonella* in Food Stuff**

Programa Doutoral em Engenharia Química e Biológica

Trabalho efetuado sob a orientação da

**Doutora Joana Azeredo**

e co-orientação do

**Doutor Leon Kluskens**

**Doutor Valery Petrenko**

Fevereiro de 2013

É AUTORIZADA A REPRODUÇÃO INTEGRAL DESTA TESE APENAS PARA EFEITOS DE INVESTIGAÇÃO, MEDIANTE DECLARAÇÃO ESCRITA DO INTERESSADO, QUE A TAL SE COMPROMETE;

Universidade do Minho,     /     /

Assinatura:

# Acknowledgments

Life is a mystery! I have been discovering my passion: constant search for why.

I did not grow up with this "dream" or a "special vocation", but the surprising is that I met people during my "path" who showed me how can we start to love what we are doing. I remember the first day I went to school, I was so enthusiastic to start learning and meet my new colleagues that I will never forget. While stepping through that path I never thought to be one day contributing to the Science in some way. I can consider myself privileged, since I had the opportunity to join different lab groups and study some time abroad. During my studies in different countries I learnt professionally and personally. I can say that if I put both fields of learning on a balance, they would be equilibrated. During the PhD trial, I contacted within research groups with high expertise and people with many years of experience. The professional knowledge combined with different labs environments made this experience unforgettable. My field of study has been built with the help of a multidisciplinary approach joining knowledge on different field. In the beginning I felt a little lost, but step by step and with the help gained in various laboratories I was creating the "pieces to my puzzle". It was not easy at all. The research is not only a field of flowers, sometimes we felt down... The feelings are like a "roller coaster" sometimes up and sometimes completely down. However, difficulties make us realize how we enjoy what we are doing. When I started this journey I had "a luggage composed of expectations, fear, curiosity", and now I "renewed that luggage with new ideas, knowledge and different perspectives". For all of this, I am eternally grateful to several people, special my supervisors Joana Azeredo and Leon Kluskens, not only for their expert guidance, but also for the continuous support. I will never forget the efforts that both did before I went to the United States in order to push me to improve my English and how they move the phage group to have meeting in another language. Beside it, their care and trust I will never forget. Another person, that I consider special is Ana Nicolau, that made this bridge and motivate me to start the PhD. I would like to thank her continuous care. To Valery Petrenko I would like to thank him the opportunity of joining his laboratory, for his suggestions and their efforts to make me understand their points of view. I will never forget the crystals example. I am also thankful to Bryan Chin for welcoming me so kindly. I would like to thank Paulo Freitas for the opportunity of being part of his group and a special thank you

for their advices. I am also thankful to Rob Lavigne for their availability to received me in his laboratory and help during my stay.

I am thankful to all my colleagues from the Applied Microbiology laboratory at the University of Minho, for the help at the beginning of this path. Additionally and on the redline I cannot forget to thank Franklin, even I do not know you since a long time, I appreciated your motivating words and help.

Also from the University of Minho I would like thank Cláudia for your help and suggestions with the flow cytometry.

To all my colleagues at the INL my sincere thanks for welcoming me so kindly, for helping each time, and a special THANKS to Verónica for the suggestions and support during this last year (not easy at all). You made my days in the lab so motivating... I will never forget your vision of the platform (like a movie;)..always on the expectation.

To the people from the other side (INESC-MN) I would like to thank all of them, specially Filipe for his suggestions and motivating words. To all my colleagues at Catholic University of Leuven I special thank you.

From Auburn University, I want to thank Deepa for their availability to help me, provides suggestions, support and specially for her friendship. I am also thankful to Natasha for her support in all moments and her care with me. Thank you to all my colleagues from Pathobiology and Materials department. I am eternally grateful to all friends that I made in Auburn, in particular Ashley, John, Colissia, Yimiao, Stephen, Shin and Alice. Thank you for everything. It was a good time there.

Some people make these days more easy with their friendship and some are very specially to me. Obrigada Pequinhos ;) Andreia, Angêlo, Bernardete, Brunos, Diana, Francisco, João, Rosana, Sofia, Sónia and Pedro!

To my family, specially my grandmother for her care and D.Mimi (the grandmother that I gained with my heart), to both of you: Obrigado pelo vosso carinho:).

I am eternally grateful to my parents that always encourage me, without their love it will be difficult to overcome all the difficulties. You always reminding me that we must run for our dreams. Without your support and care it will be too hard or even impossible. "Por todo o vosso amor" Obrigada do fundo do meu coração. To José Luís I cannot find the correct words to express my gratitude. You are always present...always and I will never forget it. Thank you

for your help, motivation, support, patience, big patience ;) "com a tua pequena ;)", and mainly for your love...



This work is funded by the Portuguese Government through FCT - Foundation for Science and Technology under the grant with reference SFRH/BD/48831/2008.

## **FCT** Fundação para a Ciência e a Tecnologia

MINISTÉRIO DA EDUCAÇÃO E CIÊNCIA



UNIÃO EUROPEIA  
Fundo Social Europeu



GOVERNO DA REPÚBLICA  
PORTUGUESA



PROGRAMA OPERACIONAL POTENCIAL HUMANO



QUADRO  
DE REFERÊNCIA  
ESTRATÉGICO  
NACIONAL  
PORTUGAL 2007.2013



COMPETE

PROGRAMA OPERACIONAL FACTORES DE COMPETITIVIDADE





# Development of a Phage-Based Biosensor to Detect *Salmonella* in Food Stuff

## Abstract

Food- and waterborne illnesses are a serious public health concern worldwide and have stimulated research aiming at a rapid and accurate detection of pathogens by applying biosensing technologies. *Salmonella*, *Campylobacter* and *E. coli* are some examples of pathogens that have an enormous impact on public health. Many publications have mentioned different type of biosensors for a broad range of bacteria. These methods may circumvent the limitations that conventional microbiological techniques have. Pathogens of interest need culture enrichment steps to reach the detection limit, a process that requires time, as well as laboratory technicians with expertise skills. Detection of pathogens at a very early stage is not as easy as it seems, due to the necessity to unite a set of characteristics that enable the development of an inexpensive and robust biosensor. The ideal biosensing system should be rapid and accurate and should combine specificity and sensitivity, leading to a marginal amount of false positive or negative results. As the biosensor is composed of two parts, a biological and a sensor element, the biorecognition element of choice plays a crucial role when creating the perfect biosensor. Bacteriophages (or simply phages) are viruses that specifically recognize bacteria and this characteristic can be used as a potential "key" to solve problems related with bacterial detection. Moreover, the easy and low cost production of these viruses combined with their stability in harsh environmental conditions make them excellent competitors with other biological elements (e.g. antibodies, enzymes). The use of phages as a therapeutic agent and as an interface in detection systems has gained special interest of the research community. In many laboratories, phage-based platforms have been developed; however only a few have broken the barrier and went to the market as a clinical diagnostic tool. Nowadays, the food sector still uses conventional methods to detect *Salmonella* in food stuff that, as mentioned before, take times and requires expert skills. Notwithstanding the great improvements in the detection area, biosensing systems still lack sensitivity and give erroneous results. Furthermore, problems related to the detection of bacteria in a viable but nonculturable (VBNC) state is one of the concerns that can give false negatives. VBNC bacteria are not able to grow

on standard bacteriological media, but are metabolically active, albeit very low, maintaining the capacity to cause diseases and therefore remain a potential risk in several health facilities and the food industry. The use of standard microbiological methods to detect if the bacterium is dead or alive is not practicable, since the presence of VBNC state is not detectable. Therefore, novel technologies that can overcome this barrier are imperative. The prevalence of this problem and the necessity of finding a detection technology that can fulfill the *Salmonella* detection needs, led to the proposal of the present work that explores phages as an interface in a magnetoresistive and magnetoelastic biosensor. The work presented herein describes the characterization of a broad host range lytic phage. PVP-SE1, is able to discriminate between cell viability states, including the VBNC condition. This phage was combined with highly sensitive magnetoresistive sensors originating a powerful detection system with high-standard performance at the accuracy, specificity but also sensitivity level, detecting bacteria concentrations in the order of 100 cells/ $\mu\text{L}$  (3-4 cells/sensor). Another strategy followed, aiming at circumventing the limitations of using whole phages in a biosensing interface, was the utilization of recognition peptides of phage origin, responsible for the identification of the hosts. The proof-of-concept was demonstrated with a model phage selected from landscape library as a streptavidin binder. The results showed that the streptavidin binding peptides extracted from the phage bind to streptavidin with the same or better affinity than the native phage. The same was demonstrated with the tail fibre proteins of phage PVP-SE1, heterologously expressed, which showed equal binding affinities compared to their parental phage. This work demonstrates how phages can be explored in the development of a biosensor, opening the possibility of using an accurate, sensitive, specific and cheaper device that can be applied to an emergent concern: foodborne pathogens.

**Keywords:** Foodborne pathogens; Detection; Bacteriophages; Specificity; PVP-SE1 phage; *Salmonella*; Biosensor; Viable But Nonculturable (VBNC) state; False positives; False negatives

# Desenvolvimento de um Biossensor à Base de Fagos para Detecção de *Salmonella* nos Alimentos

## Resumo

As doenças transmitidas através de alimentos e água contaminada são uma preocupação mundial e têm estimulado o desenvolvimento de métodos rápidos e precisos na área dos biossensores para a detecção de agentes patogénicos. *Salmonella*, *Campylobacter* e a *E. coli* são exemplos de espécies bacterianas patogénicos que tem um enorme impacto na saúde pública. Atualmente já existem diferentes tipos de biossensores desenvolvidos para uma ampla variedade de bactérias, que contornam as limitações das técnicas convencionais, tais como tempo de medida, devido à amplificação do microrganismo de interesse no seu adequado meio de cultura, e pela necessidade de técnicos com competências específicas. No entanto, a detecção de agentes patogénicos não é assim tão fácil como parece devido à necessidade de combinar um conjunto de características que permita o desenvolvimento de um biossensor robusto e pouco dispendioso. Um sistema de detecção ideal deve ser rápido, preciso e combinar características como especificidade e sensibilidade, de forma a conduzir a resultados livres de falsos positivos/negativos. Como o biossensor é composto por duas partes, i.e. um elemento biológico e um sensor, o elemento biológico escolhido tem um papel crucial no momento da criação de um biossensor perfeito. Bacteriófagos (ou simplesmente fagos) são vírus que infetam especificamente bactérias podendo essa característica ser utilizada como uma “chave” para solucionar problemas relacionados com a detecção de bactérias. Para além disso, a produção simples e económica destes vírus juntamente com a sua estabilidade em condições ambientais adversas, torna-os excelentes ferramentas de detecção, podendo competir com outros elementos biológicos (e.g. anticorpos, enzimas). A sua utilização como agentes terapêuticos e como interface em sistemas de detecção tem recebido uma atenção especial por parte da comunidade científica. Muitos laboratórios têm desenvolvido plataformas de detecção à base de fagos, no entanto, somente algumas conseguiram quebrar a barreira e entrar no mercado para serem usadas como ferramenta de detecção para uso clínico. Hoje em dia, indústrias alimentares ainda usam métodos convencionais para detetar *Salmonella* na alimentação que, tal como previamente referido, são morosas e exigem mão de obra especializada. Mesmo utilizando diversas

estratégias de detecção com diferentes plataformas e bio recetores, problemas com resultados falsos positivos e negativos permanecem difíceis de resolver. Bactérias viáveis, mas não cultiváveis são uma preocupação, porque estão relacionadas com resultados falsos negativos. Bactérias viáveis, mas não cultiváveis, não têm capacidade de crescer em meios de cultura convencional, mas encontram-se metabolicamente ativas, conservando a sua capacidade de causar doenças e de serem um potencial perigo em várias setores da saúde e na indústria alimentar. Assim, a utilização de métodos de cultura padronizados para detetar se a bactéria está viva ou morta torna-se inviável, já que a presença de bactérias num estado viável, mas não cultivável não é detetada. Portanto, novas tecnologias que possam ultrapassar essa barreira são fundamentais. A prevalência deste problema e a necessidade de encontrar uma tecnologia de detecção que possa satisfazer as necessidades de detecção da *Salmonella* conduziu à proposta deste trabalho que explora os fagos como uma possível interface a usar em biossensores magneto-resistivos e magneto-elásticos. O trabalho apresentado aqui descreve a caracterização de um fago lítico com um amplo espectro lítico, PVP-SE1. Este fago provou capacidade em discriminar os estados de viabilidade celular incluindo o estado viável, mas não cultivável. O fago foi combinado com sensores magneto-resistivos, que têm mostrado uma elevada sensibilidade. Esta combinação originou um poderoso sistema de detecção com um padrão de desempenho elevado, quer em termos de precisão e especificidade, quer em termos de sensibilidade, detetando concentrações de bactérias na ordem de 100 células/ $\mu\text{L}$  (3-4 células/sensor). Uma outra estratégia adotada, tendo por objetivo contornar as limitações da utilização dos fagos inteiros numa interface de um biossensor, passou pela utilização dos recetores dos fagos responsáveis pela identificação dos hospedeiros. Como prova de conceito um fago com especificidade de ligação à streptavidin foi selecionado a partir de uma biblioteca de fagos e usado como modelo. Os resultados demonstraram que os recetores do fago ligam-se à streptavidin com a mesma ou melhor afinidade do que o fago inteiro (original). O mesmo foi demonstrado com os recetores do fago PVP-SE1, demonstrando igualmente afinidades de ligação, comparativamente, com o seu fago parental. Este trabalho demonstrou como os fagos podem ser explorados no desenvolvimento de um biossensor abrindo a possibilidade de desenvolver um dispositivo preciso, sensível, específico e económico que possa ser aplicado a uma preocupação emergente: os patogénicos de origem alimentar.

**Palavras chaves:** Patogénicos de origem alimentar; Detecção, Bacteriófagos; Especificidade; Fago PVP-SE1 ; *Salmonella*; Biossensor; Estado viável, mas não cultivável; Falsos positivos; Falsos negativos

# Table of Contents

<b>1. General Introduction.....</b>	<b>1</b>
1.1. Foodborne Illness Caused by <i>Salmonella</i> .....	2
1.2. Detection of Foodborne Pathogens: Emerging Technologies .....	6
1.2.1. Conventional Culture Methods .....	6
1.2.2. Immunology-based Methods .....	7
1.2.3. Polymerase Chain Reaction (PCR).....	7
1.2.4. Biosensors and Biochips.....	8
1.3. References .....	29
<b>2. Selection and Characterization of <i>Salmonella</i> Phages.....</b>	<b>38</b>
2. Introduction .....	40
2.1 Materials and Methods .....	41
2.1.1 Media and Buffer Composition.....	41
2.1.2 Bacteriophages and Bacterial Strains .....	41
2.1.3 Phage Propagation.....	42
2.1.4 Phage Purification .....	42
2.1.5 Phage Propagation in a Non-pathogenic Host .....	42
2.1.6 Lytic Spectrum.....	43
2.1.7 Single-Step Growth Curve Experiments .....	43
2.1.8 Restriction fragment length polymorphism (RFLP).....	43
2.1.9 Transmission Electron Microscopy (TEM).....	44
2.1.10 DNA Manipulations .....	44
2.1.11 Construction of a short genomic library of phage PVP-SE2~ .....	45
2.2 Results .....	48
2.2.1 Phage Selection .....	48
2.2.1.1 Phage Lytic Spectrum.....	48
2.2.1.2 Phage Production in a Nonpathogenic Host.....	50
2.2.1.3 Phage Infection Parameters.....	50
2.2.1.4 Phage restriction fragment length polymorphism (RFLP) .....	51

2.2.2 Phages Characterization .....	52
2.2.2.1 Phage Morphology.....	52
2.2.2.2 Phages Sequencing .....	54
2.3 Discussion.....	65
2.4 Conclusions .....	67
2.5 References .....	67
<b>3. Magneto-resistive phage-based biosensor.....</b>	<b>72</b>
3. Introduction .....	73
3.1. Materials and Methods .....	76
3.1.1 Media and Buffers Composition .....	76
3.1.2 Bacteriophages and Bacterial Strains .....	77
3.1.3 Phage Propagation.....	77
3.1.4 Phage Buffer Exchange .....	77
3.1.5 Induction of <i>Salmonella</i> into Viable but Non-culturable (VBNC) State .....	78
3.1.6 Preparation of Gold (Au) Substrates .....	80
3.1.7 Optimization of Phage Immobilization on Au Substrates .....	80
3.1.8 X-ray photoelectron spectroscopy (XPS) .....	81
3.1.9 <i>Salmonella</i> Detection in the Magneto-resistive (MR) Biochip .....	83
3.2. Results .....	87
3.2.1 Optimization of Phage Immobilization on Gold Substrates.....	87
3.2.3 X-ray Photoelectron Spectroscopy Analysis.....	89
3.2.4 Blocking Performance Analysis .....	94
3.2.5 <i>Salmonella</i> Cell Induction to the VBNC State.....	95
3.2.6 Phage Adsorption Profile to Cells at Different Physiological States .....	99
3.2.7 Phage Performance as Biological Element on a Biosensor .....	100
3.2.8 Phage-based Magneto-resistive Biochip for Cell Viability Assessment .....	101
3.3 Discussion.....	107
3.4 Conclusions .....	109
3.5 References .....	110
<b>4. Development of a Detection Tool Based on Phage Recognition Peptides.....</b>	<b>116</b>



<b>4.1 Novel "Nano-Phages" Interfaces for Biosensors .....</b>	<b>116</b>
4.1 Introduction .....	118
4.1.1 Materials and Methods.....	119
4.1.2 Results.....	127
4.1.3 Discussion.....	140
4.1.4 Conclusions.....	141
4.2 Phage tail-fibre Proteins .....	142
4.2 Introduction .....	144
4.2.1 Materials and Methods.....	145
4.2.2 Results .....	152
4.2.3 Discussion.....	155
4.2.4 Conclusions .....	156
4.2.5 References .....	157
<b>5. Conclusions and Future Perspectives .....</b>	<b>162</b>
5.1 <i>Salmonella</i> Phage .....	162
5.2 Phage PVP-SE1 as a Biorecognition Interface.....	163
5.3 A detection tool based on host recognition peptides of phage origin.....	164
5.4 Answering the important issues.....	165
Appendix A: .....	167
Appendix B:.....	167

# List of Abbreviations

- APTES** Aiminopropyltriethoxysilane
- ATCC** American Type Culture Collection
- BE** Binding Energy
- BLAST** Basic Local Alignment Search Tool
- BPW** Buffered Peptone Water
- BSA** Bovine Serum Albumin
- CCPs** Critical Control Points
- CDC** Center for Disease Control and Prevention
- CECT** Colección Española de Cultivos Tipo
- CFUs** Colony Forming Units
- DLS** Dynamic Light Scattering
- EFSA** European Food Safety Authority
- EIA** Enzyme Immunoassay
- ELFA** Enzyme-Linked Fluorescent Assay
- ELISA** Enzyme Linked Immunosorbant Assay
- ESEM** Environmental Scanning Electron Microscope
- EU** European Union
- FDA** Food and Drug Administration
- G0** Generation zero
- G1** Generation one
- GFP** Green Fluorescent Protein
- HACCP** Hazard Analysis Critical Control Points
- HRP** Horseradish Peroxidase

**ICTV** International Committee on Taxonomy of Viruses

**IMS** Immunomagnetic Separation

**INL** Iberian Nanotechnology Laboratory

**IPF** Insoluble Protein Fraction

**IST** Instituto Superior Técnico

**GMR** giant magnetoresistive

**LFI** Lateral Flow Immunoassay

**LMW** Low Molecular Weight

**ME** Magnetoelastic

**MNPs** Magnetic Nanoparticles

**MOI** Multiplicity Of Infection

**MR** Magnetoresistive

**MTJ** Magnetic Tunnel Junctions

**NCTC** National Collection of Type Cultures

**NHS** N-hydroxysuccinimide

**NPP** Nitrophenyl Phosphate

**NPs** Nano-Phages

**NT** Not Tested

**OD** Optical Density

**PB** Phosphate Buffer

**PCB** Printed Circuit Board

**PCP** Phage Coat Protein

**PCR** Polymerase Chain Reaction

**PDMS** Polydimethylsiloxane

**PEG** Polyethylene Glycol

**PFU** Plaque Forming Units

**PI** Propidium Iodide

**PMMA** Poly(Methyl Methacrylate)

**PVDF** Polyvinylidene Difluoride

**QCM** Quartz Crystal Microbalance

**RFLP** Restriction fragment length polymorphism

**RI** Radioimmunoassay

**RT** Reverse Transcriptase

**SAW** Acoustic Wave Biosensors

**SEM** Scanning Electron Microscopy

**SGSC** *Salmonella* Genetics Stock Centre

**SPF** Soluble Protein Fraction

**SPR** Surface Plasmon Resonance

**SV** Spin-Valve

**TAE** Tris-Acetate-EDTA

**TBS** Tris-Buffered Saline

**TEM** Transmission Electron Microscopy

**TFPs** Tail Fiber Proteins

**LB** Luria broth

**TPF** Total Protein Fraction

**TSPs** Tailspike Proteins

**UM** Universidade do Minho

**USA** United States of America

**VBNC** Viable But Non-Culturable

**MWCO** Molecular Weight Cut Off

**WHO** World Health Organization

**DMSO** (ideal conditions)

**XPS** X-ray Photoelectron Spectroscopy

# List of Figures

<b>FIGURE 0:1:1:</b> INFORMAL PROPOSED APPROACH. ....	XXVIII
<b>FIGURE 1:1:</b> POSSIBLE VEHICLES OF <i>SALMONELLA</i> TRANSMISSION WHICH CAN CAUSE NON-TYPHOIDAL SALMONELLOSIS IN HUMANS .....	3
<b>FIGURE 1:2:</b> IMAGE A: DISTRIBUTION OF FOOD-BORNE OUTBREAKS WITH WEAK AND STRONG EVIDENCE (EXCLUDING STRONG EVIDENCE ON WATERBORNE OUTBREAKS) PER CAUSATIVE AGENT (I); BY FOOD VEHICLE (II) AND FOR CAUSATIVE AGENT OF EGGS AND EGG PRODUCTS CONTAMINATION (III) IN THE EU, 2010 . IMAGE B: SOME REPORTED CASES OF ENTERIC FEVER AND SALMONELLOSIS WORLDWIDE . ....	4
<b>FIGURE 1:3:</b> SCHEMATIC DIAGRAM OF A BIOSENSOR, SHOWING THE POSSIBLE BIOLOGICAL ELEMENTS (E.G. BACTERIOPHAGES, DNA) AND TRANSDUCER PLATFORMS THAT CAN BE USED TO DEVELOP A BIOSENSOR.....	9
<b>FIGURE 1:4:</b> ILLUSTRATION OF THE CONCEPT OF SPR BIOSENSING, WHERE ANALYTE MOLECULES IN A LIQUID SAMPLE BIND TO THE BIOLOGICAL ELEMENT IMMOBILIZED ON THE SENSOR SURFACE. WHEN THE BIND OCCURS AN INCREASE IN THE REFRACTIVE INDEX AT THE SENSOR SURFACE HAPPENS AND IS OPTICALLY MEASURED.....	11
<b>FIGURE 1:5:</b> SETUP FOR ME BIOSENSORS MEASUREMENT, SHOWING THE ELEMENTS INVOLVED ON THE PROCESS, NAMELY THE NETWORK ANALYZER, ME BIOSENSOR AND A BAR MAGNET THAT WILL CREATES A DC (DIRECT CURRENT) MAGNETIC FIELD. ....	14
<b>FIGURE 1:6:</b> A: SCHEME OF T4 PHAGE.B: STRUCTURE OF A TYPICAL FILAMENTOUS PHAGE VIRION. ....	19
<b>FIGURE 1:7:</b> PHAGE MORPHOLOGIES AND GENOME SIZES .....	23
<b>FIGURE 1:8:</b> ILLUSTRATION OF THE LYTIC CLYCLE.....	24
<b>FIGURE 1:9:</b> THE LYTIC AND LYSOGENIC CYCLES OF $\lambda$ (LAMBDA) PHAGE . ....	25
<b>FIGURE 1:10:</b> PHAGE APPLICATION ALONG THE FOOD CHAIN ON PHAGE THERAPY, BIOSANITATION, BIOCONTROL AND BIOPRESERVATION.....	26
<b>FIGURE 2:1:</b> ONE-STEP GROWTH CURVE OF PHAGE PVP-SE1 G0 IN <i>SALMONELLA</i> S1400/94 AND PVP-SE1 G6 IN <i>E. COLI</i> BL21.....	51
<b>FIGURE 2:2</b> RESTRICTION PROFILE OF PHAGE PVP-SE1 DNA. ....	52
<b>FIGURE 2:3:</b> TRANSMISSION ELECTRON MICROSCOPY ANALYSIS OF PHAGE PVP-SE1 (A), PVP-SE2 (B) AND PVP-SE3 (C).....	53
<b>FIGURE 2:4:</b> IMAGES OF THE PLAQUE CHARACTERISTICS OF: PVP-SE1 PRODUCED IN S1400/94 <i>SALMONELLA</i> HOST (A) AND IN A NONPATHOGENIC HOST (B); PVP-SE2 PRODUCED IN 821 <i>SALMONELLA</i> HOST (C); PVP-SE3 PRODUCED IN 869 <i>SALMONELLA</i> HOST (D).....	54

<b>FIGURE 2:5:</b> .GENOME ASSEMBLY OF PVP-SE2. OVERLAPPING SEQUENCES OF GROUPS OF CONTIGS IN BLOCKS OR SCAFFOLDS, FILLING GAPS OF THE SEQUENCE. EACH SCAFFOLD OF CONTIGS CORRESPONDS TO A "SUPERCONTIG" CALLED CONTIG ASSEMBLY 1-4. THE SEQUENCES ARE ASSEMBLED TO TWO HOMOLOGOUS PHAGES, PHAGE SE2 AND SETP3.....	62
<b>FIGURE 2:6:</b> PUTATIVE TFPS IDENTIFIED AS GP4 AND A01 AND THEIR POSITION ON THE SEQUENCE GENOME.	64
<b>FIGURE 3:1:</b> MAGNETORESISTIVE BIOCHIP. ....	84
<b>FIGURE 3:2:</b> MICROFLUIDIC SYSTEM USING A PRESSURE PLATFORM INCLUDING THE PCB ALIGNED WITH THE POLY(METHYL METHACRYLATE) (PMMA) PLATES AND THE PDMS CHANNEL. ....	86
<b>FIGURE 3:3:</b> COMPARISON OF THE BACTERIA SURFACE COVERAGE WHEN THE PHAGE WAS IMMOBILIZED BY COVALENT CROSS-LINKING AND PHYSICAL ADSORPTION. ....	88
<b>FIGURE 3:4:</b> SULFO-LC-SPDP MOLECULE STRUCTURE .....	89
<b>FIGURE 3:5:</b> XPS $S_{2p}$ SPECTRA (TOP TO BOTTOM) FOR SPDP, FLUOROETHYLAMINE WITH DMSO, FLUOROETHYLAMINE WITH MOPS AND PHAGE. ....	90
<b>FIGURE 3:6:</b> XPS $C_{1s}$ SPECTRA (TOP TO BOTTOM) FOR SPDP, FLUOROETHYLAMINE WITH DMSO AND MOPS, PHAGE.....	91
<b>FIGURE 3:7:</b> XPS $N_{1s}$ SPECTRA (TOP TO BOTTOM) FOR SPDP, FLUOROETHYLAMINE WITH DMSO AND MOPS, PHAGE.....	92
<b>FIGURE 3:8:</b> XPS $F_{1s}$ SPECTRA (TOP TO BOTTOM) FOR SPDP, FLUOROETHYLAMINE WITH DMSO AND MOPS. ....	93
<b>FIGURE 3:9:</b> A: PERCENTAGE OF THE BACTERIA SURFACE COVERAGE IN THE AREA IN WHICH PHAGE WAS IMMOBILIZED (IDENTIFIED AS "IN SPOT") AND ON THE NONSPECIFIC BINDING AREA IN WHICH PHAGE WAS NOT IMMOBILIZED (IDENTIFIED AS "OUT SPOT"). B: IMAGE OBTAINED BY NIKON SMZ 1500 STEREOMICROSCOPE SHOWING THE "IN SPOT" AND "OUT SPOT".....	95
<b>FIGURE 3:10:</b> ASSESSMENT OF PHYSIOLOGICAL STATE OF <i>SALMONELLA</i> ENTERITIDIS (S1400) CELLS AFTER TREATMENT WITH BLEACH AT DIFFERENT CONCENTRATIONS BY DIFFERENT EVALUATION METHODS.....	97
<b>FIGURE 3:11:</b> COLONY FORMING UNITS ON AGAR PLATES: A: <i>SALMONELLA</i> CELLS WITHOUT BLEACH CONTACT; B: <i>SALMONELLA</i> CELLS STRESSED BY BLEACH. ....	98
<b>FIGURE 3:12:</b> (A) BACTERIOPHAGE PVP-SE1 GROWTH CURVE IN <i>SALMONELLA</i> ENTERITIDIS (S1400) IN PHOSPHATE BUFFER AT ROOM TEMPERATURE.....	99

<b>FIGURE 3:13:</b> DENSITY OF CELLS SPECIFICALLY CAPTURED BY PHAGE AND ANTIBODY SPOTS, COVALENTLY IMMOBILIZED ON GOLD SOLID SURFACE.....	101
<b>FIGURE 3:14:</b> THE DETECTION STRATEGY USING PHAGE PVP-SE1 (A) AND A TYPICAL RESPONSE OF PHAGE-MODIFIED MAGNETORESISTIVE SPIN-VALVE SENSOR (B) WHILE MEASURING <i>SALMONELLA</i> ENTERITIDIS CONTAMINATED SAMPLES. ....	103
<b>FIGURE 3:15:</b> COMPARISON OF TWO GROUPS OF EXPERIMENTAL DATA FOR <i>SALMONELLA</i> ENTERITIDIS DETECTION.....	104
<b>FIGURE 3:16:</b> SIGNAL COMPARISON OF <i>SALMONELLA</i> ENTERITIDIS IN TWO GROWTH STATES. AS A NEGATIVE CONTROL, SENSORS COATED WITH UNSPECIFIC PHAGE WERE USED.....	105
<b>FIGURE 3:17:</b> PHAGE-BASED MAGNETORESISTIVE BIOCHIP MEASUREMENTS PERFORMED ON AN ELECTRONIC READER. ....	106
<b>FIGURE 4:1:</b> SCHEME OF THE EXPERIMENTAL SETUP USING A NPS-BASED ME SENSOR.....	126
<b>FIGURE 4:2:</b> PHAGE 7B1 CHARACTERIZATION.....	127
<b>FIGURE 4:3:</b> ISOLATION OF THE PHAGE-COAT PROTEIN BY SIZE-EXCLUSION CHROMATOGRAPHY. ....	128
<b>FIGURE 4:4:</b> ELUTION/EXCHANGE BUFFER OF A FRACTION OF THE PHAGE COAT PROTEIN (PVIII) ON A SEPHAROSE COLUMN.....	129
<b>FIGURE 4:5:</b> ANALYSIS OF THE ACTIVITY OF NPS.....	130
<b>FIGURE 4:6:</b> COMPARISON OF THE BINDING AFFINITY OF NPS AGAINST DIFFERENT CONCENTRATIONS OF AP-SA. ....	131
<b>FIGURE 4:7:</b> STABILITY TESTS CONSIDERING THE STORAGE TIME AND THE RATIO $A_{260/280}$ NM AS PARAMETERS. ....	132
<b>FIGURE 4:8:</b> SIGMOIDAL FIT TO ELISA DATA POINTS INDICATES DOSE-DEPENDENT BINDING BETWEEN NPS AND AP-SA.....	134
<b>FIGURE 4:9:</b> A: INHIBITION OF AP-SA BINDING (6.25 $\mu$ G/ML) BY NPS AT DIFFERENT CONCENTRATIONS. ....	135
<b>FIGURE 4:10:</b> WESTERN BLOT ANALYSIS SHOWING THE NPS IMMOBILIZED ON THE SENSOR SURFACE.....	136
<b>FIGURE 4:11:</b> OPTICAL IMAGES OBTAINED BY NIKON ECLIPSE L150 OF STREPTAVIDIN BEADS OF 0.99 $\mu$ M (A), POLISHED ME SENSOR (B) AND STREPTAVIDIN BOUND ON SENSOR SURFACE (C AND D). ....	137
<b>FIGURE 4:12:</b> SEM IMAGES OF THE ME BIOSENSORS .....	138
<b>FIGURE 4:13:</b> MAGNETOELASTIC BIOSENSOR'S RESPONSES, WHEN EXPOSED TO INCREASING CONCENTRATIONS OF STREPTAVIDIN POLYSTYRENE BEADS.....	139



**FIGURE 4:14:** FLUORESCENCE INTENSITY MEASURED AT 520 NM IN THE WELLS COATED WITH DIFFERENT CONCENTRATIONS OF PVP-SE1 GP40 AND PVP-SE1 GP51 IN 0.1M PB BUFFER OR SM BUFFER.....153

**FIGURE 4:15:** FLUORESCENCE INTENSITY MEASURED AT 520 NM IN THE WELLS COATED WITH 200 MG/ML PVP-SE1GP40 AND PVP-SE1GP51.....154

**FIGURE 4:16:** IMAGES OBTAINED BY NIKON SMZ 1500 STEREOMICROSCOPE SHOWING THE BACTERIA SURFACE COVERAGE IN THE AREA IN WHICH PVP-SE1GP51 WAS IMMOBILIZED ON GOLD SUBSTRATES SPECIFICALLY RECOGNIZING *SALMONELLA* ENTERITIDIS CELLS. ....155

**FIGURE B.2:** REPRESENTATIVE EXAMPLE: SDS-PAGE ANALYSIS OF THE EXPRESSION AND PURIFICATION OF PVP-SE1GP51 AND PVP-SE1GP53.....168

# List of Tables

<b>TABLE 1:1:</b> EXAMPLES OF OPTICAL TECHNIQUES APPLIED ON STUDIES RELATED WITH FOODBORNE PATHOGENS. .....	12
<b>TABLE 1:2:</b> EXAMPLES OF ELECTROCHEMICAL BIOSENSORS FOR FOODBORNE PATHOGENS.....	13
<b>TABLE 1:3:</b> CLASSIFICATION OF PHAGES BASED ON THEIR FAMILY, STRUCTURAL MORPHOLOGY AND GENETIC MATERIAL ENCLOSED .....	21
<b>TABLE 1:4:</b> SHAPE REPRESENTATION OF THE MAJOR PHAGE GROUPS .....	22
<b>TABLE 1:5:</b> THE USE OF PHAGE AS BIORECOGNITION ELEMENT IN DIFFERENT TRANSDUCERS ON THE DETECTION OF DIFFERENT ORGANISMS .....	27
<b>TABLE 2:1:</b> LYTIC SPECTRA OF ISOLATED <i>SALMONELLA</i> PHAGES AGAINST POULTRY <i>SALMONELLA</i> ISOLATES AND COMPARISON WITH FELIX 01 PHAGE .....	48
<b>TABLE 2:2:</b> LYTIC SPECTRA OF ISOLATED <i>SALMONELLA</i> PHAGES AGAINST DIFFERENT <i>SALMONELLA</i> SUBTYPES AND OTHER BACTERIA THAN <i>SALMONELLA</i> .....	49
<b>TABLE 2:3:</b> LYTIC SPECTRUM OF PVP-SE1 OVER GENERATION 0 TO 6 AGAINST POULTRY <i>SALMONELLA</i> ISOLATES .....	50
<b>TABLE 2:4:</b> DESCRIPTION OF EACH PVP-SE1 GP AND CORRESPONDING FUNCTION.....	60
<b>TABLE 2:5:</b> PERCENTAGE OF SIMILARITY BETWEEN THE SHORT SEQUENCE OF PVP-SE2 AND PHAGE SE2 AND SETP3.....	63
<b>TABLE 4:1:</b> CONCENTRATIONS OF COMPETITIVE INHIBITORS. ....	124
<b>TABLE 4:2:</b> INFORMATION OF PRIMERS USED FOR THE SEQUENCING REACTION. ....	147

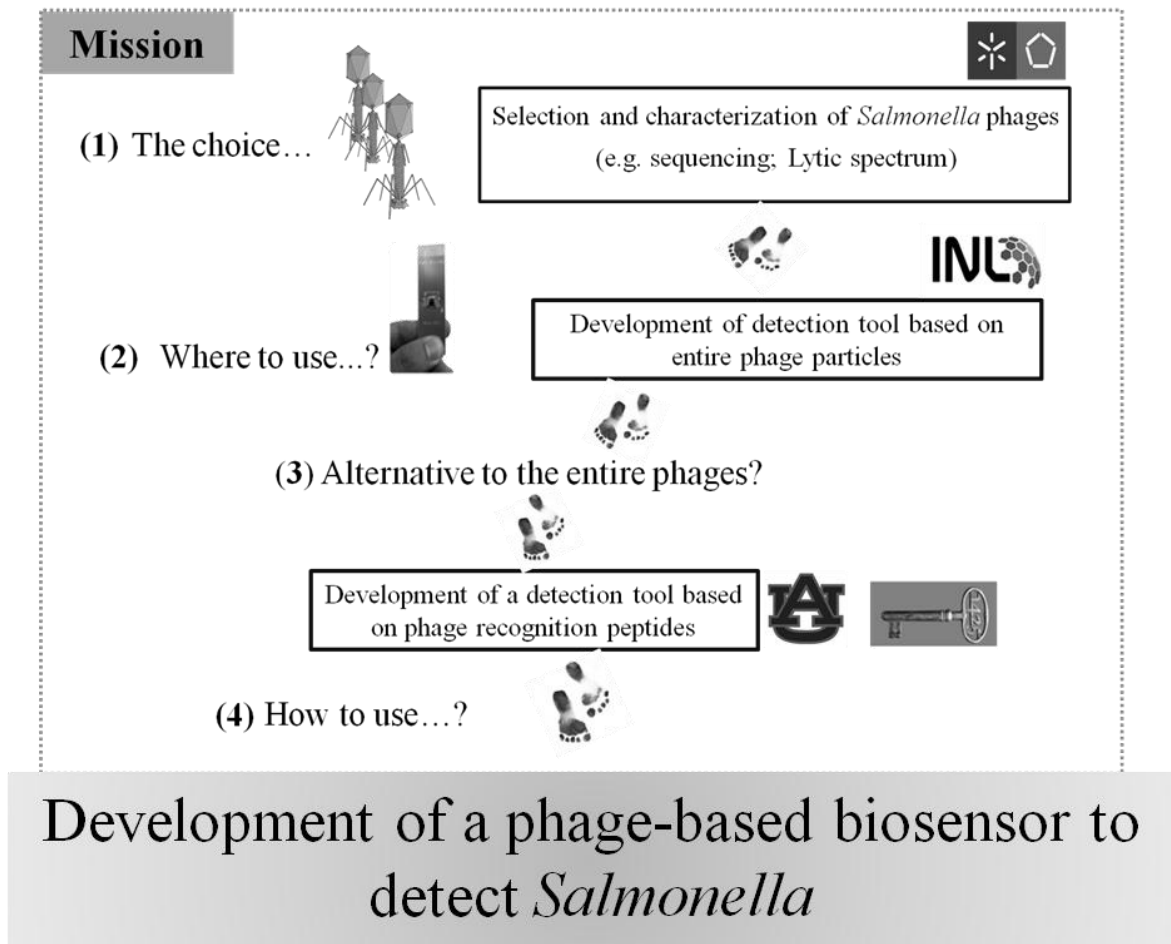


# Scope of the thesis

Problems related with *Salmonella* have generated a high social and economic impact worldwide. The difficulties that come with controlling this microorganism in the food chain are enormous and the necessity to combine a control program with an excellent detection system is an ambitious goal to achieve. Several detection technologies have emerged, but none is able to fulfill all requirements: the perfect detection system should be rapid, sensitive, specific, accurate and inexpensive and should contain all these features in "one package". I would risk to say that ideally, an excellent detection system is a small device that we take from our pocket and tells us, in a fast and accurate manner, if what we are eating is safe or not. The work described in this thesis aimed at developing a detection device for *Salmonella* taking in mind the ideal characteristics of an excellent detection system. It was based on this goal that our interest and motivation focused on a highly specific entity that could serve as a recognition tool: Bacteriophages. Bacteriophages (phages) are viruses that specifically recognize and infect bacteria. Phage's specificity and stability combined with their low production costs are features that can compete with many biological elements (e.g. antibodies). The idea was to use a lytic phage that specifically recognizes a very broad range of *Salmonella* strains, combined with a portable magnetoresistive bio-analytical device to generate a phage-based biosensor and explore its potential on the detection of *Salmonella*. Many challenges have to be faced when developing this detection tool, and many questions were formulated at the beginning of the work, helping us to accomplish each step/task. Questions as: *How can we benefit from phages as a detection agent? Will the phage preserve its excellent feature as specificity when immobilized on a sensor surface? When we only intend to have the recognition part active and available, how will we circumvent structural aspects? Can we use phage derivatives as a detection tool? Can phages distinguish cell viability?*

# Structure of the thesis

A scheme simplifying the main steps that built this thesis and helped to "fulfill" the proposed objective is shown in Figure 0:1:1.



**Figure 0:1:1:** Informal proposed approach.

This dissertation was built through a multidisciplinary approach, joining knowledge of different fields such as physics, electronics, virology and molecular biology. The work in this thesis was made possible by the scientific collaboration of the Centre of Biological Engineering, University of Minho (Portugal) with several other Laboratories: (1) Laboratory of Gene Technology, Katholieke Universiteit Leuven (Belgium) where tasks such as sequencing, cloning and protein expression were carried out; (2) Department of Pathobiology, Auburn University (USA) where the "nanophages" interface was explored for detection systems; (3) Materials Research and Education Center, Wilmore Labs, Auburn University (USA) where

magnetoelastic biosensor was used to validate that nanophage interface and (4) The International Iberian Nanotechnology Laboratory (INL, Braga), where a magnetoresistive phage-based biosensor for *Salmonella* viability assessment was developed. Besides these collaborations other laboratories had a smaller, but important contribution, like the Pharmacy Department (Auburn, USA), ICVS (UM, Braga), INESC-MN (Lisboa) and IST (Lisboa).

This thesis describes the development of a phage-based biosensor to detect *Salmonella* and is structured in the following five chapters.

**Chapter I** contains the background information of the thesis subject, covering the main concepts, i.e. *Salmonella*, bacteriophages, biosensors, the current methods used for *Salmonella* detection and the advances in food testing using phage-based pathogen biosensors.

**Chapter II** describes the characterization of three promising *Salmonella* phages based on their lytic spectrum. The results presented in this chapter led to the selection of a phage with a broad lytic spectrum and with the ability to infect and replicate in a nonpathogenic host. This phage, which was further used for the construction of the biosensor, is a safe phage product that can easily be approved for commercial applications. The sequences provided in this step opened other possibilities, regarding the use of phage derivatives products as biorecognition elements.

**Chapter III** reports the development of a magnetoresistive phage-based biosensor. The developed sensor has the ability to specifically recognize *Salmonella* and a great potential to detect viable but non-culturable bacterial cells.

**Chapter IV** focuses on the problems related with phage structure when immobilized on the sensor surface and how we can circumvent this limitation. Two different phages were evaluated on this step, namely lytic and filamentous phages. The phage tail fiber proteins of the lytic phages were used for specific detection and control of *Salmonella enterica*. Some preliminary tests of the binding affinity of the tail fiber proteins to the target (*Salmonella*) are shown. Regarding the filamentous phages, we developed a novel "nano-phages" interface for

detection systems. Our findings suggested that this new approach may be an alternative to use and replace the parental phage.

**Chapter V** summarizes the general conclusions of this thesis and show how this work contributed to the knowledge on phage-based biosensors. In addition, future perspectives and directions will be given.

## Scientific Contributions

This section refers the publications and posters in the scope of this project.

### Articles in scientific journals:

**Fernandes E.**, Martins V.C., Carvalho C.M., Nobrega C., Cardoso F., Cardoso S., Dias T., Dias J., Deng D., Kluskens L.D., Freitas P.P. and Azeredo J. *Pathogen cells viability assessment through a bacteriophage detection tool: case study of PVP-SE1 Salmonella phage* - In preparation for submission.

Ng A., Espiña B., **Fernandes E.**, Petrovykh D. *DTSSP and SPDP Bifunctional Linkers on Gold* - In preparation for submission.

Santos, S., **Fernandes, E.**; Carvalho, C.M.; Sillankorva, S.; Krylov, V.N., Pleteneva, E.A.; Shaburova, O.V.; Nicolau, A.; Ferreira, E.C.; Azeredo, J. *Selection and characterization of a multivalent Salmonella phage and its production in a nonpathogenic Escherichia coli strain*. Applied and Environmental Microbiology 76(21), 7338-7342, 2010.

### Patents:

Provisional Patent Application entitled "*Pathogen cells viability assessment through a bacteriophage detection tool: case study of PVP-SE1 Salmonella*" to be submitted.

Patent application PPI46027-12, entitled "*Phage Tail Proteins for Specific Detection and Control of Salmonella Enterica*". Inventor(s): Azeredo, J., Kluskens, L., Santos, S., Silva, S., **Fernandes, E.**, Lavigne, R., Vandersteegen, K., Cornelissen, A., August 2012

Provisional Patent Application No.61583850 entitled "*Phage Fusion Proteins as Interface for Detection Systems*". Inventor(s):Valery A. Petrenko, Deepa Bedi, **Elisabete R. Fernandes**, Vasily A. Petrenko Jr, Bryan Chin, Leon D. Kluskens, Joana Azeredo.

### **Abstracts in proceedings of international conferences:**

Carvalho, C., Romão V., **Fernandes E.**, Azeredo J., Rivas J., Freitas P., *Specific detection of Campylobacter jejuni and Campylobacter coli using lytic phages*. Abstract book of the International Conference on Nanosciences & Nanotechnologies 2012, 3-6 July 2012, Thessaloniki, Greece.

**Fernandes, E.**, Bedi, D., Li, S., Ebner, A., Leitner, M., Hinterdorfer, P., Kluskens, L., Azeredo, J., Chin, B., Petrenko, V., *Model Interface for Pathogens Detection Systems*, Abstract book of the MicroBiotec 2011, Braga, p. 469.

**Fernandes, E.**, Bedi, D., Li, S., Ebner, A., Leitner, M., Hinterdorfer, P., Kluskens, L., Azeredo, J., Chin, B., Petrenko, V., *Novel "Nano-Phage" Interfaces for Wireless Biosensors*. Abstract book of the Nanotech Conference and Expo 2011, June 13-16<sup>th</sup>, Boston, MA, U.S.A.

**Fernandes, E.**, Santos, Sílvia R.B., Kluskens, L. D., Azeredo, J., *Selection of a broad lytic spectrum phage for Salmonella detection*. Abstract Book of the BioMicroworld Conference 2009, December 2-4th, 2009 Lisbon, Portugal.





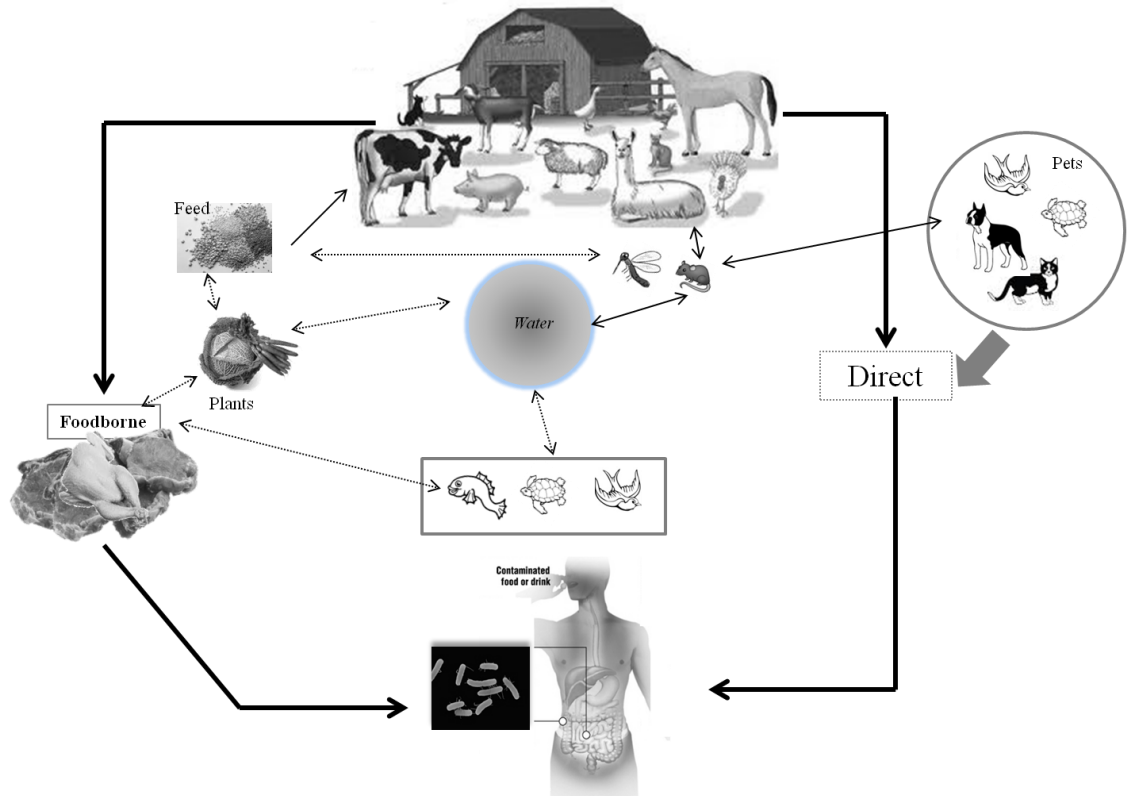
# Chapter 1

## General Introduction

Food is essential for health and well-being, although when contaminated, may cause serious problems with high social and economic impact worldwide. Foodborne illness forces a sequence of adverse events, i.e. people become ill, the food industry is damaged, and the regulatory and public health sectors are affected. Despite the great effort to combat this problem, the World Health Organization (WHO) estimates that annually in industrialized countries approximately 30% of the population passes through a disease of this nature [1]. Specific control programs to prevent and control foodborne diseases have been implemented as strategies to reduce the outbreak numbers (e.g. control program "from farm to fork") [2], but it has not been enough. Therefore it has become urgent to find rapid and accurate detection methods combined with high-quality control programs. The traditional culture methods, immunological and polymerase chain reaction based methods take hours or days to obtain results [3]. In addition, problems related with false results still occur. Biosensors appear as a promising detection tool in this field and have captured the attention of many researchers that explored this technology for many types of bacteria. This introduction will focus on the common foodborne pathogen, *Salmonella*, and on conventional and emergent detection methods.

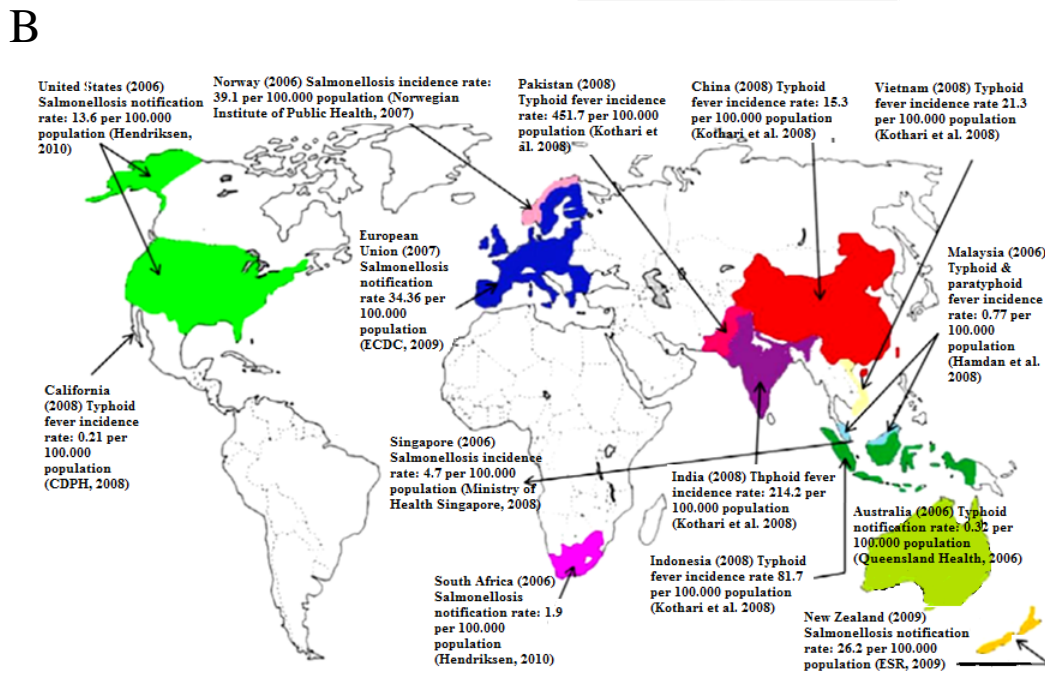
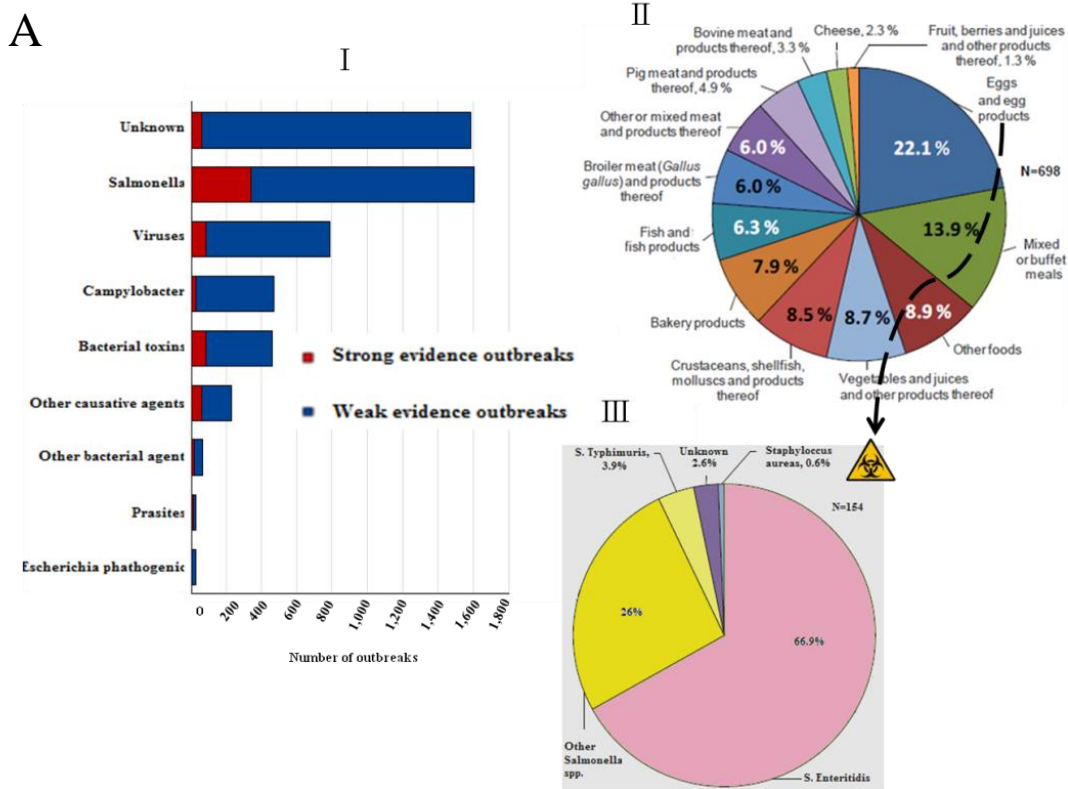
### 1.1. Foodborne Illness Caused by *Salmonella*

A foodborne illness is a disease caused by agents (e.g. bacteria, viruses) in food which, when ingested, originates severe human infections. Several types of food can be contaminated, but commonly infected are foods of animal origin, such as meat, fish and poultry [4]. Other food products from non-animal origin, like fruits, vegetables and water can also be contaminated and may lead to an infectious disease. Salmonellosis (food poisoning caused by the *Salmonella* bacterium) has been an occurring problem in industrialized countries. *Salmonella* bacterium is a gram-negative rod-shaped bacilli (typically 0.5  $\mu\text{m}$  by 1-3  $\mu\text{m}$ ) commonly found in intestinal track of domestic and wild animals [5]. There are two species of *Salmonella*: *Salmonella enterica* and *Salmonella bongori*. *Salmonella enterica* comprises six subspecies: *S. enterica* (subspecies that causes more *Salmonella* infections in humans), *S. salamae*, *S. arizonae*, *S. diarizonae*, *S. houtenae* and *S. indica*. There are about 2,500 serovars and most of them are introduced into human populations by contaminated foods, soil, water or animal contact [6]. Immunocompromised people, pregnant women, infants, and the elderly are the groups more susceptible to this zoonotic bacteria [7]. The common symptoms of salmonellosis are fever, diarrhea, and abdominal cramps and severe infections require hospitalization. *Salmonella* can spread easily from animals to humans by the consumption of food as mentioned previously and by inadequately cooked or poorly handled food. Direct contact with domestic animals is another infection line that can cause salmonellosis [2]. A summary of the direct or indirect possible transmission vehicles of *Salmonella* to humans is illustrated in Figure 1:1.



**Figure 1:1:** Possible vehicles of *Salmonella* transmission which can cause non-typhoidal Salmonellosis in humans (adapted from Hilbert et. al.[2]).

A complete depiction of salmonellosis occurrence is difficult to provide, since in general only large outbreaks are studied and reported. The European Food Safety Authority (EFSA) considered *Salmonella* as the bacterium responsible for most reported cases of foodborne diseases in the European Union (EU) in 2010 (Figure 1:2 - A). The most common serovars were *S. Enteritidis* and *S. Typhimurium* (45.0 % and 22.4 %, respectively) [8]. EFSA estimates that 100,000 cases of salmonellosis occur each year in Europe [9], predominantly transmitted by eggs, chicken and pork meat [10]. Eggs were in 2010 the main vehicle of transmission (43.7%), followed by bakery products (14.4 %) and buffet meals (12.3%) (Figure 1:2–A). However, the problem is not centred on Europe but also extends to U.S. (1.2 million illnesses/year) and other parts of the world (e.g. China, India, Australia) as shown in Figure 1:2 – B [3] [4].



**Figure 1:2:** Image A: Distribution of food-borne outbreaks with weak and strong evidence (excluding strong evidence on waterborne outbreaks) per causative agent (I); by food vehicle (II) and for causative agent of eggs and egg products contamination (III) in the EU, 2010 [8]. Image B: Some reported cases of enteric fever and salmonellosis worldwide [11].

The numbers reported each year have gained special importance worldwide and programs to control and protect the human health have been implemented. Since 2007 EU States Members were obliged to implement *Salmonella* control programs in breeding flocks of *Gallus gallus* in accordance with Regulation (EC) No 1237/2007 [13]. According to EFSA, the decrease of salmonellosis from that time to 2010 was mainly due to the control program implemented in poultry populations [8]. Some countries joined their own control programs with the international safety program recognized worldwide, the Hazard Analysis Critical Control Points (HACCP) system. Such an integration of control programs occurred in Canada, where Canadian chicken farmers combined good production practices with HACCP rules into the chicken production. In this particular case, farmers now follow narrow barn cleaning procedures and the farm water supplies are analyzed annually [14]. HACCP is a system that was implemented to guarantee the safety in all stages of the commercial food process, i.e. from ingredients, handling procedures to all activities that involve food components. The critical control points (CCPs) are the stages where the hazard is high and at which urgent proceedings should be developed to control the process. The CCPs are defined according to each case. HACCP have integrated the national food safety legislation in many countries, although different continents have a different interpretation of this system [15]. Even when using these plans to employ and control the production practices on the food chain, the verification of each HACCP stage is dependent on rapid tests that avoid the alarm or suspicion of a contamination. The detection of *Salmonella* is still a focal point in standard culture methods, which are time consuming (taking 3-5 days) and require expert skills. Therefore, the concern of finding new solutions and revolutionary technologies for an early detection of *Salmonella* has been installed in industrialized countries. The idea is to combine an excellent control program with a rapid and accurate detection system that consequently decreases the social and economic impact of foodborne outbreaks worldwide.

# 1.2. Detection of Foodborne Pathogens: Emerging Technologies

## 1.2.1. Conventional Culture Methods

The method described in ISO 6579:2002 is an example of a conventional pathogens detection technique applied to products consumed by humans, feed for animals and environment samples collected from the areas of food production and handling. The method consists of four stages: *i*) pre-enrichment in non-selective liquid medium; *ii*) enrichment in selective liquid medium; *iii*) plating out; *iv*) identification and the confirmation of identity [16]. Standard methods take three to five days to obtain a result, in general 3 days to provide a negative result and 5 days to confirm a positive one [3]. The disadvantages of the method described in ISO 6579:2002 are the time needed to obtain results and the possibility of false negatives due the dormancy state of bacteria. *Salmonella* and *E.coli* are some examples of bacteria that, under stress environment conditions, can enter a physiological state in which they become non-culturable even when they are still alive [17]. When the bacteria enter this state, they are commonly called: "Viable but nonculturable" (VBNC). The metabolic cell activity is lower and only under optimal grow conditions they can turn culturable again, renewing the ability to cause infection. Chemical and environmental factors are the reasons behind this cell state. Temperatures out of their range growth, lack of nutrients, elevated or lowered osmotic concentrations, effects caused by bactericidal agents (e.g. chlorination of wastewater) are some examples of stress conditions that induce the cells to enter the VBNC state. Therefore, the use of the standard culture can lead to an underestimation of pathogen numbers and the accuracy stays far from what is expected. Other methods have arisen to complement or substitute the traditional culture methodologies to produce rapid and sensitive detection technologies. Immunological and molecular detection methods are some of the alternatives which can decrease the time assay.

### 1.2.2. Immunology-based Methods

Methods involving antigen–antibody interaction are widely used for pathogens detection [11, 12]. The specificity and sensitivity is dependent on the choice of antibody (monoclonal or polyclonal). Radioimmunoassay (RI), the enzyme-linked immunosorbent assay (ELISA), the enzyme-linked fluorescent assay (ELFA), immunomagnetic separation (IMS) assay, and lateral flow immunoassay (LFI) are some examples of immunoassays [20]. Nowadays a variety of commercial products exists for *Salmonella* detection based on this technique. Currently, some commercially available immunoassay kits exist for *Salmonella* detection. VIDAS<sup>®</sup>SLM *Salmonella* assay (BioMérieux), *Salmonella* ELISA (BIO ART.) [20], Tecra Unique<sup>™</sup> *Salmonella* test are some examples. The main disadvantage of these tests is the cross reactivity of antibodies and their shelf-life. An excellent book chapter about the use of "Antibodies and immunoassays for detection of bacterial pathogens" can be found in reference [21], where the reader can find an overview of commercial immunoassay kits for pathogens.

### 1.2.3. Polymerase Chain Reaction (PCR)

PCR was developed by Mullis and colleagues in 1986 [22] and has been widely used for bacteria identification. This technique is based on the DNA amplification of the target of interest in millions of copies, using primers, an enzyme (*Taq* polymerase) in a process involving a set of repeated cycles of heating and cooling. Denaturation is the first step of the process and occurs at 94-98°C allowing the DNA melting and the break of the hydrogen bonds between the two strands DNA. The annealing happens at lower temperatures (50-65°C), allowing the primers to hybridize to the single-stranded DNA template. The extension or elongation step is related to the enzymatic DNA synthesis by DNA polymerase, which occurs at high temperatures. A variety of thermostable DNA polymerases exists, but the first used in PCR was *Taq* polymerase, isolated from the bacterium *Thermus aquaticus* with an optimal temperature around 75-80°C. The PCR reaction is carried out in a thermocycler device. Studies including the standard PCR with an enrichment step are also reported. Löfström et al. [23] combined the standard culture method with PCR to detect *Salmonella* in animal feed samples. In this study, the



problem related with the small numbers of *Salmonella* and the presence of feed inhibitors on samples was circumvented by using an enrichment step at 37°C for 18 hr in buffered peptone water (BPW). However, this strategy requires laboratory space, preparation of gel electrophoresis and analysis. PCR as a detection techniques was rapidly followed by other PCR-based applications (real-time, multiplex and reverse transcriptase (RT) PCR) that have all made some improvements over the classical PCR method and are usually based on fluorogenic probes. These methods have the following advantages:

- ▶ Real-time PCR allows to obtain rapid results without laborious manipulations, i.e. the equipment is composed of an optical system that follows the course of reaction in real time without a post-amplification process (e.g. gel electrophoresis) [24].
- ▶ Multiplex PCR has the advantage to detect simultaneously diverse bacterial strains by introducing different primers to amplify DNA regions coding for specific genes of each strain targeted [25].
- ▶ RT-PCR helps to overcome a limitation of both methods above: the difficulties to distinguish viable from non-viable cells [26].

Despite the advantages mentioned above, reduction of time diagnostic and its high throughput character, the PCR-based detection techniques have also some limitations regarding the possibility of sample contamination, lack of standardization, complex interpretation of results, and high cost production [27]. From an industrial point of view PCR can also be expensive and complicated, and requires expert workers. Therefore, the idea of creating a rapid, specific, sensitive, accurate and simple low cost device that allows in situ real-time monitoring has persisted. Recently, the research on pathogen detection has directed its attention to the biosensor field with some promising results.

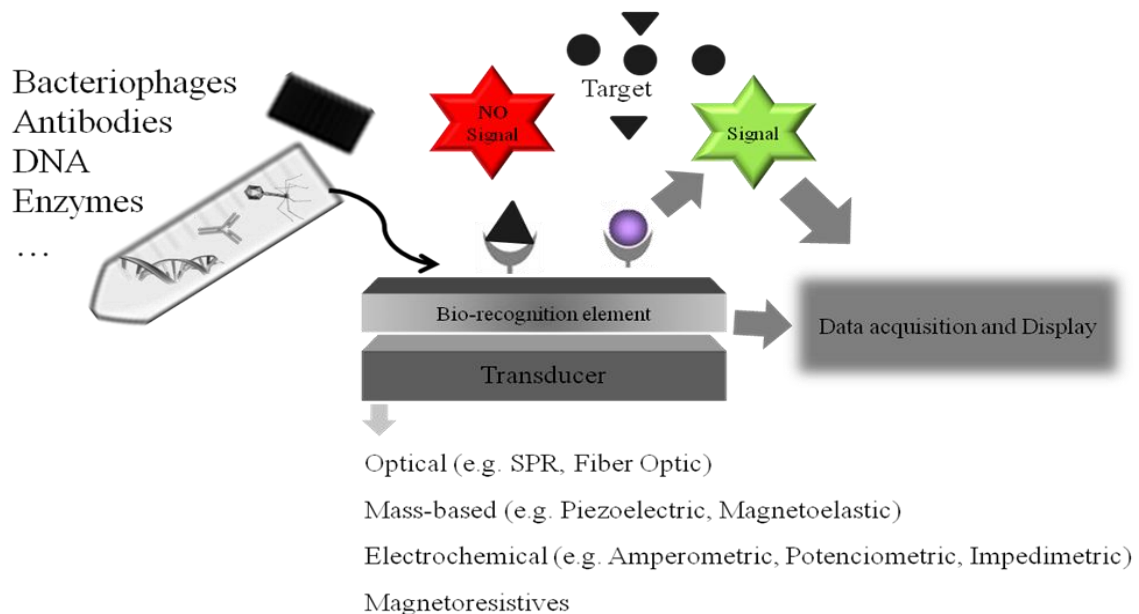
### 1.2.4. Biosensors and Biochips

In the past two decades, we have witnessed a great evolution in the biosensor and biochip field. New technologies have appeared that aim at the development of portable

devices to quickly analyze clinical, industrial and research samples. These systems should unite a set of characteristics that enable the development of an inexpensive and robust device. Requirements as accuracy - leading to low amount of false positive or negative results - , assay time, sensitivity, specificity, robustness, reproducibility and user-friendliness are demanded when the goal is to develop a quality device. Moreover, to prove those qualities the new technology needs to be validated against current standard techniques.

### 1.2.4.1 Biosensors and biochips: a definition

A biosensor, as the word itself indicates, is the combination of two components: a biological and a sensor element. Both parts play an important role in creating a sensitive and specific device. The biological element (e.g. antibodies, enzymes, or bacteriophages) recognizes the target of interest (e.g. bacterium, cancer cell) and, as soon as the identification happens, the sensor element will convert a chemical or physical change into an electrical signal. The output from the transducer is then amplified, processed and displayed/saved as a measurable effect. (Figure 1:3).



**Figure 1:3:** Schematic diagram of a biosensor, showing the possible biological elements (e.g. bacteriophages, DNA) and transducer platforms that can be used to develop a biosensor.

## **Chapter 1. General Introduction**

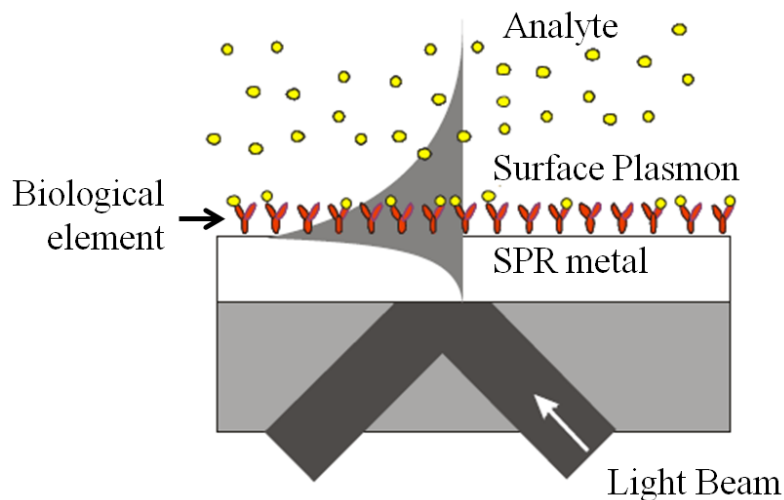
---

Biochips are the new generation of biosensors and consist of an array of single biosensors that can be individually monitored. They are often used to detect multiple targets. Biosensors/biochips can be classified based on their biological or transducer elements. There are a variety of transducers, although the ones commonly used in studies of foodborne pathogens detection are the optical, electrochemical and mass-based transducers. A brief introduction about the transduction methods and biological elements will be given in this chapter. Phages as biological element and magnetoresistive and magnetoelastic biosensors will be explained in more detail, as they were the basis of this work.

### **1.2.4.2 Transducers**

#### **1.2.4.2.1 Optical-based Biosensors**

Optical biosensors are highly sought, mainly due the inherent qualities of these systems, including high sensitivity and possible direct, real-time and label-free detection of many chemical and biological components. The concept behind the label-free optical biosensors is based on the interaction of light with the adsorbed biological elements, i.e. the light is reflected on the biosensor surface and affected by the presence of the biomolecules. The light event is measured directly based on changes in the properties of the light used (e.g., intensity, wavelength, polarization, and phase). Surface plasmon resonance (SPR) and the fluorescence are the most commonly used techniques in optical field and used in studies related with pathogens detection mainly due their sensitivity. SPR determines the presence of the target by measuring the changes in the local refractive indices caused by the alterations in the proximity of a thin film metal surface (usually gold) (Figure 1:4).



**Figure 1:4:** Illustration of the concept of SPR biosensing [28], where analyte molecules in a liquid sample bind to the biological element immobilized on the sensor surface. When the bind occurs an increase in the refractive index at the sensor surface happens and is optically measured.

Gold is widely used as surface, especially due to its oxidation stability and inertness, which is a wanted characteristic when working with biological samples [29]. Zordan et. al. [30] reported the combination of the two optical techniques mentioned above. They were able to detect *E. coli* O157:H7 combining SPR with fluorescence and suggested a "portable cytometry" and a competitive technology for the food processing industry. Moreover, they suggested further experiments using this system to image a biosensor array to perform multiplexed pathogen detection. The interest in commercializing SPR products has increased and nowadays we can have access to some commercial SPR-based biosensors for pathogens detection in food and water (e.g. SR 7000, BIAcore 3000, BIAcore J, Bios-1, SPREETA device and so on.) [31]. However, these biosensors also came with some limitations, such as the volume limits of the system. It requires small volumes and normally a pre-enrichment step to concentrate the low numbers of pathogens present on samples. Also, SPR-transducers are sensitive to room temperature drift and they are expensive. Regarding the detection limits they also need improvements due to the bacterial analytes and their size. As the sensitivity of SPR sensors decreases with an increasing distance from the surface of metal supporting (a Surface Plasmon), only a small part of the bacterium captured at the surface can contribute to a response of the SPR sensor [28]. Examples of optical techniques used for foodborne

## Chapter 1. General Introduction

pathogens are shown in Table 1:1, which information was acquired from an excellent review paper of Velusamy et al. [32].

**Table 1:1:** Examples of optical techniques applied on studies related with foodborne pathogens (information extracted and adapted from [32])

Optical techniques	Detected pathogen	Limit of detection	Assay time
<b>Optic interferometer</b>	<i>S. typhimurium</i>	10 <sup>5</sup> CFU/ml	12 h
<b>Automated optical method</b>	<i>Salmonella spp.</i> and <i>L.monocytogenes</i>	10–50 cells each in 25 g sample	24 h
<b>Surface-enhanced infrared absorption spectroscopy</b>	<i>Salmonella</i>		
<b>Imaging ellipsometry (IE)</b>	<i>E. coli</i> O157:H7, <i>S. typhimurium</i> ,	10 <sup>3</sup> to 10 <sup>7</sup> CFU/ml	
<b>Fluorescence microscopy</b>	<i>E. coli</i> O157:H7, <i>S. typhimurium</i>	10 <sup>2</sup> CFU/ml	
<b>Chemiluminescent immunoassay</b>	<i>E. coli</i> O157:H7, <i>Y. enterocolitica</i> , <i>S. typhimurium</i> , and <i>L. monocytogenes</i>	10 <sup>4</sup> to 10 <sup>5</sup> CFU/ml (for all bacterial Species)	
<b>Bacteriophage-based bioluminescence</b>	<i>Salmonella</i>	10 <sup>8</sup> CFU/ml	1–3 h

### 1.2.4.2.2 Electrochemical Biosensors

Since the introduction of glucose enzyme electrodes by Clark and Lyons electrochemical biosensors have been extensively studied for different health purposes [33]. Their revolutionary discovery proved to be an excellent tool for the diabetic community and efforts to improve it have been made, with success. Now we have in our hands an amperometric needle-type glucose biosensor that has increased the patient's life quality.

Electrochemical biosensors can be classified into four subclasses, namely as amperometer, potentiometer, impedimeter and conductometer and are based on the parameters current, potential, impedance and conductance, respectively [34]. Their low cost and the possibility to construct a portable device joined with their ability to work with turbid samples are their main advantages. In contrast, their selectivity and sensitiv-

ity are their weakest points when compared with optical biosensors. In order to circumvent some detection difficulties, they appear combined with other types of biosensors. The amperometric-based biosensors are most commonly studied to detect foodborne pathogens. Examples of some pathogens detected by electrochemical biosensors are presented in Table 1:2.

**Table 1:2:** Examples of electrochemical biosensors for foodborne pathogens [32].

Mode of detection	Detected pathogen	Limit of detection (CFU/ml)	Assay time
Amperometric	<i>S. typhimurium</i>	$1.09 \times 10^3$	2.5 h
Conductometric	<i>E. coli O157:H7</i> and <i>Salmonella spp.</i>	$7.9 \times 10^1$	10 min
Impedimetric	<i>S. typhimurium</i>	$5.4 \times 10^5$	2.2 h

#### 1.2.4.2.3 Mass-based Biosensors

Piezoelectric and magnetoelastic (another format of acoustic wave devices) biosensors are examples of mass-sensitive sensors, which means that their detection principle is based on small mass changes. The quartz crystal microbalance (QCM) and acoustic wave biosensors (SAW) are piezoelectric devices with a operate principle based on an oscillating crystal that resonates at a fundamental frequency.

##### 1.2.4.2.3.1 Magnetoelastic (ME) Sensor

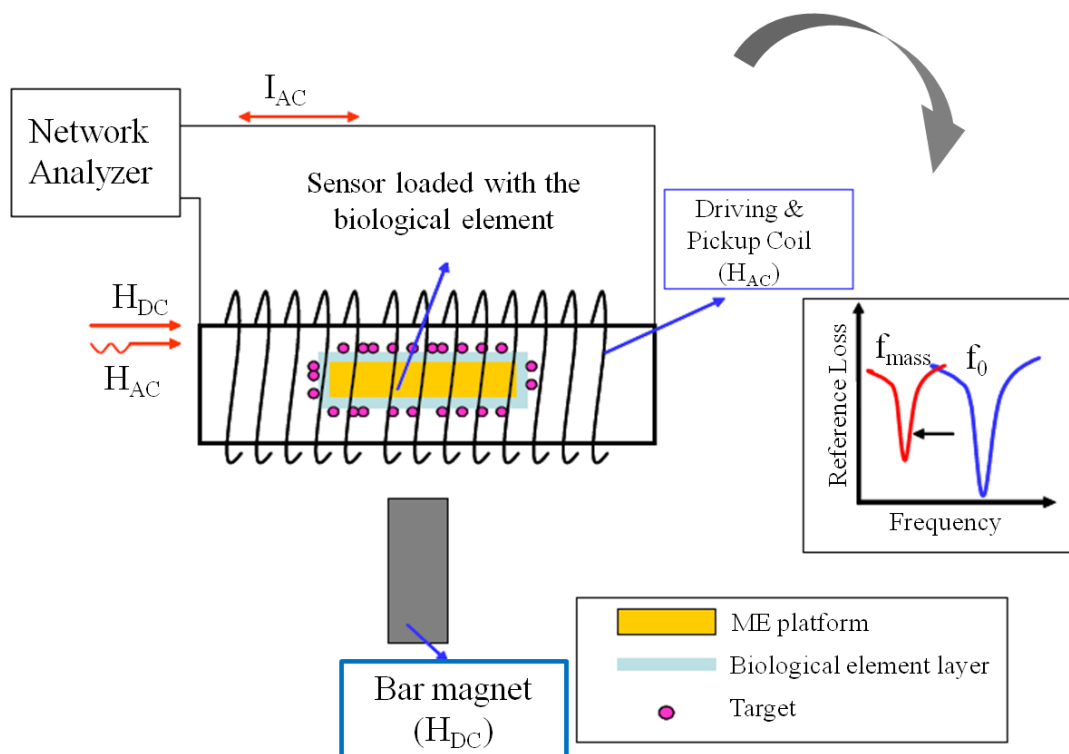
The working principle of ME sensors is based on magnetostriction properties, in which material changes in dimension due the application of a magnetic field. The magnetic energy is converted into mechanical oscillations by applying a time-varying magnetic field. The resonance frequency and amplitude of such oscillations are dependent on the sensor material and also on the surrounding medium that acts as a damping force to the sensor. The characteristic fundamental resonance frequency (equation 1) of these oscillations is dependent on the physical properties, such as elastic modulus ( $E$ ), density ( $\rho$ ), Poisson's ratio ( $\nu$ ) and the dimensions of the material ( $L$ ).

$$f_0 = \frac{1}{2L} \sqrt{\frac{E}{\rho(1-\nu)}} \quad (\text{eq.1})$$

The resonance frequency is dependent on geometry as well as mass and when an additional mass is loaded on the sensor surface, a shift in the resonance frequency ( $\Delta f$ ) occurs (equation 2) [10]:

$$\Delta f = -\frac{f_0 \Delta m}{2M} \quad (\text{eq. 2})$$

The  $\Delta f$  is the change in resonance frequency,  $\Delta m$  is the change in the sensor's mass due to the mass attached over the sensor and  $M$  is the original mass of the sensor. The negative signal ( $-$ ) is due to the shift of the resonance frequency to lower values as a consequence of the increase mass loaded over the sensor. The setup of a ME biosensor is presented in Figure 1:5. Further information of ME sensors is described by Grimes et al. and Johnson et al. [35], [36]).



**Figure 1:5:** Setup for ME biosensors measurement (adapted from [37]), showing the elements involved on the process, namely the network analyzer, ME biosensor and a bar magnet that will creates a DC (direct current) magnetic field.

ME materials are iron-based that typically include iron, nickel, molybdenum and boron (e.g. Metglas alloy 2826 MB - Fe<sub>45</sub>Ni<sub>45</sub>Mo<sub>7</sub>B<sub>3</sub>). The sensor is coated with gold to prevent corrosion and to turn the surface biocompatible. After the pre-coating and annealing [37], the ME sensor is ready to be prepared. The biological element (e.g. antibody, bacteriophage) that will recognize the target of interest is immobilized on the sensor surface by different strategies (e.g. physical or chemical immobilization). Then, the fundamental resonance frequency ( $f_0$ ) is measured and considered as the control value (i.e. value before the exposure of ME biosensor to the target). When the ME biosensor is "read", an AC- and DC-biasing magnetic field is applied to amplify the signal. After measuring the  $f_0$ , the ME biosensor is exposed to the solution containing the target and the binding occurs (biological element + target). The mass increases over the sensor and consequently the resonance frequency decreases. This system can be performed in "air" or using a flow system. The first method uses the ME biosensor dried in air following the contact with the target and washing procedures. The second method is carried out using a flow system composed by a peristaltic pump, a target analyte container, a flush out container and the measurement chamber (capillary tube inside the ME sensor).

ME biosensors have been studied for pathogen detection as well as for homeland security (e.g. *B. anthracis* - possible bioterrorism agent) [38–41]. Compared with piezoelectric devices, the ME sensors are more simple and cheaper, allowing their use in a disposable manner. An excellent advantage is their wireless characteristic. This technology offers real-time detection in air or in liquid without the need of direct contact between the sensor and the measurement device, a feature that can compete with many techniques. The limitation is their sensitivity, which can be circumvented by decreasing the sensor size [36].

#### 1.2.4.2.4 Magnetoresistive Sensors

The massive research in spintronics has given rise to a new class of biosensors [42]. In such devices the transducers are magnetoresistive sensors (MR), which presently find their major application in the data storage market, as read heads in hard disk drives, but are quickly expanding to the biosensing field. Due to the advantage of being compatible with silicon-integrated circuit fabrication technology it originates compact chips com-



prising single or multiple sensors along with the required electrical circuitry. Additional valuable assets are related to high sensitivity, low background, tunable dynamic range, fast performance, scalability and low production costs [43–46]. In a standard MR chip-based bioassay, a biorecognition element immobilized over the sensor is used to interrogate an unknown sample potentially containing a target molecule of interest (e.g. DNA strand, protein, cell antigen, toxin, etc), labeled with a magnetic particle. Whenever there is recognition between the target and its probe, a biomolecular event occurs. After washing, the recognized targets stay over the sensor while the unbound molecules are washed out. Upon application of an external magnetic field, the magnetic labels attached to the bound molecules will create a fringe field, which is further detected by the MR sensor. The discrete quantification of magnetic entities can be related to the number of molecular recognition events, which results in a quantitative analytical mode, overcoming the “yes or no” basic type of answer presented by many technologies. Moreover, the magnetic particle when associated to the target molecule offers a number of advantages, such as: *i*) target concentration from the native sample into a smaller volume of a different buffer solution, *ii*) on-chip active transportation and *iii*) site-focusing of the magnetically-labeled molecules [47].

Additionally, the combination of these MR biochips to electronic [48] and microfluidic platforms [49], may enable sample position control, temperature control, detection signal acquisition and processing, converting a bulky and complex analytical apparatus into a practical lab-on-a-chip device [50]. Since the last decade, several MR-based biochips using different types of sensors, such as large giant magnetoresistance (GMR) sensors, spin valve (SV), anisotropic magnetoresistive ring (AMR) sensors and magnetic tunnel junctions (MTJ) have been demonstrated as proof-of-concept systems. Meanwhile, most of these systems have already evolved into a prototype format and are starting to be used in several biological applications [46], [50]. Presently only two main types of MR biochip platforms have been developed, in terms of biorecognition agent in use, and applied to bioanalytical assays; DNA-chips and protein-chips. Generally, the designation of DNA- and protein-chip stands for whether single stranded DNA sequences or antibodies are used as biological probes immobilized over each sensing area, respectively. However, some limitations of these biorecognition agents, such as poor stability, high production costs and cross-reactivity, have set the need for alternatives.

### 1.2.4.3 Biological Elements

Since the first immunoassay used to identify bacterial pathogens [51], biomolecular recognition elements other than antibodies (enzymes, nucleic acids and bacteriophages) have been reported [52–54]. The instability of the biological element can be a disadvantage in a biosensor, thus their choice is an important issue to be considered.

#### 1.2.4.3.1 Enzymes

The attractive use of enzymes on biosensors is emphasized by their specific binding capability and catalytic activity. In biosensors they are used mostly as label instead of recognition elements [55]. The most studied enzyme-based biosensors are commonly glucose biosensors, which utilize the enzyme glucose oxidase. Enzyme-based biosensors are highly selective but their purification is expensive, time-consuming and their activity is limited [56].

#### 1.2.4.3.2 Antibodies

Antibodies can be polyclonal, monoclonal or recombinant, depending on their selective properties and the way that they are synthesized [24]. Recombinant antibodies have been used to improve its specificity and production costs are more reasonable, compared to enzymes [57]. They are used in some conventional immunoassays (as mentioned in point I.2.2 as well as in optic, electrochemical and mass-based biosensors [58–61]). Apart from their advantages, these biological elements are highly fragile and sensitive to harsh changes in environmental conditions [62]. Moreover, more studies using real samples should be done to understand their sensitivity under those conditions.

#### 1.2.4.3.3 Nucleic Acids

Compared with enzymes and antibodies, biosensors that use nucleic acids as biorecognition elements are simple, rapid, inexpensive, stable and can be easily synthesized and regenerated [32]. The use of nucleic acids as an interface in biosensors has

## Chapter 1. General Introduction

---

also been demonstrated by many researchers. Chen *et al.* [63] described a nucleic acid-piezoelectric biosensor for detection of *Escherichia coli* O157:H7, a bacterium that has become a serious cause of foodborne illness. Their study shows that Au nanoparticles, when functionalized with oligonucleotides, allow for the amplification of the signals in frequency change in a QCM biosensor due to the large mass of the nanoparticles compared to DNA targets. It is a strategy that can be used to improve the sensitivity of the technique and without culture enrichment. In a recent publication of Zhang *et al.* [64] an optical transducer (SPR) was created with a specific DNA probe for the invasion gene *invA* of *Salmonella*, allowing the detection of  $10^2$  CFU of *Salmonella* cells in 1 ml sample in approximately in 4.5 h. Even using those platforms their advantages have been highlighted in microarray techniques for the simultaneous detection of foodborne pathogens [65]. The only concern on their use as a probe is the possibility of damages on DNA due external factors that can impede the detection accuracy.

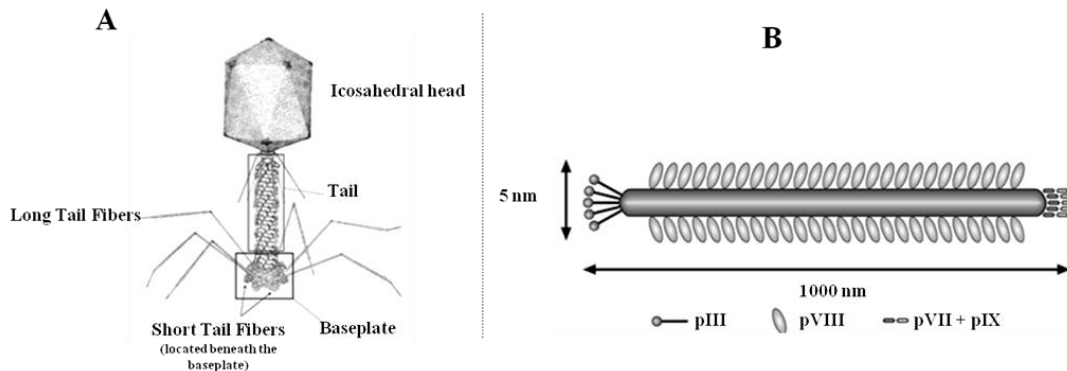
### 1.2.4.3.4 Bacteriophages

Bacteriophages or simply phages are the most ubiquitous molecules on Earth. They are viruses that infect bacteria and possess an excellent feature: specificity. The first official report about the phages existence was published by Frederick Twort in 1915 [66]. Since their discovery by this British bacteriologist, many researchers have been exploring phages for different applications [67][68]. These viruses can be easily isolated from different sources (e.g. faecal samples, sea, soil, raw domestic wastewater, sewage and treated effluents) and are stable in diverse harsh environment conditions.

#### 1.2.4.3.4.1 Phage Structure

Morphologically, all phages are composed by a protein coat, the capsid (usually referred to as 'head') which can vary in size and shape (hexagonal and filaments form or complex structures). The capsid is built by multiple copies of proteins and protects the genetic material of phage (single or double stranded DNA or RNA). The majority of phages are *Caudoviridae* and their morphology is similar to the phage showed in Figure 1:6:A. These phages have a tail attached to the capsid, which can be contractile or not. The tail is a hollow tube that allows the passage of the nucleic acid to the cell and con-

tains tail fibers that are responsible for the recognition of bacteria. An example of a tailed phage is the T4 phage (one of the largest phages) in which 25 kbp of its genome is dedicated to the tail assembly. Phage T4 at the end of its tail has a base plate and fibers [69]. However, it should be noted that not all phages have base plates and fibers. The structure of T4 and a filamentous phage is illustrated in Figure 1:6.



**Figure 1:6:** A: Scheme of T4 phage [70].B: Structure of a typical filamentous phage virion [71].

The Figure 1:6:B refers to a filamentous phage (nonlytic virus) which belongs to the family *Inoviridae*. Filamentous phages are flexible rods with approximately 1  $\mu\text{m}$  long and 6 nm in diameter. They are composed of a circular single stranded DNA genome that is enclosed in a tubular capsid that contains major coat protein pVIII and few copies of minor coat proteins at the ends of the virion (pIII, pVI, pVII and pIX) [72].

#### 1.2.4.3.4.2 Classification

The International Committee on Taxonomy of Viruses (ICTV) divides phages in one order, 13 families and a “floating genus” *Salterprovirus*. Until 2006 more than 5500 phages were analyzed using electron microscopy, with the tailed phages being the most predominant (96%) against 3.7% polyhedral, filamentous, or pleomorphic phages [73]. Their classification is based on the nature of the genomic material: single or double stranded DNA and RNA (Table 1:3). *Caudoviridae* comprise the tailed phages with a double stranded DNA and have 50:50 of DNA/protein. Phages from the *Myoviridae* family are morphologically complex, having contractile tails. An excellent example of this family is the T4 phage [69]. The well known lambda ( $\lambda$ ) phage is characterized by a long and flexible tail [74] that belongs to *Siphoviridae* family. P22 phage belongs is

## Chapter 1. General Introduction

---

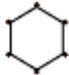

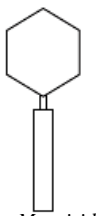
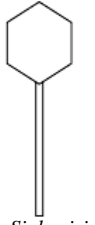
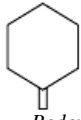

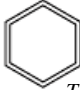






an example of the *Podoviridae* family and their short tail structure is incorporated into a unique five-fold vertex of the icosahedral phage capsid [75]. The other families that are not assigned to an order contain circular single stranded (*Microviridae* and *Inoviridae*) and double stranded (*Fuselloviridae*, *Plasmaviridae* and *Corticoviridae*) DNA. *Rudiviridae*, *Lipothrixviridae* and *Tectiviridae* have linear double stranded DNA. The family *Leviviridae* and *Cystoviridae* are the ones that contain single and double stranded RNA, respectively.

**Table 1:3:** Classification of phages based on their family, structural morphology and genetic material enclosed (adapted from [76]).

Order	Family	Morphology	Nucleic Acid
<b>Caudovirales</b>	<i>Myoviridae</i>	Non-enveloped, contractile tail	Linear dsDNA
	<i>Siphoviridae</i>	Non-enveloped, long non-contractile tail	Linear dsDNA
	<i>Podoviridae</i>	Non-enveloped, short non-contractile tail	Linear dsDNA
<b>Virus families not assigned to an order*</b>	<i>Tectiviridae</i>	Non-enveloped, isometric	Linear dsDNA
	<i>Corticoviridae</i>	Non-enveloped, isometric	Circular dsDNA
	<i>Lipothrixviridae</i>	Enveloped, rod-shaped	Linear dsDNA
	<i>Plasmaviridae</i>	Enveloped, pleomorphic	Circular dsDNA
	<i>Rudiviridae</i>	Non-enveloped, rod-shaped	Linear dsDNA
	<i>Fuselloviridae</i>	Non-enveloped, lemon-shaped	Circular dsDNA
	<i>Inoviridae</i>	Non-enveloped, filamentous	Circular ssDNA
	<i>Microviridae</i>	Non-enveloped, isometric	Circular ssDNA
<i>Leviviridae</i>	Non-enveloped, isometric	Linear ssRNA	
	<i>Cystoviridae</i>	Enveloped, spherical	Segmented dsRNA

# Chapter 1. General Introduction

**Table 1:4:** Shape representation of the major phage groups (adapted from [78]).

Nucleic acid	Shape
ssDNA	 <span data-bbox="1043 394 1158 416"><i>Microviridae</i></span>
	 <span data-bbox="1043 568 1142 591"><i>Inoviridae</i></span>
dsDNA	 <span data-bbox="794 920 887 943"><i>Myoviridae</i></span>  <span data-bbox="916 920 1008 943"><i>Siphoviridae</i></span>  <span data-bbox="1059 920 1152 943"><i>Podoviridae</i></span>
	 <span data-bbox="831 1061 956 1084"><i>Corticoviridae</i></span>  <span data-bbox="1059 1061 1168 1084"><i>Tectiviridae</i></span>
	 <span data-bbox="802 1211 927 1234"><i>Plasmaviridae</i></span>  <span data-bbox="1011 1211 1136 1234"><i>Fuselloviridae</i></span>
	 <span data-bbox="911 1301 1054 1323"><i>Lipothrixviridae</i></span>
	 <span data-bbox="927 1424 1035 1447"><i>Rudoviridae</i></span>
ssRNA	 <span data-bbox="927 1621 1035 1644"><i>Leviviridae</i></span>
dsRNA	 <span data-bbox="927 1816 1051 1839"><i>Cystoviridae</i></span>

Very recently, Abedon [77] demonstrated that it is possible to ascertain phage family by the size of the genome as illustrated in Figure 1:7. According to this classification, *Leviviridae* and *Myoviridae* families are representative of the lowest and highest genome size, respectively.

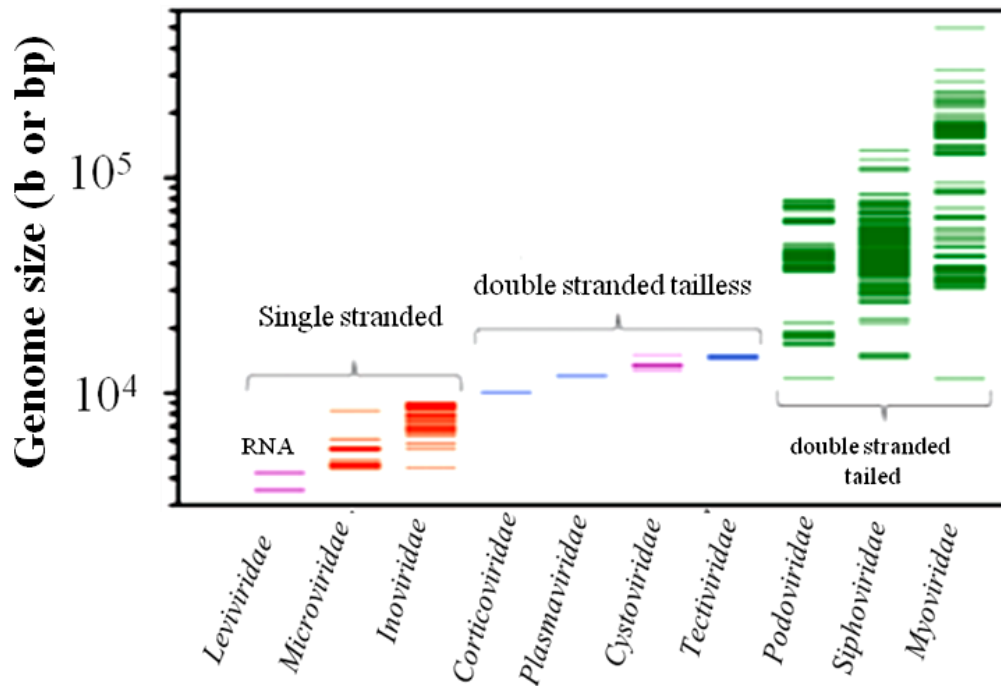


Figure 1:7: Phage morphologies and genome sizes [62]

## Life Cycle

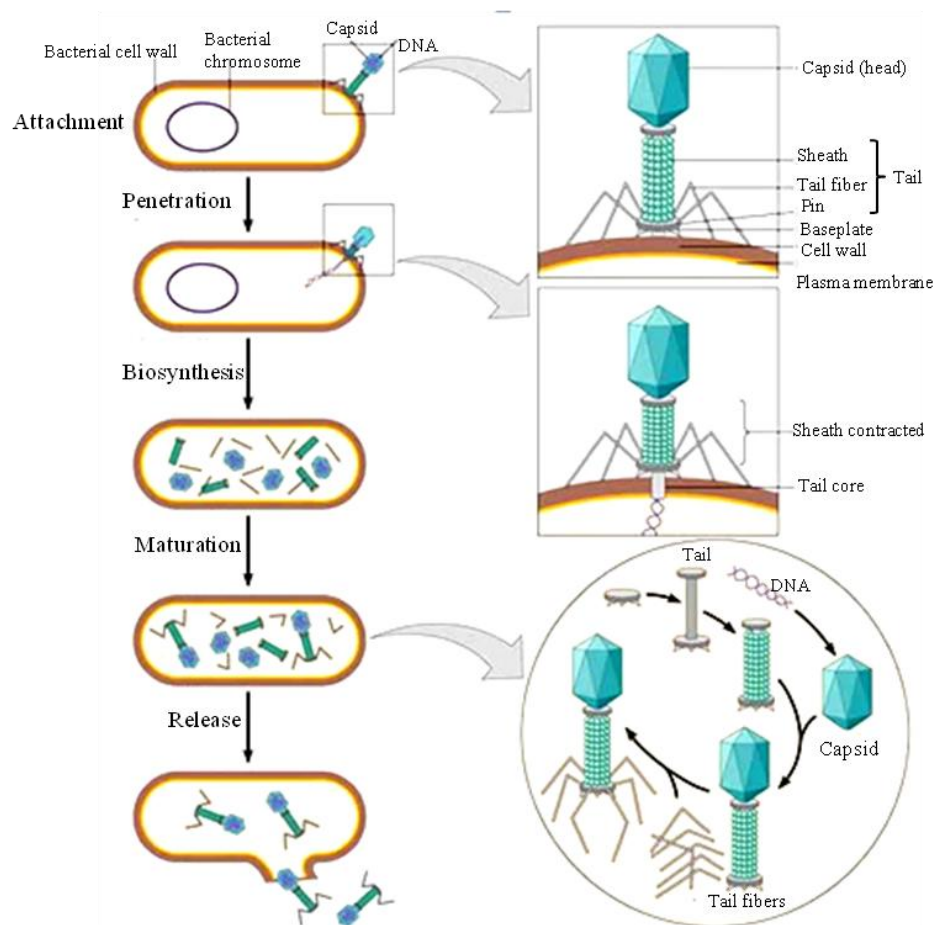
Phages can be differentiated by their life cycle, i.e. by the interaction between phage and host. Phages can absorb, infect and release the bacterium (lytic cycle) or can integrate their DNA into the host's genome after infection (lysogenic cycle).

## Lytic Cycle

Phages with this type of pathway are called lytic or virulent phages. The cycle is divided in different stages: attachment, penetration, biosynthesis, maturation and release. The first interaction between phage and bacteria happens when one or a set of adhesins present on the tail fibers or spikes that recognize the cell wall receptors, allowing phage adsorption. Phage then



penetrates and injects its nucleic acid into the cell, while the capsid and tail will remain outside the cell. After entering into bacterium, an eclipse period starts where no phage particles can be found outside and inside the cell and the viral nucleic acids assume all the activity of the host cell. Inside the host synthesis of the phage components occurs (viral lysozyme, internal proteins and coat proteins), followed by their assembly into mature phage particles. In order to release newly assembled phages, phage produce hydrolytic enzymes (endolysins) that digest the cell wall, resulting in cell lysis.

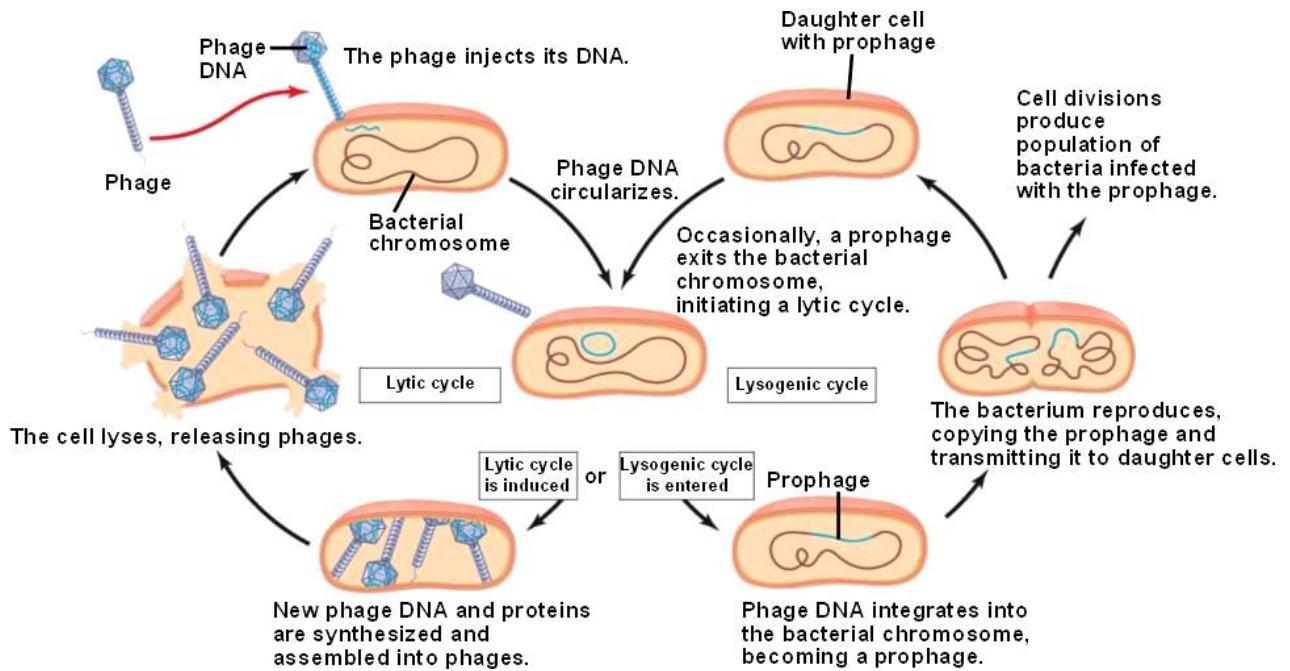


**Figure 1:8:** Illustration of the lytic cycle [79].

### Lysogenic Cycle

Lysogenic or temperate phages can either follow the lytic pathway or enter to the cell without killing the host. The phage DNA is integrated into cell chromosome and replicates along with the host DNA, passing to the daughter cells. At this stage, the virus is called prophage and the

process is known as lysogeny. This process will affect the evolution of the bacterium and contribute to the diversification of the bacterial genome architecture (lysogenic conversion) [80]. The process can confer the cell immunity to the same phage and only stress conditions, like the ultraviolet light, can induce the lytic cycle [81].



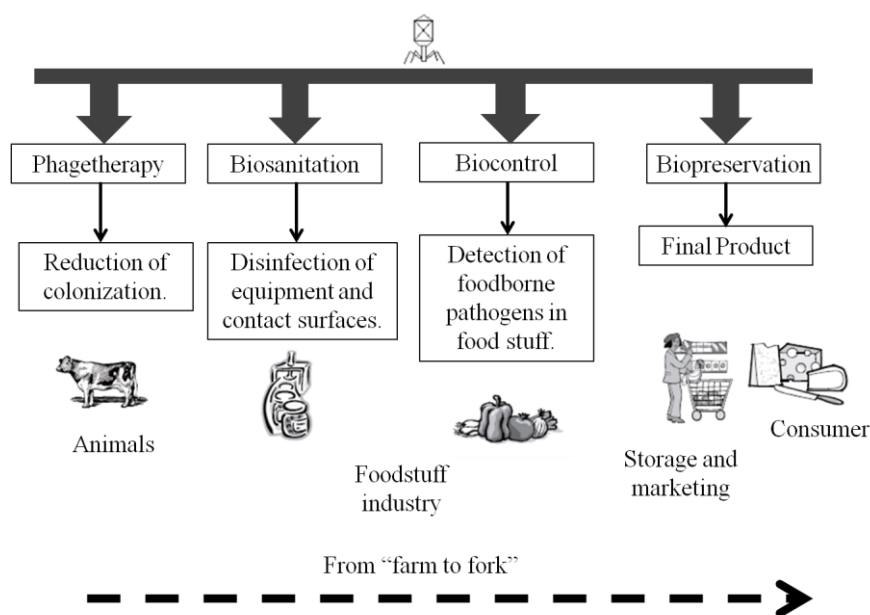
**Figure 1:9:** The lytic and lysogenic cycles of  $\lambda$  (lambda) phage [82].

## Phage Applications

Since the first report on the existence of phages the scientific community has attempted to explore and benefit from this tool, provided by Mother Nature. While discovered before the era of antibiotics, phages were abandoned for some time after the introduction of penicillin. However, the emergence of antibiotic resistance in bacteria has awakened the community and renewed the interest in phages. Many researchers have been exploring the potential of phages either for therapy purposes or as biorecognition probe to use in biosensors. The power of lytic phages lies in their ability to lyse cells and is a characteristic appreciated in phage therapy. As such, they are used in studies for the treatment and prevention of bacterial infectious diseases, such as *Listeria monocytogenes*, *Streptococcus pneumoniae*, *E.coli*, *Salmonella*, *Campylobacter jejuni*, among others [83–87]. Beside the applications in human diseases and the veterinary field, their potential has been recognized in the field of water treatment [88][89] and at

the level of development of phage products for food safety. The commercial **LISTEX™** P100 [90] used for the eradication of *L. monocytogenes* contamination is an example of a phage product that was approved by FDA. The lysogenic cycle of some phages, i.e. lacking the ability to lyse the cell, make them poor candidates for therapy. In contrast, they are a good option when the objective is to use the phages as a recognition element, for instance, as an interface to detect pathogens. Filamentous phages have shown promising results as a biorecognition element on biosensors for pathogens detection and have been explored as a target delivery of drug-load to cancer cells. Although the life cycle of phages determines their use in specific applications, these limitations can be overcome by the genetic modification of certain genes responsible for lysis or lysogenicity [91][92].

Studies related with the application of phages on the detection and control of foodborne pathogens have increased over the last years. However, regarding the biocontrol, the use of phages on foods is not considered safe by everybody. Despite some concerns and doubts about its use and mode of action, many organizations believe in the potential of phages and therefore encourage research in this field [93]. In particular, phages have proven to be an excellent tool when applied to control foodborne infections along the food chain. Figure 1:10 shows their applications as action points: phage therapy, biosanitation, biocontrol and as biopreservation elements.



**Figure 1:10:** Phage application along the food chain on phage therapy, biosanitation, biocontrol and biopreservation (adapted from García et al. [68]).

Biocontrol is an important issue nowadays; however, an early detection technology can prevent rather than control mass epidemics. When applied as a prevention tool, phages do not need to be incorporated in the food product. Ideally, a simple product sample would be required to obtain a positive or negative result. The efforts to make this possible have been made and their applicability has been tested in a variety of biosensors. Therefore, biosensors can provide a final product that combines a biological element highly specific to the target of interest with portability and easy handling.

### Phage-based Pathogen Biosensors

The urgent need for pathogen detection in agricultural, environmental and food sectors has generate different works that show the relevant use of phages in these fields. Table 1:5 shows some studies related with the use of phages attributed to the development of different types of biosensors.

**Table 1:5:** The use of phage as biorecognition element in different transducers on the detection of different organisms [94].

Transducer	Organism	Bioreceptor
SPR	<i>E. coli</i> K12	T4 Phage
SPR	<i>E. coli</i> O157:H7	T4 Phage
SPR	<i>Salmonella</i>	P22 Phage TSP
SPR	<i>C. jejuni</i>	Phage NCTC 12673 TSP
SPR	<i>S. aureus</i>	Lytic phage (phage 12600)
Bioluminescence	<i>E. coli</i>	<i>E. coli</i> phage
Bioluminescence	<i>Salmonella newport</i>	Felix phage or Newport phage
Bioluminescence	<i>Salmonella enteritidis</i>	phage SJ2
Bioluminescence	<i>E. coli</i> G2-2	AT20
Fluorescent	<i>Staphylococcal enterotoxin B</i> (SEB)	phage-displayed peptides
Fluorescent	<i>E. coli</i>	QD-labeled lambda phage
Fluorescent	<i>E. coli</i>	T7 phage
QCM	<i>Salmonella typhimurium</i>	Filamentous phage
Magnetoelastic sensors	<i>Salmonella typhimurium</i>	Filamentous E2 phage
Magnetoelastic sensors	<i>Bacillus anthracis</i> spores	Filamentous phage, clone JRB7
Amperometric	<i>Bacillus cereus</i>	B1-7064 Phage
Amperometric	<i>Mycobacterium smegmatis</i>	D29 Phage
Amperometric combined with pre-filtration	<i>E. coli</i> K12	Phage lambda
Impedimetric	<i>E. coli</i>	T4 Phage

## Chapter 1. General Introduction

---

A recent review of Schofield *et al.* [95] lists phage-based diagnostics that were approved by FDA for *Mycobacterium tuberculosis*, *Yersinia pestis*, *Bacillus anthracis*, and *Staphylococcus aureus*. In addition, significant progress has been made in the detection of food- and waterborne pathogens, such as *Salmonella*, *E. coli* and *Campylobacter* [31]. Recently, direct detection of *Salmonella* Typhimurium on fresh tomato surfaces was reported, using a phage-based magnetoelastic (ME) biosensor. The results show that direct detection of foodborne bacteria on fresh products is possible using filamentous phages immobilized on a sensor surface [96]. A study reported by Tawil *et al.* [97] describes a detection technique for *E. coli* O157:H7. The technology involves a surface plasmon resonance (SPR) platform with a T4 phage as the selected biorecognition element. It was shown that efficient detection was achieved at concentrations of  $10^3$ CFU/ml in about 20 minutes. These are some examples of ongoing works that show how phages can be used as a recognition tool for pathogens. However, problems related to the detection of bacteria in a viable but nonculturable (VBNC) state is one of the big concerns in the environmental and food sector, resulting in the observation of false negatives. Wastewater and surfaces on which food is treated are some examples where they can be found. In these conditions, they are under stress environments caused by bactericidal agents, changes in pH or temperature, or deficiency of nutrients, all factors that contribute to bacteria entering this state (a survival state) [18-19]. Bacterial downsize occurs, revealed by a change in their membrane structure, protein composition and ribosomal content [99]. These cellular changes are the weakness point of various detection systems. Studies involving the detection of VBNC bacteria using phages are still limited and some used a green fluorescent protein (GFP)-labeled phage (e.g. to analyze environment samples (river, tap water)) [19][20][101]. However, this type of approach needs a rigorous pre-treatment of environment samples due the presence of any autofluorescent or light-quenching particles that can give false positives. The prevalence of this problem and also the necessity of finding a detection technology that can measure real samples without any sample treatment (e.g. a piece of raw meat, juice, a piece of fruit or vegetables) are still a big deal. Even when testing pre-treated samples the sensitivity of the measurements have a long way to go, although with the help of phage-based detection systems it is possible to fulfil these specificity and sensitivity requirements.

### 1.3. References

- [1] “Food safety and foodborne illness,” *World Health Organization*. [Online]. Available: <http://www.who.int/mediacentre/factsheets/fs237/en/index.html>.
- [2] F. Hilbert, F. J. M. Smulders, R. Chopra-Dewasthaly, and P. Paulsen, “*Salmonella* in the wildlife-human interface,” *Food Research International*, vol. 45, no. 2, pp. 603–608, Mar. 2012.
- [3] P.-Y. Cheung and K. M. Kam, “*Salmonella* in food surveillance: PCR, immunoassays, and other rapid detection and quantification methods,” *Food Research International*, vol. 45, no. 2, pp. 802–808, Mar. 2012.
- [4] P. V Elgea, A. C. Loeckaertb, and P. B. Arrowc, “Review article Emergence of *Salmonella* epidemics: The problems related to *Salmonella* enterica serotype Enteritidis and multiple antibiotic resistance in other major serotypes,” vol. 36, pp. 267–288, 2005.
- [5] M. E. Ohl and S. I. Miller, “*Salmonella*: A Model for Bacterial,” 2001.
- [6] B. J. Haley, D. J. Cole, and E. K. Lipp, “Distribution, diversity, and seasonality of waterborne salmonellae in a rural watershed,” *Applied and environmental microbiology*, vol. 75, no. 5, pp. 1248–55, Mar. 2009.
- [7] B. M. Lund and S. J. O’Brien, “The occurrence and prevention of foodborne disease in vulnerable people,” *Foodborne pathogens and disease*, vol. 8, no. 9, pp. 961–73, Sep. 2011.
- [8] S. Report, O. F. Efsa, E. Food, S. Authority, E. European, and D. Prevention, “Trends and Sources of Zoonoses, Zoonotic Agents and Food-borne Outbreaks in 2010,” vol. 10, no. 3, pp. 1–442, 2012.
- [9] “*Salmonella*,” *European Food Safety Authority (EFSA)*. [Online]. Available: <http://www.efsa.europa.eu/en/topics/topic/salmonella.htm>.
- [10] S. M. Pires, H. Vigre, P. Makela, and T. M. Hald, “*Salmonella* spp.,” *Foodborne Pathog Disease*, vol. 11, no. 7, pp. 1351–1361, 2010.
- [11] N. Hidayah, “Review Article *Salmonella*: A foodborne pathogen,” vol. 473, pp. 465–473, 2011.
- [12] N. S. Surveillance, U. States, D. Control, E. Diseases, and L. E. D. Surveillance, “National Enteric Disease Surveillance: *Salmonella* Surveillance Overview,” no. July, pp. 1–12, 2011.
- [13] T. H. E. Commission, O. F. The, and E. Communities, “24.10.2007,” no. 1237, pp. 5–9, 2007.

## Chapter 1. General Introduction

---

- [14] I. Keery and E. A. Committee, “*Salmonella* Enteritidis Control Programs in the Canadian Poultry Industry,” 2010.
- [15] K. Ropkins and A. J. Beck, “Evaluation of worldwide approaches to the use of HACCP to control food safety,” *Trends in Food Science & Technology*, vol. 11, no. 1, pp. 10–21, Jan. 2000.
- [16] I. O. for standardization (ISO), “ISO 6579:2002, Microbiology of food and animal feeding stuffs — Horizontal method for the detection of *Salmonella* spp.,” 2002.
- [17] A. R. Gupte, C. L. E. De Rezende, and S. W. Joseph, “Induction and Resuscitation of Viable but Nonculturable *Salmonella* enterica Serovar Typhimurium DT104 †,” vol. 69, no. 11, pp. 6669–6675, 2003.
- [18] I. Abdel-Hamid, D. Ivnitski, P. Atanasov, and E. Wilkins, “Highly sensitive flow-injection immunoassay system for rapid detection of bacteria,” *Analytica Chimica Acta*, vol. 399, no. 1–2, pp. 99–108, Nov. 1999.
- [19] J. S. Kim, C. R. Taitt, F. S. Ligler, and G. P. Anderson, “Multiplexed magnetic microsphere immunoassays for detection of pathogens in foods,” vol. 4, no. 2, pp. 73–81, 2010.
- [20] V. Jasson, L. Jacxsens, P. Luning, A. Rajkovic, and M. Uyttendaele, “Alternative microbial methods: An overview and selection criteria,” *Food Microbiology*, pp. 710–730, 2010.
- [21] P. P. Banada and A. K. Bhunia, “Principles of Bacterial Detection: Biosensors, Recognition Receptors and Microsystems,” Springer New York, 2008, pp. 567–602.
- [22] K. Mullis, F. Faloona, S. Scharf, R. Saiki, G. Horn, and H. Erlich, “Specific enzymatic amplification of DNA in vitro: The Polymerase Chain Reaction, 1986.
- [23] C. Lo, R. Knutsson, C. E. Axelsson, P. Ra, and F. Taq, “Rapid and Specific Detection of *Salmonella* spp . in Animal Feed Samples by PCR after Culture Enrichment,” vol. 70, no. 1, pp. 69–75, 2004.
- [24] O. Lazcka, F. J. Del Campo, and F. X. Muñoz, “Pathogen detection: a perspective of traditional methods and biosensors.,” *Biosensors & bioelectronics*, vol. 22, no. 7, pp. 1205–17, Mar. 2007.
- [25] A. Touron, T. Berthe, B. Pawlak, and F. Petit, “Detection of *Salmonella* in environmental water and sediment by a nested-multiplex polymerase chain reaction assay.,” *Research in microbiology*, vol. 156, no. 4, pp. 541–53, May 2005.
- [26] N. D. Miller, P. M. Davidson, and D. H. D’Souza, “Real-time reverse-transcriptase PCR for *Salmonella* Typhimurium detection from lettuce and tomatoes,” *LWT - Food Science and Technology*, vol. 44, no. 4, pp. 1088–1097, May 2011.

- [27] E. a Mothershed and A. M. Whitney, “Nucleic acid-based methods for the detection of bacterial pathogens: present and future considerations for the clinical laboratory.,” *Clinica chimica acta; international journal of clinical chemistry*, vol. 363, no. 1–2, pp. 206–20, Jan. 2006.
- [28] J. Homola, K. Hegnerová, and M. Vala, “Surface Plasmon Resonance Biosensors for Detection of Foodborne Pathogens and Toxins,” vol. 7167, pp. 716705–716705–10, Feb. 2009.
- [29] F. C. Dudak and I. H. Boyaci, “Rapid and label-free bacteria detection by surface plasmon resonance (SPR) biosensors.,” *Biotechnology journal*, vol. 4, no. 7, pp. 1003–11, Jul. 2009.
- [30] M. D. Zordan, M. M. G. Grafton, G. Acharya, L. M. Reece, C. L. Cooper, A. I. Aronson, K. Park, and J. F. Leary, “Detection of pathogenic E. coli O157:H7 by a hybrid microfluidic SPR and molecular imaging cytometry device.,” *Cytometry. Part A: the journal of the International Society for Analytical Cytology*, vol. 75, no. 2, pp. 155–62, Feb. 2009.
- [31] P. Leonard, S. Hearty, J. Brennan, L. Dunne, J. Quinn, T. Chakraborty, and R. O’Kennedy, “Advances in biosensors for detection of pathogens in food and water,” *Enzyme and Microbial Technology*, vol. 32, no. 1, pp. 3–13, Jan. 2003.
- [32] V. Velusamy, K. Arshak, O. Korostynska, K. Oliwa, and C. Adley, “An overview of foodborne pathogen detection: in the perspective of biosensors.,” *Biotechnology advances*, vol. 28, no. 2, pp. 232–54, 2010.
- [33] J. Wang, “Glucose Biosensors: 40 Years of Advances and Challenges,” *Electroanalysis*, vol. 13, no. 12, pp. 983–988, Aug. 2001.
- [34] S. Viswanathan, H. Radecka, and J. Radecki, “Electrochemical biosensors for food analysis,” *Monatshefte für Chemie - Chemical Monthly*, vol. 140, no. 8, pp. 891–899, Apr. 2009.
- [35] C. a Grimes, S. C. Roy, S. Rani, and Q. Cai, “Theory, instrumentation and applications of magnetoelastic resonance sensors: a review.,” *Sensors (Basel, Switzerland)*, vol. 11, no. 3, pp. 2809–44, Jan. 2011.
- [36] M. L. Johnson, J. Wan, S. Huang, Z. Cheng, V. A. Petrenko, D.-J. Kim, I.-H. Chen, J. M. Barbaree, J. W. Hong, and B. a. Chin, “A wireless biosensor using microfabricated phage-interfaced magnetoelastic particles,” *Sensors and Actuators A: Physical*, vol. 144, no. 1, pp. 38–47, May 2008.
- [37] S. Huang, S.-Q. Li, H. Yang, M. Johnson, J. Wan, I. Chen, V. A. Petrenko, J. M. Barbaree, and B. A. Chin, “Optimization of Phage-Based Magnetoelastic Biosensor Performance,” *Sensors & Transducers*, vol. 3, pp. 87–96, 2008.



## Chapter 1. General Introduction

---

- [38] J. Wan, M. L. Johnson, R. Guntupalli, V. A. Petrenko, and B. a. Chin, "Detection of *Bacillus anthracis* spores in liquid using phage-based magnetoelastic micro-resonators," *Sensors and Actuators B: Chemical*, vol. 127, no. 2, pp. 559–566, Nov. 2007.
- [39] R. S. Lakshmanan, R. Guntupalli, J. Hu, V. A. Petrenko, J. M. Barbaree, and B. a. Chin, "Detection of *Salmonella typhimurium* in fat free milk using a phage immobilized magnetoelastic sensor," *Sensors and Actuators B: Chemical*, vol. 126, no. 2, pp. 544–550, Oct. 2007.
- [40] S. Huang, H. Yang, R. S. Lakshmanan, M. L. Johnson, J. Wan, I.-H. Chen, H. C. Wickle, V. A. Petrenko, J. M. Barbaree, and B. a. Chin, "Sequential detection of *Salmonella typhimurium* and *Bacillus anthracis* spores using magnetoelastic biosensors.," *Biosensors & bioelectronics*, vol. 24, no. 6, pp. 1730–6, Feb. 2009.
- [41] R. Guntupalli, R. S. Lakshmanan, J. Hu, T. S. Huang, J. M. Barbaree, V. Vodyanoy, and B. a. Chin, "Rapid and sensitive magnetoelastic biosensors for the detection of *Salmonella typhimurium* in a mixed microbial population.," *Journal of microbiological methods*, vol. 70, no. 1, pp. 112–8, Jul. 2007.
- [42] P. P. Freitas, *et al.*, "Spintronic platforms for biomedical applications." *Lab Chip*, vol. 12: p. 546-557, 2012
- [43] Cardoso, F.A., *et al.*, "Diode/magnetic tunnel junction cell for fully scalable matrix-based biochip." *Journal of Applied Physics*, vol.99(8): p. 08B307-3 2006.
- [44] Cardoso, F.A., *et al.* "Detection of 130 nm magnetic particles by a portable electronic platform using spin valve and magnetic tunnel junction sensors." *Journal of Applied Physics*, 103(7): p. 07A310-3 2008.
- [45] Graham, D.L., *et al.* "High sensitivity detection of molecular recognition using magnetically labelled biomolecules and magnetoresistive sensors." *Biosensors and Bioelectronics*, 18(4): p. 483-488 2003.
- [46] Wang, S.X., *et al.*, "Towards a magnetic microarray for sensitive diagnostics." *Journal of Magnetism and Magnetic Materials*, 293(1): p. 731-736 2005.
- [47] V. C. Martins, F. a Cardoso, J. Germano, S. Cardoso, L. Sousa, M. Piedade, P. P. Freitas, and L. P. Fonseca, "Femtomolar limit of detection with a magnetoresistive biochip.," *Biosensors & bioelectronics*, vol. 24, no. 8, pp. 2690–5, Apr. 2009.
- [48] J. Germano, V. C. Martins, F. a Cardoso, T. M. Almeida, L. Sousa, P. P. Freitas, and M. S. Piedade, "A portable and autonomous magnetic detection platform for biosensing.," *Sensors (Basel, Switzerland)*, vol. 9, no. 6, pp. 4119–37, Jan. 2009.
- [49] V. C. Martins, J. Germano, F. a. Cardoso, J. Loureiro, S. Cardoso, L. Sousa, M. Piedade, L. P. Fonseca, and P. P. Freitas, "Challenges and trends in the development of

- a magnetoresistive biochip portable platform,” *Journal of Magnetism and Magnetic Materials*, vol. 322, no. 9–12, pp. 1655–1663, May 2010.
- [50] P. Yager, T. Edwards, E. Fu, K. Helton, K. Nelson, M. R. Tam and B. H. Weigl, “Microfluidic diagnostic technologies for global public health.”, *Nature*, vol.442, pp. 412-418, July 2006.
- [51] R. M. Lequin, “Enzyme immunoassay (EIA)/enzyme-linked immunosorbent assay (ELISA).”, *Clinical chemistry*, vol. 51, no. 12, pp. 2415–8, Dec. 2005.
- [52] J. D. Newman and S. J. Setford, “Enzymatic biosensors.”, *Molecular biotechnology*, vol. 32, no. 3, pp. 249–68, Mar. 2006.
- [53] X. Mao, L. Yang, X.-L. Su, and Y. Li, “A nanoparticle amplification based quartz crystal microbalance DNA sensor for detection of Escherichia coli O157:H7.”, *Biosensors & bioelectronics*, vol. 21, no. 7, pp. 1178–85, Jan. 2006.
- [54] S. Hagens and M. J. Loessner, “Application of bacteriophages for detection and control of foodborne pathogens.”, *Applied microbiology and biotechnology*, vol. 76, no. 3, pp. 513–9, Sep. 2007.
- [55] M. Zourob, *Recognition receptors in biosensors*. Springer New York Dordrecht Heidelberg London, 2010.
- [56] J. P. Chambers, B. P. Arulanandam, L. L. Matta, A. Weis, and J. J. Valdes, “Biosensor recognition elements.”, *Current issues in molecular biology*, vol. 10, no. 1–2, pp. 1–12, Jan. 2008.
- [57] X. Zeng, Z. Shen, and R. Mernaugh, “Recombinant antibodies and their use in biosensors.”, *Analytical and bioanalytical chemistry*, vol. 402, no. 10, pp. 3027–38, Apr. 2012.
- [58] Y. Wang, Z. Ye, and Y. Ying, “New trends in impedimetric biosensors for the detection of foodborne pathogenic bacteria.”, *Sensors (Basel, Switzerland)*, vol. 12, no. 3, pp. 3449–71, Jan. 2012.
- [59] R. Guntupalli, J. Hu, R. S. Lakshmanan, T. S. Huang, J. M. Barbaree, and B. a Chin, “A magnetoelastic resonance biosensor immobilized with polyclonal antibody for the detection of *Salmonella typhimurium*.”, *Biosensors & bioelectronics*, vol. 22, no. 7, pp. 1474–9, Feb. 2007.
- [60] J. Waswa, J. Irudayaraj, and C. DebRoy, “Direct detection of E. Coli O157:H7 in selected food systems by a surface plasmon resonance biosensor,” *LWT - Food Science and Technology*, vol. 40, no. 2, pp. 187–192, Mar. 2007.
- [61] T. Geng, J. Uknalis, S.-I. Tu, and A. k. Bhunia, “Fiber-Optic Biosensor Employing Alexa-Fluor Conjugated Antibody for Detection of,” *Sensors*, pp. 796–807, 2006.

## Chapter 1. General Introduction

---

- [62] V. Petrenko and G. P. Smith, “Phages from landscape libraries as substitute antibodies.,” *Protein engineering*, vol. 13, no. 8, pp. 589–92, Aug. 2000.
- [63] S.-H. Chen, V. C. H. Wu, Y.-C. Chuang, and C.-S. Lin, “Using oligonucleotide-functionalized Au nanoparticles to rapidly detect foodborne pathogens on a piezoelectric biosensor.,” *Journal of microbiological methods*, vol. 73, no. 1, pp. 7–17, Apr. 2008.
- [64] D. Zhang, Y. Yan, Q. Li, T. Yu, W. Cheng, L. Wang, H. Ju, and S. Ding, “Label-free and high-sensitive detection of *Salmonella* using a surface plasmon resonance DNA-based biosensor.,” *Journal of biotechnology*, vol. 160, no. 3–4, pp. 123–8, Aug. 2012.
- [65] M. Uttamchandani, J. L. Neo, B. N. Z. Ong, and S. Moochhala, “Applications of microarrays in pathogen detection and biodefence.,” *Trends in biotechnology*, vol. 27, no. 1, pp. 53–61, Jan. 2009.
- [66] M. H. Adams, *Bacteriophages*. New York: Interscience Publishers, 1959.
- [67] F. Article, “Bacteriophage biocontrol and bioprocessing: Application of phage therapy to industry,” vol. 53, no. 6, pp. 254–262, 2003.
- [68] P. García, B. Martínez, J. M. Obeso, and a Rodríguez, “Bacteriophages and their application in food safety.,” *Letters in applied microbiology*, vol. 47, no. 6, pp. 479–85, Dec. 2008.
- [69] P. G. Leiman, S. Kanamaru, V. V Mesyanzhinov, F. Arisaka, and M. G. Rossmann, “Structure and morphogenesis of bacteriophage T4.,” *Cellular and molecular life sciences : CMLS*, vol. 60, no. 11, pp. 2356–70, Nov. 2003.
- [70] “Schematic of T4 Bacteriophage.” [Online]. Available: <http://www.nsf.gov/od/lpa/news/02/pr0207images.htm>.
- [71] L. R. H. Krumpe and T. Mori, “The Use of Phage-Displayed Peptide Libraries to Develop Tumor-Targeting Drugs.,” *International journal of peptide research and therapeutics*, vol. 12, no. 1, pp. 79–91, Mar. 2006.
- [72] G. P. Smith and V. A. Petrenko, “Phage Display.,” *Chemical reviews*, vol. 97, no. 2, pp. 391–410, Apr. 1997.
- [73] H.-W. Ackermann, “5500 Phages examined in the electron microscope.,” *Archives of virology*, vol. 152, no. 2, pp. 227–43, Feb. 2007.
- [74] C. a Roessner, D. K. Struck, and G. M. Ihler, “Morphology of complexes formed between bacteriophage lambda and structures containing the lambda receptor.,” *Journal of bacteriology*, vol. 153, no. 3, pp. 1528–34, Mar. 1983.

- [75] L. Tang, W. R. Marion, G. Cingolani, P. E. Prevelige, and J. E. Johnson, "Three-dimensional structure of the bacteriophage P22 tail machine.," *The EMBO journal*, vol. 24, no. 12, pp. 2087–95, Jun. 2005.
- [76] S. Li, L. R. S., V. A. Petrenko, and B. A. Chin, "Phage-based Pathogen Biosensors," in *Phage Nanobiotechnology*, 2008.
- [77] S. T. Abedon, "Size does matter – distinguishing bacteriophages by genome length ( and ' breadth ' )," *Microbiology Australia*, 2011.
- [78] M. H. Adams, *Bacteriophages*. New York: Interscience Publishers, 1959.
- [79] "Viral Multiplication." [Online]. Available: <http://classes.midlandstech.edu/carterp/Courses/bio225/chap13/lecture3.htm>.
- [80] H. Bru, C. Canchaya, and W. Hardt, "Phages and the Evolution of Bacterial Pathogens : from Genomic Rearrangements to Lysogenic Conversion," vol. 68, no. 3, pp. 560–602, 2004.
- [81] S. Jiang and J. Paul, "Significance of Lysogeny in the Marine Environment: Studies with Isolates and a Model of Lysogenic Phage Production," *Microbial ecology*, vol. 35, no. 3, pp. 235–43, May 1998.
- [82] "The lytic and lysogenic cycles of  $\lambda$ , a temperate phage." [Online]. Available: <http://bio1151.nicerweb.com/Locked/media/ch19/lysogenic.html>.
- [83] V. Mai, M. Ukhanova, L. Visone, T. Abuladze, and A. Sulakvelidze, "Bacteriophage Administration Reduces the Concentration of *Listeria monocytogenes* in the Gastrointestinal Tract and Its Translocation to Spleen and Liver in Experimentally Infected Mice.," *International journal of microbiology*, vol. 2010, p. 624234, Jan. 2010.
- [84] H. Poultry and C. Pei, "Effectiveness of Phages in Treating Experimental *Escherichia coli* Diarrhoea in Calves , Piglets and Lambs," pp. 2659–2675, 1983.
- [85] J. M. Loeffler, D. Nelson, and V. a Fischetti, "Rapid killing of *Streptococcus pneumoniae* with a bacteriophage cell wall hydrolase.," *Science (New York, N.Y.)*, vol. 294, no. 5549, pp. 2170–2, Dec. 2001.
- [86] L. Fiorentin, N. D. Vieira, and W. Barioni, "Oral treatment with bacteriophages reduces the concentration of *Salmonella* Enteritidis PT4 in caecal contents of broilers.," *Avian pathology : journal of the W.V.P.A*, vol. 34, no. 3, pp. 258–63, Jun. 2005.
- [87] J. a Wagenaar, M. a P. Van Bergen, M. a Mueller, T. M. Wassenaar, and R. M. Carlton, "Phage therapy reduces *Campylobacter jejuni* colonization in broilers.," *Veterinary microbiology*, vol. 109, no. 3–4, pp. 275–83, Aug. 2005.

## Chapter 1. General Introduction

---

- [88] A. A. Elshayeb, “The impact of bacteriophages in bacteria removal associated with soba stabilisation station efficiency,” vol. 4, no. 4, pp. 233–239, 2010.
- [89] W. Sciences, “Bacteriophages-Potential for application in wastewater treatment processes,” vol. 339, no. March, pp. 1–18, 2005.
- [90] M. Loessner and R. Carlton, “Virulent phages to control *Listeria Monocytogenes* in foodstuffs and in food processing plants,” U.S. Patent US 2008/0318867 A12008.
- [91] R. Awais, H. Fukudomi, K. Miyanaga, H. Unno, and Y. Tanji, “A recombinant bacteriophage-based assay for the discriminative detection of culturable and viable but nonculturable *Escherichia coli* O157:H7.,” *Biotechnology progress*, vol. 22, no. 3, pp. 853–9, 2006.
- [92] S. Matsuzaki, M. Yasuda, H. Nishikawa, M. Kuroda, T. Ujihara, T. Shuin, Y. Shen, Z. Jin, S. Fujimoto, M. D. Nasimuzzaman, H. Wakiguchi, S. Sugihara, T. Sugiura, S. Koda, A. Muraoka, and S. Imai, “Experimental protection of mice against lethal *Staphylococcus aureus* infection by novel bacteriophage phi MR11.,” *The Journal of infectious diseases*, vol. 187, no. 4, pp. 613–24, Feb. 2003.
- [93] Q. N. Efsa-q--, O. Andreoletti, H. Budka, S. Buncic, P. Colin, J. D. Collins, A. De, J. Griffin, A. Havelaar, J. Hope, G. Klein, H. Kruse, S. Magnino, M. López, J. Mcllauchlin, C. Nguyen-the, K. Noeckler, B. Noerrung, M. P. Maradona, T. Roberts, I. Vågsholm, and E. Vanopdenbosch, “The use and mode of action of bacteriophages in food production 1 Scientific Opinion of the Panel on Biological Hazards Adopted on 22 April 2009,” 2009.
- [94] A. Singh, S. Poshtiban, and S. Evoy, “Recent advances in bacteriophage based biosensors for food-borne pathogen detection.,” *Sensors (Basel, Switzerland)*, vol. 13, no. 2, pp. 1763–86, Jan. 2013.
- [95] D. Schofield, N. J. Sharp, and C. Westwater, “Phage-based platforms for the clinical detection of human bacterial pathogens.,” *Bacteriophage*, vol. 2, no. 2, pp. 105–283, Apr. 2012.
- [96] M.-K. Park, J. W. Park, and H. C. Wikle III, “Comparison of Phage-Based Magnetoelastic Biosensors with Taqman- Based Quantitative Real-Time PCR for the Detection of *Salmonella typhimurium* Directly Grown on Tomato Surfaces,” *Journal of Biosensors & Bioelectronics*, vol. 03, no. 01, pp. 1–8, 2012.
- [97] N. Tawil, E. Sacher, R. Mandeville, and M. Meunier, “Surface plasmon resonance detection of *E. coli* and methicillin-resistant *S. aureus* using bacteriophages.,” *Biosensors & bioelectronics*, vol. 37, no. 1, pp. 24–9, 2012.
- [98] J. D. Oliver, “The viable but nonculturable state in bacteria.,” *Journal of microbiology (Seoul, Korea)*, vol. 43 Spec No, no. February, pp. 93–100, Feb. 2005.
- [99] J. D. Oliver, “The viable but nonculturable state and cellular resuscitation,” 1999.

- [100] M. Ben Said, O. Masahiro, and A. Hassen, “Detection of viable but non cultivable *Escherichia coli* after UV irradiation using a lytic Qbeta phage.” *Annals of microbiology*, vol. 60, no. 1, pp. 121–127, Mar. 2010.
- [101] P. P. P. Bacteriophage, M. Oda, M. Morita, H. Unno, and Y. Tanji, “Rapid Detection of *Escherichia coli* O157 : H7 by Using Green Fluorescent Protein-Labeled PP01 Bacteriophage,” 2004.

## Chapter 2

# Selection and Characterization of *Salmonella* Phages

**Parts of the work presented in this chapter are based on:**

Santos, S. B., **E. Fernandes**, C. M. Carvalho, S. Sillankorva, V. N. Krylov, E. A. Pleteneva, O. V. Shaburova, A. Nicolau, E. C. Ferreira, and J. Azeredo. 2010. Selection and Characterization of a Multivalent *Salmonella* Phage and Its Production in a Nonpathogenic *Escherichia coli* Strain. *Appl. Environ. Microbiol.* 76(21), 7338-7342.

**... and contributed to the:**

Patent application PPI46027-12, entitled “*Phage Tail Proteins for Specific Detection and Control of Salmonella Enterica*”. Inventor(s): Azeredo, J., Kluskens, L., Santos, S., Silva, S., **Fernandes, E.**, Lavigne, R., Vandersteegen, K., Cornelissen, A., August 2012.

### Abstract

*Salmonella* is a pathogenic bacterium responsible for the majority of food-borne outbreaks and therefore it is urgent to develop therapeutic agents and detection systems that can eliminate and/or control this pathogen. Bacteriophages (phages) have the ability to specifically recognize their host, a feature that is appreciated by many researchers that seek to explore their potential as a therapeutic and detection agent. However, as the majority of phages are highly specific, recognizing a limited number of strains, their application as detection tool might be limited. Here we report the characterization of three lytic phages exhibiting a broad lytic spectrum, and thus having great potential to be used as detection tools. Furthermore, the sequences of genes encoding for the tail fiber proteins (TFPs) responsible for host recognition and binding are presented herein to be further explored in the biosensing field. In addition, we propagated the phage with the broadest host range (PVP-SE1) in an alternative nonpathogenic host, namely *E.coli* BL21. The results showed that the selected phage maintained its ability to lyse *Salmonella* strains and the phage DNA restriction profile was not modified. This work reports on the detailed characterization of a phage that can be produced in a non-pathogenic host, thereby contributing to an easier approval of a safer product based on this *Salmonella* biocontrol agent.



### 2 Introduction

*Salmonella enterica* has long been recognized as an important zoonotic pathogen of economic significance in animals and humans and remains the primary cause of reported food poisonings worldwide, with massive outbreaks occurring in recent years [1–3]. The serovars most commonly reported in human infections in the European Union (EU) and the United States have been Enteritidis and Typhimurium, comprising, respectively, 76% and 14% of the cases in the EU [4–5]. Therefore, controlling *Salmonella* infections has become an important goal for the poultry industry, the most common source of *Salmonella* Enteritidis infections [1, 2, 6, 7]. The use and misuse of antimicrobials in both humans and animals has given rise to the emergence of infectious bacteria displaying resistance toward many, and in some cases all, effective antimicrobials [1, 2, 8]. Thus, the development of alternatives to chemotherapy is imperative and a critical priority. The use of (bacterio)phages, viruses that specifically infect and lyse bacteria, as a therapeutic agent (phage therapy) is one possible option for controlling pathogenic bacteria. Phages have already been tested as biocontrol agents for salmonellae and other pathogens in humans and animals, and have showed advantages over antibiotics [9–13]. Furthermore phages are attractive tools in the biosensing field, because they display host recognition peptides on their capsids, spikes, tails or tail fibres (depending on the phage family). However, due to the high specificity of the majority of phages, their application as biocontrol or detection agents might be limited. Nevertheless few studies have reported the isolation of multivalent phages, which are phages able to infect a broad host range including different bacterial species, this is the case of Felix 01 [14]. Another drawback of phage specificity is the fact that they often can only be produced in their natural hosts [7, 14]. In the case of pathogens, this may turn out to be problematic, due to the release of cell debris and large quantities of both endotoxins and exotoxins and the presence of live cells that may occur in the crude phage lysate [12], [16–18]. The use of a nonpathogenic host in the production process would eliminate the risk of accidentally administering a pathogen [7], [10, 18]. Consequently, it would greatly simplify the purification process with a consequent reduction in cost and would furthermore increase the safety of phage preparations, leading to easy and faster approval of phage products. Nevertheless, this tends to be a difficult approach since multivalent phages are rare [7], [19–21]. Therefore, our work focused on the selection

and characterization of a *Salmonella* phage with a broad lytic spectrum and studied the possibility of producing it in a nonpathogenic *Escherichia coli* strain.

## 2.1 Materials and Methods

### 2.1.1 Media and Buffer Composition

The culture media LB broth and Agar were provided by Sigma-Aldrich. LB agar plates were prepared by adding 1.2% of agar to the LB broth, soft agar was made by adding 0.6% of agar. The reagents for SM buffer (100 mM NaCl, 8 mM MgSO<sub>4</sub>, 50 mM Tris-HCl, pH 7.5) were provided by Sigma-Aldrich.

### 2.1.2 Bacteriophages and Bacterial Strains

The three phages characterized in this work, namely PVP-SE1, PVP-SE2 and PVP-SE3, belong to phage collection of CEB-IBB and were isolated in the framework of the European Project Phagevet-P [22]. These phages were previously named as phi 2/2, 38 and 39, respectively. PVP-SE1 was isolated from a Regensburg (Germany) wastewater plant, PVP-SE2 and PVP-SE3 were isolated from Braga (Portugal) raw sewage wastewater treatment plant [23]. Following the same sequence, the phage hosts are *Salmonella enterica* serovar Enteritidis strains as S1400 that belongs to the private collection of the University of Bristol, and strains 821 and 869 from the Instituto Nacional Ricardo Jorge, Portugal [23]. The lytic spectra were compared to *Salmonella* phage Felix 01 obtained from the Profos AG collection (Regensburg-Germany). The tests were carried out against thirty eight bacterial strains, thirteen of which were isolated from contaminated food products in Portugal and from poultry farms in England [23]. Two *E. coli* strains (N5-bovine and N9-porcine) were also isolated. The remaining strains belong to the type cultures collections NCTC (National Collection of Type Cultures), ATCC (American Type Culture Collection), SGSC (*Salmonella* Genetics Stock Centre), and CECT (Colección Española de Cultivos Tipo). At least two *Salmonella* strains

from each subspecies were used. Two well known *E. coli* strains, BL21 (BL21-Gold(DE3), purchased from Stratagene) and K-12, were also included in the infection studies.

### 2.1.3 Phage Propagation

The phages were produced using the double layer agar technique as described by Sambrook and Russell [24]. Briefly, from the plaque forming units (PFU) obtained, ten were selected and transferred several times to three new Petri dishes with the proper bacterial soft agar. Using sterile paper strips, the phages were spread by passing the strips several times on the production Petri dishes and incubated overnight at 37°C. Then, 3 to 10 ml of SM buffer was added to Petri dishes and incubated overnight at 4°C (with agitation). The liquid was transferred to 50 ml tubes and centrifuged at 9000 x g during 10 min at 4°C (Hettich Zentrifugen-Universal 320) to remove the bacteria. One volume of chloroform was added to 4 volumes of supernatant and centrifuged at 9000 x g during 10 min at 4°C. The top liquid phase was removed carefully and filtered through a 0.2 µm filter (Minisart-Santorius stedim biotech). The phage titer was verified and the solution was stored at 4°C.

### 2.1.4 Phage Purification

Phage purification was performed by cesium chloride (CsCl) gradient ultracentrifugation [25]. Initially, heat-dried CsCl (MP Biomedicals, Illkirch, France) was added gradually to 15 ml of phage in order to avoid an osmotic shock. Four CsCl solutions were prepared (densities of 1.33, 1.45, 1.50 and 1.70 g/ml) and 5.7 ml per gradient was added (starting from the lowest to the higher density) and the solution was centrifuged at 28,000 x g at 4°C during 3 h. The phage was collected from the gradient (~3 ml, white cloud) and dialyzed. To hydrate the membrane, the Slide-A-Lyzer dialysis cassette (Pierce, Rockford, IL) was incubated in 1 L of 1 × phage buffer [10 mM Tris-HCl, pH 7.5, 100 mM MgSO<sub>4</sub>, 150 mM NaCl]. Three ml of phage suspension was added in the dialysis cassette and dialyzed 3 times for 30 min against 300 volumes of phage buffer. The pure phage preparation was collected and stored at 4°C

### 2.1.5 Phage Propagation in a Non-pathogenic Host

Phages were amplified by plate lysis as described by Sambrook and Russell [24]. Generation one (G1) of phage PVP-SE1 in *E. coli* BL21 was produced using the phage stock suspension obtained for PVP-SE1 in *Salmonella* S1400/94 (G0). This production was then used as a stock suspension to produce G2 of phage PVP-SE1 in *E. coli* BL21. G3 to G6 were obtained using the same procedure, i.e. each generation was obtained using phages from the previous generation.

### 2.1.6 Lytic Spectrum

To determine the phages lytic spectra, bacterial lawns were prepared by homogenizing the soft agar with fresh suspension of the test strains and applied to Petri dishes with an LB agar layer. After solidifying, drops (10  $\mu$ l) of serial dilutions of the different phage suspensions were added to bacterial lawns. The plates were incubated overnight at 37°C. Lytic activity was verified by the formation of clear areas and phage plaque formation on the bacterial lawns.

### 2.1.7 Single-Step Growth Curve Experiments

Single-step growth curve experiments were carried out at 37°C in LB medium as described by Sambrook and Russell [24] using an overnight pre-inoculum of the bacteria in the same medium. The experiments were done in duplicate and repeated twice. The values of the parameters were determined by fitting the experimental data to a four-parameter sigmoid curve using least-squares fitting.

### 2.1.8 Restriction fragment length polymorphism (RFLP)

Phage DNA was extracted using the Wizard DNA Clean-Up System from Promega Corporation (Madison, WI) and digested with *Hind*III and *Eco*RV from Sigma-Aldrich Inc. (St. Louis, MO) according to the manufacturer's instructions. Fragments were separated on a 1% agarose (Bio-Rad Laboratories Inc., Hercules, CA) gel at 70 V for 3 h (20 V for 16 h when

DNA was digested with *Hind*III) and stained with ethidium bromide (10 g/ml; Bio-Rad Laboratories Inc., Hercules, CA).

### 2.1.9 Transmission Electron Microscopy (TEM)

Phage particles were sedimented at 25,000 x g for 60 min using a Beckman (Palo Alto, CA) J2-21 centrifuge with a JA 18.1 fixed-angle rotor. Phages were washed twice in 0.1 M ammonium acetate (pH 7.0), deposited on copper grids provided with carbon-coated Formvar films, stained with 2% potassium phosphotungstate (pH 7.2), and examined using a Philips EM 300 electron microscope (Laval University, Quebec, Canada).

### 2.1.10 DNA Manipulations

For the shotgun sequencing of phage PVP-SE2 phage DNA was prepared as follows:

#### 2.1.10.1 Phage DNA Extraction

Following the phage purification, 1 ml of phage solution was incubated with 0.5% of SDS, 20 mM of EDTA, pH 8.0, and 50 µg/ml of Proteinase K during 1 h at 56°C. After incubation and cooling down to room temperature, an equal volume (1:1) of phenol was added and the mixture was centrifuged at 6000 x g for 2 min at room temperature. The aqueous phase was carefully collected to another tube. An equal volume of 0.5:0.5 of phenol-chloroform was added to the aqueous phage, homogenized and the mixture was centrifuged as before. The aqueous phase was again collected and mixed with an equal volume of chloroform (1:1), homogenized and centrifuged again. The aqueous phase was removed and DNA was precipitated by ethanol.

#### 2.1.10.2 Ethanol precipitation

Ethanol precipitation was carried out by mixing 1:10 volume of 3 M sodium acetate (pH 5.2), 1:10 volume of 125 mM EDTA and 2.5 volumes of cold 96% ethanol with the DNA obtained

in step II.2.10. The mixture was homogenized and incubated on ice during 15 min. Then, the solution was centrifuged at 18000 x g during 20 min. The supernatant was removed and the pellet was resuspended in 250 µl of cold 70% ethanol, homogenized and centrifuged at room temperature, under the same conditions as described before, during 5 min. The supernatant was removed and the pellet was air-dried and resuspended in EB buffer (composition EB buffer?). The concentration of DNA was measured on a spectrophotometer.

### **2.1.10.3 Plasmid DNA isolation**

Plasmid DNA isolation was performed using the QIAprep spin Miniprep Kit as described in manufacturer's protocol.

### **2.1.10.4 Restriction analyses**

300 ng of purified DNA of PVP-SE2 was digested with *EcoRV* in a total reaction volume of 20 µl, containing 3 µl of phage DNA, 2 µl of 10 × buffer R, 14 µl of milli-Q water and 1 µl of enzyme. The mixture was incubated 1 h at 37°C and analyzed by agarose gel electrophoresis.

### **2.1.10.5 Agarose gel electrophoresis**

The DNA fragments were separated using 1% of agarose gel electrophoresis. The agarose (Eurogenetic, Luik, Belgium) was dissolved in TAE buffer (40 mM Tris-HCl, 0.5 mM sodium acetate, 50 mM EDTA, pH 7.2), after which 2 µl of ethidium bromide (1 mg/ml) was added (Cambrex NJ, USA). Four µl of loading buffer (0.1% bromophenol blue, 49% Sucrose) was added to each 20 µl of sample and used 6 µl of ladder λ *HindIII*. The gel electrophoresis was run in TAE buffer at 90 V and visualized under UV radiation using a Nikon camera.

## **2.1.11 Construction of a short genomic library of phage PVP-SE2~**

### 2.1.11.1 Sonication

Random DNA fragments were generated by Sonication (Sonics, Vibra Cell™, USA). 75 µl of sample containing 148 ng/µl was subjected to several pulses during 1 s to 30 % of amplitude. Then, the fragments were separated on an agarose gel (1%, without ethidium bromide) versus  $\lambda$  *Pst*I ladder during 30 min at 115 V.

### 2.1.11.2 DNA Gel Extraction

The  $\lambda$  *Pst*I marker lane was carefully cut out and stained in a Tris-acetate-EDTA (TAE) buffer containing ethidium bromide during 30 min. Then, using the lanes of  $\lambda$  *Pst*I were used as a control, the appropriate size (800 bp-1500 bp) was marked under UV radiation and used as a template to excise the non-UV-exposed phage DNA fragment. The extracted fragments were placed into an Eppendorf tube and purified using the GENEJET™ Gel Extraction Kit according to manufacturer's protocol.

### 2.1.11.3 End Repair

The random DNA fragments which may contain 5' and/or 3' protruding ends were end-repaired (blunted). 70 µl mixture containing 50 µl of DNA previously purified, 0.6 µl of T4 DNA Polymerase, 0.75 µl of 10 mM dNTPs, 14 µl of 5 × T4 DNA buffer and 4.65 µl of milli-Q water was incubated at 16°C during 10 min. The reaction was stopped by inactivating the T4 DNA polymerase at 70°C during 10 min. The wash step was performed with GeneJET™ purification kit as described on manufacturer's protocol.

### 2.1.11.4 Ligation

Ligation was carried out using pUC DNA/*Sma*I cloning vector. A 20 µl reaction mixture containing 8.8 µl of DNA (random fragments), 1 µl of the vector (0.5 µg/µl), 4 µl of 25 % PEG 4000, 2 µl of 10 × T4 DNA ligation buffer, 1 µl of T4 DNA ligase and 3.2 µl of Milli-Q water. The reaction mixture was incubated at 16°C overnight and stopped at 70°C during 10

min. The ligation mixture was ethanol precipitated and used for transformation to *E.coli* XL1-Blue MRF electroporation-competent cells.

### 2.1.11.5 Transformation

42.5 µl of sample containing 2.5 µl of the ligation mixture and 40 µl of *E.coli* XL1-Blue MRF electroporation-competent cells were mixed gently and electroporated at 1.7 kV (BioRAD Gene Pulser<sup>TM</sup>). The cells were recovered by adding 960 µl of pre-warmed SOC medium (2% Trypton, 0.5% Yeast extract, 0.05% NaCl, 10 mM MgCl<sub>2</sub>, 10 mM MgSO<sub>4</sub>, and 20 mM glucose) and incubated at 37 °C during 1 h under shaking conditions at 250 rpm. Then, the cells were plated out on LB solid medium containing ampicillin (100 µg/ml), 20 mg/ml X-gal and 25 mg/ml of IPTG and incubated overnight at 37°C.

### 2.1.11.6 DNA Sequencing

Individual colonies were passed to 96-well plates containing 100 µl of selective medium (LB/Ap<sup>100</sup>) and incubated for 2 h at 37°C. One hundred µl of the selective medium containing 40% glycerol was added and stored at -20°C. A standard PCR was run to verify the presence of the insert using the corresponding primers.

The sequences of inserts in the purified plasmids were determined from one side 3 µl of sequencing reaction containing 0.75 µl of BigDye buffer, 0.5 µl of primer (MV-M13f), 0.25 µl of BigDye terminator mix and 1.5 µl of Milli-Q water was performed in a Tpersonal thermocycler (Biometra, Germany) with an initial denaturation at 96°C for 1 min, followed by 30 cycles of 96°C (30 sec), 50°C (15 sec), and 60°C (4 min) and storage at 4°C thereafter. Then, ethanol precipitation was performed as described in II.2.10.2., with the exception of the elution step in which pellet was resuspended with 20 µl of elution buffer. The samples were analyzed using ABI 3130 genetic analyzer (Applied Biosystems) and the sequences were assembled with the Sequencer 4.1 software (Genecodes).



## 2.2 Results

### 2.2.1 Phage Selection

#### 2.2.1.1 Phage Lytic Spectrum

The lytic spectra of three lytic phages were tested against thirteen poultry *Salmonella* isolates and compared with the lytic spectrum of *Salmonella* phage Felix-O1. Comparing the four phages, phage PVP-SE1 showed the broadest lytic spectrum as shown in Table 2:1.

**Table 2:1:** Lytic spectra of isolated *Salmonella* phages against poultry *Salmonella* isolates and comparison with Felix 01 phage

	Phage	PVP-SE1	PVP-SE2	PVP-SE3	Felix 01
<i>Salmonella</i> Enteritidis	AL855	+	+	+	NT
	EX2	+	L	+	-
	S1400/94	+	+	+	+
	269	+	+	+	+
	546	+	+	+	+
	629B	+	+	+	+
	657	+	L	L	+
	821	+	+	+	+
	855	+	L	+	+
	869	+	+	+	+
	905	+	+	+	+
	932	+	+	+	-
	9510.85	+	L	L	-

(-) Absence of phage halo and phage plaques; (+) Presence of phage halo and phage plaques; (L) Lysis from without: Presence of phage halo and absence of phage plaques; (NT) Not Tested;

In addition, the lytic spectra were also tested for different *Salmonella* subtypes and other bacteria than *Salmonella* (Table 2:2). Besides being able to lyse almost all *Salmonella* strains (of all *Salmonella* subtypes except IIa), PVP-SE1 was also able to infect *E. coli* BL21 and K12 and was therefore considered a multivalent phage. In contrast, phages PVP-SE2 and

## Chapter 2. Selection and Characterization of *Salmonella* Phages

PVP-SE3 were unable to infect any *E.coli* and *Salmonella* subtypes, except the *Salmonella* NCTC 13349 (subsp. I) and the thirteen poultry *Salmonella* isolates (Table 2:2).

The results obtained for the lytic spectrum of PVP-SE1, show that this phage is able to infect more strains than Felix-O1 (Table 2:1).

**Table 2:2:** Lytic spectra of isolated *Salmonella* phages against different *Salmonella* subtypes and other bacteria than *Salmonella*.

Strains	Phage		
	PVP-SE1	PVP-SE2	PVP-SE3
<i>Salmonella</i> Typhimurium NCTC 12416 - subsp. I	+	-	-
<i>Salmonella</i> NCTC 13349 - subsp. I	+	+	+
<i>Salmonella</i> spp. SGSC 3047 - subsp. II	+	-	-
<i>Salmonella</i> spp. SGSC 3039 - subsp. II	+	-	-
<i>Salmonella</i> Arizonae SGSC 3063 – Iia	L	-	-
<i>Salmonella</i> Arizonae 83 (isolate) – Iia	-	-	-
<i>Salmonella</i> spp. SGSC 3069 - subsp. IIb	+	-	-
<i>Salmonella</i> spp. SGSC 3068 - subsp. IIb	+	-	-
<i>Salmonella</i> spp. SGSC 3086 - subsp. IV	L	-	-
<i>Salmonella</i> spp. SGSC 3074 - subsp. IV	+	-	-
<i>Salmonella</i> Bongori SGSC 3103 - subsp. V	+	-	-
<i>Salmonella</i> Bongori SGSC 3100 - subsp. V	+	-	-
<i>Salmonella</i> spp. SGSC 3118 - subsp. VI	+	-	-
<i>Salmonella</i> spp. SGSC 3116 - subsp. VI	+	-	-
<i>Salmonella</i> spp. SGSC 3121 - subsp. VII	+	-	-
<i>Salmonella</i> spp. SGSC 3120 - subsp. VII	+	-	-
<i>Escherichia coli</i> N9	L	-	-
<i>Escherichia coli</i> N5	L	-	-
<i>Escherichia coli</i> CECT 434 (ATCC 25922)	L	-	-
<i>Escherichia coli</i> BL21	+	-	-
<i>Escherichia coli</i> K12	+	-	-
<i>Enterobacter amnigenes</i> CECT 4078 (ATCC 33072)	L	-	-
<i>Enterobacter aerogenus</i> CECT 684 (ATCC 13048)	-	-	-
<i>Klebsiella pseudomonas</i> 11296	-	-	-
<i>Shigella</i> ATCC 12022	-	-	-

(-) Absence of phage halo and phage plaques; (+) Presence of phage halo and phage plaques; L-Lysis from without: Presence of phage halo and absence of phage plaques.

### 2.2.1.2 Phage Production in a Nonpathogenic Host

To assess whether the phage maintains its lytic profile when grown in an alternative nonpathogenic host, the phage was produced for six generations in *E. coli* BL21. It was observed that the lytic spectrum of the phage was maintained from G0 until G6. This indicates that replication of the phage in this alternative host does not narrow its lytic spectrum. Taking into account these characteristics - a broad lytic spectrum and the ability to be amplified in a nonpathogenic strain without modification of its lytic spectrum - phage PVP-SE1 was further characterized and G6 was compared with G0. Following the production step, the lytic performance, burst size, latent period and restriction profile of phage PVP-SE1 amplified in *E. coli* BL21 and in its pathogenic host strain were determined and compared.

**Table 2:3:** Lytic spectrum of PVP-SE1 over generation 0 to 6 against poultry *Salmonella* isolates

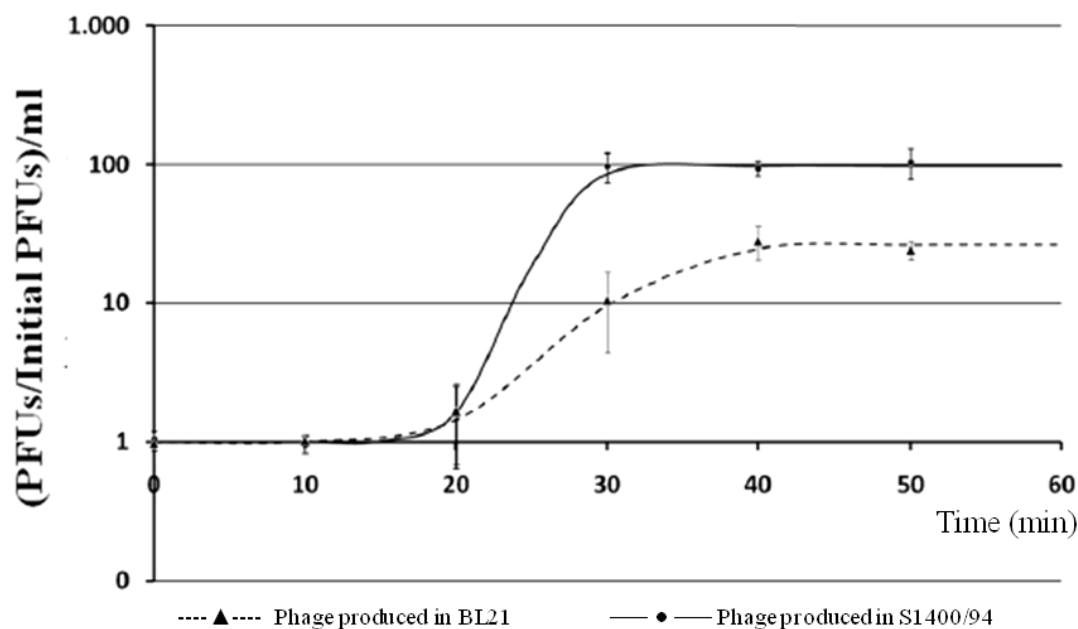
Genera- tions	<i>Salmonella</i> strains												
	9510/ 85	269	821	546	EX2	932	AL855	657	S140 0/94	629B	869	855	905
0	+	+	+	+	+	+	+	+	+	+	+	+	+
1	+	+	+	+	+	+	+	+	+	+	+	+	+
2	-	+	+	+	+	+	+	-	+	+	+	+	+
3	+	+	+	+	+	+	+	+	+	+	+	+	+
4	+	+	+	+	+	+	+	+	+	+	+	+	+
5	+	+	+	+	+	+	+	+	+	+	+	+	+
6	+	+	+	+	+	+	+	+	+	+	+	+	+

(+) Lytic halo; (-) No halo

Table 2:3 shows that phage PVP-SE1 maintained its lytic spectrum even after being produced in *E. coli* for six generations.

### 2.2.1.3 Phage Infection Parameters

The phage infection parameters of G0 and G6 were determined by a single-step growth curve. Figure 2:1 shows the increase in phage concentration over time of G0 in S1400/94 and G6 in BL21.

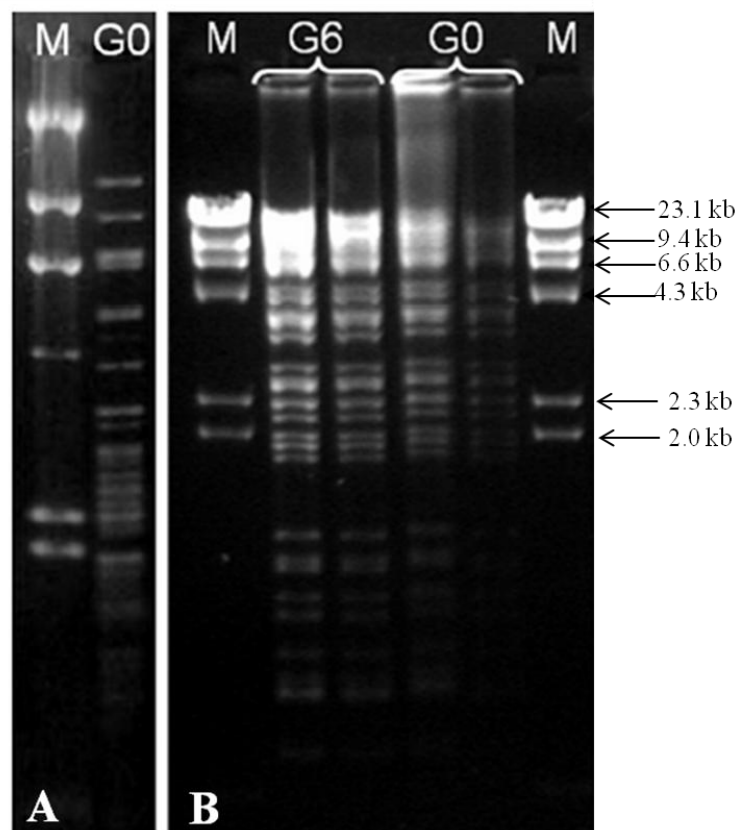


**Figure 2:1:** One-step growth curve of phage PVP-SE1 G0 in *Salmonella* S1400/94 and PVP-SE1 G6 in *E. coli* BL21. Fitted values are presented for both conditions.

Three phage infection parameters were determined, namely burst size, rise and latent period. Generation zero (G0), i.e. the phage produced on their pathogenic host (S1400/94) showed a burst size of 102 phages per infected host cell, while the generation six, i.e. phage produced in an alternative host (*E. coli* BL21), obtained a burst of 28 phages. The rise periods were 11 and 21 min, respectively, and the same latent period was verified for both phages. The production of the phage in an alternative host lead to a smaller burst size and a longer rise period compared with the original phage.

### 2.2.1.4 Phage restriction fragment length polymorphism (RFLP)

Phage PVP-SE1 was further genomically characterized by determining the restriction profile of phage DNA (Figure 2:2).



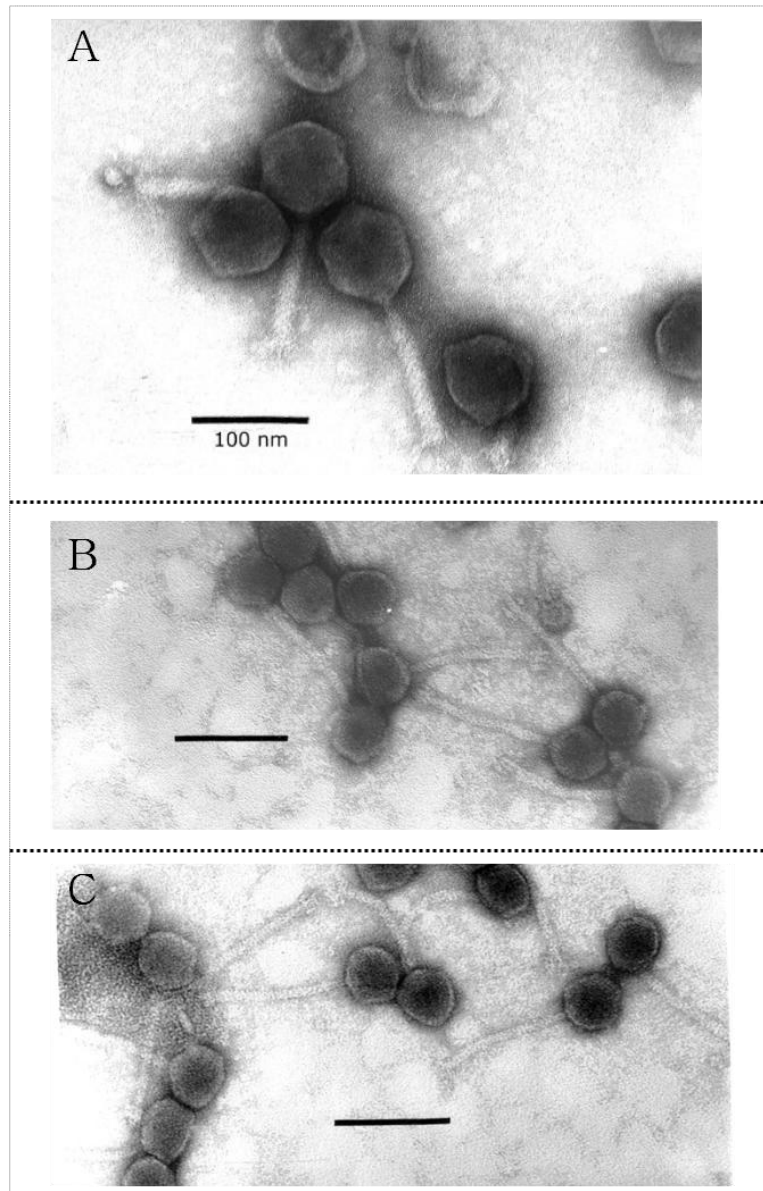
**Figure 2:2** Restriction profile of phage PVP-SE1 DNA. (A) PVP-SE1 G0 DNA digested with *Hind*III. (B) PVP-SE1 DNA (G0 and G6) digested with *Eco*RV. Lane M (marker) is a *Hind*III digest of lambda DNA.

To assess if replication of the phage in *E. coli* BL21 could cause significant mutations or modifications in the phage DNA, the DNA from G6 was extracted and digested with *Eco*RV, which produces a great number of bands with different sizes, showing a genome of 93-94 kb. Comparison of its restriction profile with that of G0 (phage grown in its natural host, *Salmonella* S1400/94) showed no difference.

## 2.2.2 Phages Characterization

### 2.2.2.1 Phage Morphology

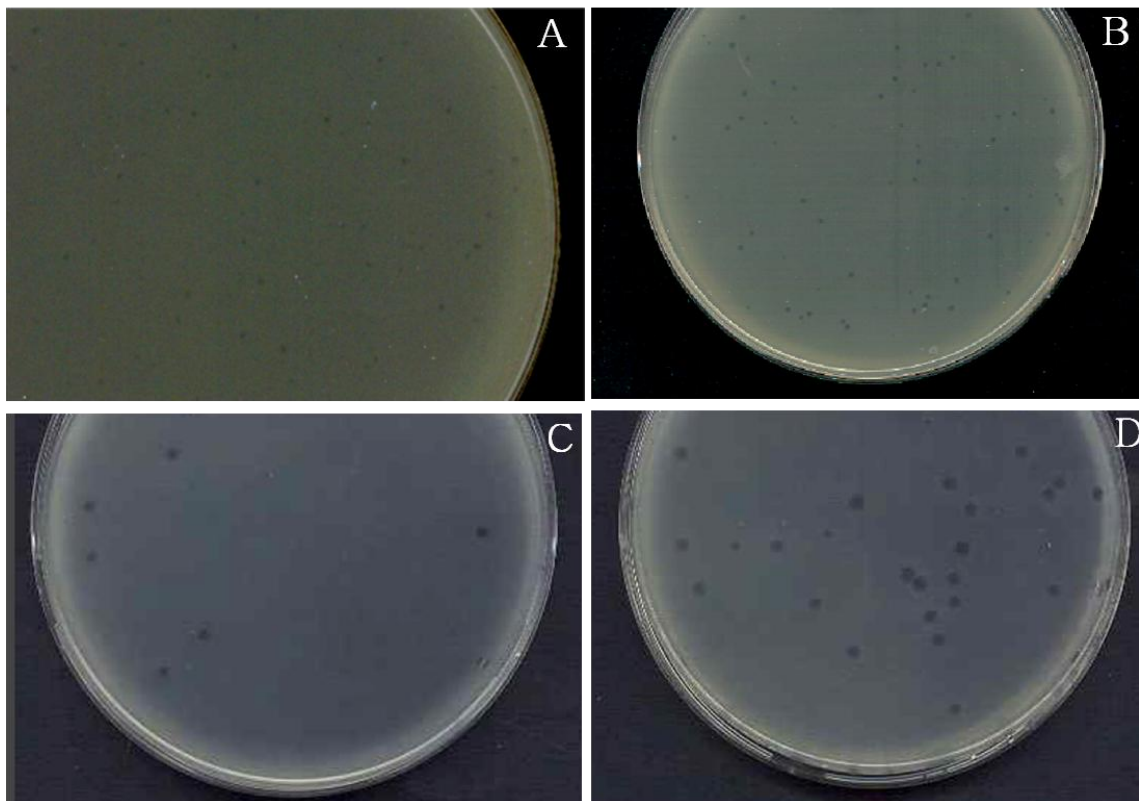
The morphology of phage PVP-SE1, PVP-SE2 and PVP-SE3 was analyzed using transmission electron microscopy (TEM) (Figure 2:3).



**Figure 2:3:** Transmission Electron Microscopy analysis of phage PVP-SE1 (A), PVP-SE2 (B) and PVP-SE3 (C).

Morphologically, phage PVP-SE1 belongs to the *Myoviridae* family, which is characterized by its contractile tail, and resembles typical O1-like phages. However, this phage has a head size of 84 nm and a tail of 120 by 18 nm, which is considerably larger than those of typical O1-like phages (72 nm, 113 by 17 nm) [23], [62], [63]. Phage PVP-SE2 and PVP-SE3 are Jersey-like *Siphoviridae* with a head size of 57 nm, tail 125 x 8 nm and base plate with three or more spikes (Figure 2:3) (Data provided by H.-W. Ackermann, Université Laval,

Quebec, Canada). The two phage families displayed plaques with different aspects, as showed in Figure 2:4 below.



**Figure 2:4:** Images of the plaque characteristics of: PVP-SE1 produced in S1400/94 *Salmonella* host (A) and in a nonpathogenic host (B); PVP-SE2 produced in 821 *Salmonella* host (C); PVP-SE3 produced in 869 *Salmonella* host (D)

The characteristics of the plaques formed by PVP-SE1 produced in S1400/94 *Salmonella* host are matted and small (Figure 2:4–A), while PVP-SE1 produced in *E.coli* BL21 displays small but clear plaques (Figure 2:4–B). Both *Siphoviridae* phages show large and clear plaques (Figure 2:4:C-D).

### 2.2.2.2 Phages Sequencing

The results obtained under the selection procedures provided us the information about the lytic spectrum of phages and their subsequent potential as a tool in a detection system. Phage

PVP-SE1 showed the ability to lyse a very broad range of *Salmonella* strains, broader than the well-described phage Felix O1 [14]. PVP-SE1 was able to infect several *Salmonella* mutants, defective in core the polysaccharide assembly, suggesting that the receptor for this phage is the conserved LPS inner core region, which explains its broad lytic spectrum [28]. Therefore it is expected that the phage recognition elements located at the tail, the tail fiber proteins (TFPs), may also exhibit binding abilities to a broad range of hosts. As a result, TFPs alone may prove to be useful entities for the construction of a diagnostic tool for the fast detection of *Salmonella* spp. and its control. Apart from PVP-SE1, the TFPs of phages PVP-SE2 and PVP-SE3, which only infect a few *Salmonella* serovars, may help us to understand whether the width of the lytic spectrum is determined by their TFPs. We therefore decided to sequence phage PVP-SE2, to identify its TFPs and compare them to their counterparts of PVP-SE1 [28].

### ***Salmonella* Phage PVP-SE1**

The isolated polypeptides sequenced in scope of this work are described below and the whole patent document can be consulted on Appendix A (inside the CD). The nucleotide sequences are identified by SEQ ID No 1-6 and protein sequences from SEQ ID No 8-12. Sequence identification corresponds to the numbers identified on patent and the information per protein sequence acquired from databases as PFAM and BlastP is presented in Table 2:4.

#### **SEQ ID No. 1: Nucleotide sequence of wt PVPSE1gp40 (1815bp)**

```
atgtatcctattccatgtctctcttgacattatctggaggaggaacagaaccactaccaccaggtagtgttaagaaggtggcctttacc  
gtggctctggttgggtggtgctacaaaagggtcaatggcgatcctcctgattgatgggagactctataccaaggggataatgcgtggtct  
gaatgcgcaaacgggaacataagcccgttaaggatcattggcacttggcggctaatggtgtagctgatgttttgggtggtgtagagc  
ctttgttgcaatacaacaatggtggctggcagtttggggacaccagtcattcactggtagtgggtctatctattctcttgacaa  
gcttccttcatcaatcacaggcacagtatccctcgcaatttacaagtgttcttgtgctctcggtaacacactctggcagatggtatg  
ggaagactttatggaagcgggtcaaacacaaatggatgccttggctctggttaatactaccgtaatatcgatccaagaagtattagtga  
tcctctgtgagagcttacagcttaaatgcttgcgtgacatacctgaacaatattggacttcccgtgtttggtggggccacccatcagatag  
atggtacttcaacaacacacaaaactttatc gatgtagtttgcctctgtgactgaaaccgtctatgttaaagagtgttagcgaac  
gaaacaaactcaatggctatcgctctacaggtgttgatgatacagagcattatfatatacagggggtatcgggacagcccaatactc  
aagaagagggtattggtccttcgagacattcagggttatcgacggtggtcagctctcatttctgattgctgataacaagctttacggtct
```



## Chapter 2. Selection and Characterization of *Salmonella* Phages

---

tggtgacctaagtgtcaacttggccttggcacaccatcaacaatggtgttagaaccgaccttgtccagttcctacaggaaggattg  
ggatcttcgaagctgacatacattgtagacatgaagacagatgtccttaaccaggggaactctatagccattggatggtgatgacgg  
gaacctttactacgctgtaacctttatggttctttgggtcaaccgatagcactgggtgagttcacaacatcccagaagcatccttgggg  
ggacaactgcggatgctatcaccacaggtctatcccatacgtatcaaagggtcgagaagtaacttacgtggactgttgagccagc  
agatgctgagatttatgatatttcgttcacatcgagtgtcctaatatcgcaactgtagactcaaagtgtatcatgacctccttgaagaggg  
tggtttgacatcacaatgactgctaaaacagggctggcgcggatgctaaaactcacagatacttctggcggttatgtttccatcttct  
ctgtgactaccgattccatcccacaaaaggaagttggtgatgttctgtgtcatggataaaaacagtctgactatacaccaggtccga  
acgtgtcggaatggaaatttctccagccaatgttgatactaactcatagacggagaattaacaactacaaatccggatgtggtgatgat  
tgatgaggggtgattccttctgtattgcagttggtgatgccggtgtggtgttccttattacagggagggtcaggttgaggcatttga  
tgattcgtatgtcagtttcagacttcacagccccaccagatcctgtggacccccgcgaaccagttgtaccttctcaaccgcaataa

**SEQ ID No. 8:** Protein sequence of wt PVP-SE1gp40 (605 amino acids)

MYPIPCFLFLTLSSGGTEPLPPGSVKKVAFTRGLVGGATKRSMALLIDGRLYTQGDN  
AWSECANGNISPFKDHWHLAANGVADVFGGGRAFVVKYNNGGWQYCGDTSQFTG  
SGSIYSSWTSFPSSITGTVSLANLQSVSCALGNTLWQMVDGRLYSGSNTNGCLGSG  
NTTVISIPRSISASSVRAYSLNACVTYLNNIGLPRVCGATHQIDGTSTTQTQNFIDVSFA  
SVTETVYVKEWLANETNSMAIASTGVDDTEHYLYTRGIGTAQYSKKEGIGPFETFRV  
IDGGQSHFLIADNKLYGLGDLAQLGLGTPSTMVLEPTLVPVPTGRDWDLSKLTIV  
DMKTDVLNQGNSISHWMVYDGNLYYAGNLYGFFGSTDSTGEFTNIPEASFGGTTAD  
AITTGSIPYAIKGSRSQLTWTVEPADAEIYDISFTSSAPNIATVDSNGIMTFLEEGGFDIT  
MTAKTGSGADAKTLTDTSGGYVSIFSVTDSIPQKEVGDVVFVMDKNSPDYTPGPNV  
VGMEISPANVDTNFIDGELTTTNP  
DVVMIDEGGFLSCIAVGDARCGVRLIYREGQVEAFDDSYVSVSDFTAPPDPVDPGEP  
VVPSQPQ

**SEQ ID No. 2:** Nucleotide sequence of wt PVPSE1gp41 (1809bp)

gtggcagacatgactcaatttgaacaggctgtcgtatcagggtgtgaagactctgaacgcctccacaaggtgtcaacggaacggcatc  
cgaaactgttgttactgaagatgtagcaccattccaacggctcgtaaagctcttcttgacaacctgttctttaaaccaccgctatgccgt  
ggatcgcgggtactcagaccagattcaaccagctttatgctttaaaggcacaatgggggtcaatggtggtatgaccaaccgcaa  
cagcaagcggcctgtcgtttaccacaaaaccagctaacagtgttaactggagattgtacaacgacgcagcggcgatggcatctat  
ctatgaccaatcaacagcccgatctgacaggaaccacaggtccaaccctgcggctaacagcaacagtacaacaattgccac  
aactgccttgttacaaccgctattgcaagcgcctgtcaagcatctcaggtggtagttaccttgcacacctgtctgtaacaggtgcta  
caactcaatagtttgggtggtggggacaatcaccctaatggcctgtaaacgcagataactcaacaggtcgttccagaacctga

tcctgacaaaagagttgtcaagcttaccttcgtatttacagacgcagataatccgacattctttaagacgcgccttgacccatatgcatc  
caaaccacagcatccagacggacattattgtcaacggaacagtggctgaagatgatacaaccatgtctctgacaggtgtgggtaata  
acgtcttcgattatgtgtatatccgtggtaacgcaagtaaagatcctacagcaccgagattaaaggtctcaggtacaactgaggtagaaa  
acctgaatattacaggaacgtaacaggtatcaccttcagtgtcaacggactgatattcaccaaactctgttacaaccgacagcgggtg  
aactgtaggtggtagcttacaggtcagtggtgttaccaccttggaaacgcaacaatcggccttgatattacaagtgatctgaccgt  
aaacggtaataacaacactcgaagatttctctgcggtaacggaacatcactggtccattcacagtggtgggtaaccagctcattg  
gtggatttacaaccggaacagcagatgttacaattggcggaaaactctctgttacaggaacgtctgagtttattgaggatcttagcgtact  
tgccgatgttacagtcaggataacctgaccgtaaaccggatgtcaaccttaacaacgcaacaggaacaacgacagttaacaacctt  
gttattcagggtacggttacaggtcttctgttgacttgacaggtcagaacatcaacgtaggatctcttctctactggtgcagtaactgcc  
aatagccttacggtagcaggatcggcaatcttaaccaaggcaagtgtgaattcctgacacttattgctgaggatattgatagctctacag  
cggcatggtcccaagtggagattccaacatctacaacgtaacagtgatgcggatttaacaattggtgcttggcctgaaccgacagat  
gcttttctgctgtgatttacctgactcaagatggtagctgacactgtgactttagatcctaactactggttttaaacagcgaaaaca  
attaacgagacggctggttcggtagctattctcaattaacctataatggtgtgaaggcgggtgtatcgacactgtaattgttcgctgctcc  
taa

**SEQ ID No. 9:** Protein sequence of wt PVPSE1gp41 (602 amino acids)

MADMTQFEQAVDQVVEDSERLHKVVNGTASETVVTEDEGSTIPTVRKALLDNLFFKT  
PPMPWIAGTQTTVFNQLYAFNGTNGVQWWYAPTATASAPVVLPQNPANSVNWRLY  
NDAAAMASIYAPINSPILTGNPQAPTPAANSNSTTIATTAFFVTTAIASALSSISGGSVTF  
ANLSVTGATTLNSLVVGGTIDLNGPVNADNSTGRFQNLILTKELSSLTFVFTDADNPT  
FFKTRLDPYAIQTHSIQTDIIVNGTVAEDDTTMSLTGVGNNVFDYVYIRGNASKDPTA  
PRLKVSQTTEVENLNITGNVTGITFSVNGLDISPNSVTTADGVTVGGDLQVSGVTNLG  
NATIGGLDITSDLTVNGNTTLEDFSAGNGNITGPFTVGGTSLNNGGFTTGTADGTIGG  
KLSVTGTSEFIEDLSVLADVTVQDNLTVNGDVNLNNAATGTTTVNNLVIQGTVTGLSV  
DLTGQNINVGSLSSSTGAVTANSLTVQDSAILTKASVEFLTLIAEDIDSSTAAWSPSGDS  
NIYNVTVDADLTIGAWPEPTDAFSAVIYLTQDGTGGHTVTLDPNYLVLNSETINETA  
GSVTILQLTYNGVEGGVIDTVIVRRP

**SEQ ID No. 3:** Nucleotide sequence of wt PVPSE1gp46 (1122bp)

atggcagcggccaacagtagctattgagattgggcttatggagatattgttcttctaaccacccatgaattaacaagaacacgctcctatcg  
atgacctgtggaacaaaggtgggaccttggtaaaagccaacagtcgaagaatttaactacgttttaaatatgctgactgcatgggcca  
agtatatcactggtagcagatccctggctcgcagagtcgttcttacgtgtgaatcagaacctgcagacctgcagacaaggccgcag  
caagaacaaacctgatgtttggagtaaacagagtctgataccagatatgtgaacattcaggcgacacctgactggtgcattatctg

## Chapter 2. Selection and Characterization of *Salmonella* Phages

---

ttccacgcctgaacctccaacctccgaatcagattacgcatacatcacgaccaccaaccagcagcagacaccacattctttgattttg  
tagttggtgataatatcggaatgccccaggtacgctgagcatcgatagatgctgttccgcttcgcccctctggtggctcaatctcaca  
atgatggagttgaatcgcatcagtgccactgctgactgtgtagggtaactgtaacattatcgcaagcgggaagtataagcggtgcaa  
gcgtcactgcaaccactgcaaacctcacaactaccgtaagcggtagctgaatgctccaactattcagtcacaacaatcaggac  
agggaccttaacggcaacaggaacgttcaagggttcaacggtgctgcaacaagctctttaacaaccccatatgccagtgtaacgga  
cagtgtaacgttaactcccttgtgtcaacaactccgctacagttggtggacgaaacggtgtgagagcaatcaatggtgcaacggc  
agatggtaacggtaacgtcacactaaactgctggtttggtcagcagatccgtttaggtaataggtttgccacaggtgtaagtgaatcc  
agattttatgcaggtcacgtcatgaccgggtgggctttcgtaacaagaaagaattgaggggagcaacttactactgcaccactaca  
gtatctcattaacggacaatgggtaactgtttccaacctggactaa

**SEQ ID No. 10:** Protein sequence of wt PVPSE1gp46 (373 amino acids)

MAAPTVPPIEWAYGDIVLPNTHLNKARPIDDLWNKGWDLGEKPTVEEFNYVLNML  
TAWAKYITGEQIPGLDSRFLRVNQNLDLADKAAARTNLDVWSKTESDTRYVNISS  
DTMTGALSVPRNLQPSESDYAYITTTNPAADTTFFDFVVDNIGNAPGTSSIDSMRF  
RFVPSGGSIFTMMELNAISGTAALCRVTGNIIASGSISGASVTATTANFTNTTVSGTLN  
APTIQSTTIRTGTLTATGNVQGFNVVATSSLTTPYASVNGQCNVNSLVNNSATVG  
GRNVVRAINGATADGNGNVTLNLSGFVQQIRLGNRFATGVSESRFYAGHVMTGWA  
FGNKKELRGATYYTAPLQYLINGQWVTVSNLD

**SEQ ID No. 4:** Nucleotide sequence of wt PVPSE1gp48 (1494bp)

gtggctgctcaatatggattaaatgactacggctttgcatccatccctcagatgattaatcgagataccaagcagtcgctgatccgaa  
ctttggtgaaaactcaacactcaggtaacactgtgttgacaaactaccacaatttgaatgaaagagaatatcagttgatccttctgg  
ctgaggctgtgtattctgcacagacactgcaggggcagaaggattttatcttgatgaactgcttgctgctggtattatcgtcgtggt  
aaaaccagaggatcaggtactatccagatggttgaacaacaccgtccgtacaacatgatttacgcttcaacatagcattgaca  
gtgtaacttcgtactcacgcaggacactcctgctgcagggaatatcctggcgcaacaatccttaaccaagattgggttcttgtaact  
atacgttccagatgattaatcagaacgatggttcaacaaatcaatgaacttgacgctaagtaataaggtgcctaacagccctcagttaa  
atgcttcatgctatcgattaaggatttcattgttgacaactccacacagttaaacgaagacaggatcttcattgactctgagggtggagc  
gatgtatcgggtatgatgtaacaagaaaatgatcgacttaacagtcgtgttgattccggtcatcaccgtagtgggccagagaac  
aattaccattgaagtaattgctgctgaagcaggggctatttctcgtgaagcaaactgtaacgaatatcacaccgacaccaagcggttt  
atcagcatgaccaacatgaccgctttaatgacggttccgatgttgagacagacactgattacaaggttcgtgcttcacaaagcaccgc  
agcaggtgctgctgccactagacctgccgttatttctcgtgaagcaaactgtaacgaatatcacaccgacaccaagcggttt  
aggggaaacagaccagtttgggttccggcatataagttgagactgtagttatggtggtccacagaagaaatcagtgaaagcactttat  
aacacaatcgattgccaacgcaacctatggtaatgtttttatgatgttaccacagaggatgatcagacggaacgtatctatcacagca

aagcacaggctcgtgagcttgagctccgtggttcgttataaaggaaagctcctgtccgtgacagagcaaaacactatcaaagatgcattg  
aaagccgttggtgacacctcaacattgcagatacactttacaacatccagttggtatccgcagttggttctctatttcaccagggcgcttc  
acgcaattgttggtgatgtaagaacactgaccaacctgacagtgcttatactaacagcgatgttggtgcaggtatgacagaagtctttg  
cttagatacagacgacattacattccagcaaatcatctaa

**SEQ ID No. 11:** Protein sequence of wt PVPSE1gp48 (497 amino acids)

MAAQYGLNDYGFAIPSLDDLIADTKQSLIRTFGENFNTQANTVVDKLTILNEREYQ  
LILLAAVYSAQTLAGAEGIYLDELLGRRGIYRRGKTRGSGTIQMVVNNTVPYNMIY  
SSSTYSIDSGNFVLTQDTPVAGNILAQQILNQDWVLGNYTFQMINQNDGSTKSMNLT  
LSNKVPNSPQLNAFMSSIKDFIVDNSTQLNEDRIFIDSAGGAMYIGYDANKKMIGLNS  
RVDFRSSPVVGQRTITIEVIAAEAGAISREANTVTNITPTPSGFISMTNMTAFNDGSDV  
ETD TDYKVRASQSTAAGAAATRPAVISA VLNVEGVSKVRVFSNNTGETDQFGVPAY  
KFETVVYGGSTEEISEALYNTIALSNATYGNV FYDVTTEDDQTERIYHSKAQARELA  
VRVRYK GKLLSVTEQNTIKDALKAVVDPLNIADTLYNIQLVSAVGS SISPRFTQLLV  
DVKNTDQPDSAYTNSD VVAGMTEVFALDTDDITFQQII

**SEQ ID No. 6:** Nucleotide sequence of wt PVPSE1gp51 (675bp)

atggcagatgtttctttccaacgggtgaaggtctctgaccttccctccgccgtcaccgtatctggtggtgactatgtagttatggatcaggc  
agacacaaccaggaaggcttctctgacaccatcatgactcgtatgggtattatgaaggtgtcttctttctgagggtgggttccttgaatc  
caagaaagaccttgattctttgatacgaatggaaggtattacacatggaatggtgtttaccgaaaacaattccaatgcatcttccccgt  
caaccacagggcggcatcagtgagaacgcctggcaagagttcggtgccagtggtggcggcggtcaacaggaaggtgtcaatcttg  
gcaatgtccaaggacagcaacatgtaaccttaacaggggtgattctttgtgccaactgacaggtggtcagtgctgtgcataattac  
caatccatcaacggctcaggatgatctcagtcgtttaccttaccttaacacaggggtacaggggcgaatttggttcatgcccagtaat  
attaagtgaattatgggcgtgtccagttcttcttataaaaccgggtccgagacatcttcagttcgtcacttatgatggtgggaatagtt  
ggttcggctcccttattatggcaggagttgagtaa

**SEQ ID No. 13:** Protein sequence of wt PVPSE1gp51 (224 amino acids)

MADV SFPTVKVSDLPSAVTVSGGDYVVM DQADTRKASLDTIMTRMGIMKV VFFSE  
GGFLESKKDLAFFDTNGKY YTWNGVYPKTIPMSSSPSTTGGISENAWQ EFGASGGGG  
STGKV VNLGNVQGTATCNLNRGDSFVANLTGGQCVVIITNPSTAQDVSQSFTLSLTQ  
GTGANL VSWPSNIKWNYGRVPVLSYKTGVRDIFQFVTYDGGNSWFGSLIMAGVE

## Chapter 2. Selection and Characterization of *Salmonella* Phages

---

The information per protein sequence, as acquired from the databases Pfam and BlastP, is presented in Table 2:4.

**Table 2:4:** Description of each PVP-SE1 gp and corresponding function.

PVP-SE1 gp	SEQ ID No	Length (a.a)	Search tool	Putative Function
40	8	605	Pfam	Structural protein
41	9	602	BlastP	Tail Fiber protein
46	10	373	BlastP	Tail Fiber protein
48	11	497		Structural protein
51	12	224	BlastP	Structural protein

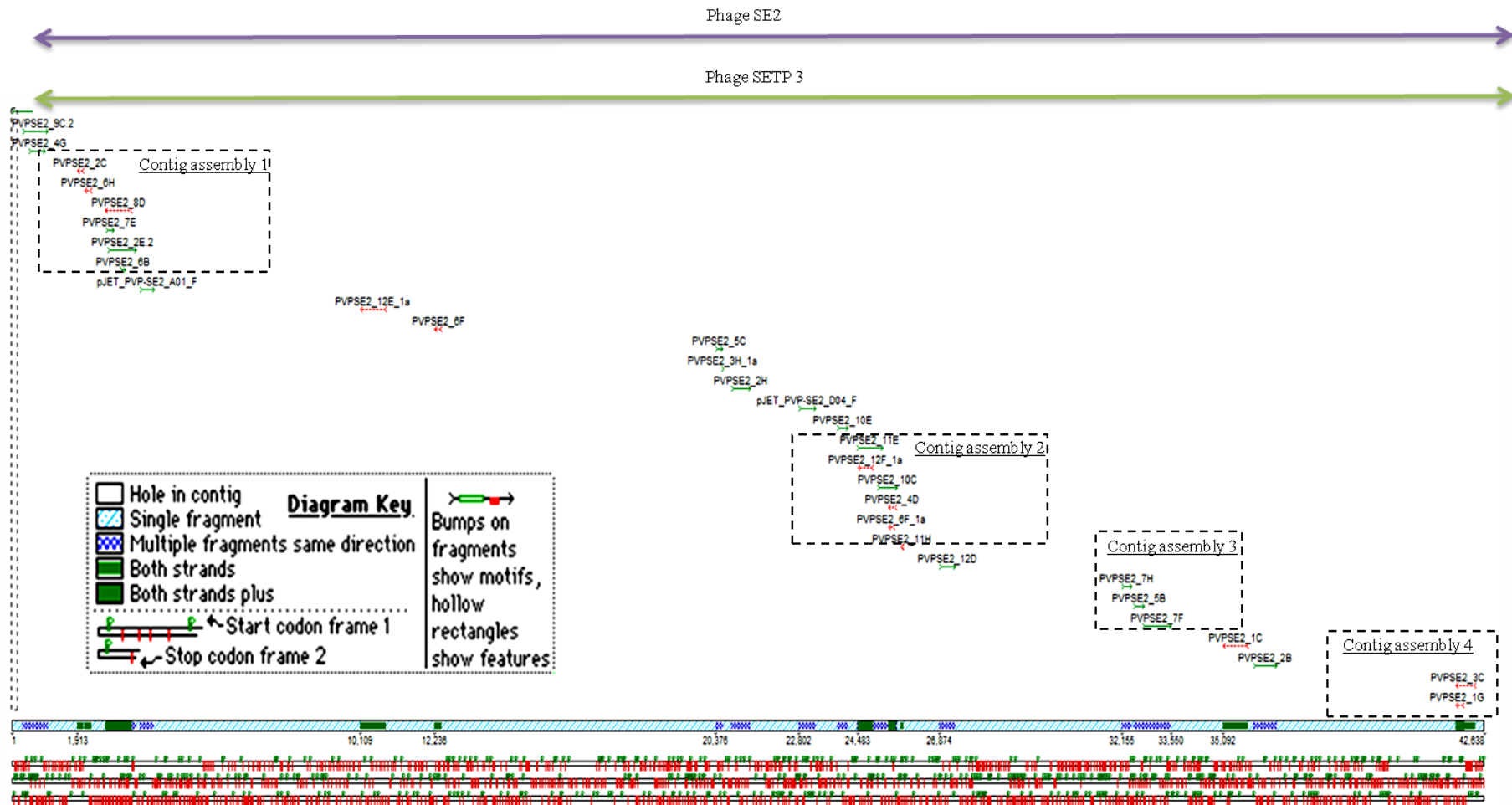
### *Salmonella* Phage PVP-SE2: Short Genomic Library

Phage PVP-SE2 was produced and purified and a shotgun library was created for sequencing. We found that the phage has an approximate size of 40.6 kb, which is in accordance with the usual size of phages that belong to the *Siphoviridae* family. The sequence was analyzed by BLAST (Basic Local Alignment Search Tool). Figure 2:5 shows the overlapping sequence of groups of contigs in blocks or scaffolds, filling gaps of the sequence. The alignment and their assembly to the two homologous phages, namely phage SE2 and SETP3, are also shown. Figure 2:5 presents the similarity (in terms of percentage) of our phage to the two homologous phages mentioned previously. The results show a genome with approximately 85 % of similarity with the sequenced phage SETP3 (NCBI Reference Sequence: NC\_009232.[29]). Another interesting phage included in this comparison was the recently sequenced phage SE2 [30], that even belongs to the same family and, despite bearing a similar name is not 100% identical to our phage. Both are *Salmonella enterica* serovar Enteritidis phages. Moreover, two putative TFPs were identified as gp4 and A01 and their position in the genome sequence is shown in Figure 2:6. Observing the sequence, the two TFPs share homology between each other, which may indicate functional similarity.

#### **Protein sequence of gp4 (684 amino acids):**

MSSGCGDVLSLNDLQVAKKHQIFEAEVITGKQGGVAGGADIDYATNQVTGQTQKTL  
PAVLRDAGFSPASFNFTTGGTLGADDADKAVLWPKEDGGDGNYYAWRGS LPKVIP  
AASTPLTAGGISDSAWVAFGDITFRAEADKKFKYSVKLSDFTTLQQ LADA AVDSILID  
RDYNFNNNETVNF GGKTLTIDCKAKFIGDGNLVFTQLGKGSIVVAPFMESATTPWVI  
KPWTDNNEWITDPAAIVATLKQSKTDGYQPTVNDYAKFPGIESLLPPEAKDQNISSV  
LEIRECTGVEIHRASGLMACFLFRGCHFCRMVDADNPSGGKDG VITFENLSGDWVK  
GNYVIGGRTSYGSVSSAQFLRNNGGFARDGGVIGFTSYRAGESGVK TWQGTVGSTT  
SRNYNLQFRDSAVLYPVWDGFDLGADTDINPEDGRPGDFPYSQYPVHMLPLNHLID  
NLLVRGSLGVGLGMDGQGLYVSNITVEDCAGSGAYLLTHETVFTNIAIIDTNTKDFP  
ANQIYISGACRVNGLRLVGIRSTSGQGMTIDAPNSTVSGITGLVDPSRIN VANLAEEG  
LGNSRINSFN SDSAALRLRIHKLSKTLDSGSVYSRINGGPGSGSAWTEITAIAGSLPDA  
VSLKINRGDYRAVEIPVAMTVLPDNAV RDNGSISLYLEGDSLKALVKRADGSYTRLT  
LA

## Chapter 2. Selection and Characterization of *Salmonella* Phages



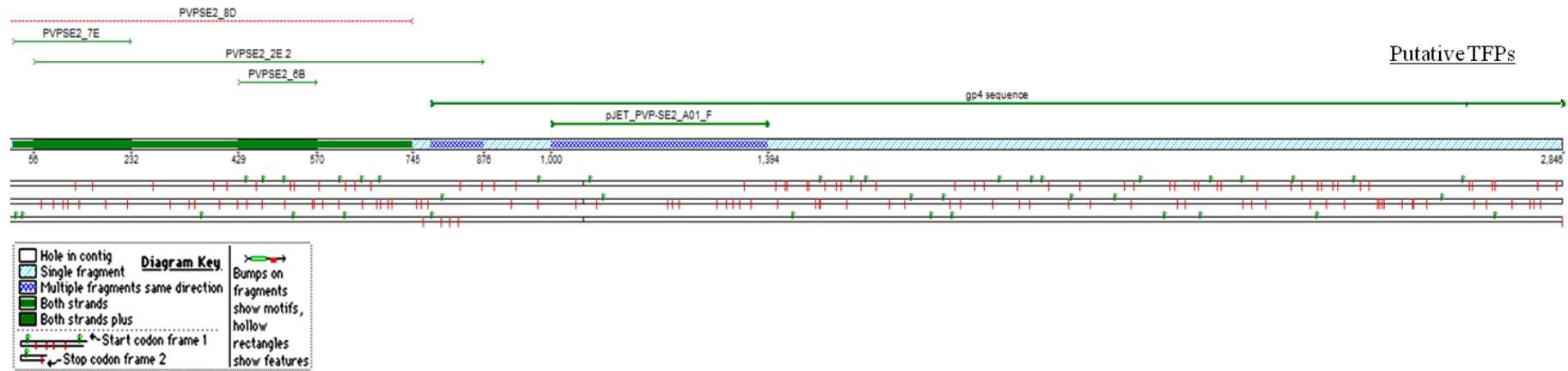
**Figure 2:5:** Genome assembly of PVP-SE2. Overlapping sequences of groups of contigs in blocks or scaffolds, filling gaps of the sequence. Each scaffold of contigs corresponds to a "supercontig" called Contig assembly 1-4. The sequences are assembled to two homologous phages, Phage SE2 and SETP3.

**Table 2:5:** Percentage of similarity between the short sequence of PVP-SE2 and phage SE2 and SETP3

	SE2_phage	SETP3	Contig 1	Contig 1#2	Contig 3	Contig 4	pJET_PVP-SE2_A01_F	pJET_PVP-SE2_D04_F	PVP-SE2_10E	PVP-SE2_11H	PVP-SE2_12D	PVP-SE2_12E_1a	PVP-SE2_1B	PVP-SE2_1C	PVP-SE2_2B	PVP-SE2_2C	PVP-SE2_2H	PVP-SE2_3H_1*	PVP-SE2_4D	PVP-SE2_5B	PVP-SE2_5C	PVP-SE2_6F	PVP-SE2_6H	PVP-SE2_7F	PVP-SE2_7H
SE2_phage	87	0	90	99	94	31	80	88	43	79	28	38	33	96	32	92	53	38	86	81	32	35	87	95	
SETP3		97	88	0	92	31	78	94	42	92	29	39	31	88	36	93	50	35	97	90	31	38	89	96	
Contig 1			0	0	0	0	0	0	0	0	0	0	0	0	0	0	0	0	0	0	0	0	0	0	0
Contig 1#2				0	0	0	0	0	0	0	0	0	0	0	0	0	0	0	0	0	0	0	0	0	0
Contig 3					0	0	0	0	0	0	0	0	0	0	0	0	0	0	0	0	0	0	0	0	0
Contig 4						0	0	0	0	0	0	0	0	0	0	0	0	0	0	0	0	0	0	0	0
pJET_PVP-SE2_A01_F							32	0	0	0	0	0	0	0	0	0	0	25	0	0	20	0	0	0	
pJET_PVP-SE2_D04_F								0	0	0	0	0	0	0	0	0	0	36	0	0	25	0	0	0	
PVP-SE2_10E									0	0	0	0	0	0	0	0	0	0	0	0	0	0	0	0	
PVP-SE2_11H										0	0	0	0	43	0	0	40	0	0	0	0	0	0	0	
PVP-SE2_12D											34	40	31	0	39	0	0	0	0	0	0	0	42	0	0
PVP-SE2_12E_1a													33	23	0	34	0	0	0	0	0	0	28	0	0
PVPSE2_1B														28	0	0	0	0	0	0	0	0	0	0	0
PVPSE2_1C															0	30	0	0	0	0	0	0	33	0	0
PVPSE2_2B																0	0	53	0	0	0	0	0	0	0
PVPSE2_2C																	0	0	0	0	0	0	30	0	0
PVPSE2_2H																		0	0	0	0	0	0	0	0
PVP-SE2_3H_1a																			0	0	0	0	0	0	0
PVPSE2_4D																				0	0	20	0	0	0
PVPSE2_5B																					0	0	0	100	0
PVPSE2_5C																						0	0	0	0
PVPSE2_6F																							0	0	0
PVPSE2_6H																								0	0
PVPSE2_7F																									0



## Chapter 2. Selection and Characterization of *Salmonella* Phages



**Figure 2:6:** Putative TFPs identified as gp4 and A01 and their position on the sequence genome.

### 2.3 Discussion

The aim of this work was to select and characterize phages with a broad host range of *Salmonella* strains and to investigate the possibility of using them as a potential tool to use in the biosensing field. The highly specialized nature of phages and the uncommon existence in nature of broad host range phages (with a host range over species borders) makes the isolation of such phages a rare situation. In particular, the narrow host specificity of *Salmonella* phages and the relatively large number of pathogenic *Salmonella* strains exacerbate this difficulty [12], [31]. Due to their broad host range among *Salmonella* strains the phages presented in this study may have added value in phage therapy or detection field. Especially phage PVP-SE1 had our particular interest, since it was able to lyse almost all of the *Salmonella* strains used in this work and also bacteria other than salmonellae, e.g. the non-pathogenic strain *E. coli* BL21. Its ability to recognize *E. coli* BL21 created the hypothesis of producing this phage in an alternative, nonpathogenic strain, since it is believed that the broader the host range of a phage, the higher the probability of success in phage therapy and of finding alternative hosts in which to reproduce the phage [32]. When comparing the lytic spectrum of this phage to that of the well known phage Felix-O1 (a virulent phage originally isolated by Felix and Callow in 1943 [33]), we observed that PVP-SE1 presents a broader host range. Felix-O1 is used routinely as a diagnostic tool in the identification of salmonellae due to its ability to lyse up to 99.5% of *Salmonella* strains [34]. Therefore, like Felix-O1, the newly isolated phage PVP-SE1 is considered to have equal or better properties as a diagnostic tool.

On the other hand, the ability of PVP-SE1 to recognize *E. coli* can be a problem when developing a phage-based biosensor to detect *Salmonella*, due to the possibility of false positives. However, this limitation may be overcome if we manage to understand which TFPs are responsible for the recognition of *E. coli*. With the help of this knowledge we may then block or eliminate this specific binding characteristic. Based on sequencing information we could have an idea of some putative tail fiber proteins and which to use in binding affinity tests. Moreover, the partial sequencing of phage PVP-SE2 provided us with the information whether we are dealing with a new phage or not. The sequence showed a high percentage of similarity with SETP 3 and SE2 phage, however our phage is not 100% identical. Two genes encoding putative TFPs were identified as gp number 4 and A01. Currently, their gene products are being produced and examined for their binding capacities. After comparing them to the

## Chapter 2. Selection and Characterization of *Salmonella* Phages

---

binding characteristics of the TFPs of phage PVP-SE1 we expect to have more insight in to what extend the width of the lytic spectrum of both phages is determined by their TFPs. Then, using recombinant technologies that allow us to remove or add TFPs to each phage, we hope to obtain more data on their binding properties, which will ultimately be used to create a phage with a tailor-made lytic spectrum.

The genotype of the host in which a virus reproduces affects the phenotype of the newly formed virus progeny [35]. In contrast to mutation, antagonist pleiotropy may be applied simultaneously to almost all the members of a developing phage population and generally is determined only by the nature of the last host in which the phage was replicated, being independent of the previous phage history [36]. As a consequence of this ubiquitous phenomenon, the growth and adaptation of the virus to the new host will lead to the achievement of a new stock that may be divergent from the original [37], [38]. Taking this into account, it would be expected that the replication of a phage in a different host would lead to progeny with different characteristics. In fact, the phenomenon of host-controlled variation has already been reported for phages and is usually implemented in a few growth cycles; in some cases, the phenotypic change is evident right after a single growth step where phages lose their ability to infect and lyse their original host [36], [38–40]. Therefore, the use of a non-pathogenic host to produce phages for therapeutic purposes could be compromised by induced changes in the phage lytic spectrum. In this study, the lytic activity of the phage after its replication in the nonpathogenic strain *E. coli* BL21 (G1 to G6) showed an efficiency equal to that of PVP-SE1 produced in *Salmonella* (G0), and thus no host-induced modification of the phage or restriction by the pathogenic target bacteria occurred, i.e. there was no increase in the specificity of the phage to that strain with consequent narrowing of the host range. Therefore, in this case, it is expected that there will be no risk of treatment failure, in contrast to what happened in the past when phages were produced in laboratory strains and then used in therapy [41].

Comparing the one step growth curve parameters of phage PVP-SE1 grown in *Salmonella* S1400/94 (G0) and in *E. coli* BL21 (G6), it was observed that differences between the burst sizes and rise periods occurred that can be attributed to the use of a different host to replicate the phage: the phage had not suffered any genetic modification, and the only variable in the experiments (besides the phage generation) was the host used. When repeating the experiment using phage from G0 and *E. coli* BL21 as the host the same results were obtained. The increased safety and consequently the lower costs when producing phage PVP-SE1 in a

nonpathogenic host (*E. coli* BL21) can overcome the disadvantages of a smaller burst size and a longer rise period when compared to the phage production in the S1400/94 *Salmonella* host.

### 2.4 Conclusions

This work reports the selection and characterization of *Salmonella* phages, allowing us to find a phage with a broad host range among salmonellae. Phage PVP-SE1 presents a broad lytic spectrum, one even broader than that of *Salmonella*-specific phage Felix-O1. That characteristic was found to be an excellent opportunity when exploring the development of a phage-based biosensor. PVP-SE1 was able to lyse and could be produced in a nonpathogenic *E. coli* strain, without modification of its lytic spectrum, in this way ensuring its stability when used in phage therapy. Furthermore, the use of this nonpathogenic *E. coli* strain for PVP-SE1 production facilitates the production and purification processes by eliminating the risk of introducing a phage-resistant pathogenic bacterium. The resulting cost reduction and increased safety of the phage preparations will lead to easier and faster approval for commercial applications. Furthermore, this phage can be used in the creation of a small cocktail of phages able to act as biocontrol agents in salmonellosis. Moreover, their tail fibers, responsible for detecting different strains, can be explored as detection tools.

### 2.5 References

- [1] T. Community, S. Report, Z. Agents, and E. Union, “The Community summary report on trends and sources of zoonoses and zoonotic agents in the European Union in 2007”, January, 2009.
- [2] P. V Elgea, A. C. Loeckaertb, and P. B. Arrowc, “Review article Emergence of *Salmonella* epidemics: The problems related to *Salmonella enterica* serotype Enteritidis and multiple antibiotic resistance in other major serotypes,” vol. 36, pp. 267–288, 2005.
- [3] R. Bishop, B. Plikaytis, P. Fields, C. R. Braden, and R. V. Tauxe, “National *Salmonella* Surveillance System Annual Summary, 2004,” 2004.

## Chapter 2. Selection and Characterization of *Salmonella* Phages

---

- [4] J. Santander and J. Robeson, “Bacteriophage prophylaxis against *Salmonella* enteritidis and *Salmonella pullorum* using *Caenorhabditis elegans* as an assay system,” *Electronic Journal of Biotechnology*, vol. 7, no. 2, Aug. 2004.
- [5] L. Fiorentin, N. D. Vieira, and W. Barioni, “Oral treatment with bacteriophages reduces the concentration of *Salmonella* Enteritidis PT4 in caecal contents of broilers.,” *Avian pathology: journal of the W.V.P.A.*, vol. 34, no. 3, pp. 258–63, Jun. 2005.
- [6] R. J. Atterbury, M. a P. Van Bergen, F. Ortiz, M. a Lovell, J. a Harris, a De Boer, J. a Wagenaar, V. M. Allen, and P. a Barrow, “Bacteriophage therapy to reduce *salmonella* colonization of broiler chickens.,” *Applied and environmental microbiology*, vol. 73, no. 14, pp. 4543–9, Jul. 2007.
- [7] A. M. Donoghue, L. R. Bielke, S. E. Higgins, D. J. Donoghue, B. M. Hargis, and G. Tellez, “Use of Wide-Host-Range Bacteriophages to Reduce *Salmonella* on Poultry Products,” *International Journal of Poultry Science*, vol. 6, no. 10, pp. 754–757, Oct. 2007.
- [8] G. Arlet, T. J. Barrett, P. Butaye, A. Cloeckert, M. R. Mulvey, and D. G. White, “*Salmonella* resistant to extended-spectrum cephalosporins: prevalence and epidemiology.,” *Microbes and infection / Institut Pasteur*, vol. 8, no. 7, pp. 1945–54, Jun. 2006.
- [9] S. Matsuzaki, M. Rashel, J. Uchiyama, S. Sakurai, T. Ujihara, M. Kuroda, M. Ikeuchi, T. Tani, M. Fujieda, H. Wakiguchi, and S. Imai, “Bacteriophage therapy: a revitalized therapy against bacterial infectious diseases.,” *Journal of infection and chemotherapy: official journal of the Japan Society of Chemotherapy*, vol. 11, no. 5, pp. 211–9, Oct. 2005.
- [10] N. K. Petty, T. J. Evans, P. C. Fineran, and G. P. C. Salmond, “Biotechnological exploitation of bacteriophage research.,” *Trends in biotechnology*, vol. 25, no. 1, pp. 7–15, Jan. 2007.
- [11] M. Skurnik and E. Strauch, “Phage therapy: facts and fiction.,” *International journal of medical microbiology: IJMM*, vol. 296, no. 1, pp. 5–14, Feb. 2006.
- [12] M. Skurnik, M. Pajunen, and S. Kiljunen, “Biotechnological challenges of phage therapy.,” *Biotechnology letters*, vol. 29, no. 7, pp. 995–1003, Jul. 2007.
- [13] A. Sulakvelidze and Z. Alavidze, “Minireview Bacteriophage Therapy,” vol. 45, no. 3, pp. 649–659, 2001.
- [14] A. Villegas, Y.-M. She, A. M. Kropinski, E. J. Lingohr, A. Mazzocco, S. Ojha, T. E. Waddell, H.-W. Ackermann, D. M. Moyles, R. Ahmed, and R. P. Johnson, “The genome and proteome of a virulent *Escherichia coli* O157:H7 bacteriophage closely resembling *Salmonella* phage Felix O1.,” *Virology journal*, vol. 6, p. 41, Jan. 2009.

- [15] Kathy Walker ,“Use of Bacteriophages as novel food additives”, Food Regulation in the United States Michigan State University October 29 , 2006.
- [16] J. R. Clark and J. B. March, “Bacteriophages and biotechnology: vaccines, gene therapy and antibacterials.,” *Trends in biotechnology*, vol. 24, no. 5, pp. 212–8, May 2006.
- [17] C. R. Merrill, B. Biswas, R. Carlton, N. C. Jensen, G. J. Creed, S. Zullo, and S. Adhya, “Long-circulating bacteriophage as antibacterial agents.,” *Proceedings of the National Academy of Sciences of the United States of America*, vol. 93, no. 8, pp. 3188–92, Apr. 1996.
- [18] C. R. Tinsley, E. Bille, and X. Nassif, “Bacteriophages and pathogenicity: more than just providing a toxin?,” *Microbes and infection / Institut Pasteur*, vol. 8, no. 5, pp. 1365–71, Apr. 2006.
- [19] L. Bielke, S. Higgins, a Donoghue, D. Donoghue, and B. M. Hargis, “*Salmonella* host range of bacteriophages that infect multiple genera.,” *Poultry science*, vol. 86, no. 12, pp. 2536–40, Dec. 2007.
- [20] V. N. Krylov, S. Miller, R. Rachel, M. Biebl, E. a. Pleteneva, M. Schuetz, S. V. Krylov, and O. V. Shaburova, “Ambivalent bacteriophages of different species active on *Escherichia coli* K12 and *Salmonella* sp. strains,” *Russian Journal of Genetics*, vol. 42, no. 2, pp. 106–114, Feb. 2006.
- [21] M. Skurnik, M. Pajunen, and S. Kiljunen, “Biotechnological challenges of phage therapy.,” *Biotechnology letters*, vol. 29, no. 7, pp. 995–1003, Jul. 2007.
- [22] S. B. Santos, E. Fernandes, C. M. Carvalho, S. Sillankorva, V. N. Krylov, E. a Pleteneva, O. V Shaburova, a Nicolau, E. C. Ferreira, and J. Azeredo, “Selection and characterization of a multivalent *Salmonella* phage and its production in a nonpathogenic *Escherichia coli* strain.,” *Applied and environmental microbiology*, vol. 76, no. 21, pp. 7338–42, Nov. 2010.
- [23] S. Sillankorva, E. Pleteneva, O. Shaburova, S. Santos, C. Carvalho, J. Azeredo, and V. Krylov, “*Salmonella* Enteritidis bacteriophage candidates for phage therapy of poultry.,” *Journal of applied microbiology*, vol. 108, no. 4, pp. 1175–86, Apr. 2010.
- [24] D. W. Sambrook, Joe; Russel, *Molecular cloning: a laboratory manual*, 3rd ed. Cold Spring Harbor, NY: Cold Spring Harbor Laboratory Press, 2001.
- [25] J. Sambrook and D. W. Russell, *Molecular cloning: a laboratory manual*, 3rd ed. NY: Cold Spring Harbor Laboratory Press, 2001.
- [26] F. B. Alberts, E. Kutter, A. Sulakvelidze, W. C. Summers, B. Guttman, R. Raya, and K. Carlson, “Bacteriophages: Biology and Applications”,

## Chapter 2. Selection and Characterization of *Salmonella* Phages

---

- [27] H.-W. Ackermann, “5500 Phages examined in the electron microscope.,” *Archives of virology*, vol. 152, no. 2, pp. 227–43, Feb. 2007.
- [28] S. B. Santos, A. M. Kropinski, P.-J. Ceysens, H.-W. Ackermann, A. Villegas, R. Lavigne, V. N. Krylov, C. M. Carvalho, E. C. Ferreira, and J. Azeredo, “Genomic and proteomic characterization of the broad-host-range *Salmonella* phage PVP-SE1: creation of a new phage genus.,” *Journal of virology*, vol. 85, no. 21, pp. 11265–73, Nov. 2011.
- [29] N. De Lappe, G. Doran, J. O’Connor, C. O’Hare, and M. Cormican, “Characterization of bacteriophages used in the *Salmonella enterica* serovar Enteritidis phage-typing scheme.,” *Journal of medical microbiology*, vol. 58, no. Pt 1, pp. 86–93, Jan. 2009.
- [30] B. R. Tiwari, S. Kim, and J. Kim, “Complete genomic sequence of *Salmonella enterica* serovar Enteritidis phage SE2.,” *Journal of virology*, vol. 86, no. 14, p. 7712, Jul. 2012.
- [31] J. P. Higgins, S. E. Higgins, K. L. Guenther, W. Huff, a M. Donoghue, D. J. Donoghue, and B. M. Hargis, “Use of a specific bacteriophage treatment to reduce *Salmonella* in poultry products.,” *Poultry science*, vol. 84, no. 7, pp. 1141–5, Jul. 2005.
- [32] A. Canada and A. Meeting, “Phage therapy – Everything old is new again,” vol. 17, no. 5, pp. 297–306, 2006.
- [33] J. Kuhn, M. Suissa, J. Wyse, I. Cohen, I. Weiser, S. Reznick, S. Lubinsky-Mink, G. Stewart, and S. Ulitzur, “Detection of bacteria using foreign DNA: the development of a bacteriophage reagent for *Salmonella*.,” *International journal of food microbiology*, vol. 74, no. 3, pp. 229–38, Apr. 2002.
- [34] D. C. Hirsh and L. D. Martin, “Bacteriophage and High-Performance Liquid Chromatography,” vol. 45, no. 1, pp. 260–264, 1983.
- [35] H. V. O. F. Bacterial, “(Adams, 1950).,” 1952.
- [36] H. Variation, R. W. Eskridge, H. Weinfeld, and K. Paigen, “Susceptibility of Different Coliphage Genomes to Susceptibility of Different Coliphage Genomes to Host-controlled Variation,” 1967.
- [37] S. F. Elena and R. Sanjuán, “Evolution. Climb every mountain?,” *Science (New York, N.Y.)*, vol. 302, no. 5653, pp. 2074–5, Dec. 2003.
- [38] W. D. Crill, H. a Wichman, and J. J. Bull, “Evolutionary reversals during viral adaptation to alternating hosts.,” *Genetics*, vol. 154, no. 1, pp. 27–37, Jan. 2000.
- [39] G. Bertani and J. J. Weigle, “Host controlled variation in bacterial viruses.,” *Journal of bacteriology*, vol. 65, no. 2, pp. 113–21, Feb. 1953.

- [40] I. Brunovskis and R. O. Burns, "Growth of coliphage T7 in *Salmonella typhimurium*," *Journal of virology*, vol. 11, no. 5, pp. 621–9, May 1973.
- [41] S. Withey, E. Cartmell, L. M. Avery, and T. Stephenson, "Bacteriophages--potential for application in wastewater treatment processes.," *The Science of the total environment*, vol. 339, no. 1–3, pp. 1–18, Mar. 2005.



## Chapter 3

# Magneto-resistive Phage-based Biosensor

### Abstract

Salmonellosis still has a huge global health and economic impact as food- and water-borne disease. Low infection doses, high survival rates, persistence over inauspicious conditions and the potential to enter a viable but non-culturable (VBNC) state, but maintaining their virulence, are challenging features for any detection method. In fact, culture methods lack the capacity to detect VBNC cells, while biomolecular methods hardly distinguish between dead innocuous cells and their viable lethal counterparts. In this context we present and validate a novel bacteriophage-based microbial detection tool able to assess for *Salmonella* cells viability. The phage PVP-SE1 tested as a biological element in a previously validated bioanalytical platform was proven to discriminate viable and VBNC cells from dead cells, thus surpassing one of the epic challenges in dealing with false-negative and false-positive results. Besides, the combination of this “smart” biological element with highly sensitive magneto-resistive sensors provides a powerful detection system with high-level performance at the accuracy, specificity but also sensitivity level, detecting bacteria concentrations in the order of 100 cells/ $\mu$ L (3-4 cells/sensor).

### 3. Introduction

Food- and waterborne microbial contaminations are a serious worldwide threat to public health. The ingestion of foodstuffs and water contaminated with microbial pathogens (e.g. *Escherichia coli*, *Campylobacter* or *Salmonella*) is responsible for about 2.2 million deaths annually. To reduce the incidence and economic consequences of foodborne diseases, the World Health Organization (WHO) has been enforcing the establishment of a surveillance program to assure the safety of food along the food chain, from “farm to fork” [1]. Such actions have greatly stimulated R&D activities around new microbial tests, in particular on the level of biosensing technologies [2,3]. Biosensors are sought to provide outstanding performance, ideally working at the point-of-use, outside the central laboratory units. In contrast to the current time-consuming culture-based methods these devices are promising to deliver faster and more accurate results. Even so, there still exist some concerns that must be taken into consideration when adopting or developing a microbial analytical method. One of these involves the failure to detect an active pathogen when present, the so called false-negative.

The occurrence of false-negatives is often attributed to technological limitations, namely low sensitivity or matrix interferences and inhibitions. Not less important, however, are biological limitations such as the viable but non-culturable (VBNC) cells, which are bacterial cells that, despite being viable, do not grow on standard solid culture media and thus fail to be detected. As a result, the absence of colony forming units (CFU) in a culture plate is not a reliable or safe indication that bacteria are absent, dead, unable to grow or even unable to cause infection. In fact, under certain conditions, VBNC cells have been shown to resuscitate from this “dormant” state and return to an active metabolizing and culturable form, while retaining virulence [4,5].

The VBNC physiological state is reported for several pathogenic bacteria and occurs under the influence of different stress conditions, such as nutrient or oxygen limitation, osmotic stress, temperature and humidity changes and the presence of disinfectant agents [6]. Given that microorganisms in most food facilities and food-contacting surfaces are submitted to numerous sources of stress, including disinfection treatments, different physiological states namely viable, dead and VBNC bacteria in variable proportions are expected to be found within a bacterial population [7].

In this context, accurate microbial detection methods, able to identify the cell's physiological state, gain particular importance. Most of the established detection methods are based either on the classical culture plate assays, immunoassays (*e.g.* ELISA – Enzyme Linked Immunosorbant Assay) or DNA-based technologies (*e.g.* PCR – Polymerase Chain Reaction); all of these methods, for different reasons, lack this accuracy and therefore cannot prevent outbreaks from occurring. On the one hand, culture plate methods known as laborious and time-consuming suffer from false-negatives originating from the impossibility to detect the VBNC population. On the other hand, antibody and DNA-based assays, despite being very promising due to the rapid, sensitive and/or specific detection, are more prone to false-positive results but also, in particular cases, can give rise to false-negatives.

In the immunoassays case, false-negatives may occur upon antibody denaturation or inactivation. Antibodies are sensitive to environmental conditions such as temperature, pH or solvent nature and easily undergo irreversible denaturation, resulting in a limited shelf-life [8]. False-positives result from the general incapacity of the antibody to distinguish viable from dead cells, specifically recognizing both populations, but also from cross-reactivity among related species of bacteria.

Conversely, in PCR analysis, false-negatives can be related to interference with target-cell lysis reagents necessary for nucleic acid extraction, DNA degradation and/or direct inhibition [9]; false-positives come either from the detection of dead cells or from other unknown DNA sources. To overcome the tendency of PCR methods to overestimate the number of viable cells (false-positives) reverse transcriptase (RT)-PCR, an increasingly popular strategy, is used [10,11]. RT-PCR detects mRNA, a biomolecule that has a half-life of 3 to 5 min after cell death [12]. More common is the use of new DNA-intercalating dyes such as ethidium monoazide and propidium monoazide to block the amplification of DNA from dead cells [13]. Still it has been reported that the length of the PCR amplicon may influence the efficiency of removal of the dead cell signal [14]. Furthermore, these dyes are said to only penetrate the damaged membranes of the dead cells, not the viable ones, and bind to the respective DNA, preventing amplification. However, a compromised membrane may not always be associated to irreversibly inactive cells.

The same principle of actuation is the basis of other viability indicator dyes, mostly fluorescent molecules widely used in epifluorescence microscopy and flow cytometry. For instance, the commercially available kit format LIVE/DEAD® BacLight™ from Invitrogen

offers a combination of two dyes. In this case a green fluorochrome (SYTO9) able to enter all cells is used to assess total cell counts, whereas the red fluorochrome (propidium iodide - PI) only enters compromised cells. In a simplistic approach the viability dyes only discriminate a viable population (green stained cells) from a dead population (red stained cell). However, many reports in flow cytometry have shown that the staining of bacterial cells does not always produce distinct “live” and “dead” populations [15,16]; intermediate states with different amounts of both dyes, presenting a yellowish to orange coloration when observed under fluorescence microscopy and identified as compromised or “unknown” population by the cytometry kit, have also been observed. As discussed in more detail by Berney et. al. [17], this unknown population can be related to the presence of intermediate cellular states. Therefore, there is a clear need for “smarter” as well as more practical detection tools able to discriminate between the different cell states, while avoiding misclassification of VBNC or detection of dead cells. In this context, to address this challenge we here present and study a highly specific biomolecular detection tool – the bacteriophage.

Bacteriophages (or simply phages) are viruses that only infect bacteria while being innocuous to humans. Mainly due to their ability to specifically attach and capture bacteria, combined with robustness, great stability even under adverse environmental conditions and extended shelf-life, phages are considered very interesting biological elements or biodetection tools [18,19]. Accordingly, significant progress in the detection of foodborne and waterborne pathogens, making use of phages, has been reported [20-22]. A recent work describes the direct detection of *Salmonella* Typhimurium on tomatoes using a phage-based magnetoelastic sensor, proving the ability of detecting foodborne bacteria on fresh products by immobilized phages on a sensor surface [23]. Also, a recent publication reviews the phage-based diagnostics, approved by Food and Drug Administration (FDA), for a list of pathogens, including *Mycobacterium tuberculosis*, *Yersinia pestis*, *Bacillus anthracis*, and *Staphylococcus aureus* [24]. However, studies on the detection of VBNC bacteria using phages are still limited [25,26]. A phage labeled with green fluorescent protein (GFP), was used to analyze VBNC cells of *E. coli* O157:H7 in fresh water samples by epifluorescent microscopy [23]. Nevertheless, using fluorescence as the detection principle demands a rigorous sample pre-treatment mainly due to the presence of autofluorescent or light quenching entities that may interfere in the measurement.

Bearing this in mind, as well as the need to find a superior analytical technology to fulfill the foodborne pathogen detection needs, a well-characterized broad-spectrum virulent phage (i.e. PVP-SE1) that infects *Salmonella* was studied. Its potential as a superior microbial biodetection tool and biological element on a biosensor interface was evaluated. In this work, *Salmonella Enteritidis* samples at different states of viability were analyzed by the phage using different techniques. The VBNC cell state was induced by the disinfectant agent sodium hypochlorine (commercial bleach) and evaluated using the SYTO9/PI fluorochrome uptake kit (LIVE/DEAD® BacLight™) in combination with epifluorescent microscopy and flow cytometry techniques. Various tests on the phage ability to discriminate *Salmonella* cells in different physiological states (viable, VBNC and heat-killed cells) were successfully accomplished resulting in phage validation as a selective biorecognition tool. In fact, the combination of the PVP-SE1 bacteriophage with a previously developed and validated magnetoresistive bioanalytical platform [27-29] is a completely novel approach that allowed us to detect, identify and quantify different microbial samples.

### 3.1. Materials and Methods

#### 3.1.1 Media and Buffers Composition

The culture media components LB broth and agar were used for phage production. LB agar plates were prepared by adding 1.2% of agar (standard) to the LB broth. The soft agar used for the bacterial lawn was made by adding 0.6% of agar (soft agar) to the LB broth. The washing step on gold substrates was carried out combining phosphate buffer (PB) 0.1 M, pH 7.5, with 0.02% (v/v) of Tween 20. Phages were suspended in SM buffer (100 mM NaCl, 8 mM MgSO<sub>4</sub>, 50 mM Tris-HCl, pH 7.5. TE was prepared by mixing 10 mM Tris-HCl with 1 mM EDTA at pH 7.4. The buffer used to substitute the SM buffer on the experiments was 0.1M MOPS buffer (3-(N-morpholino) propanesulfonic acid) at pH 5.7. The blocking buffer used was bovine serum albumin (BSA). All reagents were provided by Sigma-Aldrich.

### 3.1.2 Bacteriophages and Bacterial Strains

PVP-SE1, a phage with a broad lytic spectrum against different *Salmonella* strains, was used as a biological element, and was isolated from a Regensburg (Germany) wastewater plant in a European Project Phagevet-P [30] *Salmonella enterica* serovar Enteritidis strain S1400 was used as a host [31]. *Campylobacter coli* phage vB\_CcoM-IBB\_35, isolated from poultry intestines, was used as a control [32].

### 3.1.3 Phage Propagation

The phages were produced using the double layer agar technique as described by Sambrook and Russell [33]. Briefly, from the obtained plaque forming units (PFU) ten were selected and transferred several times to three new Petri dishes with the proper bacterial soft agar. Using sterile paper strips, the phages were spread by passing the strips several times on the production Petri dishes and incubated overnight at 37°C. Then, 3 to 10 ml of SM buffer was added to Petri dishes and incubated overnight at 4°C (with agitation). The liquid was transferred to 50 ml tubes and centrifuged at 9000 x g during 10 min at 4°C (Hettich Zentrifugen-Universal 320) to remove the bacteria. One volume of chloroform was added to 4 volumes of supernatant and centrifuged at 9000 x g during 10 min at 4°C. The top liquid phase was removed carefully and filtered through a 0.2 µm filter (Minisart-Santorius stedim biotech). The phage titer was verified and the solution was stored at 4°C.

### 3.1.4 Phage Buffer Exchange

Phage immobilization occurred on gold surfaces chemically functionalized by Sulfo-LC-SPDP, an amino- and thiol (sulfhydryl) reactive heterobifunctional protein crosslinker and therefore phage buffer exchange was needed to remove the amine groups present in the SM-Buffer.

Buffer exchange was made using Vivaspin 500 Centrifugal concentrator (MWCO 100,000 Da), starting with a pre-rinsing step as described in the manufacturer's protocol. Then, the concentrator was filled with 500 µl of PVP-SE1 at a concentration of  $1.0 \times 10^{10}$  PFUs/ml and centrifuged at 9500 x g during 15 min. After the first centrifugation, the con-

centrator was filled twice with 400  $\mu\text{l}$  of 0.1 M MOPS, pH 5.7, and centrifuged as before. At the end, the filter walls were rinsed with 200  $\mu\text{l}$  of 0.1M MOPS and the final volume was approximately 300  $\mu\text{l}$ . Following the buffer exchange the concentration of phage was verified using the double layer agar technique [33].

### 3.1.5 Induction of *Salmonella* into Viable but Non-culturable (VBNC) State

#### 3.1.5.1 Induction of VBNC State

Bacteria were induced to enter the VBNC state using sodium hypochlorite (commercial bleach - stock concentration: 5%) at different concentrations. A single colony of *Salmonella* (S1400) was inoculated in 20 ml of LB broth and incubated overnight at 37°C/200 rpm. Following the pre-inoculation, 1 ml was transferred to 15 ml of fresh LB broth and incubated approximately 2-3 h at 37°C/200 rpm until the OD<sub>600</sub> reaches 0.5-0.7 (concentration at  $\sim 1.0 \times 10^7$  CFUs/ml). The cells were washed and resuspended in 0.1 M PB, pH 7.5. From the stock solution, aliquots of 500  $\mu\text{L}$  of bacteria were transferred to 1.5 ml eppendorf tubes. The eppendorfs were centrifuged at 4°C and 2370 x g during 15 min. The supernatant was removed and 1 ml of the following concentrations of sodium hypochlorite was added: 5%, 4%, 3%, 2%, 1%, 0.5%, 0.25%, 0.125%, 0.05%, 0.03%, 0.01%, 0.00875%, 0.0075%, 0.00625%, 0.005%, 0.0025%, and 0.00125% (v/v) to the bacterial pellet. The serial dilutions of bleach were done with milli-Q water. As a negative control milli-Q water was used. The samples were mixed during 1 min at room temperature and 200 rpm (Thermomixer Comfort eppendorf 1.5 ml). Following chlorination, the suspensions were centrifuged at 3420 x g during 10 min at 4°C and resuspended twice at 4°C in 0.1M PB, pH 7.5. The number of culturable cells (after bleach treatment) was determined based on colony counting and expressed in colony forming units (CFUs). The experiments were conducted in triplicate. Since the data were collected over several trials and over multiple days, all cell counts were normalized to a control value.

### 3.1.5.2 Determination of Viability by Fluorescence Microscopy

The OLYMPUS BX51 EXTREMO microscope was used to observe cells viability. The fluorescent dyes SYTO9 and PI (propidium iodide) were components of the LIVE/DEAD® BacLight kit (Invitrogen detection technologies). SYTO9 labels bacteria with intact and damaged membranes when in contrast PI only permeates bacteria with compromised membranes. Consequently, PI will compete for the same binding sites as SYTO9, reducing the green fluorescence when both dyes are present. The concentration of each dye was chosen according to the protocol provided by the manufacturer.

### 3.1.5.3 Determination of Viability by Flow Cytometry

The bacterial samples were stained with LIVE/DEAD® BacLight™ Bacterial Viability and Counting Kit (Molecular Probes®) following the manufacturer's specifications, and incubated for 15 min under dark conditions. Finally, flow cytometry measurements were done using a FACSCalibur flow cytometer using Cell Quest software (BD Biosciences). Data were analyzed using FlowJo software (Tree Star, Ashland, OR).

### 3.1.5.4 Resuscitation Tests

The resuscitation studies were carried out by adding 1 ml of VBNC cells to 15 ml of fresh LB broth. During seven hours 1 ml samples of cells were taken from the medium, centrifuged at 3420 x g during 10 min and resuspended in 0.1 M PB, pH 7.5. A hundred µl were then plated out on agar plates for overnight growth at 37°C. The number of reculturable cells was expressed in CFUs.

### 3.1.5.5 Phage Infection Parameters

Adsorption assays were performed to access the percentage of phages that adsorb to their host *Salmonella* cells at different states of viability (Viable, VBNC, dead) and under conditions that mimics the ones used in the platform. Briefly, host cells were grown to reach the exponential phase ( $OD_{600\text{ nm}} = 0.6$ ), centrifuged at 6000 x g for 10 min and resuspended in 0.1 M



PB, pH 7.5. Different treatments of cells were made, as described previously at III. 2.5.1. One ml of cells was then infected with the *Salmonella* PVP-SE1 phage at a multiplicity of infection (MOI) of 0.001. Samples were taken every 10 min for 40 min, diluted in 1:10 of 0.1 M MOPS, pH, 5.7, and centrifuged at 10000 x g for 10 min. The supernatant was diluted using 10-fold serial dilutions in MOPS. Three independent replicates of each adsorption experiment were performed.

Single-step growth experiments were performed in order to assess the latent period and burst size of a single round of phage replication in viable exponential phase grown *Salmonella* cells. The procedure used was identical to the adsorption assays except that the samples, taken from the cell cultures infected with phages at 0, 20 and 40 min, were immediately plated (without being centrifuged) and their titre determined by the double-layer agar plate method in LB medium.

### 3.1.6 Preparation of Gold (Au) Substrates

A 15 cm (diameter) silicon wafer was provided with a thin film of chromium (Cr) (5 nm), followed by an Au layer (40 nm) by sputtering (Kenosistec11 Targets). Then, the substrates were diced in an automatic dicing-saw, resulting in  $7 \times 7$  mm<sup>2</sup> square pieces. Before the dicing process, the wafer was covered with a photoresistive polymer to protect the substrates from impurities due to the dicing process.

### 3.1.7 Optimization of Phage Immobilization on Au Substrates

Two phage immobilization methods, physical adsorption and covalent cross-linking, were tested. For both methods, Au substrates of  $7 \times 7$  mm<sup>2</sup> were incubated for 2 h in Microstrip® 3001 (Fujifilm Electronic Materials, Belgium) at 65°C to remove the protective coating of the photoresistive polymer. The substrates were then washed three times with isopropanol and sterile, distilled water and dried under a N<sub>2</sub> stream.

### 3.1.7.1 Physical Adsorption

Phage PVP-SE1 (prepared in 0.1 M MOPS buffer) was immobilized by physical adsorption over the Au substrates. The phage spots (1  $\mu$ l) at a concentration of  $1.0 \times 10^{10}$  PFUs/ml were incubated 2 h at room temperature in a humidified atmosphere to prevent evaporation. The unbound phages were removed by washing three times with the corresponding buffer.

### 3.1.7.2 Covalent Cross-linking Immobilization

Approximately 50  $\mu$ L of sulfosuccinimidyl 6-[3'-(2-pyridyldithio)-propionamido] hexanoate (Sulfo-LC-SPDP, Thermo Scientific) was placed over the Au surface and incubated at room temperature for 1 h in a humidified atmosphere. The excess of cross-linker was removed by rinsing with 0.1 M phosphate buffer (PB), pH 7.5. After the chemical functionalization, phage immobilization was continued as described for the physical adsorption method.

### 3.1.7.2 Blocking of Au Substrates

Both immobilization methodologies used 1% BSA in TE as a blocking buffer. The incubation was carried out during 45 min at room temperature. The excess of blocking solution was removed by washing the substrate with PB 0.1 M, pH 7.5. All substrates were exposed to  $2.8 \times 10^9$  cells/ml during 45 min and washed with  $\sim 3$  ml of serial solutions as follows: PB 0.1 M, pH 7.4; PB/0.02% Tween 20 and distilled water. In addition, the blocking performance was carried out using the following combinations: 1% BSA in milliQ-water; 1% BSA in TE and SH-PEG. This procedure was applied to the experiment using a covalent cross-linking immobilization. Two additional combinations were used: 1% BSA in milli-Q water and TE were incubated separately during 30 min. Next, the sequence was inverted, incubating first with TE and BSA 1% in milli-Q water at the end (30 min/component).

## 3.1.8 X-ray photoelectron spectroscopy (XPS)

The composition and chemistry of model biofunctionalized surfaces was characterized by X-ray photoelectron spectroscopy (XPS) using an ESCALAB 250 Xi system (Thermo Scientific).

### 3.1.8.1 Sample Preparation

The samples for XPS analysis were prepared on gold substrates freshly cleaned for 15 min in UV-ozone cleaner followed by soaking in ethanol for 30 min. The molecular depositions for characterization of the individual preparation steps were carried out by either soaking the substrates in the appropriate incubation solutions, or by manually spotting the solutions onto samples. After the deposition samples were rinsed with 0.1M PB, pH 7.5, and dried under a clean dry N<sub>2</sub> stream.

### 3.1.8.2 Analyses on ESCALAB 250 Xi System

ESCALAB 250 Xi is equipped with a monochromated Al K $\alpha$  X-ray source, a hemispherical electron energy analyzer, an automated sample stage, and a video camera for viewing the analysis position. The measurements were performed at room temperature in an ultra-high vacuum chamber with the base pressure  $<5 \times 10^{-10}$  mbar. Gold substrates ensured sufficiently high conductivity for the molecular film samples in this study, so additional charge neutralization was not necessary. The standard analysis spot of ca.  $900 \times 600 \mu\text{m}^2$  was defined by the microfocused X-ray source; smaller source-defined ca.  $500 \times 300 \mu\text{m}^2$  X-ray spots were used to analyze the samples prepared by spotting the incubation solutions. Line scans and control measurements at different spot sizes were performed to locate and confirm the positions of the spotted sample areas.

To produce accurate binding energy (BE) measurements, the energy of the monochromated Al K $\alpha$  X-ray source was measured to be within  $<0.2$  eV from 1486.6 eV. The BE scale of the analyzer was calibrated to produce  $<50$  meV deviations of the three standard peaks from their standard values: 83.98 eV for Au 4f<sub>7/2</sub>, 368.26 eV for Ag 3d<sub>5/2</sub>, and 932.67 eV for Cu 2p<sub>3/2</sub>. In agreement with the BE calibration, the Au 4f<sub>7/2</sub> peak was observed at  $84.0 \pm 0.1$  eV for all the samples. The aliphatic C 1s peak was typically observed at

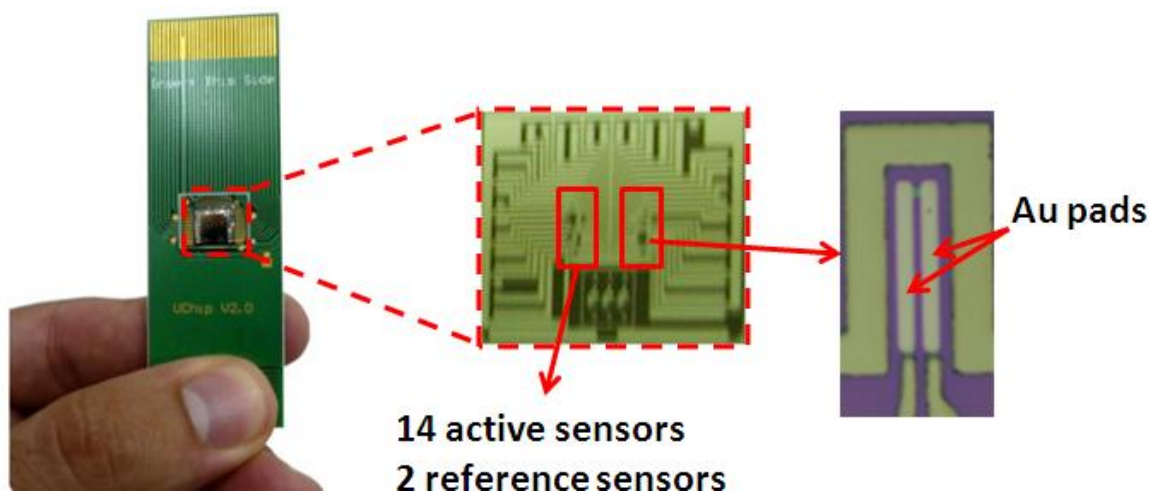
284.6±0.2 eV, i.e., at the value that is commonly measured for organic monolayers on metal substrates.

Regarding the instrument settings, a high-resolution elemental XPS data in Au 4f, C 1s, O 1s, S 2p, and N 1s regions were acquired with the analyzer pass energy set to 20 eV (corresponding to energy resolution of ca. 0.36 eV) and the step size set to 0.1 eV. Additional high-resolution scans were performed in regions corresponding to elements (including Na, P, and F) expected to be present in samples or detected in wide survey scans. All the spectra were acquired in normal emission with an effective analyzer collection angle of ca. 30°.

### 3.1.9 *Salmonella* Detection in the Magnetoresistive (MR) Biochip

#### 3.1.9.1 Biochip Design

The chips used were provided by INESC- Microsystems and Nanotechnologies and the biochip design comprises of an array of 32 U-shaped spin-valve (SV) sensors fully passivated with an oxide layer. The sensors are arranged in two sensing regions (Figure 3:1), each one including 14 active sensors plus two reference sensors. The active sensors correspond to the biological sensors and are covered with two thin gold pads (composition equal to 3. 2.6.) RF-sputtered and patterned by lift-off on top of the sensor. The reference sensor corresponds to the sensor without a gold pad, thus making it biologically inert [34]. The microfabrication process is performed in a clean room environment. The detailed process has been described previously [34-36].



**Figure 3:1:** Magnetoresistive biochip. Left: Magnetoresistive biochip mounted on a printed circuit board (PCB) chip carrier; Middle: Biochip with two columns, each containing 14 active sensors (with Au pads) and two reference sensors (without Au pads); Right: Active sensor including two Au pads on top of the sensor area for immobilization of the phage probes.

### 3.1.9.2 Phage Immobilization on Au Pads

Following the microfabrication process, chip wirebonding on a chip-carrier and wires protection with silicone gel, the chip was ready to be functionalized. First, the chip was rinsed with isopropanol and milli-Q water and then dried under a  $N_2$  stream. In order to remove the remains of the photoresistive polymer and other organic contaminants, the chip was exposed to ultraviolet light/ozone plasma (Novascan Technologies, PSDP-UVT series, IA, USA) during 15 min at  $50^\circ C$ . Next, covalent cross-linking was carried out as described in 3.2.7.2. A droplet of approximately  $1 \mu l$  of *Salmonella* phage was placed over the left column of sensors and  $1 \mu l$  of unspecific phage (*Campylobacter* phage) on right column of sensors. The phage incubation occurred during 2 h at room temperature after which the unbound phages were removed by washing three times with 0.1 M MOPS buffer. The unspecific binding sites were blocked with BSA 1% in TE during 45 min as described in 3.2.7.3.

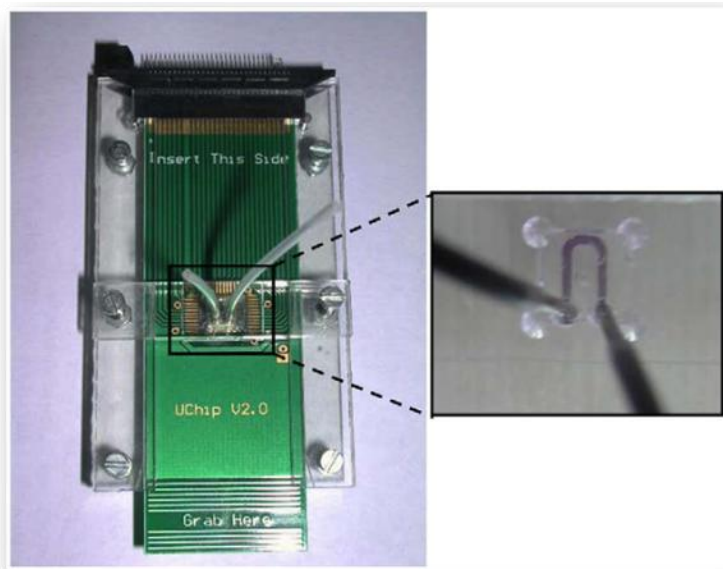
It should be noted that, to ensure that Au functionalization and phage immobilization was done properly, the experiments were conducted in parallel on Au substrates under the same conditions as the MR biochip and analyzed by Nikon SMZ 1500 Stereomicroscope.

### 3.1.9.3 Magnetic Nanoparticles (MNPs) Labeling

Protein A coated magnetic nanoparticles (Nanomag, Micromod) were labeled with anti-*Salmonella* polyclonal antibody. Protein A is a surface protein originally found in the cell wall of the bacterium *Staphylococcus aureus* and their ability to bind immunoglobulins had special interest on our antibody immobilization strategy [37,38]. Protein A specifically targets the Fc region on the antibody without requiring a chemical immobilization and thus the loss of activity of antibody can be avoided. In the magnetic concentrator (Invitrogen bead separation) a 1.5 ml Eppendorf tube, containing 1  $\mu$ l of MNPs ( $4.9 \times 10^{11}$  particles/ml) was allowed to stabilize during 3 min, until the MNPs pellet was clearly visible on the wall of the tube. The original buffer was gently removed and the particles were resuspended in 100  $\mu$ L of 0.1 M PB, pH 7.5. This procedure was repeated at least twice to completely remove the original preservative buffer. Then, MNPs were labeled with 1  $\mu$ l of anti-*Salmonella* polyclonal antibody (stock concentration at 1 mg/ml) in a total volume of 5  $\mu$ l of 0.1 M PB/0.02% Tween 20. The unbound antibody was removed by washing twice. Finally, the functionalized MNPs were resuspended in 5  $\mu$ l of 0.1 M PB/0.02% Tween 20.

### 3.1.9.4 Microfluidic System

Bacteria and MNPs suspensions are loaded in a microfluidic system that consists of a U-shaped channel printed in a polydimethylsiloxane (PDMS) block, as is shown in **Figure 3:2**. The channel is connected with metallic adapters to tubing for the inlet and outlet. The sealing of the U-shaped channel to the chip is achieved by applying pressure over the PDMS, guaranteeing at the same time a correct alignment between the channel and the sensors [29]. The samples are injected inside the fluidic system by an automated syringe pump (New Era Pump Systems, INC).



**Figure 3:2:** Microfluidic system using a pressure platform including the PCB aligned with the Poly(methyl methacrylate) (PMMA) plates and the PDMS channel. The picture on the right shows the U-shaped channel in a PDMS block filled with a color fluid [36].

### 3.1.9.5 Signal Measurement

After immobilization of the phage, the magnetoresistive biochip is introduced on the portable reading platform [27] and the microfluidic system adjusted over the sensor [29]. The sensors are biased by a 1 mA current while an external DC+AC magnetic field of  $3\text{mT} + 1.35\text{mT}_{\text{rms}}$  is applied to magnetize the MNP. The baseline signal is first acquired during 10 min with only 0.1 M PB, pH 7.5, inside the channel. *Salmonella* Enteritidis at  $1.0 \times 10^8$  cells/ml is introduced inside the channel and allowed to settle down for 40 min. Finally, the unspecifically bound bacteria are washed by introducing a solution containing 0.1 M PB with 0.02% of Tween 20 at a flow rate of 5-10  $\mu\text{l}/\text{min}$ . Then, the antibodies previously labeled with MNP (as described in 3.1.9.3) are introduced inside the channel, interacting 30 min with bacteria, previously specifically captured by phage. Then, unbound MNPs are removed by washing at 5  $\mu\text{l}/\text{min}$  and 50  $\mu\text{l}/\text{min}$  during 5 min. The difference between the signal acquired after washing and the baseline signal ( $\Delta V_{\text{binding}}$ ) is proportional to the number of cells bound to the sensor surface. To be able to compare the different sensors, the  $\Delta V_{\text{binding}}$  signal is divided by the baseline signal, as explained in [25].

### 3.1.9.6 Analysis by Scanning Electron Microscopy (SEM)

SEM analyses were performed by Quanta 650FEG, Environmental Scanning Electron Microscope (ESEM). Gold substrates containing only phages immobilized on their surface were not subjected to any treatment. The substrates with bacteria attached on the surface were treated using a fixation technique to preserve the bacterial structure. The process involves three steps: fixation, washing and dehydration. Initially, the samples were immersed in 3% of glutaraldehyde (prepared with PB 0.1 M, pH 7.5) during 30 min at room temperature and washed with 0.1 M PB. Sample dehydration was carried out using a graded ethanol series in milli-Q (30%, 50%, 70%, 80%, 90% and 96%) during 5 min/solution.

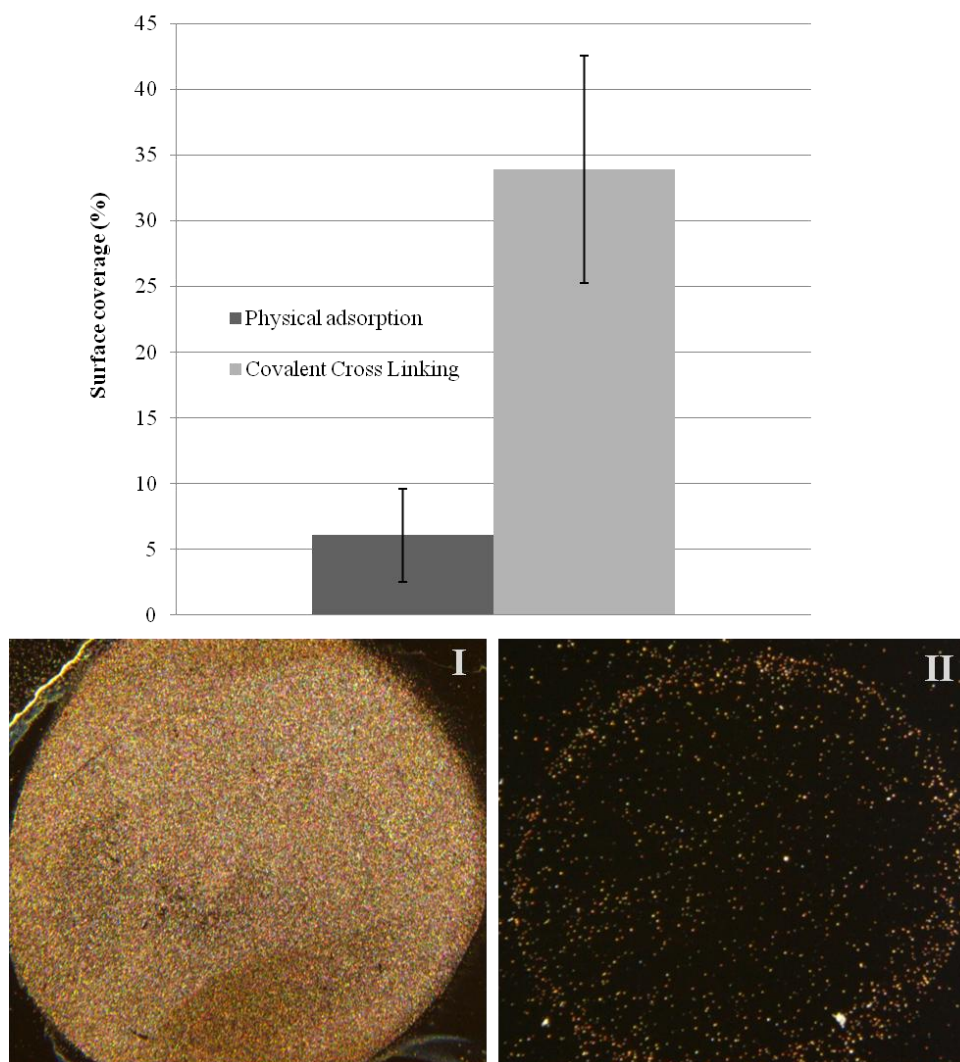
## 3.2. Results

### 3.2.1 Optimization of Phage Immobilization on Gold Substrates

When developing a detection method for a specific microorganism it is important to collect a number of elements that guarantee the quality and efficiency of the device. From the selection of both platform and biological element until the selection of the detection strategy, numerous optimizations steps should be considered to improve the sensor's performance. The techniques used for phage immobilization as well as the morphology of the immobilized phage are two important factors that can affect the binding affinity of the bioelement to the target pathogen. Researchers like Singh et al. [39], Tolba et al. [40] and Gervais et al. [41] have been studying immobilization techniques for lytic phages with morphological features similar to those of our phage. In this work, the PVP-SE1 *Salmonella* phage, belonging to the family *Myoviridae*, was used. It has an icosahedral head of 84 nm and a contractile tail of 120 × 18 nm with short tail fibers. As the phage receptors that allow target recognition are located at the tail fibers, phage immobilization on the biosensor's surface should preferentially occur through the capsid head. Our immobilization method was based on random covalent binding using the bifunctional crosslinker Sulfo-LC-SPDP on the sensor surface. Sulfo-LC-SPDP is an amino- and thiol (sulfhydryl) reactive heterobifunctional protein crosslinker and therefore phage buffer exchange was needed to remove the amine groups present in the SM-Buffer.



The chemical immobilization was compared to physical adsorption immobilization and the surfaces were analyzed by a 650 Quantum ESEM scanning electron microscope (SEM). The phage density was calculated based on the phages counted in SEM images resulting in an average surface density. The results showed a phage density of around 3.07 phages/ $\mu\text{m}^2$  when the gold surface is modified using the bifunctional crosslinker Sulfo-LC-SPDP. The bacterial captured density was visualized by Nikon SMZ 1500 Stereomicroscope and analyzed by Image J software as demonstrated in Figure 3:3.

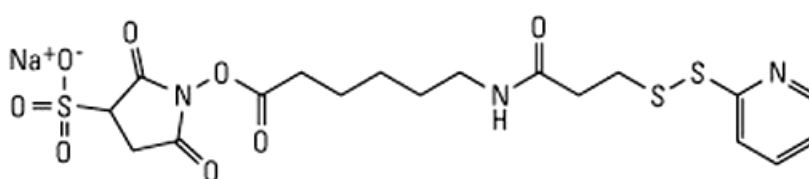


**Figure 3:3:** Comparison of the bacteria surface coverage when the phage was immobilized by covalent cross-linking and physical adsorption. The error bars are standard deviations coming from at least five surface coverage evaluations. The bottom images correspond to the chemical (I) and physical immobilization (II).

When using covalent cross-linking (Figure 3:3:I) we obtained a percentage of surface capture density of  $33.90 \pm 8.68$  against  $6.05 \pm 3.53$  by physical adsorption (Figure 3:3:II). Covalent cross-linking proved to be about 5.6-fold more efficient than physical adsorption. Non-specific binding was not observed because 1% BSA as a blocking agent was used. The positive results were also compared to those obtained on surfaces coated with only BSA.

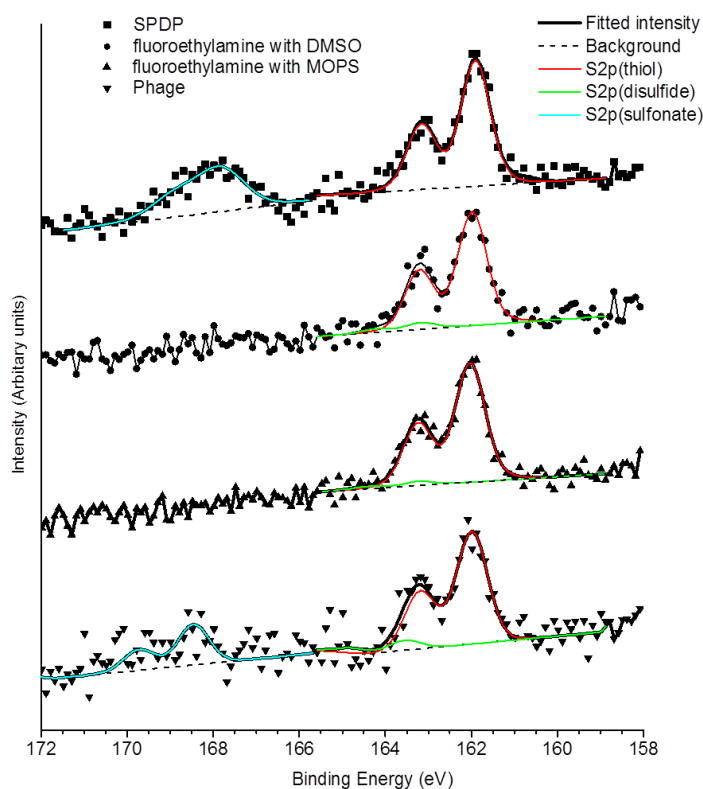
### 3.2.3 X-ray Photoelectron Spectroscopy Analysis

Besides the density studies the efficiency of Sulfo-LC-SPDP compared to a similar linker 3,3'-Dithiobis(sulfosuccinimidylpropionate) (DTSSP) was also investigated (data of DTSSP linker not shown). The efficiency and presence of the Sulfo-LC-SPDP bifunctional linker used in this experiment was analyzed and confirmed by XPS. Moreover, using the same quantitative spectroscopic technique, the covalent coupling of phage PVP-SE1 (in MOPS buffer) to the chemically modified surface was simulated using the 2-fluoro ethylamine hydrochloride compound under the same conditions as those used for phage immobilization. This technique allowed us to confirm the effectiveness of the chemical immobilization, providing the information about the attachment, composition, and chemistry of the molecular layer. Sulfur ( $S_{2p}$ ), Carbon ( $C_{1s}$ ) and Nitrogen ( $N_{1s}$ ) elemental regions provided the most important information. Figure 3:4 shows the Sulfo-LC-SPDP molecule, to help in the following XPS analysis discussion.



**Figure 3:4:** Sulfo-LC-SPDP molecule structure [42].

The graph presented in Figure 3:5 shows  $S_{2p}$  spectra for the following conditions: deposited SPDP layer, phage attachment, simulated coupling of fluoroethylamine in DMSO and MOPS.

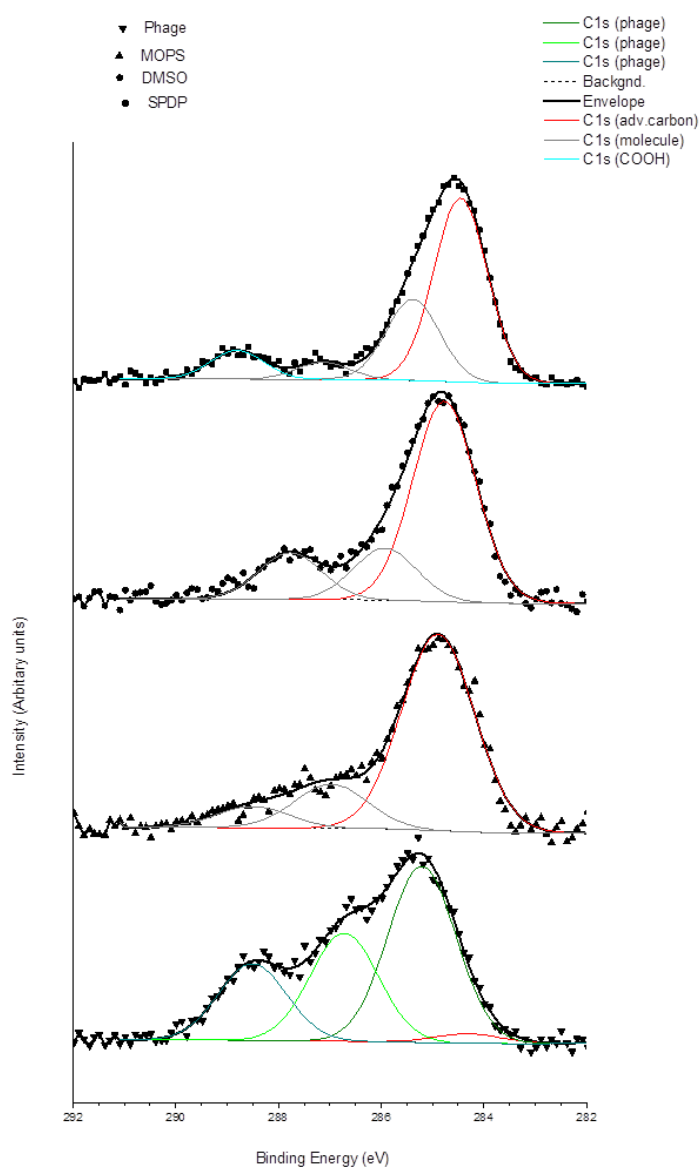


**Figure 3:5:** XPS  $S_{2p}$  spectra (top to bottom) for SPDP, fluoroethylamine with DMSO, fluoroethylamine with MOPS and phage.

Figure 3:5 provides information about the attachment of the SPDP molecule to gold and the availability of sulfo-NHS groups after the attachment. The first spectrum is for SPDP layer after deposition; referring to Figure 3:4, we can interpret this spectrum to understand how SPDP molecules are bound to gold. SPDP is a biofunction linker comprising an amine-reactive N-hydroxysuccinimide (NHS) ester group on one side of the molecule and a disulfide linkage in the molecular chain. Upon adsorption on gold, the disulfide bond (S-S) breaks and both sulfur atoms form thiolate bonds with gold, as indicated by the spectral component at 162 eV (highlighted in red). Note that the second  $S_{2p}$  component at 163 eV, which corresponds to unbound thiols or intact disulfides, [43], is not observed for SPDP and at most represents an insignificant small fraction for other samples (green lines). The large component at 168 eV marked in blue in the SPDP spectrum is related to the sulfur atom in the Sulfo-NHS reactive group of SPDP; the three oxygen atoms of the sulfonate group significantly increase the BE of this component. In contrast, this sulfo-NHS component is absent in the  $S_{2p}$  spectra obtained after fluoroethylamine coupling either in DMSO (ideal reaction conditions) or in MOPS, clearly indicating that the sulfo-NHS functional group of SPDP was available for

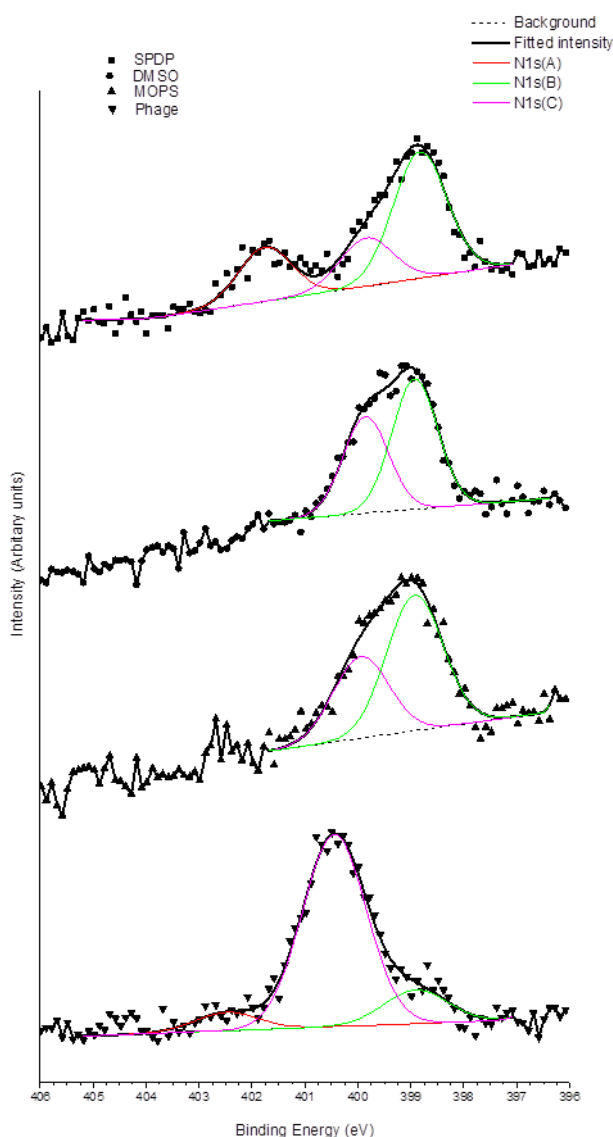
coupling and has reacted similarly under both conditions. This result shows that our reaction conditions (working with lower pH) do not interfere with the coupling of amines to the SPDP layer. In the spectrum of the phage sample, the weak intensity around 169 eV was likely produced because traces of sulfate were present in the phage incubation solution.

The carbon ( $C_{1s}$ ) and the nitrogen ( $N_{1s}$ ) regions in Figure 3:6 and Figure 3:7, respectively, provide complementary information about the NHS group.



**Figure 3:6:** XPS  $C_{1s}$  spectra (top to bottom) for SPDP, fluoroethylamine with DMSO and MOPS, phage.

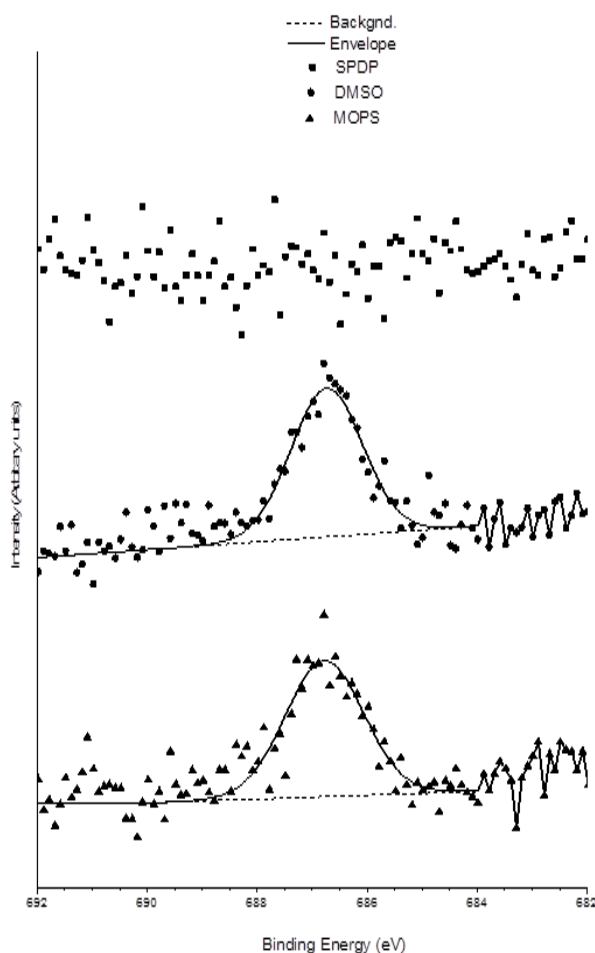
In the  $C_{1s}$  spectrum, the red line corresponds to the aliphatic carbon component, the grey lines indicate different contributions from organic molecules and the blue curve (the most important) corresponds to the carbon in the NHS group. That component disappears after the reaction with fluoroethylamine, indicating the successful coupling under both DMSO and MOPS conditions, in agreement with the  $S_{2p}$  data. In the phage spectrum, the aliphatic component (red line) is minimal, as expected, while the three components highlighted in green indicate the presence of protein and DNA of the phage.



**Figure 3:7:** XPS  $N_{1s}$  spectra (top to bottom) for SPDP, fluoroethylamine with DMSO and MOPS, phage.

The  $N_{1s}$  component marked in red for SPDP corresponds to the nitrogen in the NHS group. In agreement with evidence from both  $S_{2p}$  and  $C_{1s}$  regions, this component also disappears after the fluoroethylamine coupling. The  $N_{1s}$  component marked in purple corresponds to amide bonds: it is present in the SPDP, increases after fluoroethylamine (amide) coupling, and dominates the spectrum for the protein (and thus amide) rich phage.

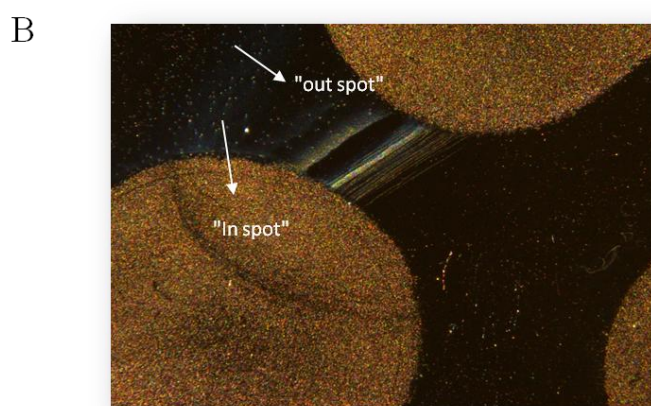
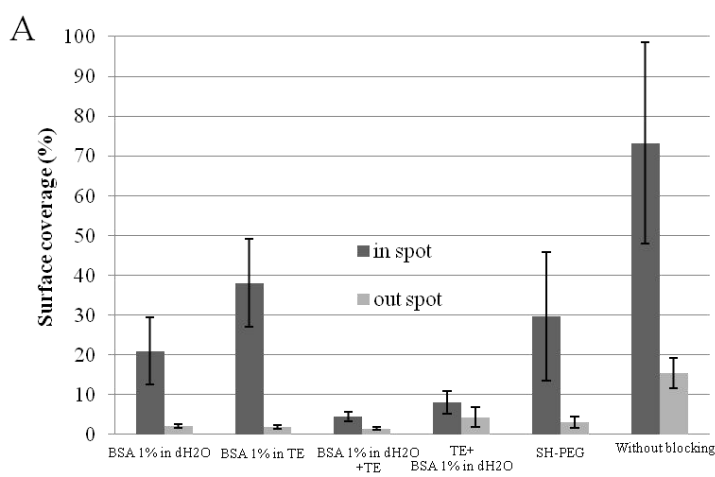
In addition to the increase of the amide signal in  $N_{1s}$  region, we verified the fluoroethylamine coupling by observing the fluorine signal ( $F_{1s}$ ) in Figure 3:8. The similar intensity of the  $F_{1s}$  peak after coupling under the DMSO and MOPS conditions directly confirms that the coupling was similarly efficient in both cases.



**Figure 3:8:** XPS  $F_{1s}$  spectra (top to bottom) for SPDP, fluoroethylamine with DMSO and MOPS.

### 3.2.4 Blocking Performance Analysis

Besides phage immobilization on a functionalized surface, the blocking performance analysis was performed to verify which blocking agent can provide or exclude non-specific binding. SH-PEG and the combination of 1% BSA with different buffers (TE, 0.1 M PB, pH 7.5, and milli-Q) were tested. The bacterial density was observed by Nikon SMZ 1500 Stereomicroscope and the images were analyzed by Image J software (Figure 3:9). Blocking buffer BSA in TE gave the best results when including surface coverage outside versus inside the spot. Similar results were obtained with BSA in water. The binding of bacteria was two times higher when TE instead of water was used. In both cases, the percentage of background remained the same. Thus, BSA in TE was shown to be the most efficient blocking buffer of nonspecific sites without inhibiting the phage receptor to bind to the bacterium.



**Figure 3:9:** A: Percentage of the bacteria surface coverage in the area in which phage was immobilized (identified as "in spot") and on the nonspecific binding area in which phage was not immobilized (identified as "out spot"). B: Image obtained by Nikon SMZ 1500 Stereomicroscope showing the "in spot" and "out spot".

Moreover, after bacteria attachment a cleaning step was carried out immersing the gold substrates in different wash solutions in the following order: 0.1 M PB, pH 7.5; PB/0.02% Tween 20 and milli-Q-. This methodology allowed the removal of the unbound bacteria over the surface.

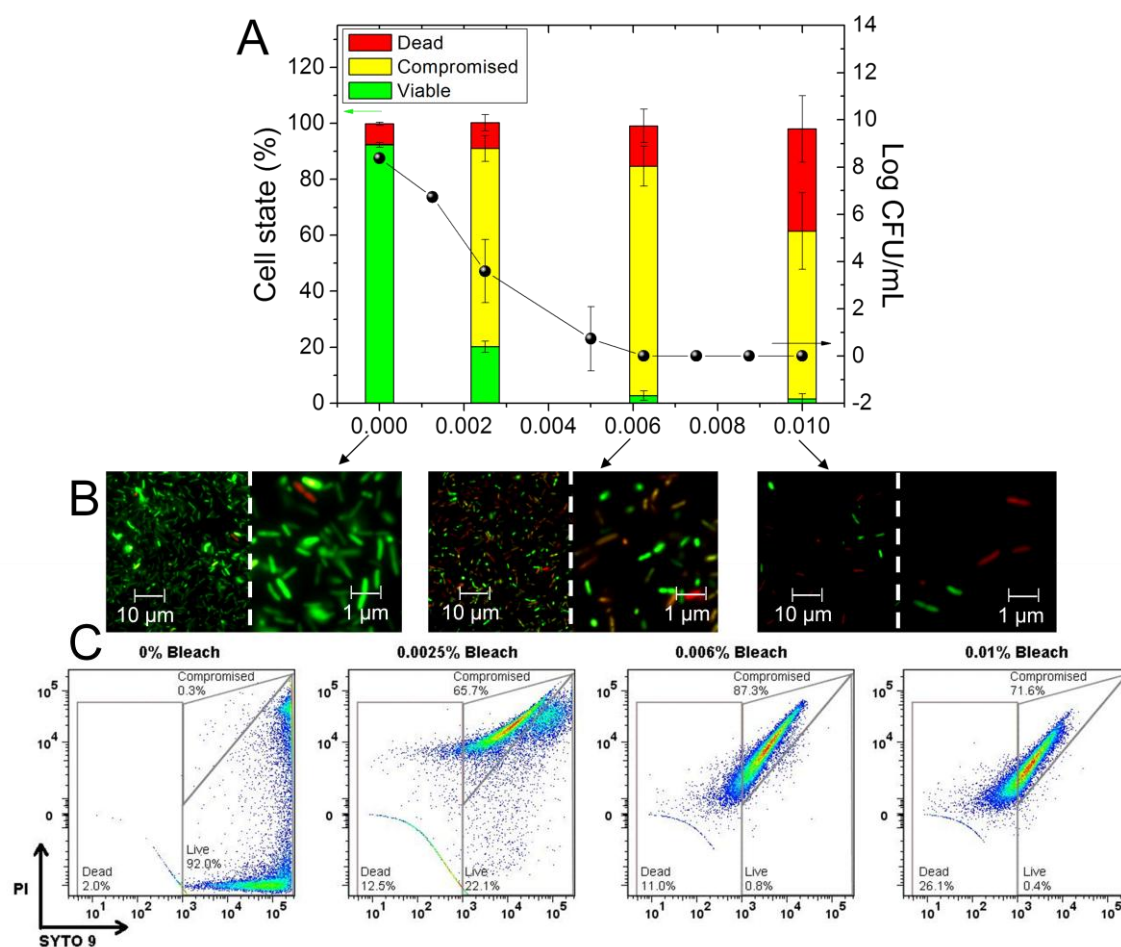
### 3.2.5 *Salmonella* Cell Induction to the VBNC State

To study the ability to detect the VBNC state of bacterial cells, a process capable to affect cell viability in a certain extent but not harsh enough to kill or lyse the cells was required.



Therefore, to induce the VBNC state in our work, bacteria were placed in contact with different concentrations of sodium hypochlorite (commercial bleach). The concentration at which the cells were nonculturable was found and identified as the break-point. Fourteen different concentrations, ranging from 0% to 5% (v/v), were tested (0% was used as a control).

*Salmonella* cells were placed in contact with different concentrations of sodium hypochlorite in water and after bleach removal the cell culturability was assessed in solid medium plates by colony counting, while enrichment in nonselective liquid media was used for resuscitation studies. Additionally, flow cytometry analysis and epifluorescence microscopy observation in combination with viability staining kit were used for cell state assessment. The break-point, the concentration at which 100% of the cells lose their culturable state and are unable to form colonies (CFU) in non-selective medium, was found to be around 0.006% (Figure 3:6-A, linear curve); below the break-point, at least a fraction of the population is still viable and able to grow in agar plates, while above that concentration no CFUs were observed. However, when exposed to fresh liquid medium at adequate growth conditions all tested concentrations of bleach, even above the break-point and up to 5%, have shown cell growth again (resuscitation times within 16 h).

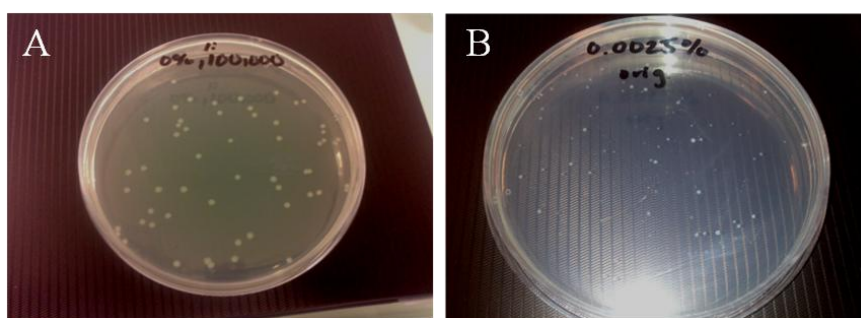


**Figure 3:10:** Assessment of physiological state of *Salmonella* Enteritidis (S1400) cells after treatment with bleach at different concentrations by different evaluation methods: (A) cfu counts on standard culture solid media compared to flow cytometry results for relative percentage of cells in the viable, compromised and dead state; (B) epifluorescence microscopy images of *Salmonella* Enteritidis cells; and (C) flow cytometry analysis showing the percentage of live, dead and compromised cells present after each treatment. For both assays, (B) and (C) cells were stained using a Live/Dead BacLight bacterial-viability kit (Invitrogen). The culturability test in (A) was collected from several trials over time and performed in triplicate, thus all cfu counts were normalized to the same initial cell concentration. Results presented for the flow cytometry analysis are the mean of independent triplicates from one representative experiment out of three.

After evaluating cell culturability by colony counts the Live/Dead BacLight bacterial viability kit containing two fluorescent stains, SYTO9 (green-fluorescent) and propidium iodide (PI) (red fluorescent), was used for epifluorescence microscopy observation and flow

cytometry measurements. These stains differ in their ability to penetrate healthy bacterial cells. When used alone, SYTO9 stains both live and dead bacteria. In contrast, PI penetrates only bacteria with damaged membranes, reducing SYTO9 fluorescence when both dyes are present. Thus, live bacteria with intact membranes appear green, while dead bacteria with damaged membranes emit red (Figure 3:10–B). Under the fluorescence microscope, intermediate cell colors ranging from orange to yellowish were also observed for bleach-treated cells, indicating the existence of other cell states than only live or dead. Additionally, bleach-treated cells exhibit morphological alterations by a decrease in cell size (Figure 3:10–B). Next, to measure the relative proportion of the different cell populations (classified as live, dead or compromised), flow cytometry analyses were conducted for the different cell samples (Figure 3:10–C). Untreated bacteria appeared mostly in the right lower corner of the plot (SYTO positive, PI negative), while with increasing concentrations of bleach the amount of green fluorescence in the cells decreases; cells move up in the plot (SYTO positive, PI positive) and the amount of viable cells loses population to the compromised and dead states. The gating strategy in flow cytometry is important to define and discriminates between the different cell populations. In this case the gating strategy adopted was from the Live/Dead Backlight kit [17], this way defining what they call an “unknown” population. This population was identified as “compromised” (Figure 3:10–C) and associated to the VBNC physiological state supported by culture medium and resuscitation results.

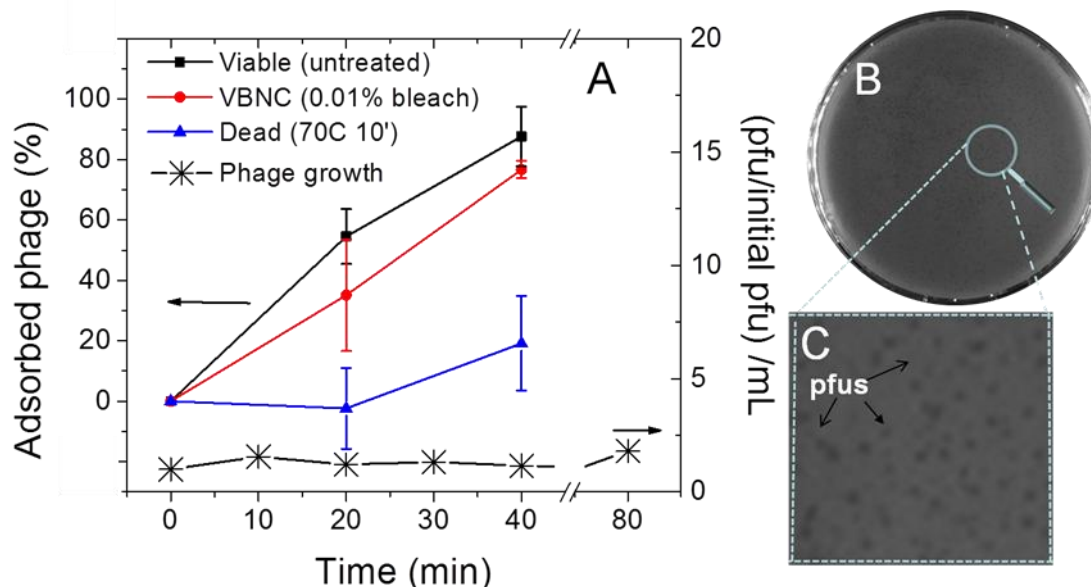
Furthermore, analysis of colony forming units on agar plates showed that the cells exhibit irregular colony shape and size as a result of sodium hypochlorite stress (Figure 3:11–B). The bacteria that were not exposed to bleach showed a more regular shape.



**Figure 3:11:** Colony forming units on agar plates: A: *Salmonella* cells without bleach contact; B: *Salmonella* cells stressed by bleach.

### 3.2.6 Phage Adsorption Profile to Cells at Different Physiological States

Lytic phages naturally infect and lyse the bacterial cell. This characteristic has kept researchers from including these phages, since it limits their use as recognition agents in detection systems for live organisms [44]. Bearing in mind this concern, the phage infection time was evaluated. The conditions used on MR platform were simulated in solution, i.e. the phage at a lower pH (0.1 M MOPS, pH 5.7) was exposed to *Salmonella* Enteritidis in 0.1 M PB, pH 7.5, without agitation, during 80 min. The phage at optimal conditions for biosensing purposes was exposed to *Salmonella* Enteritidis in solution to assess its infection time and cell lysis period. The phage infection profile was recorded by the determination of phage's concentration every 10 min and the number of total phages was plotted versus time after inoculation (Figure 3:12–A). The phage quantification was performed by double layer agar technique as described by Sambrook and Russell [33] (Figure 3:8–B and Figure 3:8–C). During the 80 min defined for the experiment, under the applied conditions, no increase in phage count was detected. Moreover, no cell lysis was observed (data not shown) indicating that the phages were not able to propagate and burst, thereby killing the host cells, at least during the 80 min of the experiment.



**Figure 3:12:** (A) Bacteriophage PVP-SE1 growth curve in *Salmonella* Enteritidis (S1400) in phosphate buffer at room temperature. The number of PFUs at each time point after inoculation was nor-

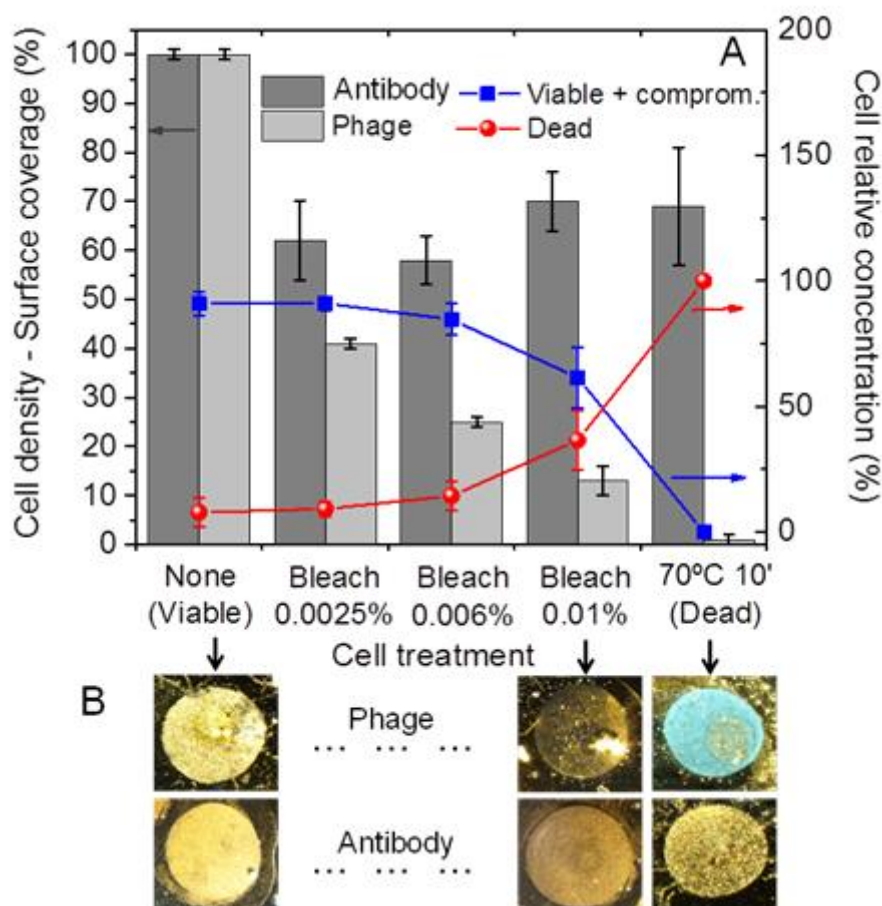
malized to the initial number of PFUs (0 min) (\*). The black, red and blue lines correspond to bacteriophage PVP-SE1 adsorption studies to *Salmonella* Enteritidis (S1400) in phosphate buffer at room temperature. (B) Picture of plaque forming units (PFU) on a culture plate for phage adsorption counts. (C) Zooming in on a couple of typical PVP-SE1 plaques.

Taking into account that, under the conditions specified, the phage was not able to induce lysis of the target cells, we next evaluated the phage adsorption capacity to *Salmonella* Enteritidis at different cell states (viable, VBNC and dead). For that purpose VBNC cells were prepared by treatment with bleach at 0.01%, whereas dead cells were prepared by heating at 70°C for 10 minutes. The phage presented an adsorption profile to VBNC cells similar to that of viable cells, but much different to that of dead cells. The fraction of adsorbed phage to the viable and VBNC cells after 20 min of incubation was about 60 and 40%, respectively. After the same period of time in the presence of dead cells, the phage remained free in solution, only reaching about 20% of adsorption after 40 min of incubation, about a fourth of the total amount of phage adsorbed to VBNC and viable cells for the same period of 40 min.

### 3.2.7 Phage Performance as Biological Element on a Biosensor

The validation of phage as a biorecognition tool consists of its immobilization on a solid sensing surface. After optimization of the surface chemistry (as explained in 3.2.1.), the phage was immobilized on a gold surface by manual spotting (Figure 3:13–B). To evaluate the immobilized phage in terms of *Salmonella* cells recognition efficiency bacteria were submitted to different bleach treatments and incubated with immobilized phage to evaluate the degree of recognition through cell surface density over the phage spot area. The acquired results for phage detection were compared to results obtained with an anti-*Salmonella* polyclonal antibody spotted in parallel. The phage was able to discriminate between viable and dead cells resulting in reduced cell densities for samples with increasing number of dead cells, but directly proportional to the relative concentration of viable plus VBNC cells (compromised population) (Figure 3:13–A). On the contrary, the antibody indiscriminately recognizes and captures all cells, independent of their physiological state, attaining almost constant cell densities even for samples with different proportions of viable to dead cells. Even more interesting is the fact that heat-killed cells were completely unnoticed by the phage but

strongly detected by the antibody. This result reveals the superior capacity of the phage to discriminate viable from dead cells and simultaneously circumvent the false-negatives and false-positives.



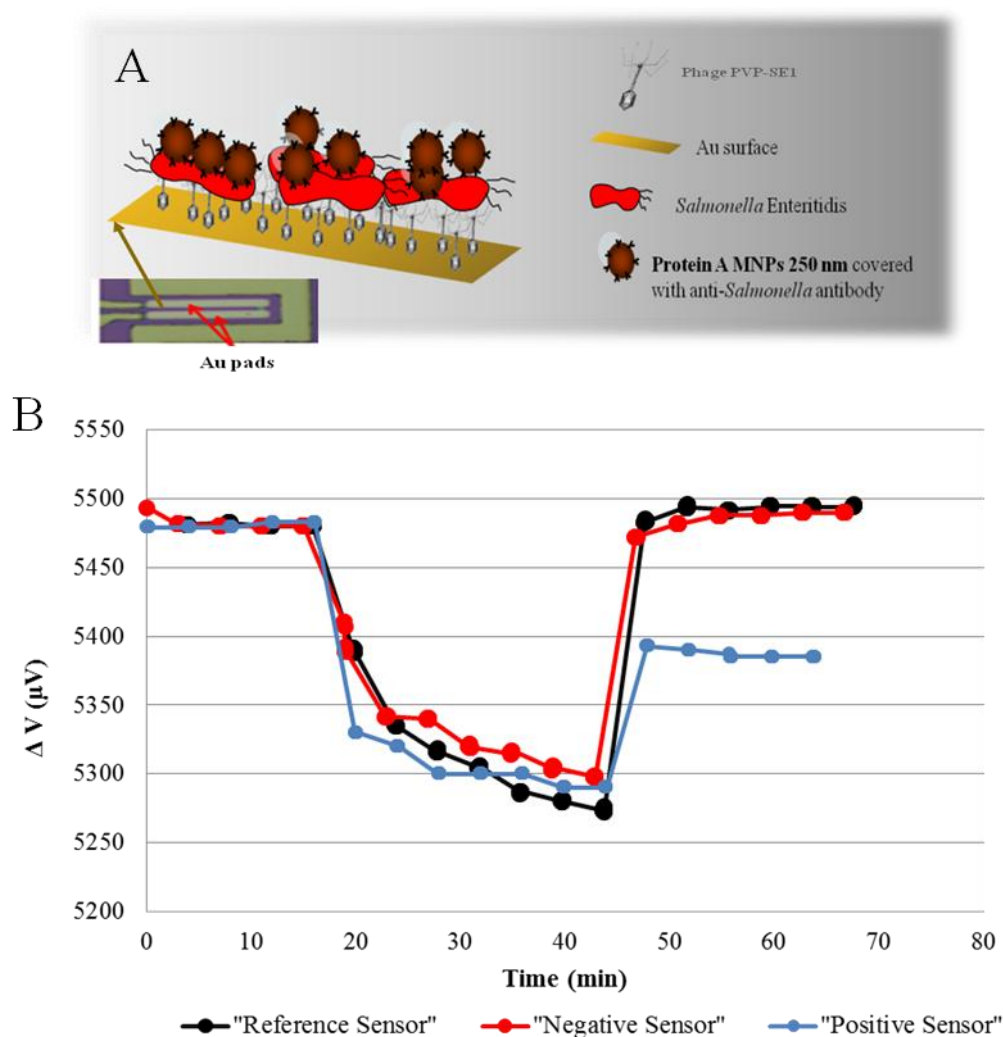
**Figure 3:13:** Density of cells specifically captured by phage and antibody spots, covalently immobilized on gold solid surface. (A) The surface coverage was analyzed by ImageJ free software and compared with the relative amount of viable + compromised cells (■ curve) and dead cells (● curve) measured by flow cytometry. (B) Stereoscope pictures for representative spots of *Salmonella* cells specifically recognized by phage PVP-SE1 (top) and anti-*Salmonella* antibody (bottom).

### 3.2.8 Phage-based Magneto-resistive Biochip for Cell Viability Assessment

The feasibility of developing a phage-based biosensing system and its potential as a cell viability determination tool was assessed by making use of an existent magneto-resistive (MR) biochip and respective electronic reader. The phage immobilization procedure previously

optimized for bulk gold surfaces was transferred to the MR biochip. The functionalized biochip was then used for quantitative analysis of *Salmonella* samples in different physiological states.

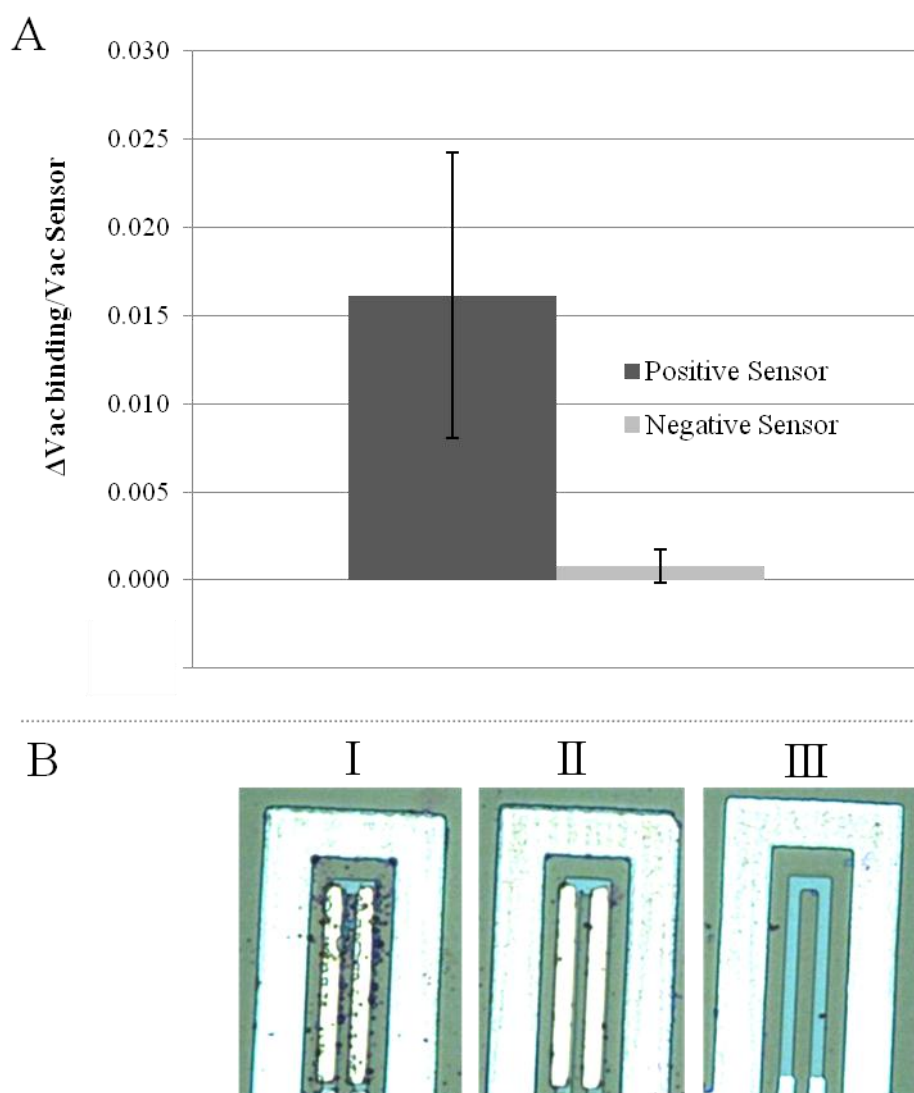
The flow cytometry analysis performed previously allowed us to identify the viability state of the bacterial cells detected by the MR biochip. The strategy used on the platform involves a heterogeneous model that is based on magnetic labels (commercial magnetic nanoparticles (MNPs) of 250 nm in diameter) coated with Protein A for site-directed immobilization of the anti-*Salmonella* antibody on their surface, combined with a specific *Salmonella* phage (PVP-SE1) immobilized on the sensor surface (Figure 3:14–A). This straightforward assay format allows a specific initial detection of bacteria by the phage, followed by the attachment of MNPs to *Salmonella*. The stray field created by the labels is detected as a variation of the sensor resistance proportional to the number of captured cells. A typical experiment of the response of three single sensors and the detection strategy applied in each sensor is demonstrated in Figure 3:14–B.



**Figure 3:14:** The detection strategy using phage PVP-SE1 (A) and a typical response of phage-modified magnetoresistive spin-valve sensor (B) while measuring *Salmonella* Enteritidis contaminated samples. The positive sensor (blue curve) is modified with a specific phage PVP-SE1, while the negative sensor (red curve) is modified with an unspecific phage (*Campylobacter coli* phage). The reference sensor (black curve) is not bioactivated.

The blue curve is the response of a positive sensor to the presence of *Salmonella* Enteritidis cells. In the positive sensor, phages specific to *Salmonella* were immobilized over the MR-sensor on the chip and an anti-*Salmonella* specific polyclonal antibody was the second recognition element immobilized on the magnetic particles. The red curve is the response of a reference sensor, where no biological element was immobilized over the MR-sensor. The analysis of the signals obtained from a set of sensors is presented in Figure 3:15–A.

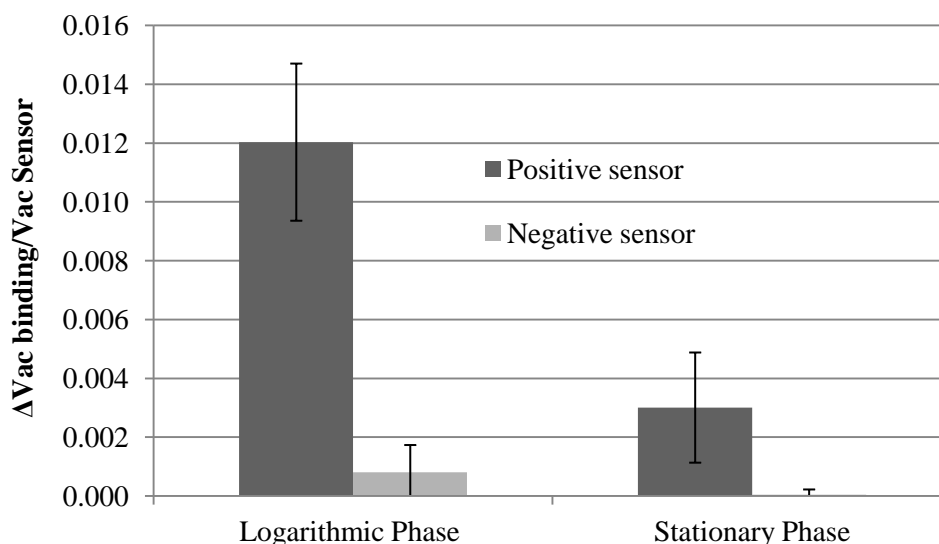




**Figure 3:15:** Comparison of two groups of experimental data for *Salmonella* Enteritidis detection (A). The positive sensors were coated with specific *Salmonella* phage and negative sensors with unspecific phage. The error bars are standard deviations of the signal coming from at least 12 sensors acquired sequentially at the same chip. The lower images correspond to microscopic visualization of a U-shaped spin valve sensor ( $2.5 \times 80 \mu\text{m}^2$ ) **I:** Positive sensor (with *Salmonella* phage immobilized over the Au pad); **II:** Negative sensor (with unspecific phage immobilized over the Au pad); **III:** Reference sensor (sensor biologically inert).

From Figure 3:15 we can conclude that the measured signals correspond to an average of 20 cells over each sensor. Compared to the negative control (unspecific phage), the binding affinity of the specific phage was around 20 times higher (average absolute value of  $100 \mu\text{V}$  against  $5 \mu\text{V}$ ), proving that the bio-assay is generating reliable results for this particular ex-

ample. The results support the evidence demonstrated on gold substrates that this technique can specifically detect *Salmonella* strains and can be used in further viability assays. To gain further insight into the capture response of phage to the target (*Salmonella*), the phage immobilized on the sensor surface was also exposed to bacteria in the stationary phase to examine whether the bacterial growth stage has an influence on the binding efficiency.

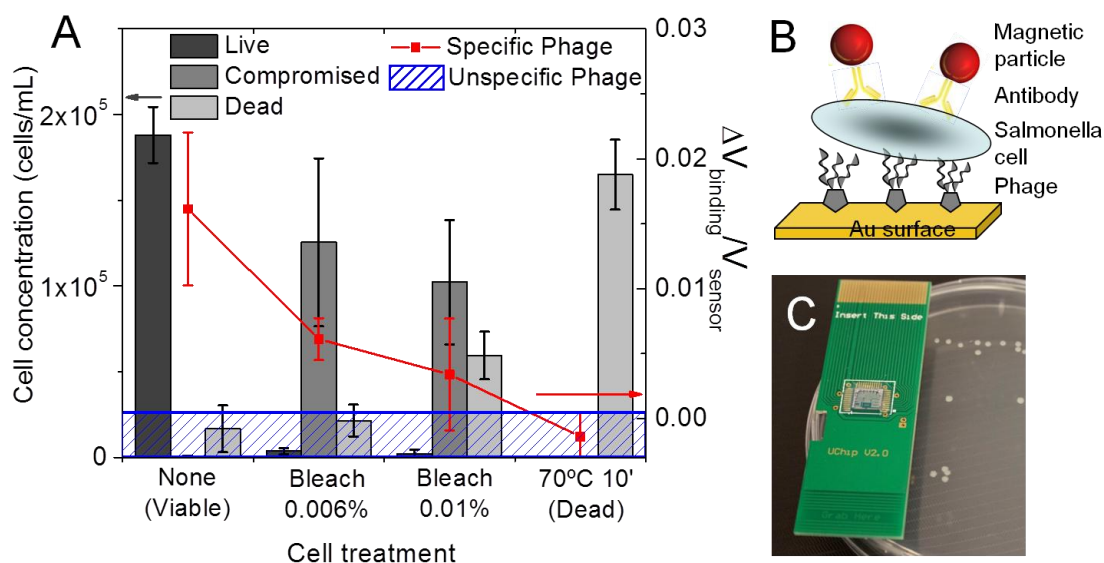


**Figure 3:16:** Signal comparison of *Salmonella* Enteritidis in two growth states. As a negative control, sensors coated with unspecific phage were used. The error bars are standard deviations of the signal coming from at least 5 sensors acquired sequentially at the same chip.

The exponential phase shows a four times higher binding signal than when cells from the stationary phase are used (Figure 3:16). This observation supported the hypothesis that our phage could be an excellent bioelement to decrease false positives or negatives when using the phage-based magnetoresistive biosensor.

Following the simulation of the VBNC state in *Salmonella* Enteritidis (as explained in 3.2.5), the phage-based MR biochip was exposed to different suspensions of bacteria exposed to different percentages of bleach. Subsequently, the voltage signal was obtained. Each solution loaded in a microfluidic system was analyzed by flow cytometry using the LIVE/DEAD<sup>®</sup> BacLight<sup>™</sup> Bacterial Viability and Counting Kit that, combined with beads (for system calibration), and allowed for the quantification and the differentiation of the bacterial population based on their viability state. Figure 3:17 shows the normalized binding signals ( $V_{\text{bindingac}}/V_{\text{sensorac}}$ ) versus viability state, where the binding signals are differential volt-

age values identified as  $V_{\text{binding ac}}$ , calculated from the difference between the sensor baseline ( $V_{\text{sensor ac}}$ ) and the signal originated from the specifically bound MPs over the sensor ( $V_{\text{particles ac}}$ ). As the binding signals are obtained from different sensors, their sensitivities must be normalized to a reference value and the sensor response ( $V_{\text{sensor ac}}$ ) to the external AC excitation field ( $H_{\text{ac}}$ ) was used as reference.



**Figure 3:17:** Phage-based magnetoresistive biochip measurements performed on an electronic reader. (A) Normalized differential voltage signal for *Salmonella* samples subjected to different treatments (square points curve). The shaded area in blue on the bottom refers to the obtained signal using an unspecific phage on the sensor. Each point and shaded area represents the average value of at least 10 independent sensors. Bars represent the concentration of cells and respective cell state for each cell sample measured on the MR-chip. Cell concentrations were obtained by flow cytometry using the Live/Dead counting Backlight kit from Invitrogen, in which each data point results from the analysis of triplicates. (B) Schematic representation of the “sandwich” type biomolecular recognition strategy adopted in the MR-biochip measurements. (C) Picture of the MR-biochip used for the detection of *Salmonella* cells shown on a standard cell culture plate.

The highest signal was obtained for bacteria in the exponential phase. The phage-based MR biosensor showed to be sensitive in the presence of bacteria on VBNC state and when the percentage of that population reduced to half (Figure 3:17–A), the detection signal decreased proportionally. Moreover, based on these results we can conclude that our phage does not recognize the dead cells, since the signal for the condition VBNC would increase with an

increase in percentage of dead cells in solution. The heat-treated cells were not detected by the biosensor, which obtained signal occurred on the negative sensors region.

### 3.3 Discussion

Most water treatment systems in the US and Europe have been using chlorine-based products, usually at 0.5 to 1.0% concentration, for disinfecting drinking water for nearly 100 years. In particular sodium hypochlorite (NaOCl), commonly known as bleach, is trusted as a powerful disinfectant. It is considered a bactericidal agent, except when it is used at lower concentrations, where it works as a bacteriostatic agent. Many scientific studies report on the inefficacy of bleach to completely kill bacteria, but rather induces latent forms [6,45,46], assisting bacteria in entering the VBNC state. This has been related to bacterial survival mechanisms, which upon the exposure to harsh but sub-lethal conditions can lead cells to enter a VBNC state that cannot be detected by traditional bacteriological culture methods [47]. The reason to choose this disinfectant agent resides in the fact that it is widely used and applied in various food processing facilities, household cleaning and even health care facilities [48]. Therefore, to induce cells into the physiological state of VBNC, *Salmonella* Enteritidis suspensions were treated with commercial bleach at a range of concentration from 0 to 5%. In fact, it was observed that *Salmonella* treated with bleach at concentrations above 0.006% were not able to grow in solid culture media. To prove the presence of viable cells under these conditions several analytical techniques were used to assess the physiological state of the cells as well as their total count number. The applied methods, fluorescent microscopy and flow cytometry [49], are common techniques in microbiology that, when associated with viability stains, allow the rapid characterization of cells from nonhomogeneous populations. Both methods, in agreement, showed that bleach induces *Salmonella* to enter the VBNC state. The different efficiencies on green and red fluorophores cell uptake rates denote the presence of a compromised population that was proven to be VBNC by resuscitation tests. These results prompted us to study whether the *Salmonella*-specific phage PVP-SE1 would be able to detect bacteria at the VBNC state. An additional important issue is the fact that PVP-SE1 is a virulent phage, able to lyse the cells, which in a solid state biosensing system could be a limitation. This opposed to other types of phages, such as filamentous phages, which do not lyse

the infected cells. This characteristic has refrained researchers from including these phages in detection systems, since it limits their use as a recognition agent for live organisms [15]. Bearing this in mind, the phage infection time was evaluated prior to the realization of phage-cell adsorption studies. Our results show that no cell lysis occurred during the period of a common biosensing experiment. This allowed us to circumvent the limitation of using lytic phages as a detection tool mentioned by other researchers [50]. A first test involved the evaluation of the phage adsorption efficiencies to cells at different physiological state in solution. We demonstrated that the PVP-SE1 phage has a completely different adsorption profile for viable (including the VBNC) cells than for cells killed by temperature treatment. Viable cells were rapidly recognized by the phage while dead cells were completely ignored (80% of adsorption against 20%, respectively). Moreover, the 20% of adsorption can be due to an un-specific attachment from phages to the cell surface, which after washing (as verified on MR platform) can be removed. Considering that the cell receptors of PVP-SE1 are lipopolysaccharides and taking into account that it has been observed that different serotypes of *Salmonella* can display different receptors under stress conditions [51], cell recognition may be affected by those changes.

As for the biological element, the detection signal generated was proportional to the concentration of viable plus VBNC cells in the sample, whereas dead cells were absolutely unnoticed. This gave us an indication of the possibility to explore this phage as a biological element in biosensing systems.

Following the optimization of phage immobilization conditions over a solid sensing surface, we therefore designed a set of experiments with the intention to explore the potential of PVP-SE1 to capture, detect and, above all, discriminate between different physiological states of *Salmonella*. Gold coated solid substrates were used as sensing surfaces for phage immobilization aside with anti-*Salmonella* antibody. The two biorecognition agents were evaluated and compared in their cell binding and capture performances for different cell populations. The bacteriophage presented a cell surface coverage proportional to the sample concentration on viable cells (including VBNC), while the antibody presented an almost constant surface density following the total number of cells in the sample (including dead cells). From these results one important assumption arises: the phage and the antibody are not recognizing the same cell membrane receptors and may work successfully in combination. In fact, one major concern when developing biomolecular recognition strategies, mainly “sandwich” type assay,

where two biological elements may specifically bind to the target analyte, is the competition for target receptors. Identical biological elements may hamper each other's proper attachment. This is a common scenario in standard immunoassays where a labeling antibody may block the epitopes to the capture antibody or vice versa. In this case by conjugating two bioligands of a different nature, antibody and bacteriophage, in a so-called heterogeneous "sandwich" assay, we took advantage of non-competitive capture and labeling steps. After setting up the phage immobilization conditions as well as the recognition strategy the phage was evaluated in terms of cell viability discrimination and detection tool. Results clearly demonstrate that a device using PVP-SE1 as the biorecognition interface has the potential to decrease both false-negative and false-positive results. The binding signals ( $\Delta V_{\text{binding ac}} / V_{\text{sensor ac}}$ ) obtained from the MR biochip measurements besides confirmation of the results obtained by direct imaging of captured cells in optical microscopy add quantitative information at much higher sensitivity than optical inspection. The amplitude of the binding signal for the different samples is matched up to the flow cytometry analyses of the samples loaded on the MR platform. When the percentage of VBNC loses population to the dead state, the biochip detection signal also decreases proportionally. Additionally, heat-killed cells did not create any signal at all, remaining at the level of the negative control for unspecific phage signal and both at the system noise level.

The results showed that, when in a buffer with lower pH, the phage can be efficiently immobilized with approximately 80% of attachment to the surface (data not shown).

### 3.4 Conclusions

The lytic phage PVP-SE1 was explored as an alternative biological element for pathogen detection and viability assessment. Taking into account the problematic occurrence of false positives associated to DNA-chips and the high production costs, poor stability and cross-reactivity related to immuno-chips, the development of phage-based biochips emerges as a valuable tool. The feasibility to conjugate this biomolecular tool with electronic analytical devices without losing functionality was proven. An existent magnetoresistive type of biochip was used as proof-of-concept system to demonstrate the potential of the phage as biological element. However, the potential of this biomolecule is not limited to one type of detection

platform or transducing principle. The countless possibilities to combine this biological element in microbial detection and characterization approaches may also include the development of a phage-based viability kit for flow cytometry, where a fluorescently labelled phage, eventually by genetic modification, is used as a viability marker. Also optical or even other detection principles have plenty of room to be explored.

Still this can be the tip of the iceberg because taking into account the diversity of phages that are currently available for different targets, this hybrid technology presents an enormous potential to be explored in a multitude of applications where bioanalytical devices are required, namely in the environmental area, food and beverage industry, or even biomedical field.

### 3.5 References

- [1] WHO in international health regulations. (ed. W.H. Organization)Geneva; 2005).
- [2] Nugen, S.R. & Baeumner, A.J. Trends and opportunities in food pathogen detection. *Anal. Bioanal. Chem.* 391, 451-454 (2008).
- [3] Velusamy, V., Arshak, K., Korostynska, O., Oliwa, K. & Adley, C. An overview of foodborne pathogen detection: In the perspective of biosensors. *Biotechnol. Adv.* 28, 232-254 (2010).
- [4] Oliver, J.D. The viable but nonculturable state in bacteria. *Journal of Microbiology* 43, 93-100 (2005).
- [5] Oliver, J.D. Recent findings on the viable but nonculturable state in pathogenic bacteria. *FEMS Microbiology Reviews* 34, 415-425 (2010).
- [6] Khamisse, E., Firmesse, O., Christieans, S., Chassaing, D. & Carpentier, B. Impact of cleaning and disinfection on the non-culturable and culturable bacterial loads of food-contact surfaces at a beef processing plant. *Int. J. Food Microbiol.* 158, 163-168 (2012).
- [7] Firmesse, O., Morelli, E., Vann, S. & Carpentier, B. Monitoring of bacterial load in terms of culturable and non-culturable cells on new materials placed in a delicatessen serve over counter. *Int. J. Food Microbiol.* 159, 179-185 (2012).

- [8] Jayasena, S. Aptamers: An Emerging Class of Molecules That Rival Antibodies in Diagnostics. *Clinical Chemistry* 45, 1628-1650 (1999).
- [9] Murphy, N.M., McLauchlin, J., Ohai, C. & Grant, K.A. Construction and evaluation of a microbiological positive process internal control for PCR-based examination of food samples for *Listeria monocytogenes* and *Salmonella enterica*. *Int. J. Food Microbiol.* 120, 110-119 (2007).
- [10] Klerks, M.M., Zijlstra, C. & van Bruggen, A.H.C. Comparison of real-time PCR methods for detection of *Salmonella enterica* and *Escherichia coli* O157 : H7, and introduction of a general internal amplification control. *Journal of Microbiological Methods* 59, 337-349 (2004).
- [11] Hoorfar, J. et al. Practical considerations in design of internal amplification controls for diagnostic PCR assays. *Journal of Clinical Microbiology* 42, 1863-1868 (2004).
- [12] Keer, J.T. & Birch, L. Molecular methods for the assessment of bacterial viability. *Journal of Microbiological Methods* 53, 175-183 (2003).
- [13] Lu, Y. et al. Specific Detection of Viable *Salmonella* Cells by an Ethidium Monoazide-Loop Mediated Isothermal Amplification (EMA-LAMP) Method. *Journal of Health Science* 55, 820-824 (2009).
- [14] Banihashemi, A., Van Dyke, M.I. & Huck, P.M. Long-amplicon propidium monoazide-PCR enumeration assay to detect viable *Campylobacter* and *Salmonella*. *J. Appl. Microbiol.* 113, 863-873 (2012).
- [15] Berney, M., Weilenmann, H.U. & Egli, T. Flow-cytometric study of vital cellular functions in *Escherichia coli* during solar disinfection (SODIS). *Microbiology-Sgm* 152, 1719-1729 (2006).
- [16] Nebe-von-Caron, G., Stephens, P.J., Hewitt, C.J., Powell, J.R. & Badley, R.A. Analysis of bacterial function by multi-colour fluorescence flow cytometry and single cell sorting. *Journal of Microbiological Methods* 42, 97-114 (2000).
- [17] Berney, M., Hammes, F., Bosshard, F., Weilenmann, H. & Egli, T. Assessing and interpreting bacterial viability using LIVE/DEAD(R) BacLight™ kit in combination with flow cytometry. *Appl Environ Microbiol* (2007).
- [18] Santos, S.B. et al. Selection and Characterization of a Multivalent *Salmonella* Phage and Its Production in a Nonpathogenic *Escherichia coli* Strain. *Applied and Environmental Microbiology* 76, 7338-7342 (2010).



- [19] Edgar, R. et al. High-sensitivity bacterial detection using biotin-tagged phage and quantum-dot nanocomplexes. *Proceedings of the National Academy of Sciences of the United States of America* 103, 4841-4845 (2006).
- [20] Hagens, S. & Loessner, M.J. Application of bacteriophages for detection and control of foodborne pathogens. *Applied Microbiology and Biotechnology* 76, 513-519 (2007).
- [21] Smartt, A.E. et al. Pathogen detection using engineered bacteriophages. *Anal. Bioanal. Chem.* 402, 3127-3146 (2012).
- [22] Singh, A., Arutyunov, D., Szymanski, C.M. & Evoy, S. Bacteriophage based probes for pathogen detection. *Analyst* 137, 3405-3421 (2012).
- [23] Liu, Y., Gilchrist, A., Zhang, J. & Li, X. Detection of viable but nonculturable Escherichia coli O157:H7 bacteria in drinking water and river water. *Appl Environ Microbiol* 74, 1502-1507 (2008).
- [24] Schofield, D.A., Sharp, N.J. & Westwater, C. Phage-based platforms for the clinical detection of human bacterial pathogens. *Bacteriophage* 2, 105–283 (2012).
- [25] Oda, M., Morita, M., Unno, H. & Tanji, Y. Rapid detection of Escherichia coli O157 : H7 by using green fluorescent protein-labeled PP01 bacteriophage. *Applied and Environmental Microbiology* 70, 527-534 (2004).
- [26] Awais, R., Fukudomi, H., Miyanaga, K., Unno, H. & Tanji, Y. A recombinant bacteriophage-based assay for the discriminative detection of culturable and viable but nonculturable Escherichia coli O157 : H7. *Biotechnology Progress* 22, 853-859 (2006).
- [27] Martins, V.C. et al. Femtomolar limit of detection with a magnetoresistive biochip. *Biosensors & Bioelectronics* 24, 2690-2695 (2009).
- [28] Freitas, P.P. et al. Spintronic platforms for biomedical applications. *Lab on a Chip* 12, 546-557 (2012).
- [29] Martins, V.C. et al. Challenges and trends in the development of a magnetoresistive biochip portable platform. *Journal of Magnetism and Magnetic Materials* 322, 1655-1663 (2010).
- [30] S. B. Santos, E. Fernandes, C. M. Carvalho, S. Sillankorva, V. N. Krylov, E. a Pleteneva, O. V Shaburova, a Nicolau, E. C. Ferreira, and J. Azeredo, “Selection and

- characterization of a multivalent *Salmonella* phage and its production in a nonpathogenic *Escherichia coli* strain.,” *Applied and environmental microbiology*, vol. 76, no. 21, pp. 7338–42, Nov. 2010.
- [31] S. Sillankorva, E. Pleteneva, O. Shaburova, S. Santos, C. Carvalho, J. Azeredo, and V. Krylov, “*Salmonella* Enteritidis bacteriophage candidates for phage therapy of poultry.,” *Journal of applied microbiology*, vol. 108, no. 4, pp. 1175–86, Apr. 2010.
- [32] C. Carvalho, M. Susano, E. Fernandes, S. Santos, B. Gannon, a Nicolau, P. Gibbs, P. Teixeira, and J. Azeredo, “Method for bacteriophage isolation against target *Campylobacter* strains.,” *Letters in applied microbiology*, vol. 50, no. 2, pp. 192–7, Feb. 2010.
- [33] D. W. Sambrook, Joe; Russel, *Molecular cloning: a laboratory manual*, 3rd ed. Cold Spring Harbor, NY: Cold Spring Harbor Laboratory Press, 2001.
- [34] V. C. Martins, F. a Cardoso, J. Germano, S. Cardoso, L. Sousa, M. Piedade, P. P. Freitas, and L. P. Fonseca, “Femtomolar limit of detection with a magnetoresistive biochip.,” *Biosensors & bioelectronics*, vol. 24, no. 8, pp. 2690–5, Apr. 2009.
- [35] J. Germano, V. C. Martins, F. a Cardoso, T. M. Almeida, L. Sousa, P. P. Freitas, and M. S. Piedade, “A portable and autonomous magnetic detection platform for biosensing.,” *Sensors (Basel, Switzerland)*, vol. 9, no. 6, pp. 4119–37, Jan. 2009.
- [36] V. C. Martins, J. Germano, F. a. Cardoso, J. Loureiro, S. Cardoso, L. Sousa, M. Piedade, L. P. Fonseca, and P. P. Freitas, “Challenges and trends in the development of a magnetoresistive biochip portable platform,” *Journal of Magnetism and Magnetic Materials*, vol. 322, no. 9–12, pp. 1655–1663, May 2010.
- [37] D. Saerens, L. Huang, K. Bonroy, and S. Muyldermans, “Antibody Fragments as Probe in Biosensor Development,” *Sensors*, vol. 8, no. 8, pp. 4669–4686, Aug. 2008.
- [38] E. Briand, M. Salmain, C. Compère, and C.-M. Pradier, “Immobilization of Protein A on SAMs for the elaboration of immunosensors.,” *Colloids and surfaces. B, Biointerfaces*, vol. 53, no. 2, pp. 215–24, Dec. 2006.
- [39] A Singh, N. Glass, M. Tolba, L. Brovko, M. Griffiths, and S. Evoy, “Immobilization of bacteriophages on gold surfaces for the specific capture of pathogens.,” *Biosensors & bioelectronics*, vol. 24, no. 12, pp. 3645–51, Aug. 2009.
- [40] M. Tolba, O. Minikh, L. Y. Brovko, S. Evoy, and M. W. Griffiths, “Oriented immobilization of bacteriophages for biosensor applications.,” *Applied and environmental microbiology*, vol. 76, no. 2, pp. 528–35, Jan. 2010.

- [41] L. Gervais, M. Gel, B. Allain, M. Tolba, L. Brovko, M. Zourob, R. Mandeville, M. Griffiths, and S. Evoy, "Immobilization of biotinylated bacteriophages on biosensor surfaces," *Sensors and Actuators B: Chemical*, vol. 125, no. 2, pp. 615–621, Aug. 2007.
- [42] "Sulfo-LC-SPDP." [Online]. Available: <http://www.piercenet.com/browse.cfm?fldID=02030365>.
- [43] D. G. Castner, K. Hinds, and D. W. Grainger, "X-ray Photoelectron Spectroscopy Sulfur 2p Study of Organic Thiol and Disulfide Binding Interactions with Gold Surfaces," vol. 7463, no. 26, pp. 5083–5086, 1996.
- [44] S. Li, L. R. S., V. A. Petrenko, and B. A. Chin, "Phage-based Pathogen Biosensors," in *Phage Nanobiotechnology*, 2008.
- [45] Rossoni, E. & Gaylarde, C. Comparison of sodium hypochlorite and peracetic acid as sanitising agents for stainless steel food processing surfaces using epifluorescence microscopy. *Int J Food Microbiol* 61, 81-85 (2000).
- [46] Oliver, J., Dagher, M. & Linden, K. Induction of *Escherichia coli* and *Salmonella typhimurium* into the viable but nonculturable state following chlorination of wastewater. *J Water Health* 3, 249-257 (2005).
- [47] Mizunoe, Y., Wai, S.N., Takade, A. & Yoshida, S. Restoration of culturability of starvation-stressed and low-temperature-stressed *Escherichia coli* O157 cells by using H<sub>2</sub>O<sub>2</sub>-degrading compounds. *Archives of Microbiology* 172, 63-67 (1999).
- [48] Rutala, W.A. & Weber, D.J. Uses of inorganic hypochlorite (bleach) in health-care facilities. *Clinical Microbiology Reviews* 10, 597-& (1997).
- [49] Porter, J., Deere, D., Hardman, M., Edwards, C. & Pickup, R. Go with the flow – use of flow cytometry in environmental microbiology. *FEMS Microbiology Ecology* 24, 93-101 (1997).
- [50] S. Li, L. R. S., V. A. Petrenko, and B. A. Chin, "Phage-based Pathogen Biosensors," in *Phage Nanobiotechnology*, 2008.
- [51] Gawande, P.V. & Bhagwat, A.A. Inoculation onto solid surfaces protects *Salmonella* spp. during acid challenge: a model study using polyethersulfone membranes. *Applied and Environmental Microbiology* 68, 86-92 (2002).



## **Chapter 4**

# **Development of a Detection Tool Based on Phage Recognition Peptides**

## **4.1 Novel "Nano-Phages" Interfaces for Biosensors**

**This work contributed for the:**

Provisional Patent Application No.61583850 entitled "*Phage Fusion Proteins as Interface for Detection Systems*". Inventor(s):Valery A. Petrenko, Deepa Bedi, **Elisabete R. Fernandes**, Vasily A. Petrenko Jr, Bryan Chin, Leon D. Kluskens, Joana Azeredo.

### Abstract

Biosensing systems are emergent in various areas of health due to limitations of conventional techniques. Developing diagnostic biosensor devices of quality involves several distinct strategies, including the choice of the biorecognition element. Qualities most sought for are: specificity, sensitivity, stability and low cost-production. If all combined in one system, the diagnostic device can lead to a rapid and real-time detection system. Bacteriophages (or phages) are viruses that infect bacteria and their elevated specificity is a potential advantage when used as a biorecognition element. In particular, filamentous phages have proven to be excellent bioelements and their exploration in the biosensor field is a challenge. Their specificity and stability under harsh environmental conditions are advantages that can compete with existing types of bioelements (e.g. antibodies). Studies involving filamentous phages as an interface describe that phages aggregate, forming bundles of fibers that cannot completely cover the sensor's interface. Subsequently, this can lead to a decrease in the sensor's performance. In this work, we report a new interface formed by biorecognition nanoparticles, called "nano-phages". "Nano-phage" comprises nanoparticles composed of self-assembled fusion major coat proteins of landscape phages selected against a target analyte. The interface was studied using a model phage selected from landscape library as a streptavidin binder. The results show that the "nano-phage" binds to streptavidin with the same or better affinity than the native phage. This new approach can be used to develop biosensors with increased performance in a wide range of applications, such as early detection of cancer diseases and other pathologies.

### 4.1 Introduction

Bacteriophages (phages) are viruses that infect bacteria and their intrinsic nature to infect bacteria make them a potential tool to detect and combat diseases. Phages can be divided in two groups depending on their life cycle: lytic or lysogenic. Virulent phages follow a strictly lytic pathway and are a good option for therapeutic use due to their ability to lyse the cell without interacting with the bacterial genome. However, this fact limits their application as biorecognition elements. In contrast, temperate phages follow a lysogenic pathway, integrating their genetic material into the host genome and therefore are considered better candidates to explore in biosensing systems [1–6]. Alternatively, filamentous phages are also good option because they are extruded across the bacterial outer membrane without causing cell lysis. Features such as specificity, sensitivity, stability and low production costs make these biomolecules a promising alternative to antibodies, nucleic acids and enzymes, which are considered expensive, fragile and sensitive to environmental conditions [7–9]. Several studies have demonstrated that phages are more efficient compared to antibodies. In particular, the environmentally robust filamentous phages have been successfully used as an alternative to fragile antibodies in wireless biosensor systems for real-time pathogen detection [10]. Filamentous phages are natural biopolymers, which can be genetically engineered to display multiple copies of foreign peptides that bind various hazardous biological agents, including bacteria, spores and cancer cells [11]. Peptide-displaying phage clones are typically selected by affinity from a landscape phage library, followed by DNA sequencing to identify the phage-displayed peptides [12]. Morphologically, filamentous phages are flexible thread-shaped bacterial viruses, with a dimension of approximately 6 nm wide and 800–900 nm long. The protein tube contains thousands of copies of pVIII (major coat protein) and pIII, pVI, pVII and pIX (minor coat protein), which are located at the tube ends [13,14]. The potential of landscape phages as a selective and robust interface in biosensors was shown in numerous publications as mentioned previously. However, due to their structure, when immobilized on sensor surfaces, they aggregate easily, forming bundles of fibers [15]. In such a situation, the bio-element cannot completely cover the sensor's interface leading to a decrease in the sensor's performance. Moreover, in detection systems false positive results may occur due their ability to detect *Escherichia coli*. In order to find a solution for this problem, we developed nanosized phage particles, called “nano-phages” (NPs). “Nano-phage” comprises nanoparti-

cles composed of self-assembled fusion major coat proteins of landscape phages selected against the target analyte. The main objective of this work was to improve the detection sensitivity, developing small molecules derived from filamentous phages (NPs) and construct a competitive interface that can be tested and used in different types of sensor's platforms. The proof-of-concept was established by using a phage previously selected from the landscape libraries as a streptavidin binder (7B1) [11]. Enzyme-linked immunosorbent assays (ELISA) were used to confirm and test the NPs specificity. Their binding affinity when they are immobilized by physical adsorption on a solid surface (e.g. gold) was confirmed by scanning electron microscopy (SEM). The ELISA assay confirmed that the NPs affinity is approximately 1.6 times higher than when the entire phage is used. Moreover, when immobilized to a magnetoelastic (ME) sensor by physical adsorption they demonstrate specificity and selectivity towards the target analyte used for selection of parental phage. Our findings suggest an interface that can lead to the development of efficient devices to apply in the food industry, environmental area and health.

### 4.1.1 Materials and Methods

#### 4.1.1.1 Bacteriophages and Bacterial Strains

Phages of the Ff class infect *E. coli* with the plasmid-encoded F-pilus [12] and *Escherichia coli* K91 BluKan cells used for phage amplification were obtained from the Natasha Lab. The phage used in this work was selected from a landscape library as a streptavidin binder. Accordingly, phage 7B1 was selected from an 8-mer library as streptavidin binder and displayed the peptide VPEGAFSS [11], [16]. In this study, the wild-type phage F8-5 was used as a negative control [17].

#### 4.1.1.1 Phage Propagation

The phage was propagated in *E. coli* K91 BluKan cells and purified by polyethylene glycol (PEG) precipitation as described before [18]. Briefly, 4 L of 2 XYT Medium (16 g, bacto-yeast extract 10 g, and NaCl 5 g/1 L, pH 7.4) containing 20 µg/ml tetracycline was inoculated



with a single colony of cells harboring 7B1 phage. The culture was grown for approximately 15 h until reaching the stationary phase. The culture was then centrifuged at 2,744 x g (Beckman Coulter Avanti J-E; Rotor JA-10) during 10 min at 4°C and, supernatant containing phage was collected and centrifuged at 7,025 x g (Beckman Coulter Avanti J-E; Rotor JA-10) for 10 min at 4°C. Cleared supernatant was transferred to a fresh centrifuge bottle, and 0.15 volume of polyethylene glycol (PEG)/NaCl (16.7% PEG, 3.3 M NaCl) was added, mixed thoroughly by inversion, and left overnight at 4°C. Phage was pelleted by centrifugation at 7,025 x g (Beckman Coulter Avanti J-E; Rotor JA-10) for 40 min at 4°C, and the pellet was resuspended in 10 ml of Tris-buffered saline (TBS). The phage suspension was clarified by centrifugation at 22,554 x g (Beckman Coulter Avanti J-E; Rotor JA-17) for 10 min at 4°C and was transferred to a fresh centrifuge tube for the second phage precipitation step with PEG/NaCl. Phage collected by centrifugation as described above was resuspended in 5 ml of TBS. The phage suspension was clarified by centrifugation at 22,554 x g (Beckman Coulter Avanti J-E; Rotor JA-17) for 10 min at 4°C and its concentration was measured spectrophotometrically and calculated in virions per milliliter, assuming that 1 (AU)<sub>269</sub> = 6.5 × 10<sup>12</sup> virions/ml (physical titer). The concentration of infective phage particles (biological titer) of the phage suspension was done by infecting the host cells, plating, and counting of colonies.

### 4.1.1.2 Peptide Sequence Determination

The peptide sequence was determined by PCR amplification of the pVIII gene of the phage and purification of PCR products, followed by sequencing. The PCR reaction was carried out using the forward primer f8s-20: (5'-CAAAGCCTCCGTAGCCGTTG -3') and the reverse primer f8as-20: (5'- CATTCCACAGACAGCCCTCA -3'). Each primer was used at a concentration of 10 pmol/μl. The phage 7B1 was diluted 1:100 in filter-sterilized water and added to the PCR reaction tube containing 24 μl reagents for PCR: 10×Mg-free reaction buffer (2.5 volumes); 25 mM MgCl<sub>2</sub> (2 volumes); 2.5 mM dNTPs (2 volumes); Taq DNA polymerase (0.04 volumes); 0.3 volumes of each primer and 16.9 volumes of filter-sterilized water. PCR was performed using GeneAmp PCR System 2400 (Perkin Elmer, Norwalk, CT, USA) using the following conditions: the first cycle corresponds to initial denaturation and occurred at 94°C during 3 min, then followed by 35 cycles at 94°C for 10 s, 46°C for 20 s, 72°C for 45

s; and finally one cycle at 72°C for 4 min. The PCR products obtained were analyzed using agarose gel electrophoresis (2% wt/vol agarose) in 1× TBE. The gel was run at 70 V during 1 hour in 1× TBE buffer. The gel was stained with SYBR Green I nucleic acid gel stain (Cambrex BioScience Rockland, Rockland, ME, USA) and illuminated on the Dark Reader (Clare Chemical Research, Denver CO). DNA bands were visualized using a Kodak EDAS 290 imaging system (Eastman Kodak Company, Rochester, NY, USA). To remove the primers and dNTPs, which can interfere with sequencing reactions, PCR products were purified using QIAquick PCR purification Kit (QIAGEN Inc., Valencia, CA) following the manufacturer's description and sequenced at the Auburn University Genomic and Sequencing Laboratory (Auburn, AL) using primer f8s-20 at 20 ng/μl (8 μl of primer solution/purified PCR sample). The sequences obtained were analyzed using CHROMAS software (version 1.45 Conor McCarthy, Griffith University, Southport, Queensland, Australia).

### **4.1.1.3 Isolation of Phage Coat Protein (PCP)**

Following phage propagation, isolation of the phage coat protein 7B1 was carried out using a Sepharose 6B-CL (column preparation procedure in Appendix B) (Amersham biosciences, NJ, USA) column (1 x 50 cm) according to the following procedure: a 1.5 ml eppendorf tube containing 350 μL of phage clone ( $1.5 \times 10^{14}$  vr/ml in TBS), 700 μL of cholate stabilizing solution (120 mM cholate with 10 mM Tris-HCl and 0.2 mM EDTA, pH 8.0) and 27 μL chloroform was incubated overnight at 37°C by rotation. Then, 1 ml of phage coat protein 7B1 was applied to the column at a flow rate of 0.5 ml/min. As a running buffer 100 mM cholate was used. Fractions were collected every 5 min, and stored at 4°C. The process was monitored by the Econo UV monitor (Bio-Rad, CA, USA). The concentration of protein per fraction was measured on a spectrophotometer (Nanodrop, Model ND-1000).

### **4.1.1.4 "Nano-Phages" Purification**

The biorecognition nanoparticles called “nano-phages” (NPs) were obtained using two techniques: chromatography by eluting the phage coat protein in 10 mM Tris-HCl, pH 8.0 and ultracentrifugation.

### 4.1.1.5.1 Chromatography

After the isolation of PCP, 1 ml fractions containing high pure protein concentrations were loaded onto a sepharose column and eluted with 10 mM Tris-HCl pH 8.0 at a flow rate of 0.5 ml/min, collecting fractions every 5 min. Protein concentration and purity of each fraction was determined by measuring the absorbance at 280 nm. The sample used for binding affinity tests was selected based on the ratio  $A_{260/280}$ .

### 4.1.1.5.2 Ultracentrifugation

One hundred microliters of phage protein in 100 mM cholate buffer was centrifuged and concentrated in 30 kDa Amicon centrifugal units at 1,362 x g (Allegra 21R Centrifuge) for 15 min to remove the excess of detergent. The residual ~30  $\mu$ l portion was diluted to 4 ml with 10 mM Tris-HCl, 0.2 mM EDTA pH 8.0 (first 1 ml was added and gently mixed, then 3 ml more was added and again mixed) followed by centrifugation for 15 min at 1,362 x g. Fifty  $\mu$ l of the concentrated protein was obtained and transferred to a 0.5-ml tube. The Amicon unit was washed with 50  $\mu$ l of 10 mM Tris-HCl, pH 8.0. The washing fraction was added to 50  $\mu$ l of the concentrated protein and characterized by UV spectroscopy.

### 4.1.1.5 Size distribution by Dynamic Light Scattering (DLS)

The size of the NPs was evaluated using the Nicomp Model 380/DLS particle sizer. The minimal volume of sample allowed by the equipment was 700  $\mu$ l. Therefore, the samples were diluted in 10 mM Tris-HCl, pH 8.0, until reaching the required volume. The size of NPs at 20  $\mu$ g/ml was also analyzed before immobilization on the sensor surface.

### 4.1.1.6 Enzyme-linked Immunosorbent (ELISA) Assays

ELISA binding assays were performed to confirm the specificity and dose-dependent binding of the NPs to the target.

### 4.1.1.8 Binding Affinity of Phage 7B1 and NPs Based on Direct ELISA

Entire phages and the NPs at concentrations of 7, 14 and 20  $\mu\text{g/ml}$  were immobilized onto a 96-well polystyrene microtiter plate by physical adsorption and incubated for 2 h at room temperature. 0.1% Bovine serum albumin (BSA-SIGMA) was used as a blocking buffer and as a negative control to evaluate nonspecific binding. Unbound NPs and phages were washed on Microplate Washer (ELX-405) using repeated washes with 100  $\mu\text{l}$  of 10 mM Tris with 0.1% Tween 20. The wells were filled with different concentrations of streptavidin conjugated alkaline phosphatase (AP-SA). After incubated during 1 h, the wells were washed and developed with *p*- nitrophenyl phosphate (NPP) at  $\text{OD}_{405}$ . The slope of color development was measured as a change in optical density (mOD/min or /hr) in a Synergy™ H1 Hybrid Microplate Reader.

### 4.1.1.9 Inhibition of AP-SA binding by NPs and 7B1 phage

In the competition assay the wells were coated with NPs and phage 7B1 and washed as described above. The wells were filled with constant concentrations of AP-SA (6.25  $\mu\text{g/ml}$ ) and competitive inhibitors at different concentrations (Table 4:1). Controls consisted of wild type phage (F8-5) and the BSA 0.1% in the absence of AP-SA.

**Table 4:1:** Concentrations of competitive inhibitors.

Phage dilutions (vr/ml)	Phage 7B1 ( µg/ml)	Phage F8-5 ( µg/ml)	NPs and BSA (µg/ml)
1.2 x10 <sup>12</sup>	46.1	41.86	60
0.4x10 <sup>12</sup>	15.36	13.95	20
1.33x10 <sup>11</sup>	5.11	4.64	6.67
0.44x10 <sup>11</sup>	1.69	1.53	2.22
1.48x10 <sup>10</sup>	0.57	0.52	0.74
0.49x10 <sup>10</sup>	0.19	0.17	0.25
1.65x10 <sup>9</sup>	0.07	0.06	0.08
0.55x10 <sup>9</sup>	0.02	0.02	0.03
0.18 x10 <sup>9</sup>	0.007	0.01	0.009

\*10 mM Tris-HCl pH 8.0 for protein and Milli-Q water for BSA

#### **4.1.1.10 Magnetoelastic Resonator Platform**

The theory behind the ME resonator platform is described in detail in Chapter 1, nevertheless, some important technical aspects of this platform are given here.

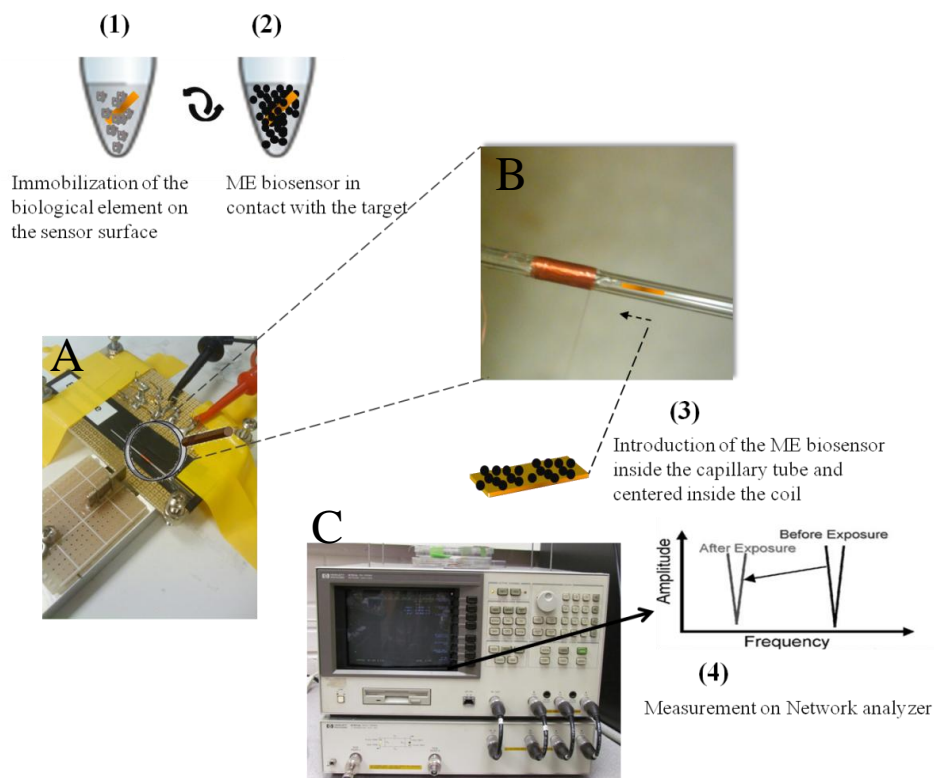
#### **Fabrication Process and Operation Principle**

The ME strip-shaped resonator platforms were supplied by METGLAS<sup>®</sup> 2826MB alloy and its microfabrication process has been described in many papers from Dr. Chin's Group [19–22]. The ME material was provided by the company in the shape of a roll of ribbon and was diced in rectangular pieces of 200 µm x 1 mm using a micro-dicing saw. ME sensors were cleaned ultrasonically with acetone and ethanol. The small pieces were coated with two film layers: chromium (Cr) and gold (Au). Cr formed the first layer deposited, allowing the adhesion of the Au layer. The main function of Au is to protect the ME material from corrosion [23], when exposed to saline solutions, and in addition it provides a bioactive surface for NPs immobilization. The operation principle of ME biosensors is based on the magnetostriction effect, where the material dimensions change in the presence of a magnetic field [24]. When exposed to an alternate magnetic field, the applied magnetic energy is converted into mechan-

ical oscillations with a characteristic resonant frequency. As the resonance frequency depends on the physical properties and materials dimensions when a non-magnetoelastic mass is added to the sensor, their mechanical oscillations decrease, consequently decreasing the resonance frequency. Resonance frequency measurements of ME biosensors were performed in an electrical circuit that consists of a network analyzer (HP/Agilent 8751A Agilent Technologies Inc., Santa Clara, CA, USA), operated in the S11 mode. A single-layer solenoid coil around a glass capillary tube (0.4 mm inner diameter) was used. The experimental setup is illustrated in Figure 4:1.

### Immobilization of the NPs and Streptavidin Detection

Unpolished magnetoelastic (ME) sensors were immersed in 100  $\mu\text{l}$  of NPs suspension at 25  $\mu\text{g/ml}$  and incubated during 1 h at room temperature under continuous smooth rotation. The rotation allows the NPs to self-assemble over the sensor surface. Then, the ME biosensors were washed three times to remove unbound NPs and incubated with 0.1% BSA (blocking buffer) during 40 min. The control sensors were treated only with 0.1% of BSA. The biosensors and control sensors were exposed to  $1.0 \times 10^7$  beads/ml (Streptavidin polystyrene beads, 0.97  $\mu\text{m}$ , Bangs Labs, Inc., Fishers, IN) and subsequently washed three times with milli-Q water to remove unbound streptavidin beads. Binding affinity of the NPs to the target (streptavidin beads) was measured as a change in resonance frequencies and visualized by scanning electron microscopy (JOEL 7001 SEM). Dose dependence experiments were conducted using the NPs-based ME biosensors exposed to different concentrations of streptavidin polystyrene beads and carried out "in air". In simple words, following NPs immobilization and blocking step each sensor was dried and the signal was measured ( $f_0$ : characteristic resonance frequency considered as a start point or reference). Then, after streptavidin exposition and washing steps, the sensors were dried in air and the frequency was measured ( $f_{\text{mass}}$ ). Subtracting the  $f_{\text{mass}}$  from  $f_0$ , the resultant resonance frequency is the result of the mass changed over the sensor ( $\Delta m$ ), described by the equation 1 (Chapter 1).



**Figure 4:1:** Scheme of the experimental setup using a NPs-based ME sensor. A: Image of the measurement circuit of the magnetoelastic sensor; B: Image of the wire coil around glass capillary and a ME sensor after exposed to the target; C: Network Analyzer.

### 4.1.1.7 Western Blot

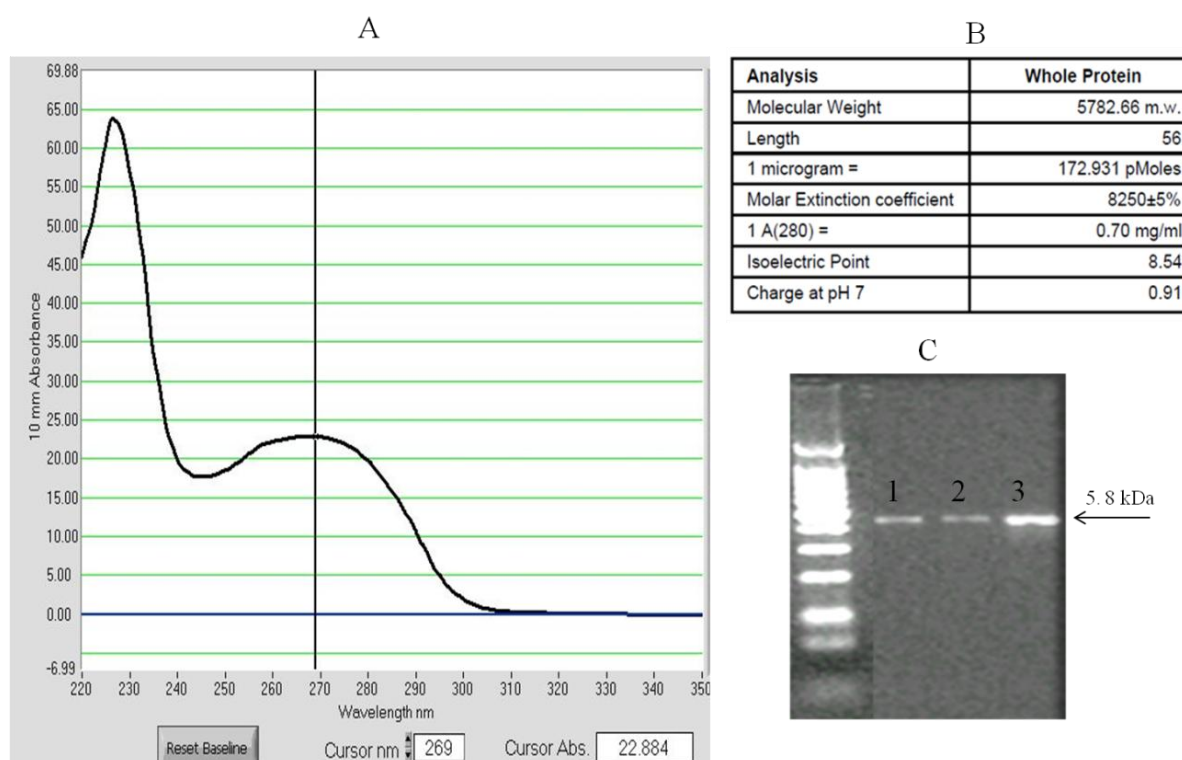
The presence of NPs was also confirmed by Western blot. NPs were immobilized on the sensor as explained previously, and the sensor was immersed in 20  $\mu$ l of Laemmli Sample buffer (BioRad) and heated at 95°C during 10 min. The sensor was washed three times and a 10- $\mu$ l sample of each washing step was treated with 10  $\mu$ l of sample buffer and heated (95°C, 10 min). Subsequently, 10  $\mu$ l samples were loaded onto a 16.5 % Tris-Tricine gel. Electrophoresis was carried out during 40 min at 100 V. Proteins were transferred to a 0.2  $\mu$ m polyvinylidene difluoride (PVDF) membrane. The resulting blots were probed with anti-fd antibody for N-terminus detection (3.3 mg/ml). Following incubation with horseradish peroxidase (HRP) conjugated antirabbit IgG (200 $\mu$ g/0.5ml) and NeutraAvidin-HRP the blots were visualized using a chemiluminescent substrate solution (West Pico: Stable Peroxide Solution and Luminol/Enhancer Solution).

## 4.1.2 Results

The aim of the present study was to analyze an alternative to using entire phages as an interface for detection systems. NPs were produced, purified and their efficiency was analyzed and confirmed using immunoassays techniques (ELISA-based formats).

### 4.1.2.1 Phage Characterization and Phage-coat Protein Isolation

Following amplification and purification, the filamentous phage 7B1 was characterized and the results are presented in Figure 4:2. The absorbance profile (Figure 4:2–A) was the first indicator that provided the elements to calculate the physical titer, as well as the information of protein and DNA ratio [25].

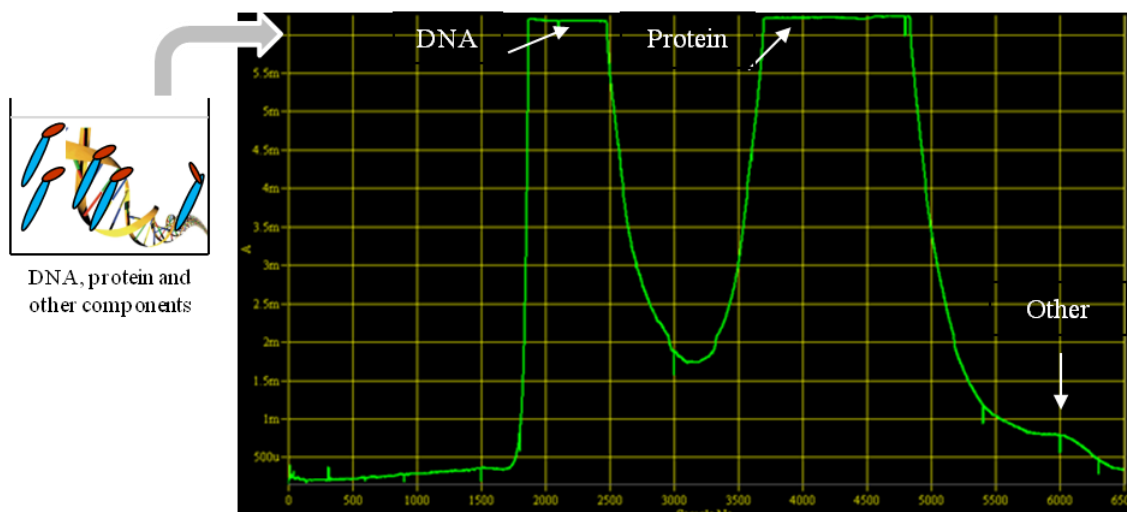


**Figure 4:2:** Phage 7B1 characterization: A - Absorbance profile obtained with a NanoDrop spectrophotometer; B - Phage characteristics C- PCR products of three 7B1 phage stocks with the following biological titers: 1-  $7.9 \times 10^{11}$  vr/ml; 2-  $8.5 \times 10^{11}$  vr/ml; 3-  $1.49 \times 10^{12}$  vr/ml.



The adsorption spectrum in Figure 4:2 shows a broad plateau in the area 260-280 nm with a maximum at 269 nm as expected for filamentous phages [26]. The absorbance was used to calculate the physical titer as follows:  $6.5 \times 10^{12} \times 23 = 1.5 \times 10^{14}$  vr/ml. The ratio  $A_{260/280}$  was 1.12. PCR amplification of the pVIII gene of the 7B1 phage and the sequencing of the amplified DNA fragment allowed the confirmation that phage production was carried out well, as shown in Figure 4:2-C (bands of ~5.8 kDa) and has the following sequence: AAVPEGAFSSDPAKAAFDS LQASATEYIGYAWAMVVVIVGATIGIKLFFKKFTSKAS.

After the analysis of the phage propagation parameters, the coat protein was isolated from the phage particle by solubilization with sodium cholate solution and subsequent size exclusion chromatography (Figure 4:3).

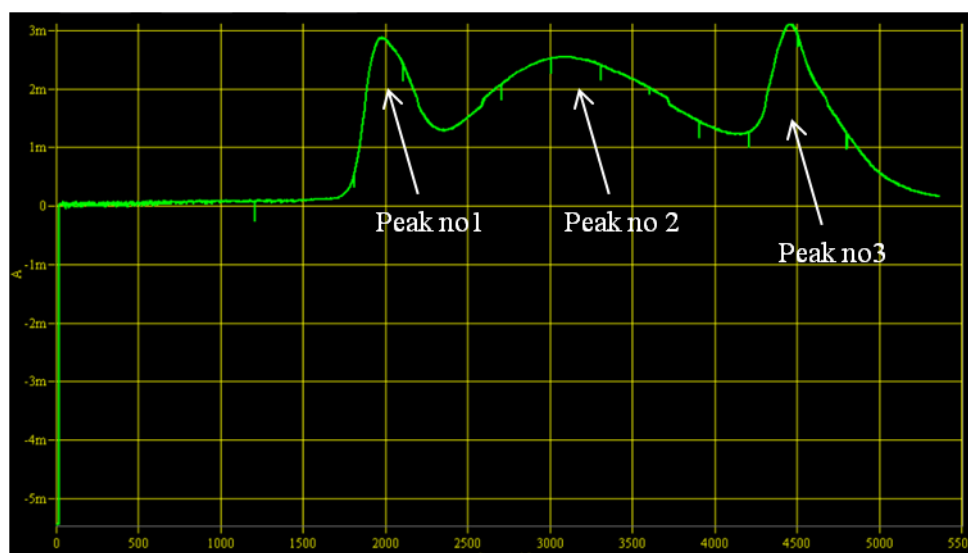


**Figure 4:3:** Isolation of the phage-coat protein by size-exclusion chromatography. Phage 7B1 (VPEGAFSSD) was loaded on a Sepharose column with 100 mM sodium cholate running buffer flow rate of 0.5 ml/min and fractions were collected every 5 min. Phage-coat protein was collected in a 100 mM sodium cholate buffer solution, which was subsequently exchanged for biosensor purposes

### 4.1.2.2 NPs Formation

The sodium cholate buffer containing the phage coat protein was exchanged for 10 mM Tris-HCl, pH 8.0, by an additional chromatography step as presented in Figure 4:4. The surfactant

from the solution was removed allowing NPs formation and further improvement of the adhesion quality of these biomolecules to the sensor surface during the immobilization step.

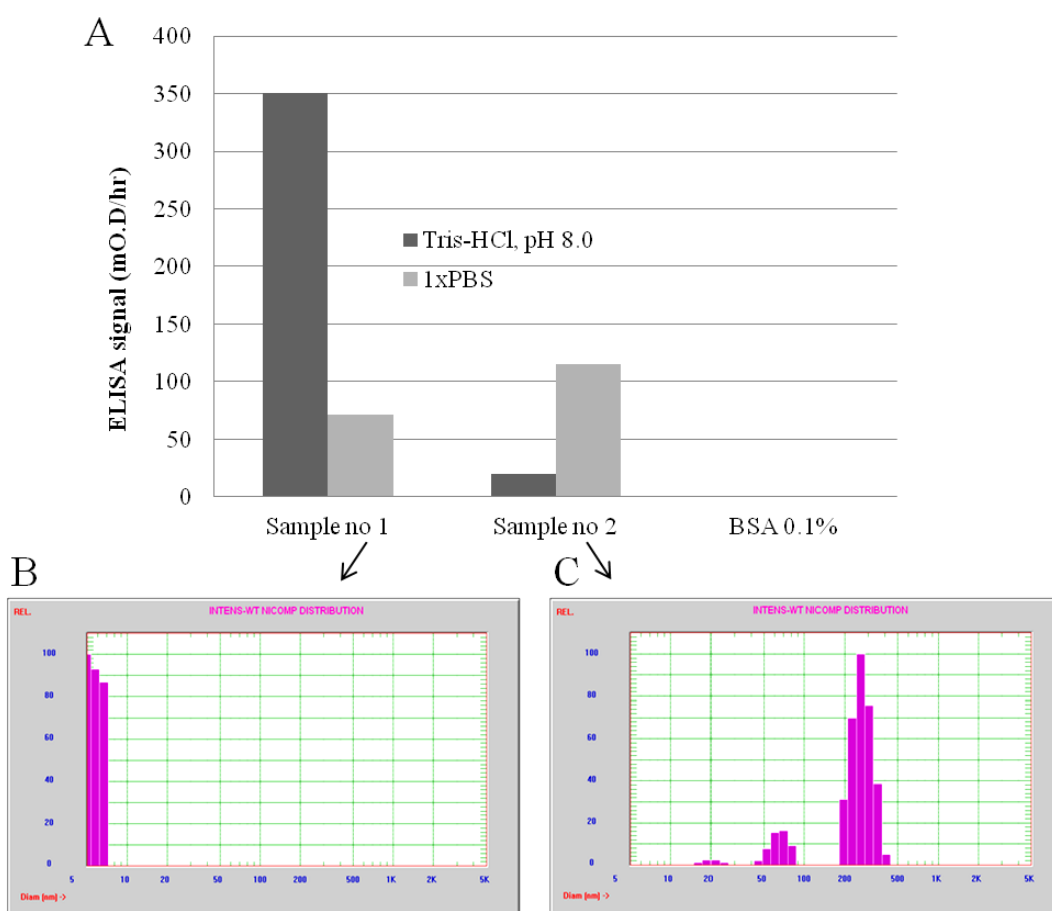


**Figure 4:4:** Elution/exchange buffer of a fraction of the phage coat protein (pVIII) on a sepharose column with 10 mM Tris-HCl, pH 8.0, at a flow rate of 0.5 ml/min. Fractions were collected every 5 min. Peak 1, 2 and 3 correspond to the NPs fractions obtained. Chromatography allowed the NPs for formation at a slow flow rate, which may assist in maintaining the correct particle configuration preserving their biological activity.

### 4.1.2.3 Assessments of the NPs Activity

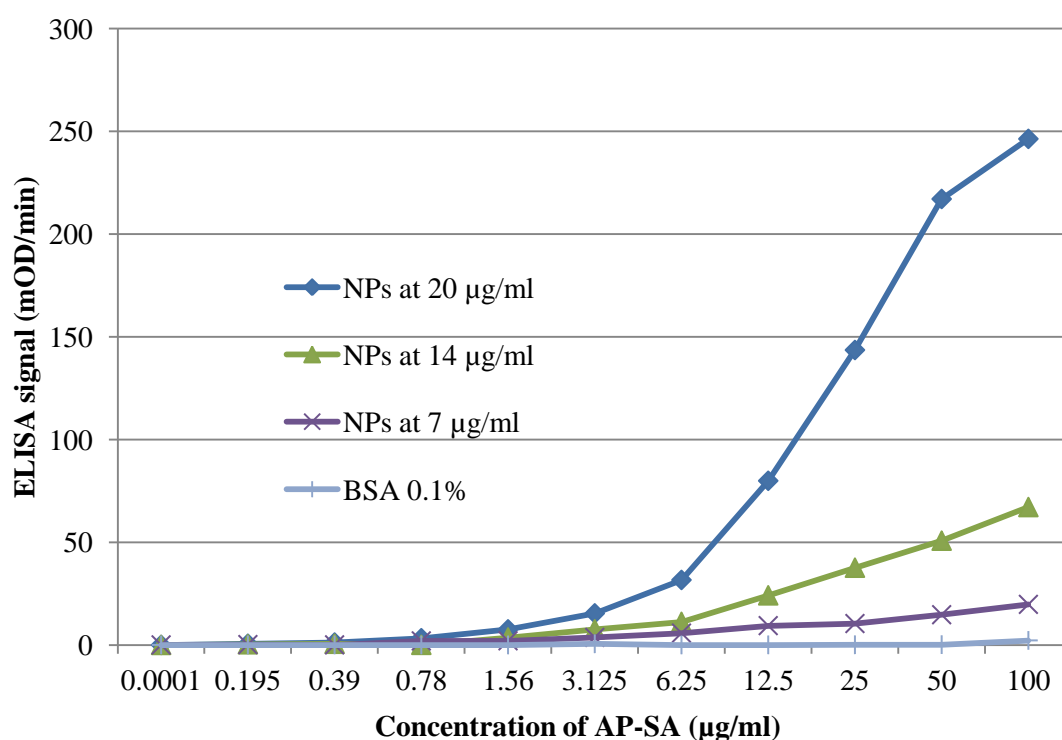
Production and purification conditions like buffer composition, pH, temperature, centrifugation velocity are aspects that may compromise the biological activity of nanoparticles and need to be considered during the process of NPs formation [16]. Accordingly, assessments to verify the stabilization and binding affinity of NPs were performed. Initially, the objective was to obtain higher concentrations of NPs and verify their behavior or activity under those conditions. Therefore, during NPs formation, fractions were collected from the third peak and their activity was tested. From that peak two type of samples were used, i.e. a sample containing one collected fraction and a second sample joining three fractions. It should be noted that all fractions used belong to the third peak. The idea was to understand if it is possible to increase the concentration and if the NPs activity can be compromised using these conditions; the NPs, when too concentrated, can aggregate. As a result, the active part may not be availa-

ble to recognize the target of interest. The process was carried out by ultracentrifugation and their activity analyzed using a direct ELISA assay. PBS and Tris-HCl, pH 8.0, were also used to verify if the Tris-HCl buffer is a favorable option to use in NPs formation. The binding affinity (Figure 4:5–A) represented by mOD/hr is the linear rate of change in absorbance over the time period during which the absorbance was monitored. The NPs were tested against 50 µg/ml of streptavidin conjugated alkaline phosphatase (AP-SA). The size distribution in each sample was evaluated, using dynamic light scattering (DLS) represented (Figure 4:5–B and C).



**Figure 4:5:** Analysis of the activity of NPs using one or three fraction mixtures prepared in two different buffers: Tris-HCl, pH 8.0, and 1xPBS, sample no 1 and no 2, respectively. The 0.1% BSA was used as a control. A: Signal obtained for both samples by direct ELISA assay against 50 µg/ml of AP-SA. B-C: Intensity-Weighted Gaussian distribution obtained by NICOMP 380 DLS.

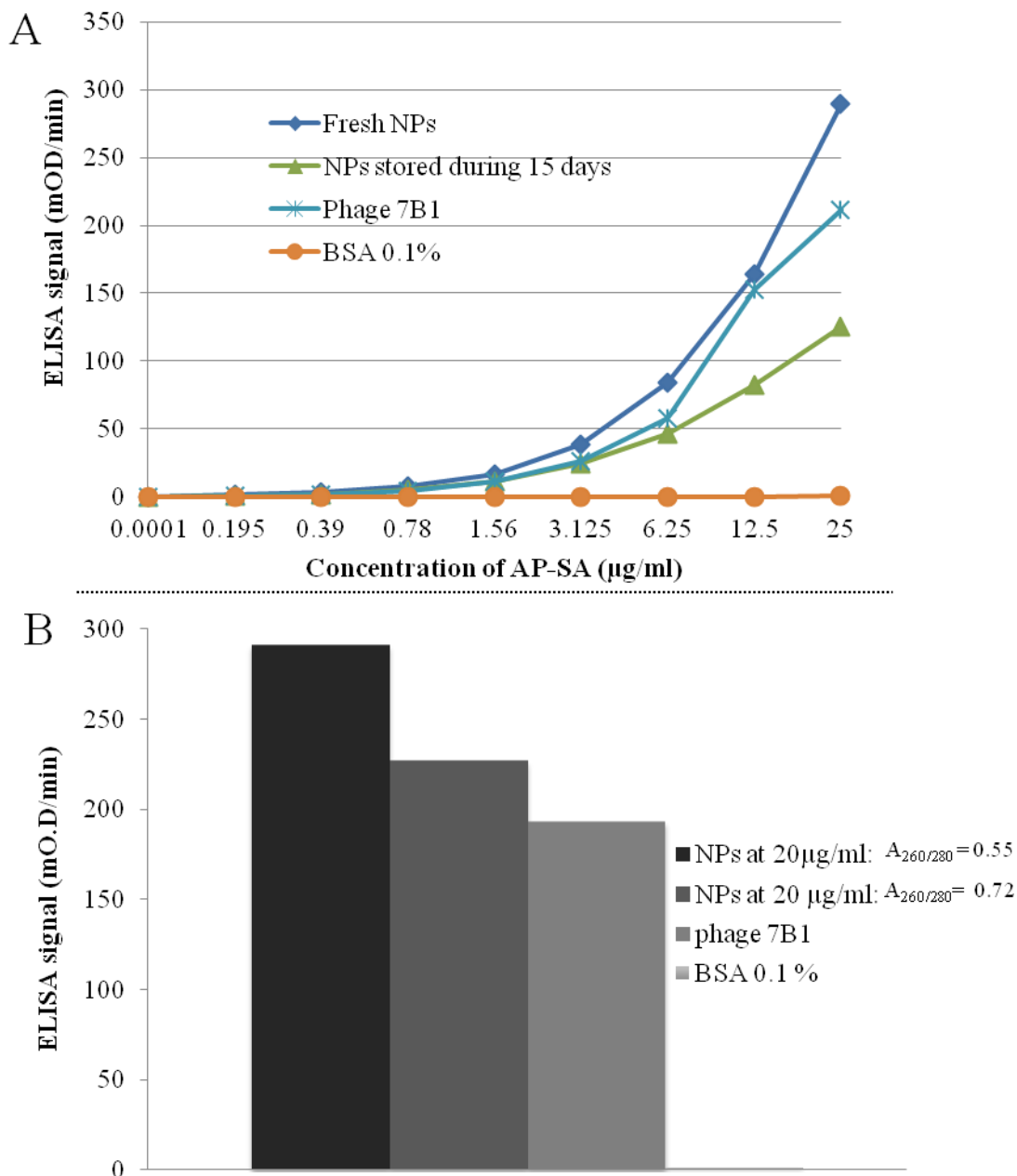
Figure 4:5–A shows that the higher sensitivity was confirmed for sample No 1, which contains NPs collected from one fraction (diameter of  $5.8 \text{ nm} \pm 0.9 \text{ nm}$ ). When mixing more than one fraction, the DLS results showed three size NPs populations (Figure 4:5–C). The first population (2.1%) presented an average diameter of  $20.4 \text{ nm} (\pm 2.4 \text{ nm})$ , the second (13.7%) displayed an average size of  $66.6 \text{ nm} (\pm 9.1 \text{ nm})$  and the last presented the largest size (84.2%) with a mean diameter of  $270.9 \text{ nm} (\pm 53.6 \text{ nm})$ . Correlating these values with NPs sensitivity, the heterogeneous population exhibited a decreased sensitivity, suggesting that aggregation may interfere with their activity. Homogeneous NPs size population presented a higher signal for the solution prepared with Tris-HCl buffer. The results obtained so far enabled the establishment of the protein fraction to be recovered and the optimal buffer to prepare NPs. After this first optimization, three concentrations of phage particles, 7, 14 and 20  $\mu\text{g/ml}$ , were tested with the purpose of verifying which concentration improves the sensitivity of the signal (Figure 4:6).



**Figure 4:6:** Comparison of the binding affinity of NPs against different concentrations of AP-SA.

The efficiency of each NPs suspension (eluted in 10 mM Tris-HCl, pH 8.0) was tested by direct ELISA against different concentrations of AP-SA. The highest signal was obtained for NPs at 20  $\mu\text{g/ml}$ . In addition, a few stability tests were conducted, taking into consideration

the ratio  $A_{260/280}$  nm and the storage time (Figure 4:7). The results showed that the binding affinity of fresh NPs was greater than the NPs stored during 15 days (Figure 4:7–A), suggesting that improvements should be considered to increase the shelf-life of these biomolecules.



**Figure 4:7:** Stability tests considering the storage time and the ratio  $A_{260/280}$  nm as parameters. A: Dose-dependent binding comparison of fresh samples of NPs to a sample stored during 15 days. Different concentrations of AP-SA were used. B: Binding affinity of NPs at two different ratios when exposed to 50 µg/ml of AP-SA. BSA 0.1% and phage 7B1 were used as a negative and positive control, respectively.

When using equal NPs concentration but different  $A_{260/280}$  ratio (Figure 4:7–B), the binding affinity increased considerably for a ratio of  $0.7 < A_{260/280} \leq 0.5$ . The binding affinity of stored samples decreased approximately 56.5% compared to fresh samples (when NPs are exposed to 25  $\mu\text{g/ml}$  of AP-SA). Based on these results, freshly NPs at 20  $\mu\text{g/ml}$  were considered for the following affinity tests. In order to use a phage concentration equal to that of the NPs (20  $\mu\text{g/ml}$ ), calculations - as shown in an example below - were carried out to estimate the phage coat protein present in whole phage:

### **Parameters:**

Concentration of phage solution =  $2.64 \times 10^{14} \text{ vr/ml} \gg 2.64 \times 10^{17} \text{ vr/L}$

*Avogadro Constant:*

1 mol  $\equiv 6.022 \times 10^{23}$  elementary entities

4000 copies of major coat protein pVIII

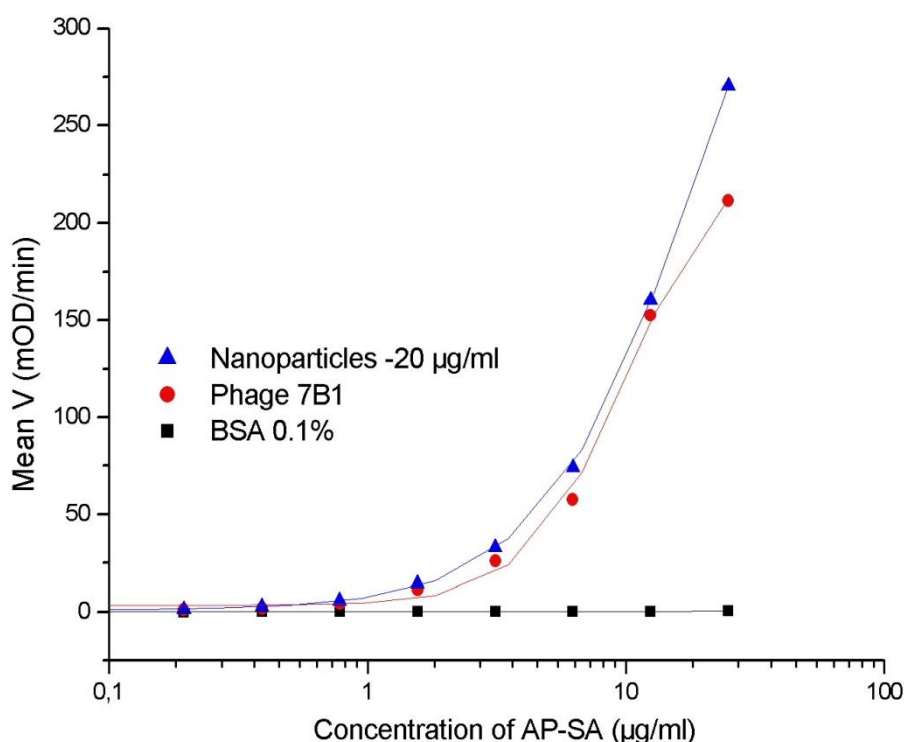
*Molecular Weight* = 5782.66 Da  $\equiv 5782.66 \text{ g/mol}$

### **Calculation:**

$$\begin{aligned} [\textit{Phage coat protein}] &= 0.14 \times 10^{14} \frac{\textit{vr}}{\textit{L}} \times \frac{1 \textit{mol}}{6.022 \times 10^{23}} \times 4000 \times 5782.66 \frac{\textit{g}}{\textit{mol}} \\ &= 0.01536 \frac{\textit{g}}{\textit{L}} = 15.36 \mu\textit{g/ml} \end{aligned}$$

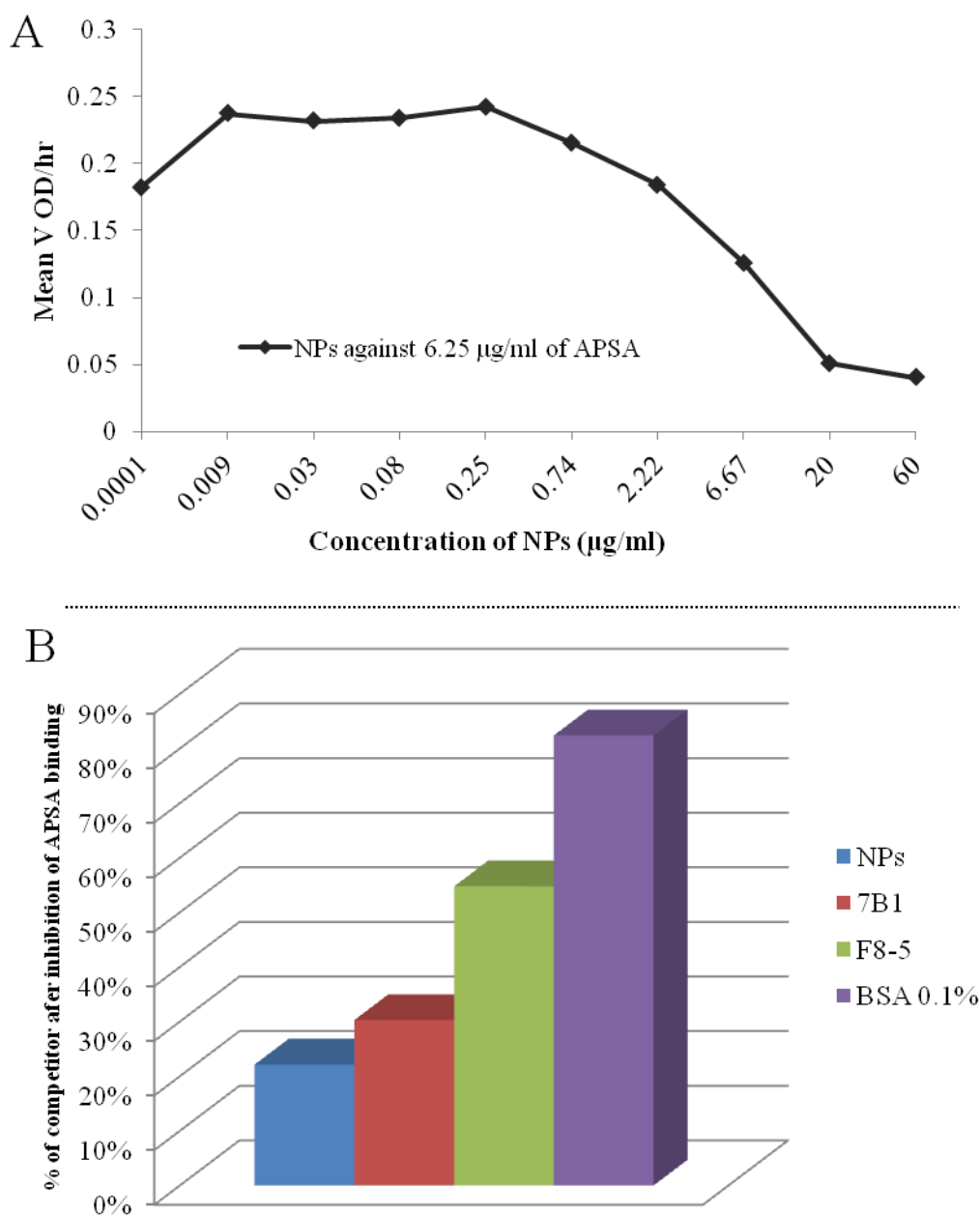
#### **4.1.2.4 . Binding Affinity of NPs Versus Parental Phage**

A direct ELISA was performed, allowing the confirmation of the specificity and dose-dependent binding of NPs to the analyte - different concentrations of AP-SA.



**Figure 4:8:** Sigmoidal fit to ELISA data points indicates dose-dependent binding ( $r^2 = 0.94$ ) between NPs and AP-SA. Phage 7B1 and 0.1% BSA were used as a positive and negative control, respectively.

The dose-dependent binding obtained in Figure 4:8 showed NPs with the same affinity to the analyte as a parental phage, however based on sigmoidal fit, the NPs showed a sensitivity slightly higher than phage. The 0.1 % BSA solution demonstrated no binding. These results gave also the information on which concentration of AP-SA generates a suitable signal for inhibition (6.25 µg/ml). The affinity of NPs was also demonstrated using other ELISA format, i.e. by measuring the ability of NPs at different concentrations in solution to competitively inhibit binding of AP-SA to an immobilized phage 7B1 (Figure 4:9). The competitive assay involved 0.1% BSA and the wild-type phage F8-5 as controls, which displayed 129 times less binding to streptavidin than 7B1 phage, as demonstrated by [27].



**Figure 4:9:** A: Inhibition of AP-SA binding (6.25 µg/ml) by NPs at different concentrations. B: compared with parental phage (7B1) Wild-type phage F8-5 and BSA 0.1% were used as a control.

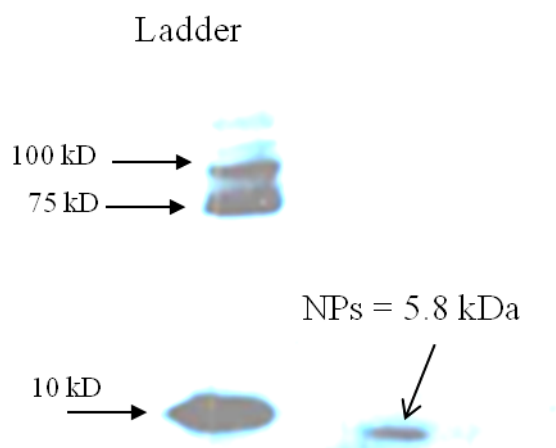
In the competitive assay, the parental phage 7B1 was immobilized on well surfaces that were filled with competitive phages and NPs. The inhibition ELISA assay presented in Figure 4:9 showed that the non-immobilized NPs compete with immobilized phage for binding to their respective target (AP-SA), producing total inhibition when their concentration is between 20-60 µg/ml. Comparing the NPs inhibition in Figure 4:9-B with the positive control



(parental phage 7B1) and negative control (wild-type phage F8-5 and BSA) we can observe that NPs was a good competitor, displaying ~78% of efficient inhibition against 70%, 45 % and 18% obtained by 7B1, F8-5 and BSA, respectively.

### 4.1.2.5 NPs Immobilization on Gold Surfaces

NPs were immobilized on the sensor's surface by physical adsorption and the initial confirmation that NPs were successfully immobilized was obtained by Western blotting. This assay allowed us to measure the relative amount of the protein present in the sample and to confirm whether, after several washes, the NPs were correctly immobilized on the sensor surface with the assurance that unbound protein was completely removed.

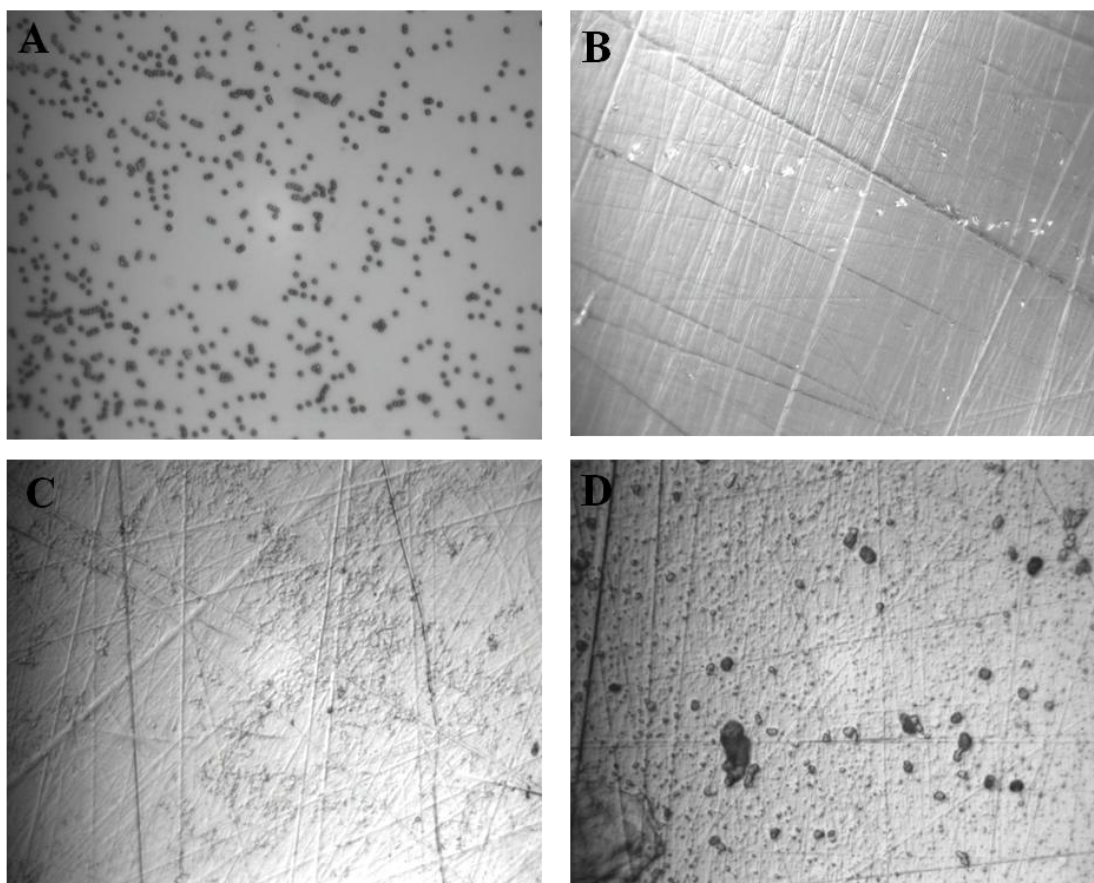


**Figure 4:10:** Western blot analysis showing the NPs immobilized on the sensor surface (band of ~5.8 kDa). Kaleidoscopic ladder (on the left side).

As can be observed in Figure 4:10, the band of 5.8 kDa refers to 7B1 NPs that remained immobilized on the surface after several washes. It was found that, after the third wash, all unbound NPs were removed (results not shown).

Following the evidence obtained by the binding affinity tests and the information that our NPs were immobilized over the gold surface (Figure 4:10), unpolished ME biosensors were coated with 20  $\mu\text{g/ml}$  of NPs and exposed to  $1.0 \times 10^8$  streptavidin beads/ml. The decision of using an unpolished or polished sensor surface was based on preliminary observations in an optical microscope (Figure 4:11) which showed that the polished one contained some

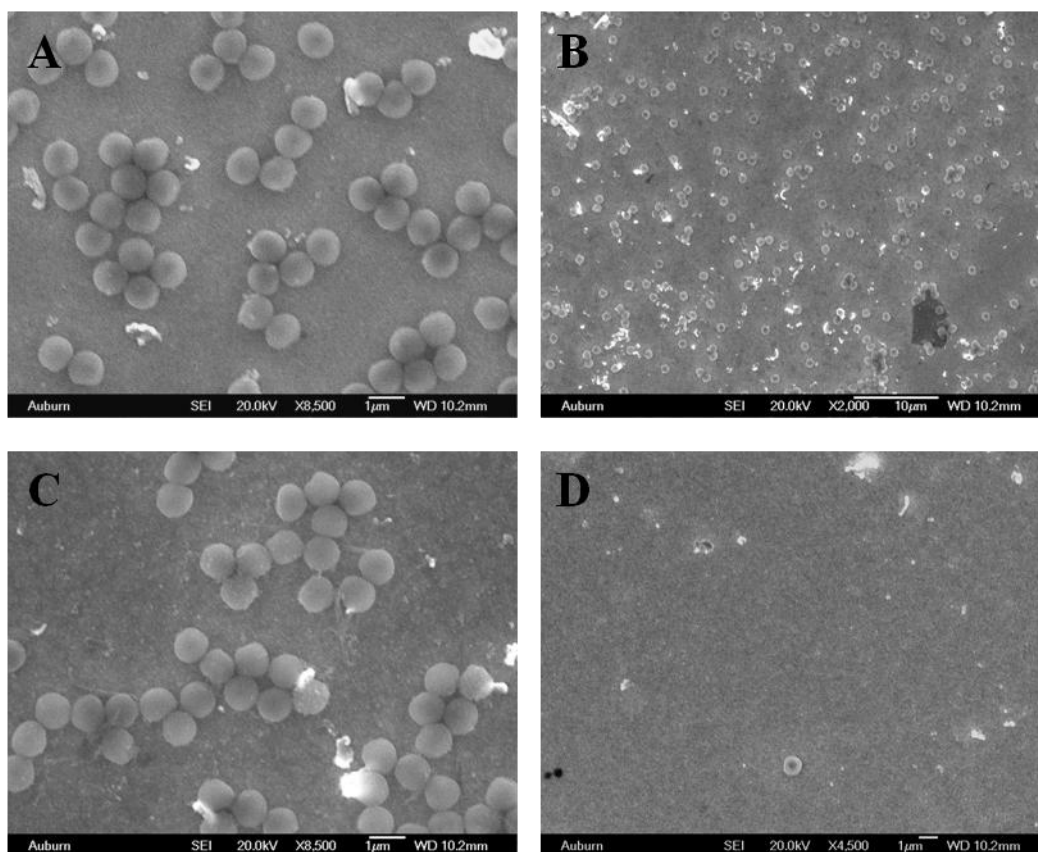
scratches that might affect the binding of the biological element and unspecific streptavidin binding to the sensor surface.



**Figure 4:11:** Optical images obtained by Nikon Eclipse L150 of streptavidin beads of  $0.99\ \mu\text{m}$  (A), polished ME sensor (B) and streptavidin bound on sensor surface (C and D).

Indeed, beads retained on the scratched area were observed (Figure 4:11–C and Figure 4:11–D) and consequently may result in a false positive signal during the measurement process. Therefore, following experiments were done using unpolished sensors. The binding affinity images acquired by SEM are shown in Figure 4:12.

Figure 4:12:A-C shows the binding affinity of NPs to the target (streptavidin beads). Streptavidin beads with a diameter of approximately  $1\ \mu\text{m}$  were selected to simulate the dimension of a bacterium, making this the ideal strategy model. Based on SEM observations and compared to the control sensor (Figure 4:12–D: sensor surface covered with 0.1% BSA) we can conclude that, when used as an interface, NPs display the same affinity and specificity as their parental phage.



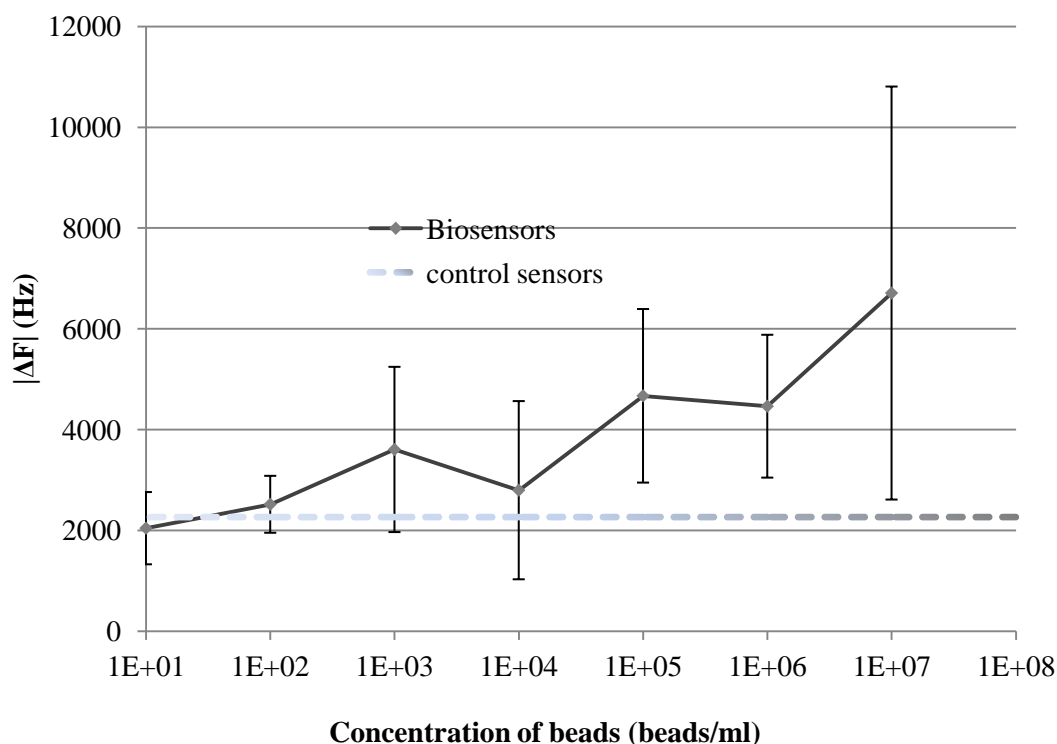
**Figure 4:12:** SEM images of the ME biosensors exposed to  $1.0 \times 10^8$  beads/ml when: A - sensor surface is covered with nano-phages (NPs); B - sensor surface covered with entire phage 7B1; C – enlarged view of the area of the sensor surface covered with nano-phages; D - sensor surface covered with 0.1% BSA (negative control).

The enlarged view of the sensor surface on Figure 4:12–B allows us to observe how NPs were dispersed along the surface. The fact that no higher target density was obtained cannot directly be associated with NPs surface coverage. The loss of beads may be related to other aspects, for instance the intensity of the washing procedure, which may remove some beads that were bound specifically. Moreover, the weak bond of NPs to the sensor surface caused by the immobilization technique could be another reason for the target absence in various sites on the sensor surface.

### 4.1.2.6 Analyte Binding Measurement

Figure 4:13 shows the resonance frequency shifts of ME biosensors as a function of the concentration of streptavidin polystyrene beads, where each data point corresponds to the

mean value of the frequency readings from at least three sensors. It should be noted that the data were typically collected from a daily experiment and for each sensor the frequency was measured five times, followed by the calculation of the mean value.



**Figure 4:13:** Magnetoelastic biosensor's responses, when exposed to increasing concentrations of streptavidin polystyrene beads. Negative controls were coated only with BSA 0.1%. The dotted line represents the mean value reached for control sensor when exposed to the highest concentration of streptavidin beads.

When exposing the biosensors to an increasing concentration of streptavidin beads we observed an amplified signal compared to the control sensors. However, the results show some signal variability which is also reflected by the standard deviation. This fluctuation can be attributed to the sensor position inside the coil center; for each biosensor five measurements were taken, meaning that the biosensor exits the coil center. After returning it is not able to take its exact previous position, which may result in signal variation.

Damages on the sensor surface can also occur during the experiment, due to successive washing processes which lead to the removal of small portions of gold on the surface. As a

result, the resonance frequency will decrease and false negatives may occur. Despite the signal variation, the difference between biosensors and control sensors is notorious.

### 4.1.3 Discussion

Particles in nano-scale are relevant in various areas, with the food industry (e.g. nanoencapsulated vitamins) and the health sector (e.g. drug delivery) as good examples where this technology is needed. Filamentous phages are viruses that specifically recognize bacteria and therefore are promising entities to use as nanocarriers for drug delivery and as a detection tool for pathogens. In the biosensing field, the idea of using nano interfaces that can increase the biosensor sensitivity and consequently increase its performance, has gained more importance when phages are concerned. The entire phage forms aggregates, blocking the availability of receptors recognizing the target. In this work, we found that NPs (phage-derived products) have affinity and sensitivity equal to their parental phage. When examining the dose-dependent binding we found that NPs had a 1.6 times higher affinity than the parental phage. Moreover, competitive assay showed that NPs-APSA interaction occurred, which inhibited the ligation between Phage and AP-SA. These results suggested that NPs may be used as a new type of substitute for entire phages and explored as a biological element in biosensors with the same elevated specificity as their parental phage. Despite the promising results obtained with NPs, our findings suggested that specificity and sensitivity features can be further improved, taking in account some aspects. To avoid problems related with the NPs stability and activity we used immobilization by physical adsorption, however the ME surfaces were not completely covered with the target. Two reasons may be behind that result: either the washing procedures were too harsh or the immobilization technique failed. Other studies have reported different immobilization strategies using chemical functionalization and physical adsorption [17,18]. Both have advantages and disadvantages: physical adsorption is the simplest method, but the adsorbed biological elements can easily be removed during the washing steps due to the weak binding. On the other hand, chemical attachments can interfere with their stability and activity [15]. Researchers from Austria Biophysics Institute conducted some immobilization techniques and nanolithography tests using NPs. Two types of functionalization were tested to obtain a stable attachment of the phage-particle to the surface: the use of bivalent ions and a single molecule layer of aminopropyltriethoxysilane (APTES). The

APTES allows the binding of molecules by electrostatic interaction as well as by charge effects, showing that using APTES coated mica led to a densely covered surface of nanophages. These results give the impression that an efficient immobilization step combined with the small size of the NPs enables a uniform surface coverage density, improving the interface sensitivity. Even further studies of NPs stability, specificity and immobilization need to be done, our results clearly show that replacement of filamentous phage for NPs is possible, increasing the sensors sensitivity. This new approach can be used to develop biosensors with increased performance for early detection of food borne pathogens, cancer diseases and other pathologies.

### 4.1.4 Conclusions

As a proof-of-concept the features of NPs were demonstrated. This study proved that NPs can bind to streptavidin-coated beads with a binding affinity equal to or better than a parental phage. The two binding assays tested confirmed the NP's binding specificity and sensitivity. When examining the dose-dependent binding we found that NPs had a 1.6 times higher affinity than the entire phage. When immobilized to the ME sensor by physical adsorption NPs demonstrated specificity and selectivity towards the target analyte used for selection of the parental phage. However, the gold surface was not completely covered with the target, which led us to conclude that more studies related to the type of immobilization or the optimization of washing steps need to be implemented, to increase the target density on the surface without compromising the NPs activity. Besides their advantages concerning specificity and sensitivity, NPs may lead to a decrease of false positives at the detection level, since the protein responsible for infecting *Escherichia coli* is not present (pIII). This new perspective of phages by the introduction of a phage-derived product - NPs can be a new format of interfaces that can contribute to the development of a robust and inexpensive biosensors for several applications.

## **Chapter 4**

### **4.2 Phage tail-fibre Proteins**

**Parts of the work presented in this chapter is based on:**

Patent application PPI46027-12, entitled “*Phage Tail Proteins for Specific Detection and Control of Salmonella Enterica*”. Inventor(s): Azeredo, J., Kluskens, L., Santos, S., Silva, S., **Fernandes, E.**, Lavigne, R., Vandersteegen, K., Cornelissen, A., August 2012.

### Abstract

Bacterio(phages) have been studied by many researchers as a potential recognition tool for detection systems due their excellent features, in particular their specificity. However, phages also have disadvantages such as their size, which can influence the successful capture of the interest target. The *Salmonella* phage used in this study belongs to the family *Myoviridae* and is characterized by an icosahedral head of 84 nm in apical diameter and a contractile tail of 120 x 18 nm with short tail fibers. Since the recognition elements are peptides present in the phage tail fibers, the possibility to obtain a phage-derived detection tool, composed only by the recognition peptides, with the same specificity as their parental phage and excluding the rest of phage structure was studied. The phage tail fiber proteins (TFPs) were expressed heterologously in *E. coli*. The binding abilities of the expressed TFPs were assessed by immunofluorescence assays and by stereomicroscopic observations. The results revealed that TFPs exhibited the same signal intensity as the parental phage, showing the high binding efficiency of TFPs. This new approach can be used as a detection tool or a kit for the identification of *Salmonella* strains in foodstuff, food processing equipment, food processing plants, food processing surfaces and in other areas where *Salmonella* might be present.



### 4.2 Introduction

Foodborne diseases are of major concern due to their worldwide impact. The Center for Disease Control and Prevention (CDC) estimates that 76 million cases of foodborne diseases occur every year in the United States, causing roughly 5000 deaths [28]. From the reported cases, it has been observed that *Salmonella* is the most common and widely distributed causing agent constituting thus a major public health burden with significant impact in the society costs worldwide. Besides the effort that has been done to control this pathogen, including the general improvement of food safety knowledge and good practices, they are still a major cause of the increasing occurrence of foodborne diseases [29]. Moreover, the production and distribution of foodstuff increased dramatically in volume and in number of consumers, increasing the risk of mass epidemics. Consequently, it is critical to identify and quantify the presence of such pathogen to monitor the safety of foodstuff and also to define strategies to reduce the number of outbreaks. The golden standard for *Salmonella* detection is still the bacteriological culture (ISO 6579:2002) which is time-consuming, laborious, expensive and ineffective in detecting non-cultivable organisms [30]. *Salmonella* detection methods typically take 3-5 days to obtain a result and during this long period portions of the food may have been distributed, marketed, sold, and eaten before a problem is even detected. A number of methods aiming at reducing the time required for the identification of foodborne pathogens have been developed, which include the use of antibodies to detect microbial antigens such as the enzyme-linked immunosorbent assay (ELISA) and nucleic acid-based techniques such as the polymerase chain reaction (PCR), DNA microarrays/DNA chips, sequencing-based identification and DNA hybridization [31–34]. However, the sensitivity of immunological methods has been found to be low, with a variable specificity depending on the antibody used, commonly with the occurrence of cross-reactivity phenomena. Often, these methods do not allow the discrimination between dead and living microorganisms. Also, the feasibility of the method depends on the origin of samples [35]. Despite the high sensitivity of the nucleic acid-based techniques and their increased value in the detection of fastidious microorganisms, they usually require extensive sample preparation, often including a DNA extraction step. These procedures are laborious, expensive and time consuming and may not be enough to remove all the contaminants, commonly found in the samples, that may inhibit (or influence) the reactions needed for the microorganisms detection. Moreover, the nucleic acid-based tech-

niques such as the PCR and microarrays demand a high initial investment in equipment and expertise personnel [36]. Bacteriophages (phages) are naturally evolved entities that due to their intrinsic characteristics present high potential in the control and detection of bacteria, namely foodborne pathogens. Phages are viruses that only infect bacteria and are obligate intracellular parasites lacking their own metabolism. They are extremely specific, usually infecting a single species or even strain and consequently they have been found to present potential in the rapid detection of bacteria [37]. Phage PVP-SE1 belongs to the family *Myoviridae* and is characterized by an icosahedral head of 84 nm in apical diameter and a contractile tail of 120 x 18 nm with short tail fibers. This phage has the ability to bind to a very broad range of *Salmonella* strains which makes it an interesting phage to be used in the detection of *Salmonella* [38]. In addition the lytic spectrum of this phage is broader than that described by Felix O1. PVP-SE1 is able to infect *Salmonella* several mutants defective in core polysaccharide assembly suggesting that the receptor for this phage is the conserved LPS inner core region and explains its broad lytic spectrum [39]. Therefore it is expected that the phage recognition elements located at the tail fibers, the tail fiber proteins (TFPs), may also exhibit binding abilities to a broad range of hosts. In the work described herein, TFPs were expressed heterogeneously and their binding abilities to *Salmonella* strains were assessed. This work constituted the first step towards the development of a phage-based sensor that makes use of the recognition elements instead of the entire phage particle.

### 4.2.1 Materials and Methods

#### 4.2.1.1. Bacteriophages and Bacterial Strains

In this work were used two *Salmonella* phages: PVP-SE1 and PVP-SE2. The phage PVP-SE1 with a broad lytic spectrum against different *Salmonella* strains was isolated from a Regensburg (Germany) wastewater plant in a European Project Phagevet-P [38] and their host is *Salmonella enterica* serovar Enteritidis strain S1400 [40]. The Phage PVP-SE2 was isolated from raw sewage, wastewater treatment plant (Braga; Portugal) [40]. Their host is *Salmonella*

*enterica* serovar Enteritidis strain 821 was provided by Instituto Nacional Ricardo Jorge, Portugal [40].

### 4.2.1.2 Phage Propagation

The phages were produced using the double layer agar technique as described by Sambrook and Russell [41]. Briefly, from the plaque forming units (PFU) obtained ten were selected and transferred several times to three new Petri dishes with the proper bacterial soft agar. Using sterile paper strips, the phages were spread by passing the strips several times on the production Petri dishes and incubated overnight at 37°C. Then, 3 to 10 ml of SM buffer was added to Petri dishes and incubated overnight at 4°C (with agitation). The liquid was transferred to 50 ml tubes and centrifuged at 9000 x g during 10 min at 4°C (Hettich Zentrifugen-Universal 320) to remove the bacteria. One volume of chloroform was added to 4 volumes of supernatant and centrifuged at 9000 x g during 10 min at 4°C. The top liquid phase was removed carefully and filtered through a 0.2 µm filter (Minisart-Santorius stedim biotech). The phage titer was verified and the solution was stored at 4°C.

### 4.2.1.3 Phage Purification

The phage purification was performed by cesium chloride (CsCl) gradient ultracentrifugation [42]. Initially, heat-dried CsCl (MP Biomedicals, Illkirch, France) was added gradually to 15 ml of phage in order to avoid an osmotic shock. Four CsCl solutions were prepared (densities of 1.33, 1.45, 1.50 and 1.70 g/ml) and 5.7 ml per gradient was added (starting from the lowest to the higher density) and the solution was centrifuged at 28,000 x g at 4°C during 3 h. The phage was collected from the gradient (~3 ml, white cloud) and dialyzed. To hydrate the membrane, the Slide-A-Lyzer dialysis cassette (Pierce, Rockford, IL) was incubated in 1 L of 1 × phage buffer [10 mM Tris-HCl, pH 7.5, 100 mM MgSO<sub>4</sub>, 150 mM NaCl]. Three ml of phage suspension was added in the dialysis cassette and dialyzed 3 times for 30 min against 300 volumes of phage buffer. The pure phage preparation was collected and stored at 4°C.

### 4.2.1.4 Isolation of the TFPs of Phage PVP-SE1

## Chapter 4. Development of a Detection Tool Based on Phage Recognition Peptides

Followed the general procedures explained previously, the cloning, expression and purification of the tail proteins of the *Salmonella* Enteritidis phage PVP-SE1 was performed as detailed below.

### 4.2.1.5 Design of Primers

Primers used for the gene amplification were based on the genes encoding the tail fiber proteins of PVP-SE1 and developed using programs like Expsy Translate, BLAST analysis and Phyre.

**Table 4:2:** Information of primers used for the sequencing reaction.

Name	Sequence	GC (%)
gp40F	TACTTCCAATCCATGTATCCTATCCATGTCTCTTC	38,88
gp40R	TATCCACCTTTACTGTTATTGCGGTTGAGAAGGTACAAC	41,02
gp41F	TACTTCCAATCCATGGCAGACATGACTCAATTGAAC	41,54
gp41R	TATCCACCTTTACTGTTACGGACGACGAACAATTACAGTG	42,50
gp46F	TACTTCCAATCCATGGCAGCGCCAACAGTACC	53,12
gp46R	TATCCACCTTTACTGTTAGTCCAGGTTGGAAACAG	42,86
gp48F	TACTTCCAATCCATGGCTGCTCAATATGGATTAAATG	37,84
gp48R	TATCCACCTTTACTGTTAGATGATTTGCTGGAATG	37,14
gp51F	TACTTCCAATCCATGGCAGATGTTTCTTTTCCAACG	41,67
gp51R	TATCCACCTTTACTGTTA CTCAACTCCTGCCATAATAAGG	40,00
gp53F	TACTTCCAATCCATGGCATCAATTCAACGTATGG	41,18
gp53R	TATCCACCTTTACTGTTATTTGTTGGGTGGGTTGG	42,86

### 4.2.5.1 PCR Amplification

50 µl of PCR sample was performed using: 15 µl of genomic DNA; 5 µl of 10 x *Pfu* buffer + MgSO<sub>4</sub>; 1 µl of 10 mM dNTP Mix; 0.5 µl of forward primer; 0.5 µl of reverse primer; 0.5 µl of *Pfu* DNA polymerase and 27.5 µl of Milli-Q water. The samples were sealed with a drop of mineral oil. PCR amplification was carried out in a thermal cycler with an initial denatura-

tion at 95°C (2 min), followed by 35 cycles at 95°C (30 s), incubation at the annealing temperature for each primer pair during 30 s and extension at 72°C during 4 min for gp40, 41 and 46; 2 min for gp51 and 53; finishing with a final extension at 72°C during 10 min and storage at 4°C thereafter. Amplified products were subjected to electrophoresis on 1 % agarose gels (the agarose (Eurogenetic, Luik, Belgium) was dissolved in TAE buffer (40 mM Tris-HCl, 0.5mM sodium acetate, 50mM EDTA, pH 7.2) and added 2 µl of ethidium bromide at 1 mg/ml (Cambrex NJ, USA)). PCR products were purified using QIAquick PCR purification kit (Qiagen). After purification, the samples were stored at -20°C.

### 4.2.5.2 Vector Preparation

An overnight culture was prepared with 14 ml of LB medium, 4 µl of kanamycin at 50 µg/ml and 25 µl of XL1-Blue / pNIC28-Bsa4 from glycerol stock.

The plasmid DNA extraction and purification was performed using QIAprep spin Miniprep Kit as described in manufacture's protocol. The elution step was done with 30 µl of Milli-Q water and the plasmid DNA analyzed by electrophoresis.

### 4.2.5.3 Restriction with *BsaI*

The vector was cut with restriction enzyme *BsaI*. A reaction mixture containing 23.40 µl of pNIC28-Bsa4, 10 µl of 10 × Buffer G (Fermentas), 3 µl of *BsaI* restriction enzyme (Fermentas) and Milli-Q water was added to obtain a total volume of 100 µl and was incubated during 3 h at 37°C and stored a 4°C. However, during the time of incubation, 3 µl of extra restriction enzyme was added after 1 h. The restriction step was verified by agarose gel and the plasmid DNA was purified.

### 4.2.5.4 Generation of Cohesive Ends

The insert preparation was done in 10 µl reaction mix: 3 µl of DNA (PCR product), 2 µl of 5x T4 DNA polymerase buffer, 0.25 µl of 100 mM dCTP, 0.5 µl of 100 mM DTT, 0.1 µl of 100 × BSA, 0.25 µL of T4 DNA polymerase and 3.9 µl of Milli-Q water. The reaction mix

was incubated at 22°C during 30 min and inactivated at 75°C during 20 min and stored until use at 4°C.

The vector preparation was conducted in a total volume of 100 µl with the exception of addition of dGTP. The reaction mixture was done using: 50 µl of *Bsa*I-digested plasmid, 20 µl of 5 × T4 DNA polymerase buffer, 2.5 µl of dGTP (100 mM), 1 µL of 100 × Bsa, 5 µl of DTT (100 mM), 19 µl of Milli-Q water and 2.5 µl of T4 DNA polymerase. The mixture was incubated for 3 h at 37°C and stored a 4°C.

### 4.2.5.5 Ligation

6 µl of a ligation mixture containing 2 µl of treated vector and 4 µl of treated insert was incubated at 22°C during 20 min and then transferred to ice.

### 4.2.5.6 Transformation

Initially LB agar plates with 50 µg/ml of kanamycin and 5% (w/v) of sucrose were prepared and an electroporation of *E.coli* XL Blue was done at 1.7 kV. The cells were recovered by adding 960 µl of pre-warmed SOC medium (2% Trypton, 0.5% Yeast extract, 0.05% NaCl, 10 mM MgCl<sub>2</sub>, 10 mM MgSO<sub>4</sub>, and 20 mM glucose) and incubated at 37°C during 1 h at 250 rpm. The cells were then plated on LB solid medium containing kanamycin and incubated overnight at 37°C.

### 4.2.5.7 Colony Analysis

Individual colonies of each transformation were collected with a toothpick and placed in glass tube containing 4 ml of LB medium and 4 µl of kanamycin and incubated overnight at 37°C. The cultures were used for colony PCR and for glycerol stock preservation at -20°C and - 80°C. 1.5 ml of liquid culture was used for plasmid purification. 10 µl of the overnight culture was used in a 50 µl PCR mix and the end products verified on a 1 % agarose gel.

### 4.2.5.8 DNA Sequencing

Purified plasmids containing inserts were sequenced from one direction. 10  $\mu$ l of sequencing reaction was prepared containing 1  $\mu$ l of DNA plasmid, 1  $\mu$ l of primer, 2  $\mu$ l of 5  $\times$  sequencing Buffer, 0.5  $\mu$ l of BigDye terminator and 5.5  $\mu$ l of Milli-Q water. The samples were prepared in a thermal cycler using the program described previously. After standard ethanol precipitation and added formamide the samples were analyzed using ABI 3130 genetic analyzer (Applied Biosystems) and the sequences were assembled with the Sequencer 4.1 software (Genecodes).

### 4.2.5.9 Small-scale Protein Expression

Small-scale protein expression was carried out at two different temperatures: 16°C and 37°C.

### 4.2.5.10 Cell Growth and Induction

A volume of 80  $\mu$ l of overnight culture was inoculated in 4 ml of LB medium with 4  $\mu$ l of kanamycin (50  $\mu$ g/ml) and incubated at 37°C until  $OD_{600nm}=0.6$ . Then, two cultures were induced with 4  $\mu$ l of IPTG (1/1000) and incubated overnight at 16°C and during 4 h at 37°C. As a control, two non-induced cultures were included.

### 4.2.5.11 Induced Culture

A: After 4 h of induction, the induced cultures were centrifuged at 8,500  $\times$  g during 10 min. The supernatant was removed and the pellet was resuspended with 1 ml of lysis buffer (10 mM imidazole). The volume was frozen and thawed three times, followed by sonication of 15 sec in 3 cycles (1 cycle/5 sec) at 40 % of amplitude.

B: Total protein fraction (TPF): a mixture containing 150  $\mu$ l of the sample prepared before, 50  $\mu$ l of SDS-PAGE (sodium dodecyl sulphate polyacrylamide gel electrophoresis) and 4  $\times$  loading buffer was prepared. This mixture was stored at 4°C.

## Chapter 4. Development of a Detection Tool Based on Phage Recognition Peptides

---

Soluble protein fraction (SPF): 150  $\mu$ l of the sample prepared in A was centrifuged at 8,500 x g during 10 min. Then, 120  $\mu$ l of supernatant was transferred to a new tube and 40  $\mu$ l of 4  $\times$  SDS-PAGE loading buffer was added. This mixture was stored at 4°C.

C: Insoluble protein fraction (IPF): the remaining supernatant was removed and the pellet was resuspended in 200  $\mu$ l of Milli-Q water. The mixture was centrifuged at 8,500 x g during 10 min and the supernatant was removed. The pellet was resuspended in 150  $\mu$ l of lysis buffer (10 mM imidazole) and 150  $\mu$ l of 4x SDS-PAGE loading buffer was added. The mixture was stored at 4°C.

The different fractions TPF, SPF and ISF were analyzed by SDS-PAGE and compared to a low molecular weight (LMW) ladder. A sample of 16  $\mu$ l stored at 4°C was heated at 95°C during 2 min and then loaded on the appropriate gel. The gel was run at 200 V during approximately 1 h.

### 4.2.5.12 Binding Ability of the Tail Proteins of Phage PVP-SE1 by Immunofluorescence Assay

The TFPs at concentrations of 100  $\mu$ g/ml, 200  $\mu$ g/ml, 300  $\mu$ g/ml, 400  $\mu$ g/ml and 500  $\mu$ g/ml in PB (phosphate buffer 0.1 M, pH 7.5; 3.1 g NaH<sub>2</sub>PO<sub>4</sub>.H<sub>2</sub>O, 10.9 g Na<sub>2</sub>HPO<sub>4</sub>) or SM (100 mM NaCl, 8 mM MgSO<sub>4</sub>, 50 mM Tris-HCl, pH 7.5) and the positive/negative controls were immobilized onto a polystyrene microtiter plate by passive adsorption and incubated during 2 h at room temperature, followed by a three times washing procedure with PB or SM. Positive controls consist of *Salmonella spp* Polyclonal Antibody (200  $\mu$ g/ml) and PVP-SE1 (phage stock at a concentration 1.0x10<sup>10</sup> pfu's/ml). Negative controls consisted of bovine serum albumin (BSA) 5% in PB and PB or SM. After the immobilization of tail proteins, 1% of BSA in PB was added as a blocking agent to each well followed by a 40 min incubation at room temperature and three times washing with PB. One hundred milliliter of an exponential culture of *S. Enteritidis* S1400 grown in LB (37°C, 120 rpm) until an optical density of 0.4 at 600 nm (corresponding to 1.0x10<sup>9</sup> cells/ml), was added to each well followed by a 1 h incubation period at room temperature. After a washing step with PB to remove unbound bacteria, the wells were filled with 100  $\mu$ l of *Salmonella spp*. Polyclonal Antibody, Biotin conjugated



at 200 µg/ml (Thermo Scientific, ref PA1-73022) and incubated during 1 h. After, the wells were washed with PB and filled with 100 µl conjugated Streptavidin Rhodamine (TRITC, Pierce, ref 21724) at 20 µg/ml and incubated for 40 min at room temperature. After several washes with PB, a volume of 100 µl of PB was added to each well and the fluorescence was measured by a Synergy H1 microplate reader at 520 nm of excitation and at 570 nm of emission.

### 4.2.5.13 Binding Affinity of the Tail Proteins of Phage PVP-SE1 Immobilized on Gold (Au) Substrates

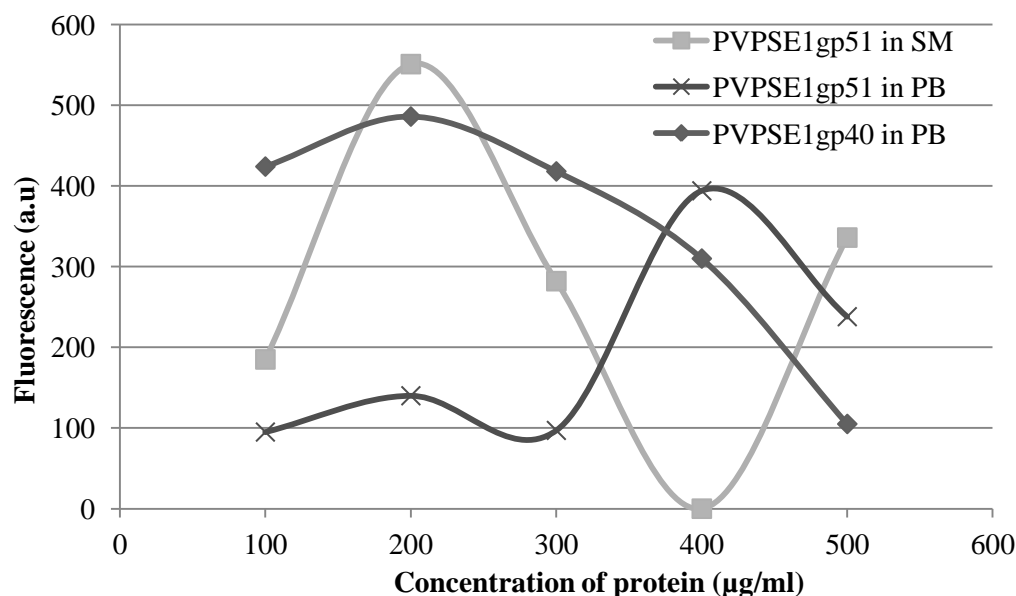
Au substrates (7x7 mm) were incubated for 2 h in Microstrip® 3001 (Fujifilm Electronic Materials, Belgium) at 65°C for removal of the protective coating of photoresistive polymer. The substrates were then washed three times with isopropanol and sterile, distilled water and dried under a N<sub>2</sub> stream. After the cleaning step, the tail proteins (200 µg/ml, prepared in SM buffer) were immobilized by physical adsorption on the Au substrates in spots of 1 µl and incubated for 4 h at room temperature in a humidified atmosphere, in order to prevent evaporation. The unbound tail proteins were removed by washing three times with SM buffer. The spots were then incubated with the blocking agent BSA 1% prepared in TE during 45 min and the excess of blocking solution was removed by washing the substrate with PB (0.1 M, pH 7.5). All substrates were exposed to 2.8x10<sup>9</sup> cells/ml during 1 h and washed with PB (0.1M, pH 7.4) and distilled water. The bacterial coverage extent “in spot” and “out spot” was visualized by a Nikon SMZ 1500 microscope.

## 4.2.2 Results

The tail fiber proteins (TFPs) used for the preliminary binding ability tests were gp40 and gp51. Protein expression was tested using two different temperatures (16 and 37°C). After the establishment of the optimal temperature, both TFPs were expressed and purified according the protocol described in the materials and methods section. A representative image of protein expression and purification is shown in Appendix B.2.

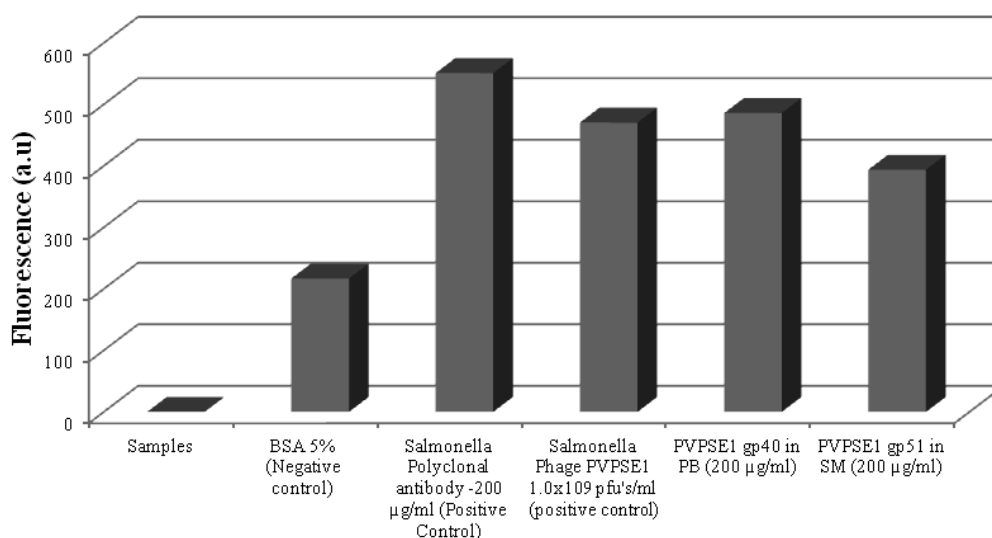
#### 4.1.4.1 Binding Ability of the Tail Fiber Proteins (TFPs)

The TFPs were tested using an immunofluorescence assay and based on intensity signal it was possible to confirm their binding affinity as shown in Figure 4:14.



**Figure 4:14:** Fluorescence intensity measured at 520 nm in the wells coated with different concentrations of PVP-SE1 gp40 and PVP-SE1 gp51 in 0.1M PB buffer or SM buffer.

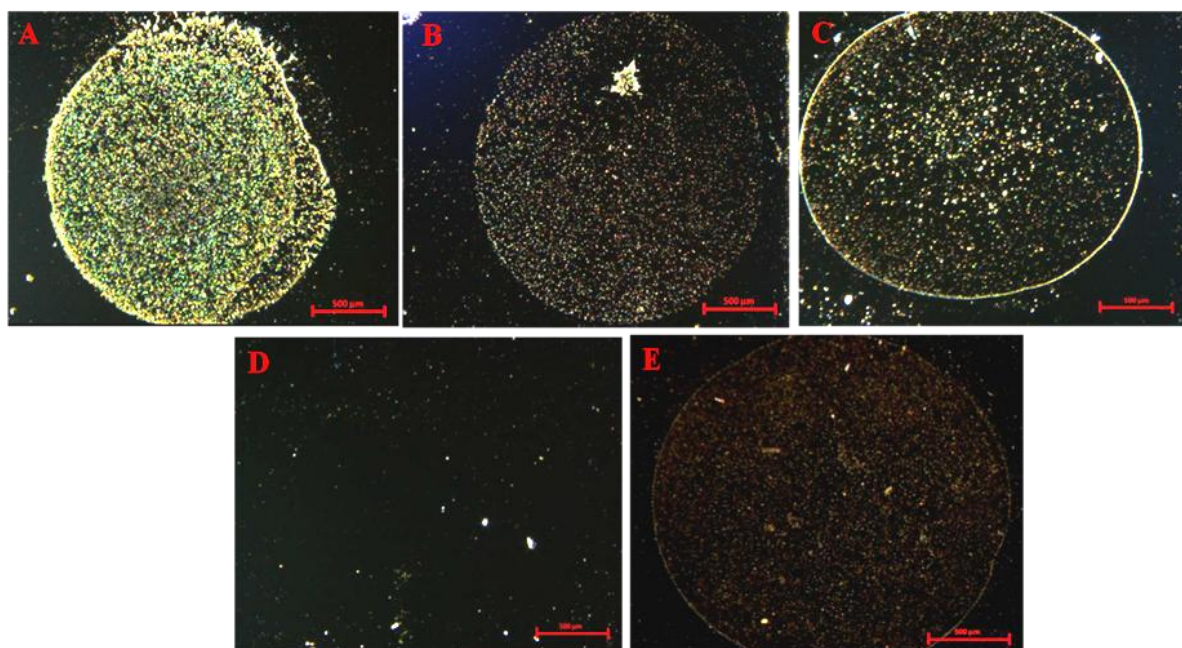
The results of the fluorescence intensity in Figure 4:14 showed that both the buffer composition and the protein concentration influence the signal intensity. Gp40 presents a higher signal in 0.1 M PB buffer at 200 µg/ml, while gp51 gives better results in SM buffer at 200 µg/ml. This preliminary study has shown that these two variables need to be optimized for each tail protein. The peptides in their optimal concentration (which gave the higher intensity signal) were tested and compared with positive controls such as phage PVP-SE1 and *Salmonella* Polyclonal antibody. As a negative control BSA 5% was used (Figure 4:15).



**Figure 4:15:** Fluorescence intensity measured at 520 nm in the wells coated with 200 µg/ml PVP-SE1gp40 and PVP-SE1gp51. Negative control was BSA (5%) and as positive controls: the phage PVP-SE1 ( $1 \times 10^9$  pfu's/ml) and *Salmonella* Polyclonal Antibody.

When comparing the tail fiber peptides gp40 and 51 with the positive and negative controls we can observe that the tail proteins show a signal intensity similar to that of the *Salmonella* Polyclonal antibody and the entire phage particle.

Following the confirmation by the immunofluorescence assay, the TFPs were immobilized by physical adsorption on gold substrates. The bacterial attachment was optically confirmed (Figure 4:16).



**Figure 4:16:** Images obtained by Nikon SMZ 1500 Stereomicroscope showing the bacteria surface coverage in the area in which PVP-SE1gp51 was immobilized on gold substrates specifically recognizing *Salmonella* Enteritidis cells. A: PVP-SE1gp51 at 200  $\mu\text{g/ml}$ , B: PVP-SE1gp51 at approximately 10  $\text{mg/ml}$ , C: PVP-SE1gp51 at 10  $\text{mg/ml}$  and a Negative control of *Salmonella* Enteritidis cells detection using a spot of unspecific protein (Bovine Serum Albumin-BSA) (Image D). The Positive Control (E) shows spots of immobilized PVP-SE1 phage on gold substrate specifically recognizing *Salmonella* Enteritidis cells.

In Figure 4:16, the surface coverage obtained was consistent with the results reported previously by immunofluorescence assay, meaning that the tail protein concentration influences its binding ability. Moreover, the binding ability of the tail protein seems equal to that of the entire phage PVP-SE1.

### 4.2.3 Discussion

The specificity and the low cost production are unquestionable qualities of phages. However, bearing in mind their use as a detection tool, the phage structure can be a limitation, because its size can compromise the number of cells attached to the surface. Moreover, the presence of the lytic activity can also be a problem when our purpose is to only recognize, without lysing the cell. Thus, TFPs can circumvent these limitations due to their small size and inabil-

ity to lyse bacterial cells. PVP-SE1 has a broad host range among salmonellae [38] which represents an added value when the goal is to select a TFP specific for a *Salmonella* strain, However this phage is also able to infect some *E. coli strains* [38] and therefore it is necessary to test the binding affinity in order to understand which tail is responsible for the recognition of what strain. It is likely that more than one tail is required for the recognition of a broader panel of strains and we therefore need to consider the use of a mixture of tails. The TFPs tested in the work described herein work showed a binding affinity similar to the parental phage and only slightly inferior to that of a specific antibody (~10% less binding). The use of phage-derived molecules has been suggested by other researchers [43], with the studies involving P22 as a good example [44, 45]. A recent publication of Singh *et al.* [44] suggested the use of tailspike proteins (TSPs) to detect *Salmonella* Typhimurium. The TSPs were engineered to express cysteine tags at their N- or C-termini, immobilized onto gold substrates using thiol-chemistry. The authors found that the appropriate orientation of the TSPs on the surface is important for efficient capture of the host bacterium. When applying that information to our study, we might be able to explain the difference of binding between the TFPs and the polyclonal antibody. It may be that, due to their orientation, a small amount of the phage derivatives was not able to detect *Salmonella*. When immobilized over the gold substrates the results were also promising, proving that further tests should be implemented to improve even more their potential as a detection tool. Immobilization techniques, stability and specificity are some examples of the points that need more attention. Despite their specificity, in general, the tail proteins are more stable than antibodies and their manufacturing costs can also be competitive. Thus, we have in our hands an excellent tool to explore in the biosensing area, leading to the development of a helper device that could be applied in the biomedical field.

### 4.2.4 Conclusions

The use of phages has been mentioned in different studies related with biosensors, but applying them as whole entity in a detection tool can be a problem, since this may limit the surface to capture a high target density. The development of nanomolecules to use in biosensors has kept the interest of many researchers. Accordingly, TFPs can be considered as a potential nanomolecule to compete with their parental phage. Considering this particular case, our

phage dimensions are 84 nm (head) and 120 by 18 nm (tail) and therefore too big when the aim is to obtain a thin and uniform active layer. The tails used in this work, namely gp40 and gp51, showed a binding ability similar to that of the parental phage, suggesting that their replacement can be possible. When immobilized over the gold substrates the results were in agreement with those from tests in an immunofluorescence assay. However, TFP efficiency can still be further improved by studying their stability and binding affinity in detail.

TFPs are promising biological elements that may find use in various detection systems or even in treatment of Gram-negative contamination of foodstuff, food processing equipment, food processing plants, surfaces coming into contact with foodstuff, medical devices, surfaces in hospitals and surgeries, or environmental samples.

### 4.2.5 References

- [1] E. . Olsen, S. . Pathirana, a. . Samoylov, J. . Barbaree, B. . Chin, W. . Neely, and V. Vodyanoy, “Specific and selective biosensor for *Salmonella* and its detection in the environment,” *Journal of Microbiological Methods*, vol. 53, no. 2, pp. 273–285, May 2003.
- [2] E. V Olsen, I. B. Sorokulova, V. A. Petrenko, I.-H. Chen, J. M. Barbaree, and V. J. Vodyanoy, “Affinity-selected filamentous bacteriophage as a probe for acoustic wave biodetectors of *Salmonella typhimurium*,” *Biosensors & bioelectronics*, vol. 21, no. 8, pp. 1434–42, Feb. 2006.
- [3] V. A. Petrenko, “2008 Evolution of phage display from bioactive peptides to bioselective nanomaterials.pdf.”
- [4] W. Shen, R. S. Lakshmanan, L. C. Mathison, V. A. Petrenko, and B. a. Chin, “Phage coated magnetoelastic micro-biosensors for real-time detection of *Bacillus anthracis* spores” *Sensors and Actuators B: Chemical*, vol. 137, no. 2, pp. 501–506, Apr. 2009.
- [5] J. Wan, M. L. Johnson, R. Guntupalli, V. A. Petrenko, and B. a. Chin, “Detection of *Bacillus anthracis* spores in liquid using phage-based magnetoelastic micro-resonators,” *Sensors and Actuators B: Chemical*, vol. 127, no. 2, pp. 559–566, Nov. 2007.
- [6] I. B. Sorokulova, E. V Olsen, I.-H. Chen, B. Fiebor, J. M. Barbaree, V. J. Vodyanoy, B. a. Chin, and V. A. Petrenko, “Landscape phage probes for *Salmonella typhimurium*,” *Journal of microbiological methods*, vol. 63, no. 1, pp. 55–72, Oct. 2005.

- [7] A. Yarman, G. Gröbe, B. Neumann, M. Kinne, N. Gajovic-Eichelmann, U. Wollenberger, M. Hofrichter, R. Ullrich, K. Scheibner, and F. W. Scheller, "The aromatic peroxygenase from *Marasmius rutola*--a new enzyme for biosensor applications.," *Analytical and bioanalytical chemistry*, vol. 402, no. 1, pp. 405–12, Jan. 2012.
- [8] X. Zhang and V. K. Yadavalli, "Surface immobilization of DNA aptamers for biosensing and protein interaction analysis.," *Biosensors & bioelectronics*, vol. 26, no. 7, pp. 3142–7, Mar. 2011.
- [9] R. Guntupalli, J. Hu, R. S. Lakshmanan, T. S. Huang, J. M. Barbaree, and B. a Chin, "A magnetoelastic resonance biosensor immobilized with polyclonal antibody for the detection of *Salmonella typhimurium*.," *Biosensors & bioelectronics*, vol. 22, no. 7, pp. 1474–9, Feb. 2007.
- [10] V. A. Petrenko, "Landscape Phage as a Molecular Recognition Interface for Detection Devices.," *Microelectronics journal*, vol. 39, no. 2, pp. 202–207, Feb. 2008.
- [11] V. A. Petrenko, G. P. Smith, X. Gong, and T. Quinn, "A library of organic landscapes on filamentous phage.," *Protein engineering*, vol. 9, no. 9, pp. 797–801, Sep. 1996.
- [12] G. P. Smith and V. A. Petrenko, "Phage Display.," *Chemical reviews*, vol. 97, no. 2, pp. 391–410, Apr. 1997.
- [13] Calendar, R. (2006). *The bacteriophages*. (R. Calendar, Ed.). Oxford.
- [14] S. Li, L. R. S., V. A. Petrenko, and B. A. Chin, "Phage-based Pathogen Biosensors," in *Phage Nanobiotechnology*, 2008.
- [15] S. Horikawa, D. Bedi, S. Li, W. Shen, S. Huang, I.-H. Chen, Y. Chai, M. L. Auad, M. J. Bozack, J. M. Barbaree, V. A. Petrenko, and B. a Chin, "Effects of surface functionalization on the surface phage coverage and the subsequent performance of phage-immobilized magnetoelastic biosensors.," *Biosensors & bioelectronics*, vol. 26, no. 5, pp. 2361–7, Jan. 2011.
- [16] V. A. Petrenko and G. P. Smith, "Phages from landscape libraries as substitute antibodies.," *Protein engineering*, vol. 13, no. 8, pp. 589–92, Aug. 2000.
- [17] V. A. Petrenko, G. P. Smith, M. M. Mazooji, and T. Quinn, "2002  $\alpha$ -Helically constrained phage display library.pdf," *Protein Engineering*, vol. 15, no. 11, p. 943:950, 2002.
- [18] J. R. Brigati, T. I. Samoylova, P. K. Jayanna, and V. A. Petrenko, *Phage display technique for generating peptide reagents. .*
- [19] S. Huang, S.-Q. Li, H. Yang, M. Johnson, J. Wan, I. Chen, V. A. Petrenko, J. M. Barbaree, and B. A. Chin, "Optimization of Phage-Based Magnetoelastic Biosensor Performance," *Sensors & Transducers*, vol. 3, pp. 87–96, 2008.

- [20] R. Guntupalli, R. S. Lakshmanan, J. Hu, T. S. Huang, J. M. Barbaree, V. Vodyanoy, and B. a Chin, "Rapid and sensitive magnetoelastic biosensors for the detection of *Salmonella* typhimurium in a mixed microbial population.," *Journal of microbiological methods*, vol. 70, no. 1, pp. 112–8, Jul. 2007.
- [21] S. Huang, H. Yang, R. S. Lakshmanan, M. L. Johnson, J. Wan, I.-H. Chen, H. C. Wikle, V. A. Petrenko, J. M. Barbaree, and B. a Chin, "Sequential detection of *Salmonella* typhimurium and *Bacillus anthracis* spores using magnetoelastic biosensors.," *Biosensors & bioelectronics*, vol. 24, no. 6, pp. 1730–6, Feb. 2009.
- [22] S. Huang, J. Hu, J. Wan, M. L. Johnson, H. Shu, and B. a. Chin, "The effect of annealing and gold deposition on the performance of magnetoelastic biosensors," *Materials Science and Engineering: C*, vol. 28, no. 3, pp. 380–386, Apr. 2008.
- [23] R. S. Lakshmanan, R. Guntupalli, J. Hu, V. A. Petrenko, J. M. Barbaree, and B. a. Chin, "Detection of *Salmonella* typhimurium in fat free milk using a phage immobilized magnetoelastic sensor," *Sensors and Actuators B: Chemical*, vol. 126, no. 2, pp. 544–550, Oct. 2007.
- [24] M. L. Johnson, J. Wan, S. Huang, Z. Cheng, V. A. Petrenko, D.-J. Kim, I.-H. Chen, J. M. Barbaree, J. W. Hong, and B. a. Chin, "A wireless biosensor using microfabricated phage-interfaced magnetoelastic particles," *Sensors and Actuators A: Physical*, vol. 144, no. 1, pp. 38–47, May 2008.
- [25] T. I. Samoylova, M. D. Norris, A. M. Samoylov, A. M. Cochran, K. G. Wolfe, V. A. Petrenko, and N. R. Cox, "Infective and inactivated filamentous phage as carriers for immunogenic peptides.," *Journal of virological methods*, vol. 183, no. 1, pp. 63–8, Jul. 2012.
- [26] A. Casadevall and L. A. Day, "DNA packing in the filamentous viruses fd, Xf, Pfl and Pf3," *Developmental and Structural Biology*, vol. 10, no. 7, pp. 2467–2481, 1982.
- [27] G. a Kuzmicheva, P. K. Jayanna, I. B. Sorokulova, and V. A. Petrenko, "Diversity and censoring of landscape phage libraries.," *Protein engineering, design & selection: PEDS*, vol. 22, no. 1, pp. 9–18, Jan. 2009.
- [28] D. G. Nyachuba, "Foodborne illness: is it on the rise?," *Nutrition Reviews*, vol. 10, no. 04, pp. 5–6, 2010.
- [29] P. Gerner-Smidt and W. JM., "Foodborne disease trends and reports.," *Foodborne Pathog Dis*, vol. 3, pp. 261–4, 2009.
- [30] M. Uyttendaele, K. Vanwildemeersch, and J. Debevere, "Evaluation of real-time PCR vs automated ELISA and a conventional culture method using a semi-solid medium for detection of *Salmonella*," *Letters in Applied Microbiology*, vol. 37, no. 5, pp. 386–391, Nov. 2003.



- [31] P. E. Andreotti, G. V Ludwig, A. H. Peruski, J. J. Tuite, S. S. Morse, and L. F. Peruski, "Immunoassay of infectious agents.," *BioTechniques*, vol. 35, no. 4, pp. 850–9, Oct. 2003.
- [32] K. B. Barken, J. a J. Haagensen, and T. Tolker-Nielsen, "Advances in nucleic acid-based diagnostics of bacterial infections.," *Clinica chimica acta; international journal of clinical chemistry*, vol. 384, no. 1–2, pp. 1–11, Sep. 2007.
- [33] P. M. Fratamico, "Comparison of culture, polymerase chain reaction (PCR), TaqMan *Salmonella*, and Transia Card *Salmonella* assays for detection of *Salmonella* spp. in naturally-contaminated ground chicken, ground turkey, and ground beef," *Molecular and Cellular Probes*, vol. 17, no. 5, pp. 215–221, Oct. 2003.
- [34] D. R. Call, M. K. Borucki, and F. J. Loge, "Detection of bacterial pathogens in environmental samples using DNA microarrays," *Journal of Microbiological Methods*, vol. 53, no. 2, pp. 235–243, May 2003.
- [35] A. H. Peruski, L. F. P. Jr, and L. F. Peruski, "Immunological Methods for Detection and Identification of Infectious Disease and Biological Warfare Agents Immunological Methods for Detection and Identification of Infectious Disease and Biological Warfare Agents," vol. 10, no. 4, 2003.
- [36] I. Abubakar, L. Irvine, C. F. Aldus, G. M. Wyatt, R. Fordham, S. Schelenz, L. Shepstone, A. Howe, M. Peck, and P. R. Hunter, "Detection and identification of bacterial intestinal pathogens in faeces and food," *Health Technology Assessment*, vol. 11, no. 36, 2007.
- [37] S. Hagens and M. J. Loessner, "Application of bacteriophages for detection and control of foodborne pathogens.," *Applied microbiology and biotechnology*, vol. 76, no. 3, pp. 513–9, Sep. 2007.
- [38] S. B. Santos, E. Fernandes, C. M. Carvalho, S. Sillankorva, V. N. Krylov, E. a Pleteneva, O. V Shaburova, a Nicolau, E. C. Ferreira, and J. Azeredo, "Selection and characterization of a multivalent *Salmonella* phage and its production in a nonpathogenic *Escherichia coli* strain.," *Applied and environmental microbiology*, vol. 76, no. 21, pp. 7338–42, Nov. 2010.
- [39] S. B. Santos, A. M. Kropinski, P.-J. Ceysens, H.-W. Ackermann, A. Villegas, R. Lavigne, V. N. Krylov, C. M. Carvalho, E. C. Ferreira, and J. Azeredo, "Genomic and proteomic characterization of the broad-host-range *Salmonella* phage PVP-SE1: creation of a new phage genus.," *Journal of virology*, vol. 85, no. 21, pp. 11265–73, Nov. 2011.
- [40] S. Sillankorva, E. Pleteneva, O. Shaburova, S. Santos, C. Carvalho, J. Azeredo, and V. Krylov, "*Salmonella* Enteritidis bacteriophage candidates for phage therapy of poultry.," *Journal of applied microbiology*, vol. 108, no. 4, pp. 1175–86, Apr. 2010.

## Chapter 4. Development of a Detection Tool Based on Phage Recognition Peptides

---

- [41] D. W. Sambrook, Joe; Russel, *Molecular cloning: a laboratory manual*, 3rd ed. Cold Spring Harbor, NY: Cold Spring Harbor Laboratory Press, 2001.
- [42] J. Sambrook and D. W. Russell, *Molecular cloning: a laboratory manual*, 3rd ed. NY: Cold Spring Harbor Laboratory Press, 2001.
- [43] S. Steinbacher, U. Baxa, S. Miller, a Weintraub, R. Seckler, and R. Huber, “Crystal structure of phage P22 tailspike protein complexed with *Salmonella* sp. O-antigen receptors.,” *Proceedings of the National Academy of Sciences of the United States of America*, vol. 93, no. 20, pp. 10584–8, Oct. 1996.
- [44] A. Singh, S. K. Arya, N. Glass, P. Hanifi-Moghaddam, R. Naidoo, C. M. Szymanski, J. Tanha, and S. Evoy, “Bacteriophage tailspike proteins as molecular probes for sensitive and selective bacterial detection.,” *Biosensors & bioelectronics*, vol. 26, no. 1, pp. 131–8, Sep. 2010.
- [45] Singh, A., Arutyunov, D., Szymanski, C.M. & Evoy, S. Bacteriophage based probes for pathogen detection. *Analyst* 137, 3405-3421 (2012).

## Chapter 5

# Conclusions and Future Perspectives

The research work described in this thesis aimed at addressing the necessities in developing a biosensor that can fulfil the requirements of systems that detect foodborne pathogens, using bacteriophages as a potential recognition tool.

This chapter is divided into four sections, corresponding to the main conclusions and future perspectives obtained along the different steps, which contributed to achieve the overall objective of the work described herein.

### 5.1 *Salmonella* Phage

The initial experimental work of this thesis was the selection and characterization of *Salmonella* phages with the objective to find a good candidate to explore as a biological element for biosensing purposes. The phage PVP-SE1 was the one exhibiting the broadest lytic spectrum and thus the phage with the greatest potential as bioelement in biosensing systems. Due to its multivalent characteristics we proved that PVP-SE1 can be propagated in a nonpathogenic strain, maintaining its binding abilities. In economic and market perspectives, this property can be used to develop a safe product, and might even lead to lower production costs. To de-

velop reliable bio-interfaces in a detection device, the biological element should be a small active molecule, allowing a homogenous and uniform surface coverage with an efficient binding ability to the target. Biorecognition is not necessarily restricted to the phage's whole structure, since the binding ability of phages is made through their host recognition peptides. Accordingly, genes encoding the host binding peptides of two of the selected phages were identified, aiming at using this information for the development of biosensing systems with host recognition peptides as an interface.

### 5.2 Phage PVP-SE1 as a Biorecognition Interface

The first approach used in the development of a biosensing system to detect *Salmonella* was based on the use of entire phage particles. The proof-of-concept was established with phage PVP-SE1 using a magnetoresistive platform. This was the first time that lytic phages were used as bioelements in biosensing devices, in fact, only temperate and filamentous phages have been previously tested due to their non-lytic behavior. Accordingly, the great challenge of this work was obtain an active and non-lytic interface built with entire phage particles. This was possible after testing and optimizing the immobilization conditions of the phage on the sensor's surface. Furthermore, the binding ability of phages immobilized over a magnetoresistive platform (MR) to bacteria in different viability states was assessed. Surprisingly, the phage-based magnetoresistive biosensor showed a great ability to distinguish among viable, VBNC and heat-killed cells. The phage infection parameters were also tested and confirmed the results given by the MR platform. Indeed, phage PVP-SE1 has a different adsorption profile for viable (including the VBNC) cells than for cells killed, namely 80% of adsorption against 20%, respectively. Besides the evidence showing that phage may not recognize bleach-killed cells, we suggested to include viability assessment tests, cells killed under different conditions, simulating real environment situations. Including this type of experiments, it will be possible to determine whether the phage's behavior maintains constant for a diverse range of samples. Another interesting feature to develop in the future, which was not possible in this work due to equipment limitations, is to sort the different viability states of the cell populations by flow cytometry and test them in a MR platform. This technique will allow us to obtain separate samples from a heterogeneous population with different viability

states and will analyze how each bacterial population contributes to the measured signal. Beside the binding affinity tests, the shelf-life of the phage-based biosensor should be an important issue to be considered and monitored in the future.

### 5.3 A detection tool based on host recognition peptides of phage origin

The second approach used in the development of a biosensing system to detect *Salmonella* was based on the use of host recognition peptides derived from lytic and filamentous phages. The proof-of-concept was established with filamentous phages, by creating peptides called "nano-phages" (NPs) with the ability to bind to streptavidin. The binding ability of NPs to streptavidin beads (mimeticizing bacterial cells) was compared to that of filamentous phages by different ELISA assay formats. NPs bound approximately 1.6 times better than the parental phage, which was an excellent indicator that this different application of phage compounds can be used as an alternative, increasing thus the sensor's performance. Tests were also conducted in a magnetoelastic (ME) sensor. Although the results presented some variation, SEM observations of the gold surfaces coated with NPs or phage confirmed the different binding patterns to streptavidin beads. Nevertheless, the binding efficiency can be improved, testing other types of immobilization techniques to allow the orientation of the NPs on the surface leaving the active parts available to capture the target. Moreover, changes in the washing procedures should be implemented in order to understand how these implicate the binding efficiency. The results obtained were the starting point of multiple assays that may lead to development of a robust and reliable biosensor.

This new approach was also confirmed using two heterologously expressed tail fiber proteins (TFPs) of PVP-SE1. The binding affinity of these proteins tested in an ELISA format was found to be equal to that of the entire phage. The results showed that TFPs binding affinities are sensitive to buffers changes, suggesting that more conditions should be considered to test their stability. When immobilized on gold substrates (a metal widely used on transducer platforms) results showed that this substrate can be used without losing the TFP's binding capability.

Overall the results presented in this thesis showed that with phages is possible to construct smart biofunctional surfaces with high specificity, sensitivity and, contribute for the decreasing of false and negative results, leading to the introduction of phage-based biosensors as a new generation of biosensors.

### 5.4 Answering the important issues...

- 1) *Will the phage preserve its excellent feature as specificity when immobilized on a sensor surface?* Yes, PVP-SE1 as entire phage was immobilized in a MR platform and their specificity was evident against the target. Also, they challenged their capabilities when showing their potential as a viability assessment tool.
- 2) *Can we use phage derivatives as a detection tool?* Yes, phage derivatives from two different types of phages were tested and both showed to have potential as an alternative for the entire phage structure.
- 3) *Even showing promising results, what is missing?* Validation. Regarding the phage-based MR platform, the specificity should be analyzed with samples containing different targets and real samples also still need to be tested, in order to understand how they can influence the measurement. The binding affinity should be tested compared against other validated platforms under the same conditions. With regard to using phage derivatives as an interface, the same tests need to be considered. Stability tests are also necessary to construct a robust and reliable biosensor.



# Appendices

## Appendix A:

Information on the CD attached to this document.

## Appendix B:

### B.1. Preparation of Sepharose column

(Sepharose CL-6B -Amersham Biosciences)

**Packing Buffer:** *Packing Buffer/Running Buffer*

- a) 10mM Sodium Chloride
- b) 10mM Tris-HCl, pH 8.0
- c) 0.2mM EDTA

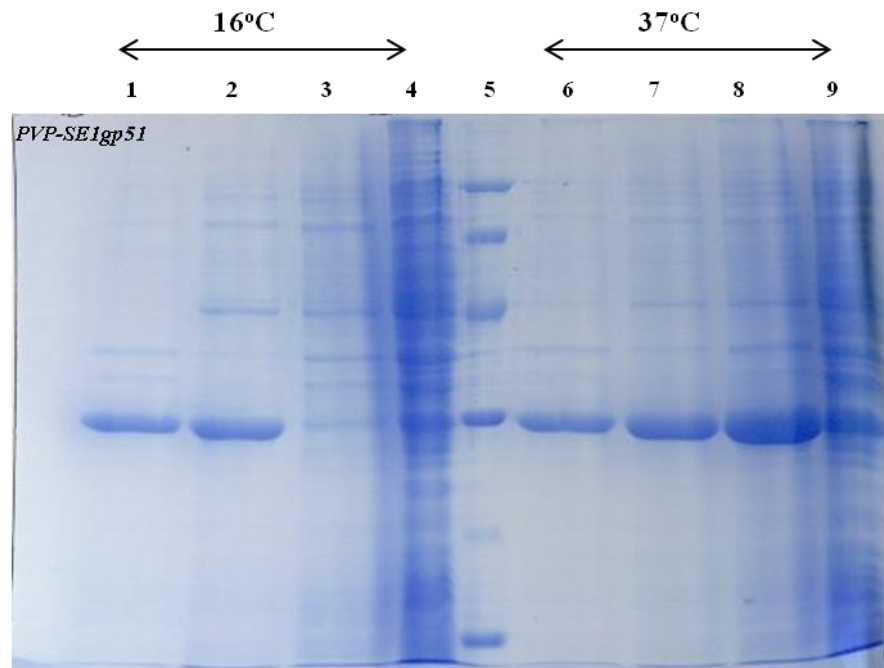
**Sepharose Chromatography Column:**

- a) Mix 48mL sepharose with 192mL Packing Buffer.
- b) Degas slurry for **20min**.
- c) Mix by swirling gently and pour the slurry into the column in one continuous motion along a glass rod held against the column.
- d) Fill the column reservoir to the top with buffer.
- e) Allow the column to pack, ensure that the buffer doesn't drain out of the column. Leave about 1cm of buffer above the surface of the column.
- f) Stop the flow by closing the stopcock at the bottom of the column.
- g) When the column is ready, connect all tubing and ensure there is no air bubbles in the flow path.
- h) Equilibrate the column with packing buffer until a stable baseline is achieved.



## B.2. Phage tail-fibre Proteins

The small-scale protein expression of the tail protein gp51 tested at different temperatures: 16°C and 37°C.



**Figure B.2:** (representative example) SDS-PAGE analysis of the expression and purification of PVP-SE1gp51 and PVP-SE1gp53. The SDS-PAGE analysis shows non-induced protein (1 and 6), total protein fraction (2 and 7), soluble protein fraction (3 and 8), insoluble protein fraction (4 and 9) and the LMW ladder (5).

Optimal temperature = 37°C.

